



University
of Glasgow

Kettlewell, Sarah (2002) *The electrophysiological and mechanical effects of gap junction uncoupling in cardiac muscle*. PhD thesis.

<http://theses.gla.ac.uk/6223/>

Copyright and moral rights for this thesis are retained by the author

A copy can be downloaded for personal non-commercial research or study, without prior permission or charge

This thesis cannot be reproduced or quoted extensively from without first obtaining permission in writing from the Author

The content must not be changed in any way or sold commercially in any format or medium without the formal permission of the Author

When referring to this work, full bibliographic details including the author, title, awarding institution and date of the thesis must be given

**THE ELECTROPHYSIOLOGICAL AND MECHANICAL EFFECTS OF
GAP JUNCTION UNCOUPLING IN CARDIAC MUSCLE**

by
SARAH KETTLEWELL

**Submitted in fulfilment of the degree
Doctor of Philosophy**

to
**University of Glasgow
Faculty of Medicine**

April 2002

For Nanna Lightfoot

Abstract

Introduction. The disruption of electrotonic interactions between cells is observed in heart failure as a result of cellular uncoupling. This disruption may unmask intrinsic dispersion of repolarisation. It is known that inhomogeneities in the recovery of excitability and restitution properties may be arrhythmogenic. Cellular uncoupling may be experimentally induced by gap junction uncouplers such as 1-heptanol and carbenoxolone.

Aims. The aim of this study was to study the electrophysiological and mechanical effects of the gap junction uncoupler 1-heptanol in the left ventricle (epicardial surface) of the artificially perfused Langendorff rabbit heart. Specifically, electrical restitution and the dispersion of repolarisation were studied.

Methods. Using a single monophasic action potential (MAP) electrode, in the healthy and failing (coronary ligated) heart, the effect of 1-heptanol was studied on rate dependent changes in action potential duration. Dispersion of repolarisation was measured sequentially.

A 32 MAP electrode array was developed to *simultaneously* record dispersion of repolarisation from the epicardial surface of the left ventricle of healthy hearts. Restitution was studied using an extrastimulus protocol that involved electrically stimulating the heart with 16 S1 stimuli (350ms intervals), and an extrastimulus S2. S1-S2 interval was increased progressively from 70 to 600ms. S1-S2 changes of 5ms were made between 70 and 150ms, 10ms between 150 and 350ms, and 50ms between 350 and 600ms. Protocols were run at 37°C, initially in Tyrode's solution, then after addition of 0.3mM 1-heptanol.

Results. The single catheter study showed that failure significantly ($P<0.05$) prolongs MAP duration between cycle lengths of 250ms and 650ms. No base to apex changes, changes in dispersion of repolarisation or ventricular fibrillation thresholds were observed. 1-Heptanol, at cycle lengths above 350ms, significantly ($P<0.05$) decreased MAP duration in failing and healthy hearts. 1-Heptanol

however did not alter the dispersion of repolarisation or ventricular fibrillation threshold in healthy and failing hearts.

The last S1 MAP in the 16 beat train and the S2 MAP obtained using the 32 electrode array were analysed at 90% repolarisation (MAPD₉₀). S2 MAPD₉₀ increased with S1-S2 interval up to ~180ms but decreased at longer intervals. 0.3mM 1-heptanol exacerbated this negative slope in the restitution curve from (mean±SEM) -0.031±0.004 in Tyrode's compared to -0.063±0.005 in 0.3mM 1-heptanol (P<0.001). Dispersion of repolarisation was increased (p>0.05) in the presence of 0.3mM 1-heptanol. Conduction delay was increased from (mean±SEM) 44.2±0.82ms to 49.2±0.87ms (P<0.001).

The possibility of an effect on the single cell being the mechanism behind the exacerbation of the negative slope by 1-heptanol was investigated in a single cell study. The effect of 1-heptanol on single cell fractional shortening and Ca²⁺ handling was examined. At 1 and 3Hz 1-heptanol decreases fractional cell shortening from (mean±SEM): at 1Hz 9.3±0.8% in Krebs to 5.7±0.7% (0.03mM 1-heptanol), 5.6±0.9% (0.1mM 1-heptanol) and 3.2±0.8% (0.3mM 1heptanol) (P<0.01); at 3Hz 10.6±0.8% in Krebs to 6.5±1.4% (0.03mM 1-heptanol), 7.7±1.4% (0.1mM 1-heptanol) and 4.7±1.5% (0.3mM 1-heptanol) (P<0.01). The negative inotropic (i.e. the reduction in contractility) effect of 1-heptanol indicated that this agent is not a specific gap junction uncoupler. SR Ca²⁺ release was reduced at 3Hz only by (mean±SEM) 7.8±0.04% (0.03mM 1-heptanol), 5.0±0.03% (0.1mM 1-heptanol) and 7.9±0.02% (P<0.05), indicating an effect on the L-type Ca²⁺ channel or ryanodine receptor.

The effect on the L-type Ca²⁺ channel was investigated by the use of nifedipine firstly in single cells then in the whole heart. Nifedipine decreased single cell fractional shortening at 1Hz from (mean±SEM) 8.9±0.7% in Krebs to 5.8±0.7% (0.1µM nifedipine), 3.4±0.9% (0.15µM nifedipine, P<0.001) and 0.8±0.2% (0.2µM nifedipine, P<0.001). SR Ca²⁺ release was also reduced from (mean±SEM) 0.75±0.017% in Krebs to 0.72±0.024% (0.1µM nifedipine), 0.73±0.024% (0.15µM nifedipine), 0.71±0.016% (0.2µM nifedipine) (P<0.05). In the whole heart

nifedipine did not induce a negative slope in the restitution curve indicating no role of the L-type Ca^{2+} channel in this phenomenon.

Carbenoxolone, a novel specific gap junction uncoupler failed to induce a negative slope in the electrical restitution curve of the whole heart, but did increase dispersion of repolarisation ($P>0.05$) and caused a significant conduction slowing from (mean \pm SEM) $45.50\pm 2.12\text{ms}$ in Tyrode to $55.11\pm 2.82\text{ms}$ in carbenoxolone ($P<0.05$). Carbenoxolone has an inconsistent effect on single cell fractional shortening and Ca^{2+} handling.

Conclusions. The biphasic relationship and the increased dispersion of repolarisation in the presence of 0.3mM 1-heptanol may have implications for the development of alternans and/or arrhythmias (Gilmour and Chialvo, 2000). The cause of the negative slope is as yet unknown, but it is likely that it is an effect on the single cell rather than gap junction uncoupling.

Key words: 1-heptanol, gap junction uncoupling, carbenoxolone, nifedipine, restitution, Ca^{2+} , heart failure, fractional shortening,

Acknowledgements

I would like to take this opportunity to thank the people who during the last 3 years have given to me their help, assistance, friendship and advice, without which the completion of this thesis would have been a greater task. I would like to thank:

Dr. Francis Burton who has given me invaluable technical, practical, and theoretical advice.

Professor Godfrey Smith for most importantly his encouragement but also for his guidance and help throughout this project.

Professor Stuart Cobbe for his most invaluable comments and guidance.

Aileen Rankin and Anne Ward for their wonderful technical support, friendship and kind words during the harder times.

Alix, Deb, Susan and all others who have been there for helpful discussion and friendship.

All at the Royal Infirmary for the animals they provided for this study.

To my mum just for being my mum.

And to Al, who has given me love and support and has helped me keep things in perspective.

Table of contents

Title	I
Abstract	III
Acknowledgements	VI
Table of contents	VII
List of figures	XIV
List of tables	XX
Aims and objectives	XXIII
Abbreviations	XXIII
Declaration	XXV
Publications	XXV
CHAPTER 1 – GENERAL INTRODUCTION	1
1.1 Introduction	2
1.2 Dispersion of ventricular repolarisation/refractoriness	2
1.2.1 Transmural dispersion	4
1.2.2 Apex to base dispersion	5
1.2.3 Heart rate	5
1.3 Electrical restitution	6
1.3.1 Cellular mechanisms responsible for restitution	7
1.3.2 Ion accumulation	8
1.3.3 Incomplete recovery of ionic currents	8
1.3.4 Dispersion of restitution	9
1.4 Intercellular coupling	9
1.4.1 Gap junction structure and function	9
1.4.2 Gap junction channels and cardiac conduction	12

1.4.3 Electrotonic interactions and gap junction uncoupling	12
1.5 Arrhythmias	13
1.5.1 Unidirectional block	14
1.5.1.1 Due to non-uniform recovery of excitability	14
1.5.1.2 Due to geometrical factors	14
1.5.1.3 Based on asymmetrical depression of conduction and excitability	15
1.5.2 Conduction delay	15
1.5.3 Re-entry	16
1.5.3.1 Anatomical re-entry	17
1.5.3.2 Functional re-entry: The leading circle theory	18
1.5.3.3 Anisotropic re-entry	20
1.6 The action potential	21
1.6.1 The ionic basis of the action potential	21
1.6.1.1 Resting potential (Phase 4)	22
1.6.1.2 Action potential upstroke (Phase 0)	22
1.6.1.3 Phase 1	23
1.6.1.4 The Plateau (Phase 2)	23
1.6.1.5 Repolarisation (Phase 3)	24
1.6.2 Refractory periods	26
1.6.2.1 Measuring refractoriness	27
1.7 Excitation-contraction coupling and Ca²⁺ handling	29
1.7.1 Intracellular Ca ²⁺ removal	32
1.7.2 Contraction-excitation feedback	33
CHAPTER 2 - GENERAL METHODS	34
2.1 Langendorff perfusion of whole hearts	34
2.1.1 The perfusion system	34
2.1.2 Experimental procedure	38
2.1.2.1 The infarct model of heart failure	38
2.1.2.2 Heart preparation and experimental set-up	39
2.1.3 Electrical recording	41

2.1.4 MAP analysis	44
2.2 Single cell preparation	47
2.2.1 Single cell dissociation	47
2.2.2 Single cell shortening/ Ca^{2+} measurements	49
2.2.3 Data analysis	52
2.3 Statistical analysis	54
2.3.1 Student's t-test	54
2.3.2 ANOVA (Analysis of variance)	55
CHAPTER 3 - METHODS OF RECORDING CARDIAC ELECTRICAL ACTIVITY	56
3.1 Development of methods used to record MAPs	57
3.1.1 Unipolar and bipolar recordings	57
3.1.2 Transmembrane action potentials	59
3.1.3 Monophasic action potentials	59
3.1.3.1 Suction electrode	61
3.1.3.2 The contact catheter electrode	62
3.1.3.3 MAP genesis	64
3.2 The contact catheter electrode - preliminary investigations and limitations	69
3.2.1 Methods	69
3.2.2 Results	70
3.2.2.1 Time to steady state	70
3.2.2.2 The effect of electrode contact pressure on MAP recordings	72
3.3 The syringe electrode – construction and preliminary investigations	75
3.3.1 Construction	75
3.3.2 Methods	78
3.3.3 Results	78
3.4 The jacket electrode – development, construction, and preliminary investigations	83

3.4.1 General construction of latex jackets and electrodes	83
3.4.1.1 The 4 electrode array	84
3.4.1.1.1 Methods	84
3.4.1.1.2 Results	85
3.4.1.2 The 8 and 16 electrode arrays	87
3.4.1.3 The 32 electrode array	87
3.5 Discussion and conclusions	90
CHAPTER 4 – THE EFFECT OF HEART FAILURE ON WHOLE HEART ELECTROPHYSIOLOGY RECORDED BY THE FRANZ MAP CATHETER TECHNIQUE	94
4.1 Introduction	95
4.2 Methods	97
4.3 Results	100
4.3.1 Cycle length dependent effects on MAP duration in sham operated and failure hearts	100
4.3.2 Global differences in MAP duration between heart failure and sham operated hearts	105
4.3.3 Base to apex differences between sham operated and failing hearts	107
4.3.4 The effect of failure on dispersion of repolarisation	109
4.3.5 Ventricular fibrillation thresholds	111
4.4 Discussion	113
4.4.1 Ionic basis of action potential duration prolongation in heart failure	113
4.4.2 Base to apex differences	114
4.4.3 Dispersion of repolarisation/refractoriness and ventricular fibrillation threshold	116
4.4.4 Conduction delay	119

CHAPTER 5 – THE EFFECT OF 1-HEPTANOL ON WHOLE HEART ELECTROPHYSIOLOGY IN NORMAL AND FAILING HEARTS RECORDED BY THE FRANZ MAP CATHETER TECHNIQUE	121
5.1 Introduction	122
5.1.1 Gap junction uncoupling and 1-heptanol	122
5.1.2 Mechanisms of action of 1-heptanol	123
5.2 Methods	125
5.3 Results	127
5.3.1 The effect of ethanol on whole heart electrophysiology	127
5.3.2 1-Heptanol dose response curve	129
5.3.3 1-Heptanol reversibly modifies the mechanical activity in the whole heart	131
5.3.4 1-Heptanol reversibly modifies the electrical activity of the whole heart	134
5.3.5 The effect of 0.3mM 1-heptanol on electrical activity in sham operated hearts	136
5.3.6 The effect of 0.3mM 1-heptanol on electrical activity in failure hearts	141
5.3.7 The effect of 0.3mM 1-Heptanol on sham hearts v failure hearts	146
5.3.9 The global effect of 0.3mM 1-heptanol on MAP duration in failure hearts	152
5.3.10 The effect of 0.3mM 1-heptanol on dispersion of repolarisation in sham operated hearts	154
5.3.11 The effect of 0.3mM 1-heptanol on dispersion of repolarisation in failure hearts	156
5.3.12 The effect of 0.3mM 1-heptanol on ventricular fibrillation threshold	159
5.5 Discussion	162
5.5.1 Effect on contractility	162
5.5.2 Reduction in action potential duration	163
5.5.3 Dispersion of repolarisation and effect on arrhythmogenesis	164

CHAPTER 6 – THE EFFECT OF THE GAP JUNCTION UNCOUPLER 1-HEPTANOL ON THE ELECTROPHYSIOLOGY OF THE WHOLE HEART AS RECORDED BY THE 32 MAP ELECTRODE ARRAY	167
6.1 Introduction	168
6.2 Methods	170
6.2.1 Protocols	170
6.2.2 Data acquisition and analysis	174
6.3 Results	175
6.3.1 Stabilisation of the basic S1 MAPs <i>prior</i> to the extrastimulus	175
6.3.2 Dispersion of repolarisation	178
6.3.3 Conduction delay	180
6.3.4 The negative slope	182
6.4 Discussion	185
6.4.1 Conduction delay and velocity	185
6.4.2 Dispersion of repolarisation	187
6.4.3 The negative slope in the restitution curve	188
CHAPTER 7 - THE EFFECT OF 1-HEPTANOL AND NIFEDIPINE ON SINGLE CELL FRACTIONAL SHORTENING AND CALCIUM HANDLING	190
7.1 Introduction	191
7.2 Methods	193
7.2.1 Fractional shortening and Ca ²⁺ measurement stimulation protocols	193
7.2.2 Caffeine induced sarcoplasmic reticulum Ca ²⁺ release stimulation protocols	194
7.2.3 Statistical analysis	195
7.3 Results	197
7.3.1 Relative end-diastolic lengths	197
7.3.2 Fractional shortening	200
7.3.3 Calcium handling	205

7.3.4 Sarcoplasmic reticulum Ca ²⁺ content	209
7.4 Discussion	214
CHAPTER 8 – THE EFFECT OF THE L-TYPE CALCIUM CHANNEL BLOCKER NIFEDIPINE ON THE NEGATIVE SLOPE OF THE RESTITUTION CURVE IN THE WHOLE HEART	217
8.1 Introduction	218
8.2 Methods	219
8.3 Results	220
8.3.1 The effect of nifedipine on LVDP	220
8.3.2 The negative slope	222
8.3.3 Conduction delay	225
8.3.3 Dispersion of repolarisation	227
8.4 Discussion	231
CHAPTER 9 – THE EFFECTS OF GAP JUNCTION UNCOUPLER CARBENOXOLONE ON WHOLE HEART ELECTROPHYSIOLOGY AND SINGLE CELL CONTRACTILITY AND CALCIUM HANDLING	234
9.1 Introduction	234
9.2 Methods	236
9.2.1 Whole heart experiments	236
9.2.2 Single cell experiments	237
9.3 Results – Whole heart	238
9.3.1 Monophasic action potential duration	238
9.3.2 Conduction delay	240
9.3.3 Dispersion of repolarisation	242
9.3.4 The negative slope	245
9.4 Results – Single Cells	247
9.4.1 Relative end diastolic lengths	247

9.4.5 Sarcoplasmic reticulum Ca ²⁺ content	256
9.5 Summary and discussion	258
CHAPTER 10 – SUMMARY AND CONCLUSIONS	261
10.1 Summary	262
10.2 Electrophysiological abnormalities associated with heart failure	262
10.3 Simultaneous recording of cardiac electrical activity	263
10.3.1 The 32 MAP electrode array	263
10.4 Gap junction uncoupling	264
10.5 Restitution	265
10.5.1 Measurement of restitution	265
10.5.2 The negative slope in the restitution curve	266
10.5.2.1 Phenomena related to gap junction uncoupling	266
10.5.2.2 Disruption of E-C uncoupling	267
10.6 Tried but failed	268
10.7 Future directions	268
REFERENCES	270

List of figures

CHAPTER 1 – GENERAL INTRODUCTION

Figure 1.1 A typical electrical restitution curve.	7
Figure 1.2 The connexon and connexin.	11
Figure 1.3 Mines model of anatomical re-entry.	17
Figure 1.4 Schematic representing the leading circle theory of re-entry.	20
Figure 1.5 Phases of the action potential and indication of the ionic influxes involved.	21
Figure 1.6 Membrane conductance to Na ⁺ , Ca ²⁺ and K ⁺ during a rabbit cardiac action potential.	25
Figure 1.7 Refractory periods of the MAP.	27
Figure 1.8 Excitation-contraction coupling.	30

CHAPTER 2 – GENERAL METHODS

Figure 2.1 The Langendorff perfusion system.	37
Figure 2.2 A schematic of the electrical set-up used for stimulation and recording during whole heart Langendorff perfused experiments.	43
Figure 2.3 Illustrative MAP showing analysis parameters.	46
Figure 2.5 Schematic of the single cell shortening/Ca ²⁺ measurement set up.	51
Figure 2.6 The parameters used for measurement of single cell fractional shortening (A) and Ca ²⁺ transients (B).	53

CHAPTER 3 - METHODS OF RECORDING CARDIAC ELECTRICAL ACTIVITY

Figure 3.1 Schematic drawings of the suction (A) and contact catheter (B) electrodes.	63
Figure 3.2 Diagram illustrating the hypothesis underlying the genesis of MAP recording by contact electrode .	65
Figure 3.3 Experimental set-up used by Franz <i>et al</i> (1992) to simultaneously record 3 MAPs using a cantilever and spring mechanism.	68

Figure 3.4 Typical experiment illustrating the time required to ensure stabilisation of MAP recordings.	71
Figure 3.5 The effect of contact pressure on MAP duration and amplitude.	73
Figure 3.6 The effect of contact pressure on the ratio MAPD ₅₀ :MAPD ₉₀ .	74
Figure 3.7 The syringe electrode.	77
Figure 3.8 A typical restitution curve obtained from the epicardial surface of the left ventricle with the syringe electrode.	79
Figure 3.9 The effect of rotation of the syringe electrode.	82
Figure 3.10 Simultaneously recorded MAPs obtained from the epicardial surface of the left ventricle by the 4 electrode array.	86
Figure 3.11 The 32 electrode array.	88

CHAPTER 4 - THE EFFECT OF HEART FAILURE ON WHOLE HEART ELECTROPHYSIOLOGY RECORDED BY THE FRANZ MAP CATHETER TECHNIQUE

Figure 4.1 Schematic of the heart showing the division of the left ventricle for dispersion analysis..	99
Figure 4.2 MAP duration v CL in failure hearts and sham operated hearts.	103
Figure 4.3 The effect of heart failure on global MAPD ₉₀ .	106
Figure 4.4 Base to apex differences in MAP duration.	108
Figure 4.5 The effect of failure on dispersion of repolarisation at a range of cycle lengths.	110
Figure 4.6 Experimental trace showing ventricular fibrillation induction.	112
Figure 4.7 The effect of heart failure on ventricular fibrillation threshold.	112

CHAPTER 5 – THE EFFECT OF 1-HEPTANOL ON WHOLE HEART ELECTROPHYSIOLOGY IN NORMAL AND FAILING HEARTS RECORDED BY THE FRANZ MAP CATHETER TECHNIQUE

Figure 5.1 The effect of 0.005% ethanol on MAPD ₉₀ (A) and conduction delay (B).	128
Figure 5.2 The effect of increasing heptanol (mM) concentration on left ventricular developed pressure (LVDP).	130

Figure 5.3 Reversible effect of perfusion with 0.3mM 1-heptanol on LVDP.	132
Figure 5.4 The effect of 0.3mM 1-heptanol on LVDP as illustrated by experimental traces.	133
Figure 5.5 Reversible effect of perfusion with 0.3mM 1-heptanol on MAPD ₉₀ .	135
Figure 5.6 The effect of 0.3mM 1-Heptanol on single MAPs.	135
Figure 5.7 Curve fitted graphs illustrating the effect of 0.3mM 1-heptanol on stable state restitution in sham-operated hearts.	139
Figure 5.8 Curve fitted graphs illustrating the effect of 0.3mM 1-heptanol on stable state restitution in failure hearts.	144
Figure 5.9 Curve fitted graphs illustrating the effect of 0.3mM 1-heptanol on stable state restitution in sham-operated v failure hearts.	149
Figure 5.10 The effect of 0.3mM 1-heptanol on MAPD ₉₀ in sham operated hearts.	151
Figure 5.11 The effect of 0.3mM 1-heptanol on MAPD ₉₀ in failure hearts.	153
Figure 5.12 The effect of 0.3mM 1-heptanol on dispersion of repolarisation in sham operated hearts.	155
Figure 5.13 The effect of 0.3mM 1-heptanol on dispersion of repolarisation in failing hearts.	157
Figure 5.14 The effect of failure on the dispersion of repolarisation in the 0.3mM 1-heptanol perfused heart.	158
Figure 5.15 The effect of 0.3mM 1-heptanol on ventricular fibrillation thresholds.	161

CHAPTER 6 – THE EFFECT OF THE GAP JUNCTION UNCOUPLER 1-HEPTANOL ON THE ELECTROPHYSIOLOGY OF THE WHOLE HEART AS RECORDED BY THE 32 MAP ELECTRODE ARRAY

Figure 6.1 Whole heart perfusion protocol.	171
Figure 6.2 Whole heart extrastimulus protocols.	173
Figure 6.3 Typical experiments showing the stability of the S1 MAP on giving 8 S1 (A and B, 3 MAPs obtained simultaneously) and 16 S1 (C and D, 7 MAPs obtained simultaneously).	177
Figure 6.4 Effect of 0.3mM 1-heptanol on dispersion of repolarisation in S2 MAPs.	179

Figure 6.5 Effect of 0.3mM 1-heptanol on conduction delay.	181
Figure 6.6 Restitution data obtained from a single experiment where 6 MAPs have been obtained simultaneously.	183
Figure 6.7 The effect of 0.3mM 1-heptanol on the slope of the restitution curve.	184

CHAPTER 7 - THE EFFECT OF 1-HEPTANOL AND NIFEDIPINE ON SINGLE CELL FRACTIONAL SHORTENING AND CALCIUM HANDLING

Figure 7.1 Stimulation and perfusion protocols for fractional cell shortening (A) and Ca ²⁺ handling (B) experiments.	196
Figure 7.2 The effect of 1-heptanol on end diastolic length.	198
Figure 7.3 The effect of 0.1μM, 0.15μM and 0.2μM nifedipine on relative end diastolic length.	199
Figure 7.4 The effect of 1-heptanol on relative fractional cell shortening.	202
Figure 7.5 Trace showing the effect of 0.1mM 1-heptanol on single cell shortening.	203
Figure 7.6 The effect of 0.1μM, 0.15μM and 0.2μM nifedipine on relative fractional shortening.	204
Figure 7.7 Experimental trace illustrating the effect of 0.15μM nifedipine on single cell contractility.	204
Figure 7.8 The effect of 1-heptanol on relative peak Fura-2 ratios.	206
Figure 7.9 The effect of 0.1μM, 0.15μM and 0.2μM nifedipine on relative peak Fura-2 ratio.	207
Figure 7.10 Experimental trace showing the effect of 0.1mM 1-heptanol on single cell Fura-2 ratio.	208
Figure 7.11 Experimental trace showing the effect of 0.15μM nifedipine on Fura-2 ratio.	208
Figure 7.12 The effect of 0.1mM 1-heptanol on sarcoplasmic reticulum Ca ²⁺ content.	212
Figure 7.13 The effect of 1-heptanol on SR Ca ²⁺ content: experimental traces.	211
Figure 7.14 The effect of 0.15μM nifedipine on SR Ca ²⁺ content.	212

Figure 7.15 Experimental traces showing the effect of nifedipine on SR Ca²⁺ content.

213

CHAPTER 8 - THE EFFECT OF THE L-TYPE CALCIUM CHANNEL BLOCKER NIFEDIPINE ON THE NEGATIVE SLOPE OF THE RESTITUTION CURVE IN THE WHOLE HEART

Figure 8.1 The effect of nifedipine on LVDP. 221

Figure 8.2 Restitution curves from a typical experiment where the heart was perfused with normal Tyrode's solution (A) followed by 0.1 μM nifedipine solution (B). 223

Figure 8.3 The global effect of nifedipine on electrical restitution. 224

Figure 8.4 The effect of nifedipine on the gradient of the slope of the restitution curve. 224

Figure 8.5 The effect of nifedipine on conduction delay. 226

Figure 8.6 The effect of nifedipine on dispersion of repolarisation. 230

CHAPTER 9 – THE EFFECTS OF THE GAP JUNCTION UNCOUPLER CARBENOXOLONE ON WHOLE HEART ELECTROPHYSIOLOGY AND SINGLE CELL CONTRACTILITY AND CALCIUM HANDLING

Figure 9.1 The effect of carbenoxolone on MAPD₉₀. 239

Figure 9.2 The effect of 50 μM carbenoxolone on conduction delay. 241

Figure 9.3 The effect of 50 μM carbenoxolone on dispersion of S1 (A) and S2 (B and C) repolarisation. 244

Figure 9.4 The effect of 50 μM carbenoxolone on the gradient of the slope of the restitution curve. 246

Figure 9.5 The effect of 50 μM carbenoxolone on end diastolic length. 248

Figure 9.6 The effect of 50 μM carbenoxolone on fractional cell shortening. 250

Figure 9.7 The effect of 50 μM carbenoxolone on end diastolic Fura-2 ratio. 252

Figure 9.8 The effect of 50 μM carbenoxolone on relative peak Fura-2 ratio. 253

Figure 9.9 Analysis of Ca²⁺ transient kinetics. 254

Figure 9.10 The effect of 50 μ M carbenoxolone on the kinetics of Ca²⁺ decay at 1Hz (A) and 3Hz (B). **255**

Figure 9.11 The effect of 50 μ M carbenoxolone on SR Ca²⁺ content. **257**

List of tables

CHAPTER 2 - GENERAL METHODS

Table 2.1 Criteria for an optimum quality monophasic action potential.	45
---	-----------

CHAPTER 3 - METHODS OF RECORDING CARDIAC ELECTRICAL ACTIVITY

Table 3.1 The advantages and disadvantages of unipolar (A) and bipolar (B) electrode recording.	58
Table 3.2 Techniques for measuring repolarisation times.	93

CHAPTER 4 - THE EFFECT OF HEART FAILURE ON WHOLE HEART ELECTROPHYSIOLOGY RECORDED BY THE FRANZ MAP CATHETER TECHNIQUE

Table 4.1 The effect of heart failure on MAPD ₉₀ .	104
Table 4.2 Absolute changes in mean dispersion of repolarisation.	109

CHAPTER 5 - THE EFFECT OF 1-HEPTANOL ON WHOLE HEART ELECTROPHYSIOLOGY IN NORMAL AND FAILING HEARTS RECORDED BY THE FRANZ MAP CATHETER TECHNIQUE

Table 5.1 The effect of 0.3mM 1-heptanol on MAPD ₉₀ in sham operated hearts.	140
Table 5.2 The effect of 0.3mM 1-heptanol on MAPD ₉₀ in failure hearts.	145
Table 5.3 Sham and failure n-numbers.	146
Table 5.4 Dispersion of repolarisation in sham operated hearts.	154
Table 5.5 Dispersion of repolarisation in failure hearts.	156

CHAPTER 6 – THE EFFECT OF THE GAP JUNCTION UNCOUPLER 1-HEPTANOL ON THE ELECTROPHYSIOLOGY OF THE WHOLE HEART AS RECORDED BY THE 32 MAP ELECTRODE ARRAY

Table 6.1 The effect of 0.3mM 1-heptanol on dispersion of S2 repolarisation. 178

CHAPTER 7 - THE EFFECT OF 1-HEPTANOL AND NIFEDIPINE ON SINGLE CELL FRACTIONAL SHORTENING AND CALCIUM HANDLING

Table 7.1 The effect of 1-heptanol at 1Hz and 3Hz, and nifedipine at 1Hz, and on mean fractional cell shortening. 201

CHAPTER 8 - THE EFFECT OF THE L-TYPE CALCIUM CHANNEL BLOCKER NIFEDIPINE ON THE NEGATIVE SLOPE OF THE RESTITUTION CURVE IN THE WHOLE HEART

Table 8.1 The effect of nifedipine on the gradient of the slope of the restitution curve. 222

CHAPTER 9 – THE EFFECTS OF THE GAP JUNCTION UNCOUPLER CARBENOXOLONE ON WHOLE HEART ELECTROPHYSIOLOGY AND SINGLE CELL CONTRACTILITY AND CALCIUM HANDLING

Table 9.1 The effect of 50µM carbenoxolone on the mean MAPD₉₀ of S1 and S2 MAPS. 238

Table 9.2 The effect of 50µM carbenoxolone on dispersion of repolarisation. 242

Aims and objectives

The initial aim of the study was to investigate the electrophysiology of the whole heart using a single monophasic action potential (MAP) contact catheter electrode. Left ventricular epicardial MAP recordings were obtained from healthy and failing Langendorff perfused rabbit hearts. Dispersion of repolarisation was mapped sequentially. Using the gap junction uncoupler 1-heptanol it was the aim to compare the intrinsic dispersion of repolarisation from healthy and failing hearts using a steady state restitution protocol.

The sequential recording of electrical activity is limited in accuracy. A further aim of this study was to develop and construct a method of simultaneously recording up to 32 MAPs from the epicardial surface of the left ventricle. Due to restrictions in the use of the electrode array in failing hearts and the apparent induction of a negative slope in the electrical restitution (extrastimulus protocol) curve by the gap junction uncoupler 1-heptanol, the focus of the study changed. The mechanism by which the (non-specific) gap junction uncoupler 1-heptanol induced a negative slope in the restitution curve became the primary aim of the study.

The negative inotropic effect of 1-heptanol indicated that 1-heptanol may have an effect on single cell Ca^{2+} handling. The effect of 1-heptanol on single cell fractional shortening and Ca^{2+} handling was investigated. Nifedipine was also used in these cells with the intention of investigating the effect of partial L-type Ca^{2+} channel blockade on the slope of the restitution curve in the whole heart.

Whole heart and single cell studies were also undertaken with the novel specific gap junction uncoupler carbenoxolone. The aim of this section of the study was to determine whether the induction of a negative slope in the restitution curve is attributable to gap junction uncoupling or to other mechanisms.

Abbreviations

A ₂ C	2-(methoxyethoxy)ethyl 8-(cis-2- <i>n</i> -octylcyclopropyl)-octanoate
ANOVA	Analysis of variance
ARI	Activation recovery interval
ARP	Absolute refractory period
ATP	Adenosone triphosphate
AVN	Atrioventricular node
BCL	Basic cycle length
BDM	2,3-Butanedione Monoxime
BSA	Bovine serum albumin
CD	Conduction delay
CL	Cycle length
CICR	Calcium induced calcium release
DAD	Delayed afterdepolarisation
DHE	Dehydroergosterol
EAD	Early afterdepolaristaion
E-C	Excitation-contraction
EDL	End diastolic length
ERP	Effective refractory period
ESL	End systolic length
g_j	Gap junctional conductance
LA	Left atrium
LV	Left ventricle
LVD	Left ventricular dysfunction
LVDP	Left ventricular developed pressure
MAP	Monophasic action potential
MAPD ₅₀	MAP duration at 50% repolarisation
MAPD ₇₀	MAP duration at 70% repolarisation
MAPD ₉₀	MAP duration at 90% repolarisation
MI	Myocardial infarction
PP	Perfusion pressure
RA	Right atrium
RFS	Relative fractional shortening

RMP	Resting membrane potential
RRP	Relative refractory period
r_{ss}	Steady state anisotropy
RV	Right ventricle
SAN	Sino-atrial node
SD	Standard deviation
SEM	Standard error of the mean
SR	Sarcoplasmic reticulum
TAP	Transmembrane action potential
VF	Ventricular fibrillation
VFI	Ventricular fibrillation induction
VFT	Ventricular fibrillation threshold
VT	Ventricular tachycardia
WCP	Whole cell program

Ions and ionic currents

Ca^{2+}	Calcium
K^+	Potassium
Na^+	Sodium
Cl^-	Chloride
I_b	Inwardly directed Na^+ current
I_{Kl}	Outwardly directed K^+ current
	I_{Ks} - slow component
	I_{Kr} - fast component
I_{Na}	Fast inward sodium current
I_{si} or I_{Ca}	Slow inward Ca^{2+} current
I_{to}	Transient outward current
	I_{to1} - slow component
	I_{to2} - fast component
$I_{K(Ca)}$	Calcium-activated K^+ current
I_{Na-Ca}	Sodium-calcium exchanger current
I_{Kp}	Plateau current

Declaration

The coronary ligation and sham operated rabbits were provided by the staff (Mrs. Diane Smillie and Mr Michael Dunne under the supervision of Dr. Martin Hicks) in the Department of Medical Cardiology, Glasgow Royal Infirmary. The material contained within this thesis was carried out by myself and has not been submitted for the fulfilment of any other degree. Some of the results obtained were published in abstract form and are detailed as follows.

Publications

S. Kettlewell, S.M. Cobbe, G.L. Smith and F.L. Burton (2001). Effect of 1-Heptanol on cardiac electrophysiology and E-C coupling in the rabbit heart. *Journal of Physiology*. 536P.

S. Kettlewell, S.M. Cobbe, G.L. Smith and F.L. Burton. (2001) 1-Heptanol induces a negative slope in the restitution curve in the Langendorff-perfused rabbit heart. *Biophysical Journal*. 643a.

Chapter 1 – General introduction

1.1 Introduction

This introductory chapter deals primarily with the dispersion of cardiac ventricular repolarisation/refractoriness and also electrical restitution and their consequent effects on arrhythmogenesis. The effect of electrotonic interactions and the uncoupling of cells on the dispersion of repolarisation are all addressed. It is known that cardiac arrhythmias can be due to inhomogeneities in the recovery of excitability and restitution, and that this in itself may be a result of the disruption of electronic interactions by gap junction uncoupling.

1.2 Dispersion of ventricular repolarisation/refractoriness

In early studies by Han and Moe (1964) dispersion of refractoriness was described as a measure of the non-uniform recovery of excitability in the myocardium. In a separate study Han, Garcia DeJalon and Moe (1964) established a connection between non-uniform recovery of excitability and a reduction in fibrillation threshold. They concluded that whether the average refractory period was increased or decreased, agencies found to favour the development of ventricular fibrillation were found to increase the temporal dispersion of recovery of excitability.

In normal atrial or ventricular tissue refractoriness is proportional to the duration of repolarisation, whereas in the diseased or otherwise altered myocardium the recovery of excitability may lag behind repolarisation. Activation times, refractoriness and action potential duration all determine the dispersion of refractoriness. If dispersion of activation times remain constant then the dispersion

of refractoriness is greater at faster heart rates. Kuo *et al* (1983) found that in dog hearts a five-fold increase in dispersion of refractoriness did not induce arrhythmia, however it did facilitate arrhythmia induction by premature stimulus.

Han & Moe (1964) showed that non-uniform recovery of excitability exists in ventricular muscle. Re-entry (see section 1.5.3) could be facilitated by unidirectional block caused by a differential dispersion of repolarisation between adjacent myocardial fibres (Han, 1969). A prolongation of action potential duration is associated with heart failure although this is not an arrhythmogenic mechanism in itself if the prolongation is homogeneous (Tomaselli *et al*, 1994). However, variations in action potential duration can cause a dispersion of refractoriness that may be arrhythmogenic.

In the normal healthy heart the characteristics of the action potential and the distribution of ion channels varies between atrial, nodal, Purkinje, and ventricular cells and also within each of these. The variation in action potential duration occurs in both the intact heart and single myocytes isolated from individual regions. However, action potentials are generally longer at early activation sites and shorter at later activation sites to ensure homogeneous recovery of excitability. It is therefore normal for hearts to have a certain degree of intrinsic dispersion of repolarisation. Because repolarisation is important to cardiac arrhythmogenesis there is much interest in the variability of ionic currents that govern repolarisation. Variations or gradients in action potential duration may occur between cell layers and also across the epicardium.

1.2.1 Transmural dispersion

Regional, or transmural (i.e. transversely across the ventricle endocardium to epicardium), variations in action potential configuration and ionic currents in the left ventricle of the rabbit heart have been noted by several authors (Fedida & Giles, 1991; Cook *et al*, 1997; Antzelevitch *et al*, 1991; Anyukhovskiy *et al*, 1996; Drouin *et al*, 1995). The epicardial action potential shows a shorter duration and also has a prominent ‘spike and dome’ morphology that is lacking in the endocardium. Fedida & Giles (1991) and also Li *et al* (1999) in their work on isolated cells from the human right ventricle, suggested that the heterogeneities in the action potential duration and the spike and dome morphology was due to the transient outward current, I_{to} . The transient outward current is much more evident in the epicardium than the endocardium and therefore explains this heterogeneity.

Laurita *et al* (1996) in work using the guinea pig heart found that the cellular kinetics of repolarisation across the epicardial surface vary despite normal cellular coupling. It is thought that regional differences in the K^+ currents I_K and I_{K1} play a role in the heterogeneity of the action potential configuration. M cells, present in the mid myocardial wall, show repolarisation properties that are strongly influenced by a reduction in the expression of the delayed rectifier (I_{Ks}) which renders these cells susceptible to factors which cause prolongation of the action potential (Viswanathan *et al*, 1999). It is indeed the case that M cells have a longer action potential duration than either epicardial or endocardial cells and they also have a greater V_{max} (rate of rise of action potential upstroke). M cells also have a more prominent late fast sodium inward current (I_{Na}) (Eddlestone *et al*, 1996).

These transmural differences in action potential duration are more prominent in dissociated isolated myocytes than the intact heart. In the intact heart intrinsic differences in action potential duration are masked by electrotonic interactions between cell layers. However, in the diseased heart these electrotonic interactions may be disrupted and intrinsic dispersions revealed.

1.2.2 Apex to base dispersion

In addition to heterogeneities in action potential duration between cell layers, a trans-epicardial dispersion in the left ventricle has also been reported. Action potential durations have been seen to be longer in the basal regions of the heart compared to apical regions. Brahmajothi *et al* (1997) found that in the ferret ventricle the expression of ERG, the gene that encodes the protein responsible for the fast component of the outwardly directed K^+ current (I_{Kr}), was more abundant in apical areas. This is consistent with the findings of Cheng *et al* (1999) in their study on the heterogeneous distribution of I_{Kr} and I_{Ks} (slow component) in the left ventricle of the rabbit heart. The greater abundance of I_{Kr} in the apex produces action potentials of shorter duration.

1.2.3 Heart rate

The balance between various K^+ currents and their consequent importance in repolarisation can be drastically altered by heart rate (editorial: van Ginneken and Veldkamp, 1999). Cheng *et al* (1999) found that, upon stimulating single rabbit cardiac myocytes at 1Hz, action potential duration was longer in the apex than the base and that at stimulation frequencies higher than this the role of I_K is more important than the transient outward current (I_{to}). The role of I_{Kr} in repolarisation

is less frequency dependent than I_{Ks} . When the heart rate is increased there is less time for the decay of the slower K^+ current after each action potential. Changes in heart rate are also important in relation to electrical restitution.

1.3 Electrical restitution

It is essential that in the working heart an increase in heart rate is accompanied by a decrease in the duration of systole to ensure enough time for the ventricles to fill during diastole. In vivo adrenergic stimulation is partly responsible for this, although in the isolated heart there is a purely rate dependent shortening of action potential duration that may contribute to the shortening of systole.

One very important determinant of action potential duration is the length of the preceding diastolic interval. In multicellular mammalian preparations (Boyett and Jewell, 1978; Litovsky and Antzelevitch, 1989; Bass, 1975), electrical restitution is the rate dependent phenomenon that describes the relationship between action potential duration and the preceding diastolic interval (Elharrar and Surawicz, 1983). Action potential duration remains constant where diastolic interval is constant, but this changes where there is a premature action potential. Action potential duration lengthens as the preceding diastolic interval becomes longer. However, in some species (e.g. rabbit) action potential duration can lengthen as diastolic interval decreases over some portions of the restitution curve (Hiraoka, and Kawano, 1987).

1.3.1 Cellular mechanisms responsible for restitution

The typical electrical restitution curve, as shown in Figure 1.1, reflects the time course over which membrane ionic currents return to their pre-stimulus values. Action potential duration depends on the inactivation of the slow inward current and activation of the outward current. Following repolarisation of a cardiac myocyte, changes in the state of individual ion channels still occurs. If another action potential is triggered prior to recovery of ionic currents its duration will be decreased because less inward current can be generated or because the outward current has not had enough time to decay.

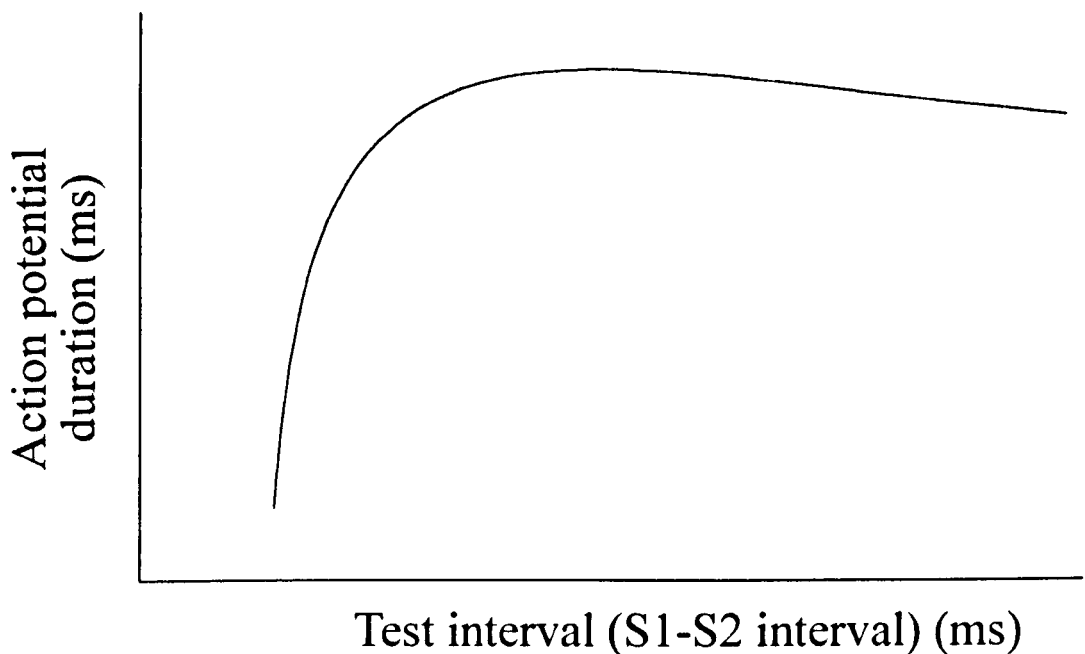


Figure 1.1 A typical electrical restitution curve. A typical electrical restitution curve. Action potential duration decreases as the preceding diastolic interval is shortened.

1.3.2 Ion accumulation

A possible mechanism for the rate dependent shortening of action potential durations is that of ion accumulation. Boyett and Jewell (1978) discussed the involvement of Ca^{2+} and K^+ , and later in 1980 the involvement of Na^+ ions in this hypothesis. Intracellular Ca^{2+} ions may accumulate at the higher stimulation rates and hence produce a shorter action potential by i) a reduction in the slow inward current or by ii) an increase in the outward current (Reuter, 1973). Shortening may also arise from extracellular accumulation of K^+ .

1.3.3 Incomplete recovery of ionic currents

Incomplete recovery of ionic currents can be a cause of rate dependent changes in action potential duration. Following each action potential, time is required for recovery from inactivation and activation of currents, namely the Na^+ current I_{Na} , a slow inward current I_{si} , transient outward current I_{to} , and time-dependent K^+ currents (see section 1.6.1). If a premature stimulus occurs prior to the recovery of these currents, less I_{Na} , I_{si} , and I_{to} and more time-dependent K^+ current will be activated. Therefore incomplete recovery will have significant consequences on action potential configuration.

Membrane potential governs the speed of recovery of ionic currents, and since recovery is slower at more positive potentials it will be after repolarisation that recovery will mainly occur. Hence recovery depends on diastolic interval (time between repolarisation of one action potential and depolarisation of the next) rather than the interval between consecutive stimuli.

1.3.4 Dispersion of restitution

By measuring restitution properties across the heart the influence of restitution heterogeneities on the substrate for re-entry (see later in introduction) could be investigated. The heterogeneity of ion channel distribution across the epicardium, between ventricles, and transmurally may be expected to produce a heterogeneity of rate dependence and restitution. Not only is there a spatial heterogeneity of rate dependence and restitution but there also exists a beat to beat variation in restitution at constant pacing rates. However, the limitations that conventional electrical recording techniques impose on multiple simultaneous recording restrict the measurement of the spatial heterogeneity of restitution in the whole heart to a few sites only. Little is known about how dispersion of restitution interacts with normal or pathological substrates to produce arrhythmias.

1.4 Intercellular coupling

1.4.1 Gap junction structure and function

In the working myocardium, adjacent myocytes are abutted onto each other, end to end, via intercalated discs. Three types of junction act in unison to make up the intercalated disc, these are the desmosome, the fascia adherens and the gap junction. The desmosome and fascia adherens are anchoring junctions and are primarily concerned with attachment between cells. Gap junctions ensure intercellular communication and electrical coupling of the cells by connecting the cytoplasmic compartments of adjacent cells. Whilst gap junctions provide an intercellular gap between adjacent plasma membranes of 2-3nm, desmosomes and fasciae adherens have a much wider intermembrane space. The small intercellular gap allows the rapid spread of excitation from one cell to the next.

The gap junction channel consists of two hexameric hemichannels, or connexons (see Figure 1.2), one provided by each myocyte. These integral membrane proteins span the full depth of the membrane and have a central channel of <2.5nm at the widest point. This channel provides a pathway for the direct exchange of nutrients, metabolites, ions and small molecules (<1kDa), described by Delmar (2000) as an 'information superhighway'. The main function of the gap junction however is to allow low resistance electrical coupling of excitable cells that is necessary for normal cardiac conduction and contractile function.

Each one of the six subunits of the connexon structure consists of one connexin molecule. In mammals connexins are part of a multigene family of at least 15 distinct proteins (Gros *et al*, 1996) of which at least 3 are expressed as different cellular subtypes of the heart; Connexin43, Connexin45 and Connexin40 (Johnson *et al*, 1999), each subtype being named by its size in kDa. The connexins of each connexon are arranged in a circular fashion with each unit protruding so as to interlock with the neighbouring connexon. Each connexin consists of four hydrophobic transmembrane domains with the N- and C- termini located on the cytoplasmic side of the membrane.

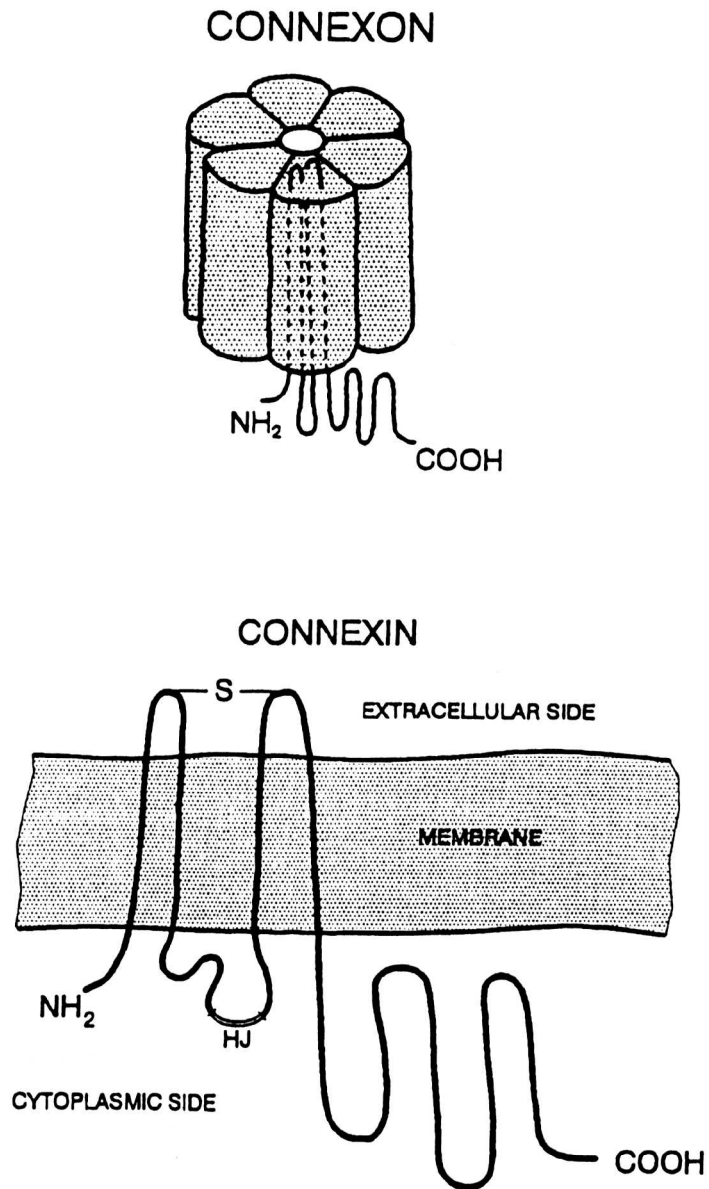


Figure 1.2 The connexon and connexin. The connexon is a hexameric structure. Each of the 6 subunits consists of a single connexin molecule. (Taken from Severs, 1994)

1.4.2 Gap junction channels and cardiac conduction

The size and distribution and the properties of the intercellular channels contribute importantly to conduction velocity and conduction patterns in the myocardium. The conductance of each of the channels that a gap junction is composed of determines the overall conductance of the gap junction. At a given potential difference across the cell membrane, the more channels between cells the more current can flow between them and the higher the conduction velocity (Jongsma, 1997). In the heart longitudinal conduction is faster than transverse conduction due to the distribution of the gap junction around the perimeter of the cell. This is an important factor in determining the pattern of impulse conduction.

1.4.3 Electrotonic interactions and gap junction uncoupling

The heart normally acts as an electrical syncytium coupled via gap junctions. Changes in intercellular coupling may predispose the heart to arrhythmias by i) slowing conduction and ii) by increasing dispersion of repolarisation and refractoriness. Myocardial ischaemia and hypertrophy further complicate the complex electrical arrangement in the heart and are associated with ventricular arrhythmias. In these conditions an increase in electrical heterogeneity in the heart can be attributed, in part, to functional or mechanical intercellular uncoupling. However, in the normal heart, electrotonic interactions between cells (which are mediated by gap junctions) act to reduce or mask the intrinsic differences in repolarisation between cells. Therefore, if gap junction coupling or gap junctional resistance are altered, an increased heterogeneity of repolarisation can be expected. This exaggerated dispersion may be arrhythmogenic.

Dhein *et al* (1999) used the gap junction uncoupler palmitoleic acid to pharmacologically intervene on gap junction coupling. They found that, using a 256 unipolar electrode array, that 20 μ M palmitoleic acid caused activation recovery intervals (ARIs) to become highly heterogeneous. They saw a dramatic 6 fold increase in the dispersion of ARIs (from 6 to 35ms). 1-Heptanol has also been used to attempt to study the effect of gap junction uncoupling in both the intact heart (Keevil *et al*, 2000) and paired myocytes (Rudisuli and Weingart, 1989; Takens-Kwak *et al*, 1992). However, the effect of 1-heptanol on dispersion of repolarisation and its possible arrhythmogenic effects were not determined.

1.5 Arrhythmias

Under normal circumstances the propagating action potential, originating at the sino-atrial node (SAN), will sequentially stimulate the atria and ventricles to contract in sequence before dying out when refractory tissue is encountered. However, under abnormal circumstances, where there is an obstacle, the propagating action potential may continue to stimulate non-refractory tissue in a self-sustained fashion thus giving rise to a re-entrant circuit. This is known to be the mechanism for several important cardiac arrhythmias. Tachyarrhythmias are a result of re-entrant excitation and have been investigated since the turn of the century.

There are three prerequisites for re-entry to occur: i) unidirectional conduction block, ii) slow conduction to permit recovery of excitable tissue and allow the re-entrant circuit to continue, and iii) a closed circuit around an anatomical or

functional obstacle. On the basis of mechanisms, re-entry may be divided into three groups: i) anatomical re-entry, ii) functional re-entry, and iii) anisotropic re-entry.

1.5.1 Unidirectional block

1.5.1.1 Due to non-uniform recovery of excitability

Differences in refractory period durations may cause impulse propagation to fail in regions with longer refractory periods. Even at fast heart rates there is a sufficient diastolic interval where excitability is normal. Therefore, such a situation as conduction block is more likely to occur in the instance of a premature stimulus. A premature stimulus facilitates re-entry as refractory period shortens as cycle length shortens and hence the pathway for impulse propagation is shortened. There is only a small degree of non-uniformity of refractory periods that is necessary to induce conduction block following a premature stimulus. Allesie *et al* (1976) measured refractory periods in isolated rabbit left atria. They found that a minimal difference of 11-16ms was necessary for unidirectional block following a premature stimulus. They also argued though, that this is not the decisive factor for the initiation of re-entry. Conduction velocity and the volume of the unidirectional block are also important. The critical timing of the premature stimulus is essential for the initiation of re-entrant arrhythmias if it occurs on the basis of temporal dispersion of recovery of excitability.

1.5.1.2 Due to geometrical factors

Unidirectional block may occur where there is a sudden increase in the cross-sectional area of interconnected cells. Re-entry may have both a functional and an anatomical basis (Pye & Cobbe, 1992). Re-entry may be functional in that

it does not occur around an anatomical obstacle but the anisotropy provided by the anatomical structure of the muscle fibres causes the re-entrant circuit to occur, and not the transmembrane properties of the myocytes. Spach *et al* (1982) showed that the anisotropy of the muscle fibre orientation might allow re-entry to occur, even in cardiac tissue with normal transmembrane properties and uniform refractoriness. They suggested that the direction of the muscle fibres is important as conduction velocity tends to be faster in the direction that the long axis of the fibres run rather than perpendicular to it, although in certain regions of the infarct border zones the reverse may be true.

1.5.1.3 Based on asymmetrical depression of conduction and excitability

Unidirectional block may also occur as a result of asymmetry in a region of depressed excitability. Experiments by Schmitt and Erlanger (1928) produced asymmetrical conduction block by localised pressure and elevated extracellular K^+ . This led to a sudden increase in the excitation threshold in one direction but a slower rise in the other, inbetween which was an inexcitable gap. In the retrograde direction, where the abrupt change was encountered, if the gap was below a critical length the impulse was transmitted, but not in the other direction where there was a gradual decrease of excitability which decreased the amplitude and driving force of the electrotonic transmission. (Kleber *et al* in: Handbook of Physiology, 2001)

1.5.2 Conduction delay

One of the conditions that can make re-entry possible is the slowing of conduction. It has been shown that zones of slow conduction present in the infarcted heart facilitate re-entry due to the extra time given for the tissue in the re-entrant circuit to regain its excitability and allow the excitation wavefront to enter again (de

Bakker *et al*, 1993). Several factors determine the velocity of the propagated action potential, but are of no concern here. A focus of conduction slowing in this introductory section is intercellular coupling resistance. Conduction depends on local current circuits, where once cell excites the next. Conduction velocity is one of the factors that is determined by coupling resistance between cells. As coupling resistance increases, conduction velocity decreases. A sizeable increase in coupling resistance is required to produce a marked decrease in conduction velocity. Tissue anisotropy caused by differences in coupling resistance perpendicular and parallel to the fibre axis can predispose to unidirectional block and re-entry.

1.5.3 Re-entry

Depending on the area of the block around which the wave is propagated, the re-entrant movement may be classified as anatomical or functional, although can be classified as both. Several factors influence re-entry. Anatomical re-entry requires a large barrier around which the wavefront circulates whilst altered electrophysiological properties allow functional and anisotropic re-entry to occur. In the case of functional re-entry, transmembrane potential properties are responsible for providing the conditions for re-entry to occur; in the case of anisotropic re-entry, microanatomy is the crucial factor. Another difference lies in anisotropic re-entry having a large excitable gap. Dispersion of refractoriness and/or non-uniform anisotropy around an infarction site may be a cause of slow conduction and unidirectional block (Vassallo *et al*, 1988).

1.5.3.1 Anatomical re-entry

Mines described the simplest model of re-entry which is illustrated in Figure 1.3 (adapted from Wit & Dillon, 1990). He was the first to suggest re-entrant excitation as a reason for arrhythmias in humans. Mines formulated criteria for the re-entrant basis of arrhythmia in 1914, and are summarised as follows:

- i) Unidirectional block must be demonstrated
- ii) There must be a circuit to allow the wavefront to return to its origin.
- iii) “The best test for circulating excitation is to cut through the ring at one point. If the impulse continues to arise in the cut ring, circus movement as a cause can be ruled out” (Mines, 1914)

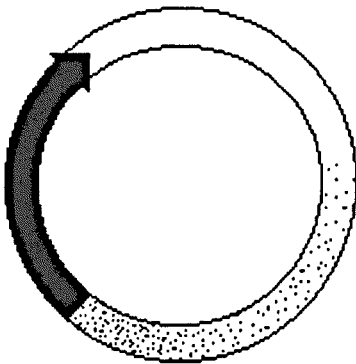


Figure 1.3 Mines model of anatomical re-entry. (Adapted from Kleber *et al* in: Handbook of Physiology, 2001). The arrow is the head of the wavefront, the black area is absolute refractory tissue, the stippled area illustrates relative refractoriness and the white area shows the excitable gap.

In this type of re-entry the wavefront propagates around an inexcitable obstacle. The length of a pathway involving an anatomical circuit is dictated by the size of the obstacle around which it travels, and the length of this pathway is fixed. An anatomical circuit has a fully excitable gap; the length of the re-entrant pathway is significantly greater than the wavelength of the re-entrant impulse (conduction velocity x effective refractory period). The time taken for an excitation wave to complete one revolution of an anatomical circuit, where there is an excitable gap, is determined by the conduction velocity. Therefore, if an impulse initiated outside the circuit can invade, via the excitable gap, the arrhythmia may be terminated. Due to the excitable gap and the stability of the circuit, propagation can be maintained for hours (Kleber *et al* in: Handbook of Physiology, 2001). Dispersion of refractoriness must be relatively large to influence conduction velocity.

In the case where the wavelength is longer than the re-entrant circuit the front of the wave is situated within its own refractory tail. In this situation there is no longer an excitable gap and external stimuli cannot penetrate in to the circuit. There is instability in the re-entrant circuit where there is an interaction between head and tail. This instability originates from two sources: a restitution dependent instability as well as one arising from the reliance of conduction velocity on the excitation interval.

1.5.3.2 Functional re-entry: The leading circle theory

Re-entry in cardiac tissue may occur in structurally intact tissue with altered functional properties such as heterogeneities of refractory period. The leading circle phenomenon of re-entry was proposed (Allessie *et al*, 1976, 1977) and explains this (Figure 1.4). They induced circuit movement in isolated rabbit atrial

tissue, where no anatomical obstacle is present, by premature stimulus. Here, the propagating impulse travels around a centre of refractory tissue, it follows the path of shortest refractory period with unidirectional block occurring in those fibres with a longer refractory period. The activation spreads in an arc around the block before merging again and re-exciting the tissue proximal to the block. The leading circle theory, as proposed by Allesie *et al* (1977), is described as “the smallest possible pathway in which the impulse continues to circulate and in which the stimulating efficacy of the wavefront is just enough to excite the tissue ahead which is still in its relative refractory period”. Dispersion of repolarisation and conduction velocity may influence the size of the circuit and hence the time taken to complete one revolution of the circuit. Due to this lack of an excitable gap, impulses initiated outside the circuit cannot easily penetrate into it. In some cases of functional re-entry there may be a large difference in refractoriness (dispersion) and therefore there is the existence of an excitable gap. In these cases, an external stimulus may penetrate the circuit and termination of the tachycardia may occur. The length of a functional circuit is variable and is determined by the electrophysiological properties of the cardiac fibres that it is composed of.

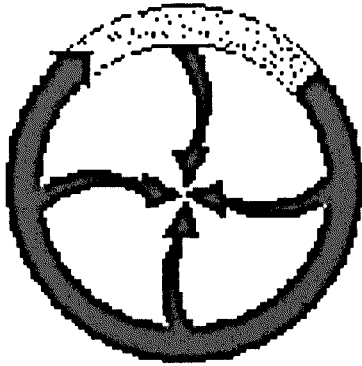


Figure 1.4 Schematic representing the leading circle theory of re-entry. The arrows represent the crest of the circulating wavefront. Black areas show areas of absolute refractoriness, dotted areas relative refractoriness.

The border zone of infarcted tissue may provide the ideal setting in which re-entrant arrhythmias can occur. Fibrosed tissue in the peri-infarct area may cause a loss of cellular electrical coupling resulting in slow conduction or unidirectional block and dispersion of refractoriness which may predispose to re-entry (Kurz *et al*, 1993). Hypertrophied, non-infarcted, myocardium that is remote from the infarcted tissue also has altered electrophysiological characteristics. Heterogeneity of refractoriness in the tissue remote from the infarct may be involved in the degeneration of VT to VF (Ramdat Misier *et al*, 1995).

1.5.3.3 Anisotropic re-entry

In the absence of an anatomical obstacle, unidirectional block may arise as a result of non-uniform recovery of excitability (dispersion of repolarisation), differences in conduction velocity as a result of altered cellular connections, or depression of electrophysiological properties. The conduction of impulses moving through a volume of myocardium with regional differences in refractoriness may fail where

there is a long refractory period. This form of re-entry, termed anisotropic re-entry, also demonstrates an excitable gap.

1.6 The action potential

1.6.1 The ionic basis of the action potential

The action potential consists of 5 phases as illustrated below in Figure 1.5: phase 4, the resting membrane potential; phase 0, rapid depolarisation/upstroke; phase 1, early repolarisation; phase 2, the plateau and; phase 3, final repolarisation. Each phase is determined by different ionic fluxes across the cell membrane and are described as follows.

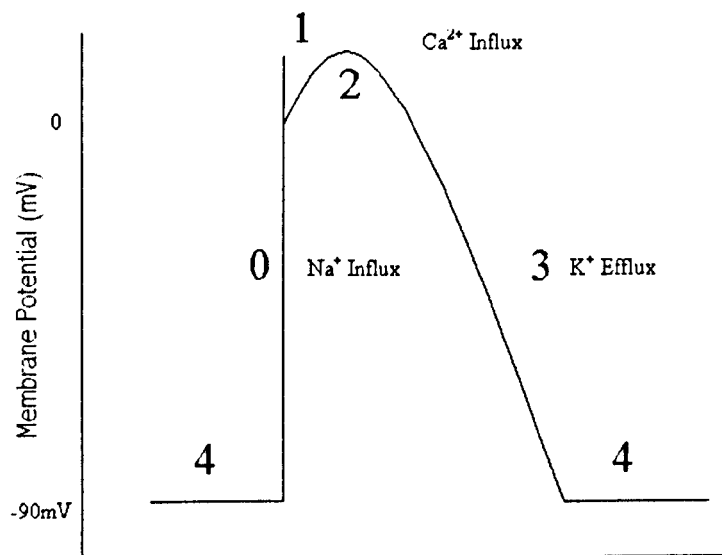


Figure 1.5 Phases of the action potential and indication of the ionic influxes involved.

1.6.1.1 Resting potential (Phase 4)

Phase 4, or the resting membrane potential, is due mainly to the high intracellular K^+ concentration and the high permeability of the sarcolemma to these ions. Although there is a tendency for the K^+ ions to move out of the cell down a concentration gradient, the negative intracellular ions are unable to accompany them. There is a separation of charge across the sarcolemma and the interior of the cell becomes negative with respect to the exterior. The intracellular K^+ concentration remains high and the Na^+ concentration low due to the electrogenic Na^+-K^+ ATPase pump (3 Na^+ out for 2 K^+ in) that operates at the sarcolemma. Background currents involved in phase 4 of the action potential include an inwardly directed Na^+ current, I_b , and an outwardly directed K^+ current, I_{KI} . This movement of ions across the cell membrane determines the resting membrane potential of the myocyte, which in the ventricles is between -80 and -90mV and is stable until stimulated to contract.

1.6.1.2 Action potential upstroke (Phase 0)

In ventricular myocytes the action potential upstroke, phase 0, is very rapid with a large V_{max} . The main current involved in this phase is the fast inward Na^+ current (I_{Na}) which lasts for approximately 1-2ms. When the membrane potential reaches between -70mV to -60mV, the membrane ionic conductances suddenly change and there is a rapid influx of Na^+ through the fast channels. This produces a regenerative depolarisation that activates the slow inward Ca^{2+} current, I_{si} or I_{Ca} , through which the membrane is depolarised to between +30 and +40mV. Thus towards the latter part of phase 0, current flows through fast and slow type channels. Two types of inward Ca^{2+} current are also involved in this phase; the

slow or L-type current and the fast or T-type current. The L-type Ca^{2+} channel begins to open in phase 0 when the membrane voltage approaches -40mV .

1.6.1.3 Phase 1

During phase 1 of the action potential, I_{Na} is inactivated and a transient outward current (I_{to}) is activated which facilitates the rapid repolarisation of the membrane to near 0mV . I_{to} is a current carried mainly by K^+ and shows voltage dependent activation and inactivation (Antzelevitch *et al*, 1991). Two subtypes of I_{to} have been described in the rabbit left ventricle; a slow component I_{to1} , and a fast component I_{to2} (Fedida and Giles, 1991). I_{to} is an important repolarising current that can influence action potential duration and configuration by interacting with the inward Ca^{2+} current, I_{Ca} . Another transient outward current that is activated during the plateau phase of the action potential is the Ca^{2+} -activated K^+ current, $I_{\text{K(Ca)}}$. Since this current is activated by intracellular Ca^{2+} there is an overlap with the slow inward current. A slight Cl^- influx and a Na^+ - K^+ exchanger pump (3Na^+ out for 2K^+ in) also contribute to the earlier phases of repolarisation.

1.6.1.4 The Plateau (Phase 2)

Phase 2 of the action potential is a long plateau mediated by a balance between an outwardly directed K^+ current (I_{Kl}), an inward Ca^{2+} current (I_{Ca}), and an inward slow inactivating Na^+ current. It is thought that 2 subtypes of I_{K} exist: a slow, (I_{Ks}) and a fast (I_{Kr}) component. The Ca^{2+} channels are voltage-gated channels that are activated during phase 0 when the membrane potential reaches approximately -40mV . This current is responsible for the Ca^{2+} induced Ca^{2+} release (CICR) via

the ryanodine receptor in the sarcoplasmic reticulum that initiates contraction of the myocyte (see E-C coupling).

During phase 2 Na^+ conductance is low due to Na^+ channel inactivation. A Na^+ - Ca^{2+} ($I_{\text{Na-Ca}}$) exchanger current (3Na^+ in for 1Ca^{2+} out) sustains the late plateau phase and removes intracellular cytoplasmic Ca^{2+} . $I_{\text{Na-Ca}}$ can operate in either an outward or an inward direction depending on the membrane potential and Na^+ and Ca^{2+} concentrations (Coraboeuf and Nargeot, 1993). During plateau potentials the Na^+ - Ca^{2+} exchanger operates in reverse mode to pump Ca^{2+} in and Na^+ out. The balance between the movement of ions across the cell membrane during the plateau phase maintains the membrane potential at around 0mV for up to several hundred milliseconds.

1.6.1.5 Repolarisation (Phase 3)

Repolarisation occurs rapidly during phase 3 of the action potential, this is due to the increase in K^+ conductance and the inactivation of the Ca^{2+} channels. In ventricular myocytes several types of K^+ are involved in repolarisation of the action potential. These are the inward rectifier (I_{K1}); the delayed rectifier (I_{K}); the transient outward current (I_{to}); and possibly the plateau current (I_{Kp}) (Luo and Rudy, 1991). At a membrane potential of approximately -50mV the fast Na^+ channels are closed from an inactive state and hence the myocyte is excitable again, although a larger than normal stimulus is required to produce a smaller than usual action potential. Figure 1.6 (Bers, 2001) illustrates the basic membrane conductances to individual components of the action potential.

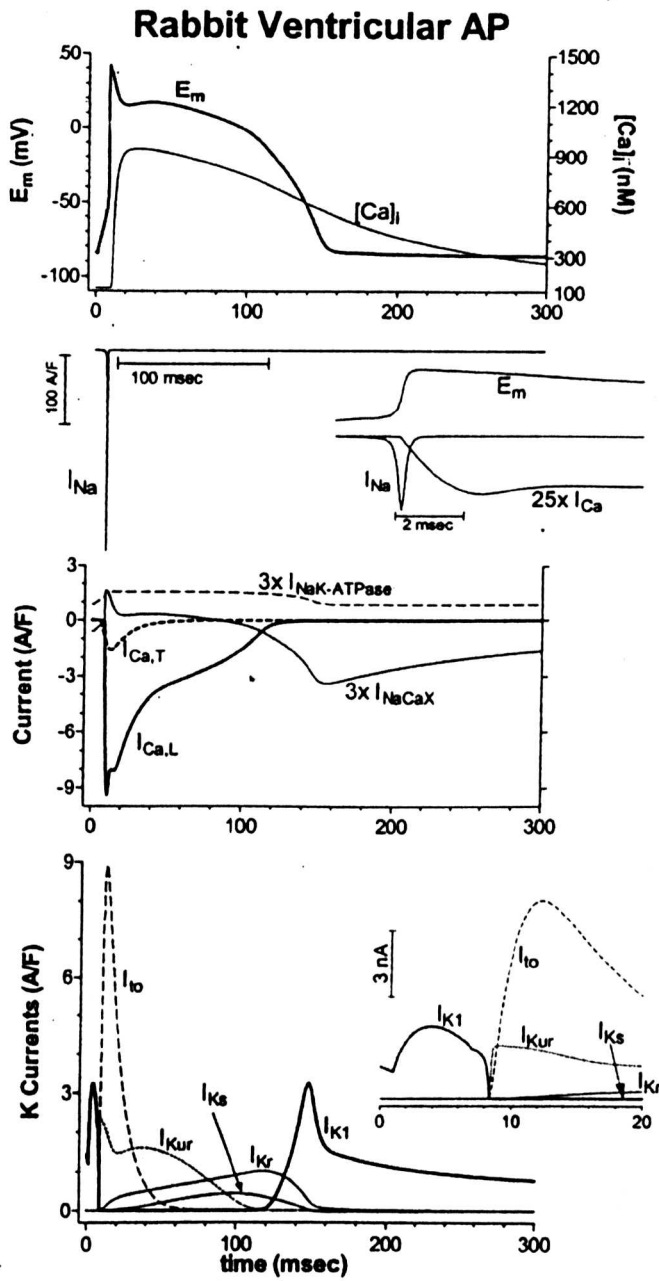


Figure 1.6 Membrane conductance to Na^+ , Ca^{2+} and K^+ during a rabbit cardiac action potential (taken directly from Bers, 2001).

1.6.2 Refractory periods

Periods of refractoriness are essential to the action potential to ensure that the heart has enough time to refill prior to the next contraction. If a cell is excited by a stimulus at some time and another stimulus arrives before the cell returns to rest, the second stimulus may elicit no response at all. If the second stimulus is delayed slightly, it may elicit a reduced or "graded" response. If the strength of the second stimulus is sufficient, and the onset is delayed enough, it may elicit another full action potential, in which case we say it has come during the relative refractory period (RRP).

Figure 1.7 illustrates these refractory periods. During the absolute refractory period (ARP) the myocardium is completely inexcitable and stimulation is ineffective. The effective refractory period (ERP) includes the ARP but extends into a period where the myocardium may be stimulated but an action potential is not propagated. During the RRP the myocardium may be stimulated but the propagated action potential is weaker than normal and thus moves slower. The supernormal (SNP) period is a hyper-excitable time period. The actual full recovery time is indicated in Figure 1.7 as FRT as is the time when a full 'normal' action potential can be produced again.

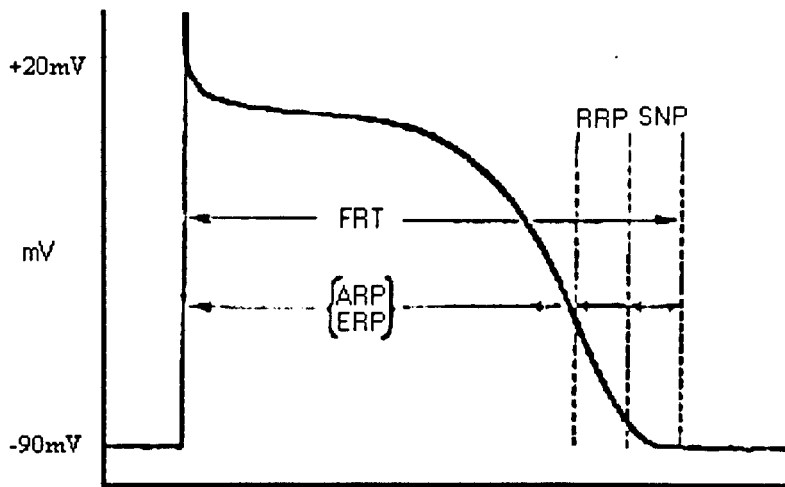


Figure 1.7 Refractory periods of the MAP.

1.6.2.1 Measuring refractoriness

Refractory periods can be measured and used to determine the minimum length of a re-entrant circuit that may lead to the introduction of a ventricular arrhythmia (Burton & Cobbe, 1998). Refractory periods may be determined directly using the premature extrastimulus technique. This is the most common and conventional method used to map refractoriness. The heart is paced at a basic cycle length (S_1) and a premature extrastimulus (S_2) is applied at an interval S_1 - S_2 . The S_1 - S_2 interval is decreased until the refractory period is found. If multiple sites are to be mapped, this may be a time consuming process as varying intervals must be tested separately at each recording site. It must also be assumed that the refractory period at one site does not alter whilst the other measurements are made. The problems associated with multiple site recording using a limited number of electrodes prompted the introduction of multi-site simultaneous recordings.

Ventricular fibrillation intervals (VFIs) can be used as an indirect measurement of refractoriness at multiple sites (Burton *et al*, 1998). When a heart is in VF cells

become re-excited as soon as they have recovered from the previous excitation, the time interval between these activations is the VFI. VFI has been closely correlated with the action potential and ERP durations (Surawicz, 1997; Ramdat Misier *et al*, 1995). Providing a train of extrastimuli at progressively increasing current stimulus induces VF. The details of this method are described in the relevant methods sections of individual results chapters.

Simultaneous multiple recordings of monophasic action potentials (MAPs) provide an indirect measurement of refractoriness. MAPs reliably reproduce the repolarisation time course of the transmembrane action potential, and are described in detail in chapter 3. MAP recording can also be used as an index of refractoriness provided that the APD/ERP relationship is constant, i.e. there is no post-repolarisation refractoriness. Kuo *et al* (1983), in studies on the arrhythmogenic role of dispersion of repolarisation, used suction electrodes to simultaneously record MAPs from six sites in the open chested dog. Behrens *et al* (1997) simultaneously recorded ten MAPs from the epicardial and endocardial surfaces of the Langendorff-perfused rabbit heart using the Franz contact MAP catheter (refer to chapter 3) mounted on a spring mechanism to help eradicate motion artefacts. However, even in experienced hands, the number of simultaneous recordings that can be made is limited. Although not MAP recording, a non-invasive method of recording myocardial electrical activity at multiple sites was made by Burton and Cobbe in 1998. They used a flexible epicardial array containing multiple unipolar electrodes to simultaneously record up to 240 unipolar electrograms from the epicardial surface of the left ventricle.

Intracellular microelectrodes (refer to chapter 3) adequately measure action potential durations and repolarisation but are unsuitable for multiple recordings due to the technical difficulty in maintaining more than one impalement. The limitations of the intracellular and suction electrode methods for multiple site recordings prompted the introduction of optically recording electrical activity using voltage sensitive dyes (refer to chapter 3).

1.7 Excitation-contraction coupling and Ca²⁺ handling

Cardiac myocytes are single contractile units within the heart which under normal circumstances act as a syncytium to allow the heart to perform efficiently in helping to pump blood through the body. Excitation-contraction coupling (E-C coupling) is initiated by the depolarisation of the sarcolemma by an action potential. The arrival of the action potential at the sarcolemmal membrane causes a transient increase in the sarcoplasmic Ca²⁺ concentration that subsequently activates contractile proteins resulting in contraction of the cardiac myocyte. The part that the action potential plays in E-C coupling has been described (see above). The following section of this introduction will concentrate on the role that Ca²⁺ plays in cardiac contraction. Refer to Figure 1.8 for details.

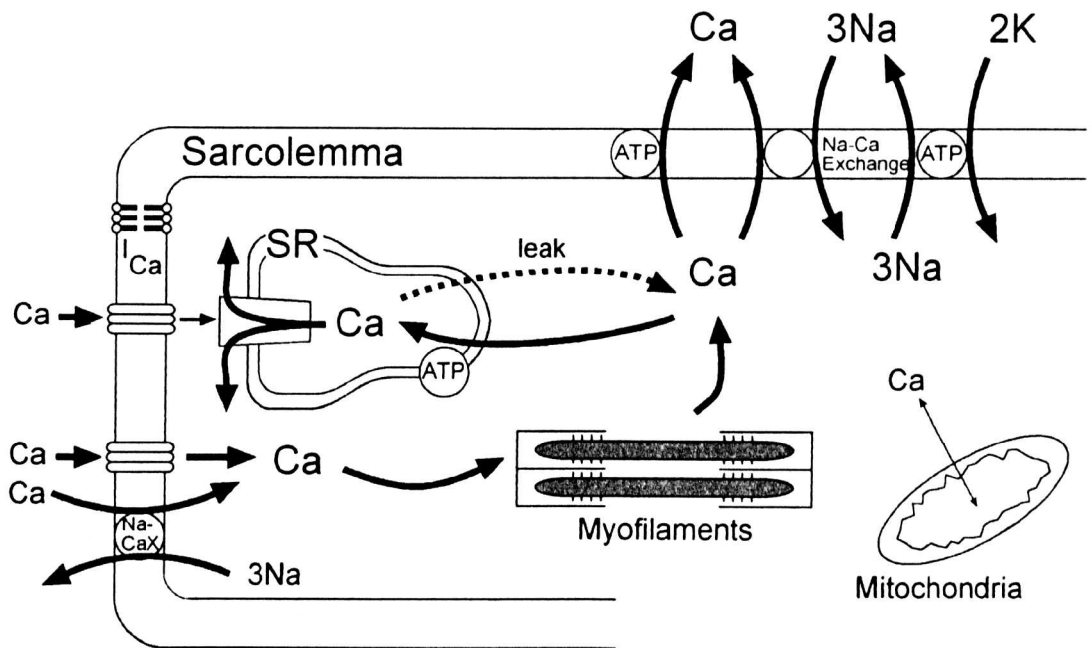


Figure 1.8 Excitation-contraction coupling. Schematic of Ca^{2+} handling within a single cardiac myocyte. Adapted from Bers, 1993.

The action potential is propagated along the sarcolemma and into the cell along the T-tubules. T-tubules are invaginations of the sarcolemma that run in to the cell interior. Within the cell, junctional sarcoplasmic reticulum (SR) lies in close proximity to the sarcolemma or the T-tubules. The SR is the main Ca^{2+} store within the myocyte. The SR contains Ca^{2+} release channels (ryanodine receptors) which are in the closed state during diastole and hence when diastolic cytoplasmic Ca^{2+} is low ($\sim 100\text{nM}$) the Ca^{2+} does not bind to the Ca^{2+} binding sites associated with the contractile apparatus (myofibrils – see below). As the action potential travels along the T-tubule I_{Ca} causes a small rise in the intracellular Ca^{2+} concentration. This small influx of Ca^{2+} activates the ryanodine receptors which causes the release of a large quantity of stored Ca^{2+} from the SR in to the cytoplasm to occur – a process known as Ca^{2+} induced Ca^{2+} release (CICR).

The myocyte contains contractile apparatus called myofibrils. Each myofibril is composed of smaller units called sarcomeres that are joined end to end. This gives the myocyte a striated appearance. The sarcomere contains thick (myosin) and thin (actin) filaments that interdigitate. Actin comprises a double helix of F-actin and G-actin. Embedded in this helix are 2 proteins – tropomyosin (closely associated with actin) and troponin (binds to the tropomyosin). Troponin has 3 distinct subunits: troponin-T links to tropomyosin; troponin-C has a high affinity for Ca^{2+} ; and troponin-I interacts with the actin. At rest the troponin/tropomyosin complex inhibits the binding of actin to myosin. When calcium is released from the SR it binds to Troponin-C producing a configurational change in the troponin unit. Because troponin is tightly bound to tropomyosin, this results in a secondary configurational change in tropomyosin. This permits formation of the actomyosin complex and capacity for developing tension. Tropomyosin exerts its inhibitory effect to reduce tension when Ca^{2+} is reduced.

The interaction of these contractile proteins, which induces a sliding mechanism which is activated by Ca^{2+} and causes the cell to contract, is a process known as cross bridge cycling. This mechanism was termed the sliding filament theory by Huxley in 1969. Ca^{2+} released from the SR raises the cytoplasmic Ca^{2+} concentration, Ca^{2+} diffuses the short distance in to the sarcomere, and the cell develops tension. Ca^{2+} enters the cell during the action potential via the L-type Ca^{2+} channels and also via the Na^+ - Ca^{2+} exchanger working in reverse. During systole the Ca^{2+} concentration is raised to $\sim 1\mu\text{M}$. Following contraction Ca^{2+} must be extruded from the cytoplasm in order to return the Ca^{2+} concentration to diastolic levels.

1.7.1 Intracellular Ca^{2+} removal

There are 4 main mechanisms which aid in the removal of Ca^{2+} from the cytoplasm: the SR Ca^{2+} -ATPase pump (SERCA); the sarcolemmal Na^+ - Ca^{2+} exchanger; the sarcolemmal Ca^{2+} ATPase, and; the mitochondrial Ca^{2+} uniporter. SERCA and the sarcolemmal Na^+ - Ca^{2+} exchanger are the 2 dominant Ca^{2+} removal mechanisms.

SERCA

The released Ca^{2+} ions are pumped back in to the SR by ATP-dependent Ca^{2+} pumps which are located in the network SR. Regulation of SERCA depends on the phosphorylation state of another protein, phospholamban (PLB). Dephosphorylation of PLB inhibits the pump, whilst in its phosphorylated state SERCA is activated.

SARCOLEMMAL Na^+ - Ca^{2+} EXCHANGER

Depending on the membrane potential and the intracellular and extracellular Na^+ and Ca^{2+} concentrations, the Na^+ - Ca^{2+} exchanger can also function in reverse. The exchanger is an electrogenic pump, so for every 3 Na^+ it pumps in, 1 Ca^{2+} is pumped out.

SARCOLEMMAL Ca^{2+} ATPase

The sarcolemmal Ca^{2+} ATPase pumps 1 Ca^{2+} out for each ATP molecule that is hydrolysed.

1.7.2 Contraction-excitation feedback

Contraction-excitation feedback, or mechanoelectrical feedback, is the reverse scenario of excitation-contraction coupling. Contraction-excitation coupling describes the process by which mechanical stress or strain produces changes in membrane potential, either as a change in action potential duration or as a transient depolarisation (Lab, 1982).

Chapter 2 - General methods

2.1 Langendorff perfusion of whole hearts

2.1.1 The perfusion system

Before the experiments, a modified Krebs-Henseleit buffer solution, of the following composition (mM): 120.9 NaCl, 2.8 KCl, 2.5 CaCl₂, 1.5 MgSO₄, 1.5 KH₂PO₄, 24.8 NaHCO₃, 11 glucose, 2.0 sodium pyruvate was pumped through the perfusion system to prime it. Figure 2.1 shows a detailed diagram of the Langendorff perfusion system. The pH of the solution was maintained at 7.4 by continuously bubbling with a 95% O₂ / 5% CO₂ mixture. A 2-way tap incorporated into the perfusion lines allows the rapid changing of solutions that is needed in some protocols. Specific variations of the general methods and protocols involving solution changes and/or stimulus regimes are discussed in the relevant chapters.

A cellulose nitrate membrane filter (5µm) (Whatman International Ltd, UK) was incorporated in to the perfusion system to ensure the removal of contaminant particles in the saline solution and tubing. This was renewed prior to each experiment. A heated water bath was used to supply warm water to glass water-jackets. One coiled water jacket heated the perfusion solution; another maintained the temperature of the atmosphere surrounding the heart. The coiled water jacket warmed the perfusion solution immediately prior to it descending the tubing in to the cannula and heart. The water jacket encompassing the heart directly warmed the atmosphere surrounding the heart. Therefore, a constant temperature of 37°C was maintained.

Small air bubbles that form in the plastic down-tube that feeds into the stainless steel aortic cannula coalesce to produce larger bubbles. If this spans the width of

the tubing it may descend through the tubing and enter the heart via the aorta causing an air embolus. Therefore, the system was continually observed for the formation of bubbles. This air formation is due to the cooling properties of liquid where gas becomes less soluble in the cooler solution, and hence comes out of solution. Air emboli can block blood vessels within the heart thereby stopping blood flow and causing regional ischaemia. Figure 2.1 illustrates the Langendorff perfusion system.

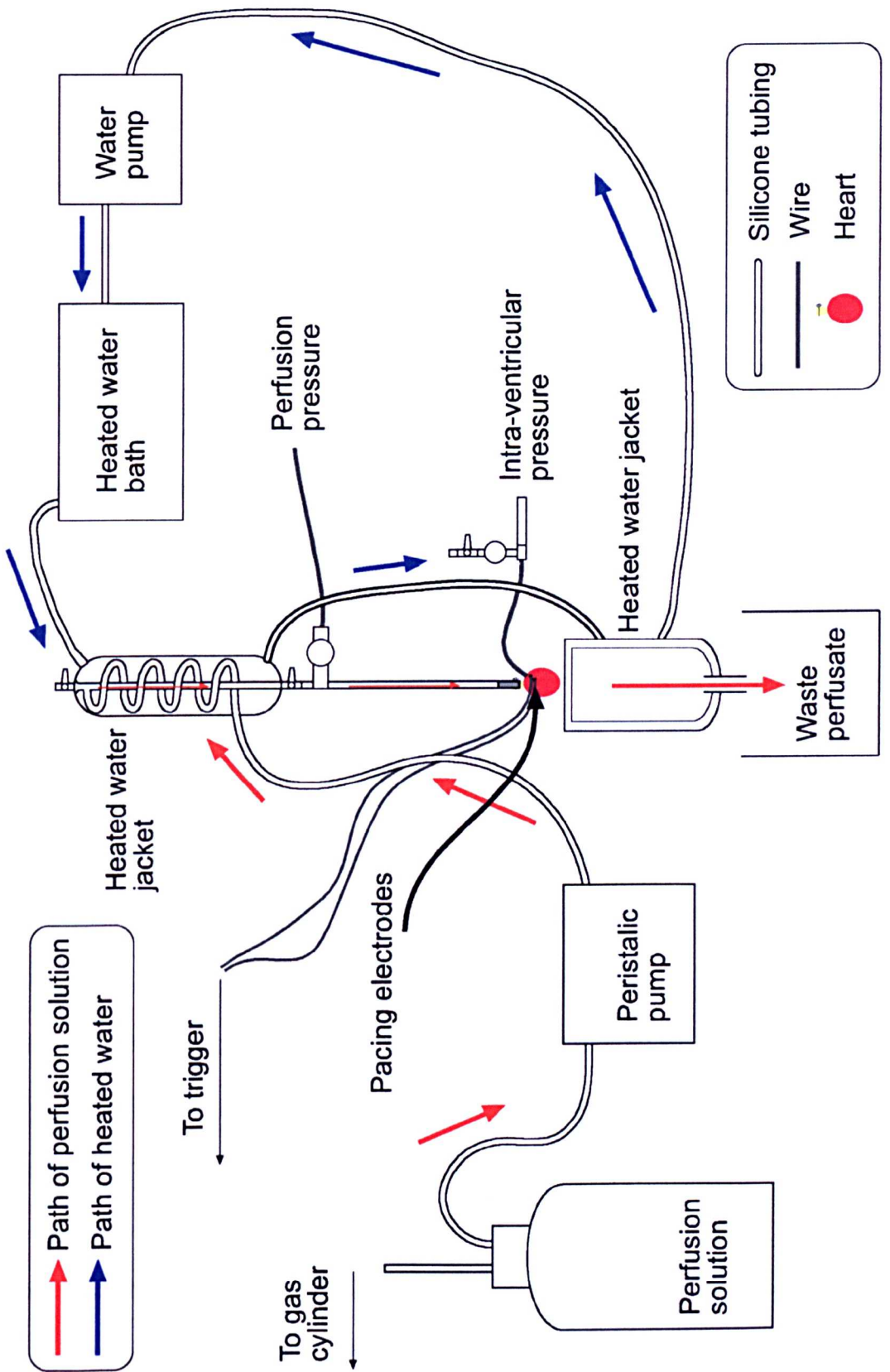


Figure 2.1 The Langendorff perfusion system.

2.1.2 Experimental procedure

2.1.2.1 The infarct model of heart failure

A rabbit coronary artery ligation model of heart failure/left ventricular dysfunction was used for some parts of this study. The rabbit coronary artery ligation model of heart failure produces heart failure as a result of left ventricular dysfunction following myocardial infarction. Coronary ligation causes eccentric hypertrophy leading to increased left ventricular dimension. It also causes a significant increase in myocyte length and a non-significant increase in myocyte diameter (McIntosh *et al*, 2000). Heart failure causes manifestations such as liver and lung congestion and heart and liver enlargement.

Before sacrifice all animals had echocardiography done to assess the degree of left ventricular dysfunction produced by the procedure. End diastolic left ventricular diameter and ejection fraction were measured. This model was developed by Dr. M. Pye and Prof. S. Cobbe in the Department of Cardiology, Glasgow Royal Infirmary. Surgery was performed by technicians at the animal house at the Infirmary. Briefly, the procedure is as follows. Anaesthesia was induced using Hypnorm and maintained with halothane and nitrous oxide/oxygen prior to performing a left thoracotomy. The left anterior descending coronary artery was ligated to produce an ischaemic area approximately 1/3 the size of the left ventricle. Post-operative analgesia was administered and the animals monitored. Heart failure was allowed to develop for 8 weeks prior to sacrifice for experiment. Sham-operated animals underwent the same operation as the failure animals but without coronary artery ligation. These animals were also allowed 8 weeks prior to sacrifice for experiment.

2.1.2.2 Heart preparation and experimental set-up

Sham-operated and coronary-ligated animals were sacrificed by intravenous administration of sodium pentobarbitone (100mg/kg) with 1000 IU heparin into the left marginal ear vein. The absence of corneal and limb withdrawal reflexes were checked prior to making the initial transverse subcostal incision into the abdomen. The diaphragm was cut, and lateral incisions made along both sides of the rib cage to expose the heart and lungs. With fingers carefully placed behind the heart to protect the atria, the trachea and blood vessels supplying the heart were cut. Care was taken to ensure that a reasonable length of aorta was preserved to allow later cannulation. The heart was then placed into a beaker of ice cold saline solution. The transfer to cold solution is made to stop contraction and reduce metabolic rate.

Two pairs of small, serrated, tipped forceps were used to pick the heart up by the aorta and slip it over the cannula on the down tube of the perfusion apparatus. The down tube is a short piece of silicon tubing that descends from the heated water jacket and joins on to a small steel tube, the cannula. An arterial clip held the heart in place whilst a silk ligature was tied around the aorta. A fine groove lathed in to the stainless steel cannula prevented the ligature from slipping. The flow rate was increased to give a constant perfusion rate of 40ml/min by a peristaltic pump (Gilson Minipuls 3). The time taken from removal of the heart (and asystole) to artificial reperfusion with saline solution was usually less than 2 minutes. Once the heart was mounted on the apparatus a small incision was made in the pulmonary artery to allow the perfusion solution to flow freely. The heart then began to beat as coronary vessels were flushed of blood. Fatty and fibrous tissue was then removed.

Next, a latex water filled balloon was inserted in to the left ventricle (LV) via the left atrium (LA) and secured with a silk ligature. A pressure transducer monitored the left ventricular developed pressure (LVDP). The balloon was initially empty, but was inflated after insertion to fill the cavity of the left ventricle. Balloon inflation was adjusted to give a zero end-diastolic pressure. The volume of the balloon could be set either manually or with a computer-controlled linear motor driven pump. A second pressure transducer, situated at the top of the down pipe, was used to measure the perfusion pressure. An increase in perfusion pressure might indicate a block in the coronary vessels either by air, blood clot or debris. Perfusion pressure, peak-systolic and end-diastolic pressures were used to monitor the condition of the heart throughout the experiment.

Many experiments in this study involved pacing the heart over a range of cycle lengths (typically between 150ms and 1250ms). To obtain this large range in CL the intrinsic heart rate had to be reduced. The intrinsic heart rate of the rabbit is normally 180 beats/minute (CL=350ms), therefore the heart can normally be paced faster than intrinsic, but not slower. Therefore, the entire right atrium (RA) was dissected away from the whole heart. This procedure removed the sinoatrial node (SAN) and hence the heart's primary pacemaker. The exact location of the atrioventricular node (AVN) could often be discerned by a short period of asystole that occurred when light pressure was applied to the correct region of the interventricular septum. The AVN was located using a pair of fine tipped forceps. A small amount (<0.05ml) of 5% formaldehyde was injected locally over several applications. Usually this slowed the heart rate considerably, although sometimes further action needed to be taken which involved stabbing the AVN region with the syringe, or pinching the AVN region with fine tipped forceps. Often it was only

necessary to give the AVN region a small pinch, this omitted the requirement of an injection of formaldehyde. It was an unusual occurrence that this procedure did not work. However, occasionally it was not possible to slow heart rate by these methods. It was important to not compromise the condition of the heart by over damage through ablation.

A pair of platinum pacing electrodes was hooked into the base of the right ventricle (RV). Stimulation voltage was adjusted to twice diastolic threshold. A Digitimer DS2 stimulator was used to provide constant voltage pulse with a width of 2ms. Timing of the pulse was controlled with a PC running a locally developed program.

2.1.3 Electrical recording

Figure 2.2 shows a schematic diagram of the electrical equipment used in whole heart experiments. MAPs, perfusion pressure and intraventricular pressure were displayed on, and a paper record produced, by a chart recorder (Gould Electronics, Ohio, USA.). Single channel MAPs were displayed on an oscilloscope (Nicolet Instrument Corporation, Wisconsin, USA.). MAPs were recorded from the epicardial surface of the LV via contact electrodes that were connected to a 32 channel custom-built MAP amplifier (Dr. Mark Watts, Glasgow Royal Infirmary). The signals were digitised by a multichannel analogue-to-digital board (National Instruments Corporation (UK) Ltd). All 32 channels could be displayed simultaneously on the computer screen in real time. Data were stored on computer disc for analysis. Data acquisition was via a custom made computer program (Dr. Francis Burton, University of Glasgow).

The heart was stimulated via bipolar pacing electrodes that were driven by a computer system to allow customised pacing protocols to be used. One particular pacing protocol (refer to specific methods sections of results chapters) was used to induce VF via a catheter inserted in to the right ventricle. The catheter was connected to a stimulator (Digitimer, UK) which allowed increasing current pulses to be applied to the heart. This stimulator was different to the afore mentioned one that delivered a voltage pulse. The VF induction stimulator supplies a constant current pulse.

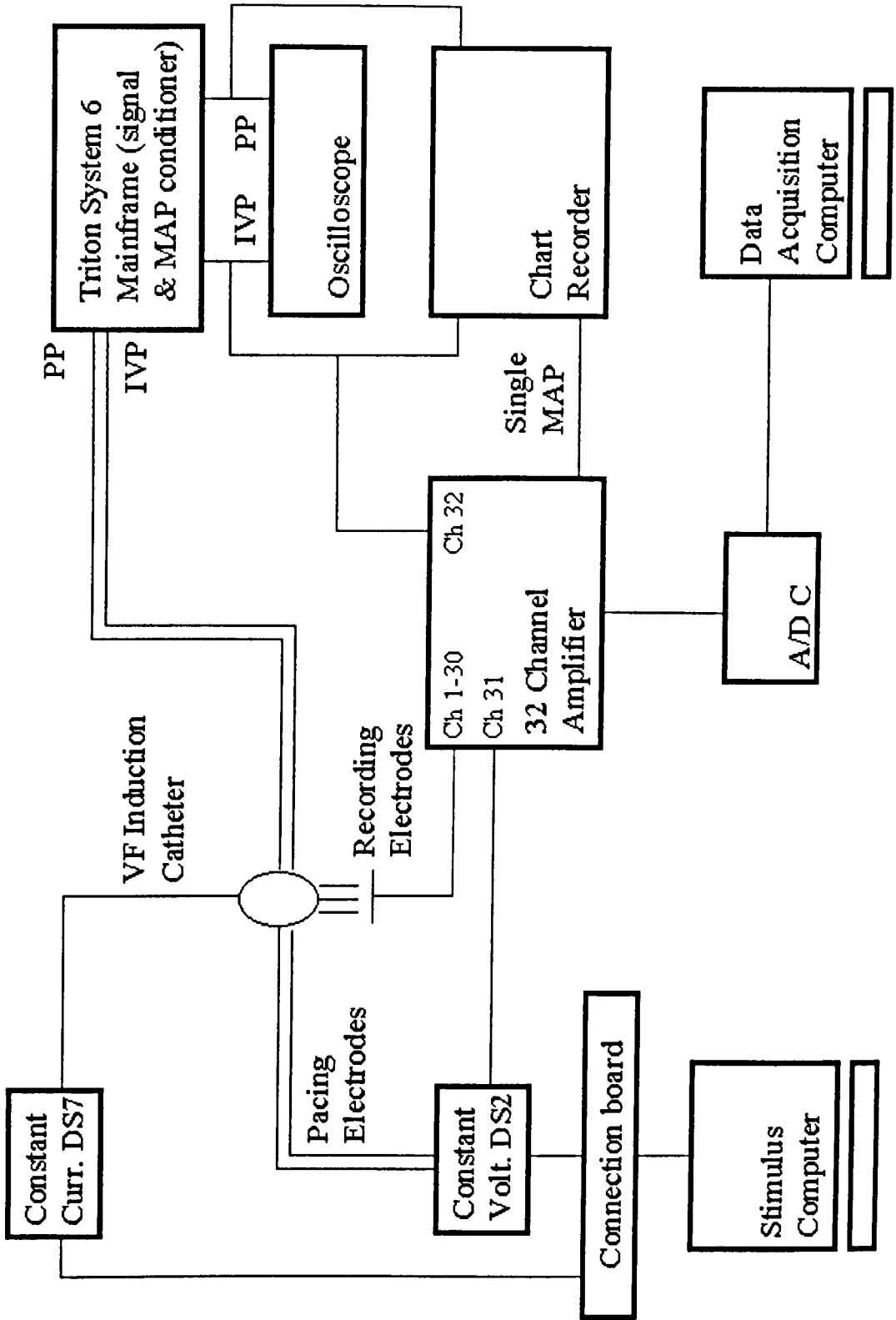


Figure 2.2 A schematic of the electrical set-up used for stimulation and recording during whole heart Langendorff perfused experiments.

2.1.4 MAP analysis

MAPs were analysed off line using a computer program developed locally. This allowed semi-automated analysis of up to 32 channels of MAP signals. Measurements extracted included: MAP duration at 50% and 90% repolarisation (MAPD₅₀ and MAPD₉₀ respectively), conduction delay (time from stimulus artefact to MAP upstroke) and MAP amplitude,. Figure 2.3 illustrates these parameters diagrammatically.

The MAP amplitude is measured from the baseline (the resting membrane potential, RMP) to the crest of the MAP plateau. The peak of the upstroke (or ‘overshoot’) is an intrinsic deflection indicative of the time at which the excitation wavefront passes underneath the electrode. MAP upstroke may be used to define and characterise local electrical activity (Levine *et al*, 1986).

MAP duration is the time from onset of Phase 1 to return to the RMP. The time to 100% repolarisation (second derivative d^2V/dt^2) is not commonly used as a measure of repolarisation although Efimov *et al* (1994) used this measure of repolarisation and obtained accurate data. Using the second derivative amplifies noise, making measurement of repolarisation inaccurate. MAPD₉₀ is the most commonly used point to provide information regarding repolarisation of the MAP and is generally the accepted level for analysis as it is so ubiquitously used. MAPD₅₀ is also used as changes in this can be indicative of ischaemia.

In this study, agents were used that affected conduction delay. Conduction delay was measured as the period of time between stimulus artefact and maximum

upstroke (V_{max}), i.e. the time taken for the wavefront to move from the point of stimulus to under the electrode(s).

Table 1.1 (taken directly from Franz, 1999) outlines the criteria set to describe a good quality MAP.

-
1. MAP amplitude (baseline to plateau crest) not <10mV
 2. Fast, clean upstroke (rise time not longer than 5ms)
 3. No major contamination by intrinsic deflection or QRS
 4. Smooth, upwardly convex plateau
 5. Horizontal diastolic baseline (no undershoot during mechanical diastole, and no upsloping potential for remainder of diastole)
 6. MAP wave forms closely similar during normal and ectopic activation sequence
-

Table 2.1 Criteria for an optimum quality monophasic action potential.

The quality of MAPs obtained in this study is considered, for several different methods of MAP recording, in chapter 3.

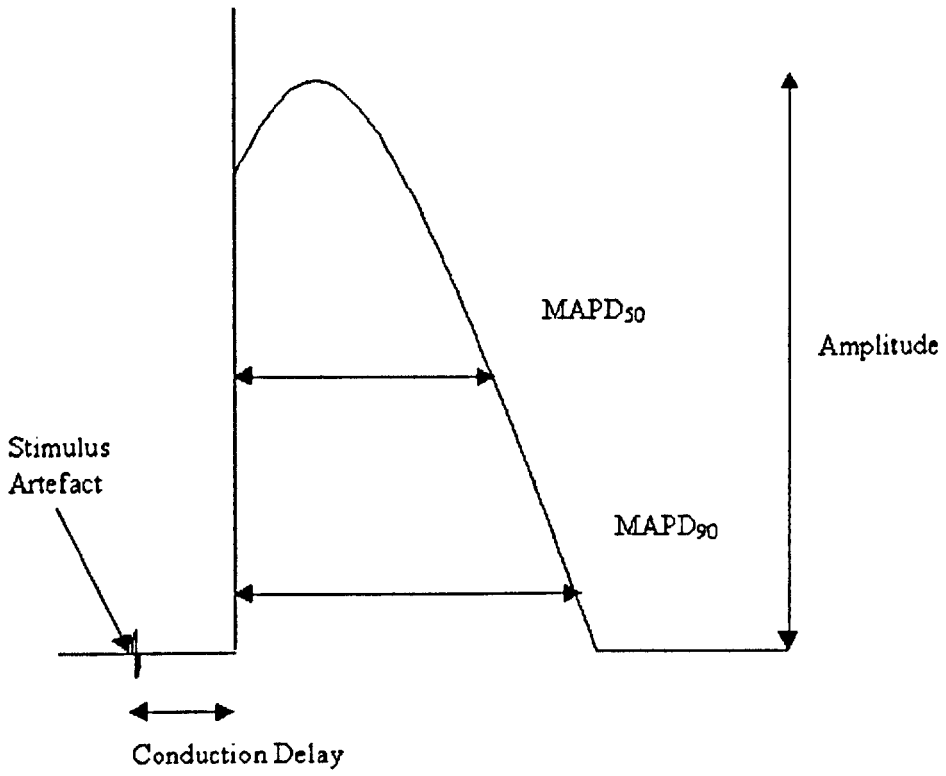


Figure 2.3 Illustrative MAP showing analysis parameters.

2.2 Single cell preparation

2.2.1 Single cell dissociation

Single left ventricular epicardial myocytes for fractional cell shortening and Ca^{2+} handling measurements were obtained using a different Langendorff perfusion system to that described for whole heart electrophysiology experiments.

Prior to cannulation of the heart, de-ionised water was perfused through the system to cleanse it. Base Krebs solution of the following composition (mM): 120 NaCl, 20.0 Hepes, 5.4 KCl, 0.56 NaH_2PO_4 , 3.5 $\text{MgCl}_2 \cdot 6\text{H}_2\text{O}$, 20.0 Taurine, 10.0 Creatine, 11.1 Glucose, was heated to 37°C . Two small beakers of Base Krebs were placed in the freezer to cool ready for the heart dissection. Base Krebs solution containing 0.075, 0.125, 0.25, 0.5 and a 1.0mM CaCl_2 and 1% Bovine Serum Albumin (BSA) solution were made. These were also heated to 37°C .

The dissection of the heart was performed as described for the whole heart electrophysiology experiments. On removal, the heart was placed in the pre-chilled Krebs solution and fatty and fibrous tissue quickly removed. The heart was cannulated on the Langendorff apparatus and perfused with Base Krebs and then a protease (0.0004%)/collagenase (0.07%) enzyme solution. After 1 minute the enzyme was collected and re-circulated. Approximately 2-3 minutes in to the digestion time CaCl_2 was added to the re-circulating enzyme to make a $46.67\mu\text{M}$ solution. After approximately 9-10 minutes (dependent on the size of the heart) perfusion was switched to a low Ca^{2+} (0.075 mM)/BSA solution.

The atria and right ventricle were removed and discarded. The epicardial layer of the left ventricle, which comprises approximately the top 1mm of the myocardium, was dissected away from the left ventricle. The section was finely cut and placed in low Ca^{2+} (0.125mM)/BSA solution (further referred to as (concentration) CaCl_2 solution). The preparation was then shaken at 37°C in a heated water bath for 60 minutes. After this time the supernatant from the preparation, containing single cardiac myocytes, was decanted in to a centrifuge tube which was then gently spun. The supernatant resulting from the spin was then discarded and the cells re-suspended in 0.25mM CaCl_2 . The cells were then left to settle, which took approximately 20 minutes. Once cells settled the supernatant was discarded and the cells were re-suspended in 0.5mM CaCl_2 . Again, the cells were left to settle, the supernatant discarded and the cells re-suspended in 1.0mM CaCl_2 solution. The cells were then ready for use.

2.2.2 Single cell shortening/ Ca^{2+} measurements

Cell length shortening measurements and changes in cytosolic Ca^{2+} concentration were measured using the set-up that is schematically illustrated in Figure 2.5. The system was initially primed with a HEPES buffered Krebs solution of the following composition (mM): 140 NaCl, 4.0 KCl, 0.3 Na_2HPO_4 , 1.0 MgCl_2 , 5.0 HEPES, 11.1 glucose, 1.8 CaCl_2 . Cells were loaded with an initial concentration of $10\mu\text{M}$ Fura-2 AM in Krebs for 5 minutes at room temperature. The cell aliquot was diluted with double the volume of superfusate to prevent any further loading of the cells with Fura-2 AM. The pH of the solution was adjusted to pH 7.4 at 37° using NaOH. The cell bath was superfused at 37° . A small heater located within the tubing from the stock solution to the cell bath warmed the superfusate. The metallic cell bath was also heated. The superfusate outlet was mounted on a micromanipulator that allowed perfusion directly next to the cell. Solution changes were performed using a custom made 4-way solution changer. Single cells were stimulated using 2 Ag-AgCl electrodes that were positioned either side of the superfusate outlet and hence single cells were also stimulated directly. Square wave pulses of 10ms duration were delivered to the electrodes at 80-90V using a Digitimer DS2 stimulator.

The area of the microscope field in which fluorescence was measured was restricted by an adjustable rectangular window on the side port of the microscope. Cell orientation and window size was adjusted so that fluorescence and shortening of a single cell was measured. A Xenon arc lamp source and spinning wheel system rotating at 60Hz (Cairn Research Systems) stimulated fluorescence at 340nm and 380nm. A red filter selects the bandwidth of light that passes to the cells, allowing only the bandwidth of light corresponding with the emission spectra

of Fura-2 to pass. A 500nm longpass filter was used to collect wavelengths above 500nm which were then passed through a dichroic mirror to a photomultiplier. A spectrophotometer (Cairn Research Systems) was used to measure the output from the photomultiplier. A ratiometric measurement of intracellular Ca^{2+} concentration was obtained from fluorescence emitted at 340nm and 380nm. These measurements plus a ratio of the two were displayed on a chart recorder (Gould Instruments Ltd), recorded to video tape, digitised to the data acquisition computer program Whole Cell Program (WCP) (John Dempster, Strathclyde University) and stored on hard disk. A schematic illustrating the single cell shortening/ Ca^{2+} measurement set-up is shown in Figure 2.5.

Cell shortening measurements were recorded simultaneously with Ca^{2+} transients where possible. Ca^{2+} transients and shortening measurements from cells stimulated at 1hz and 3hz were recorded under a variety of conditions. The variable rectangular window was used to capture a single cell, which was displayed on a monitor and recorded on to video tape. The intensity profile of the cell along a line was positioned to run from one end of the cell to the other (length) and was represented on an oscilloscope. The edges of the cell were represented as a positive deflection for the left edge and a negative deflection for the right edge of the cell. The windows and thresholds were adjusted so as to obtain a shortening measurement alongside the Ca^{2+} transient on a separate oscilloscope. The contractions were displayed and recorded in the same way as for the Ca^{2+} .

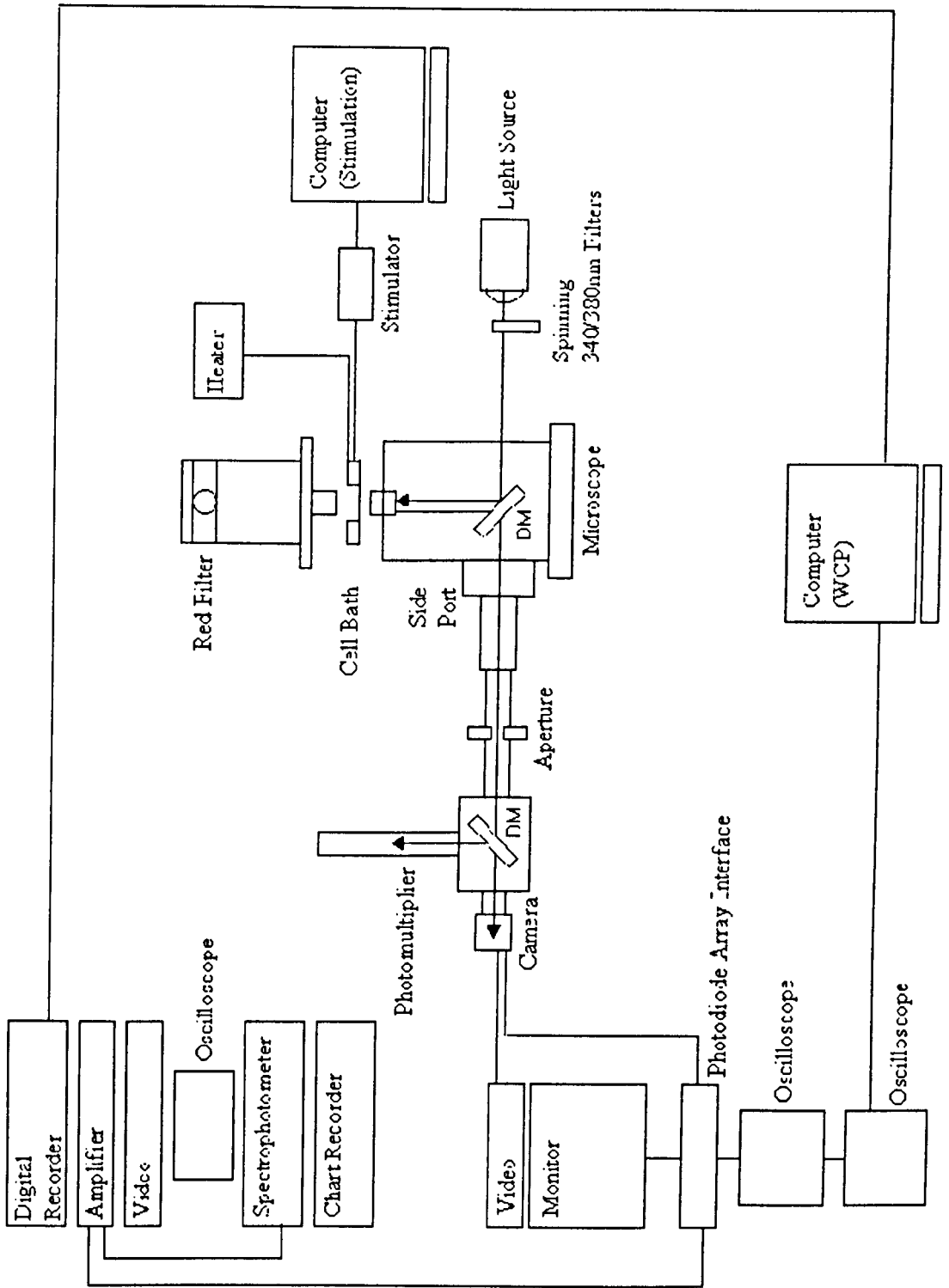
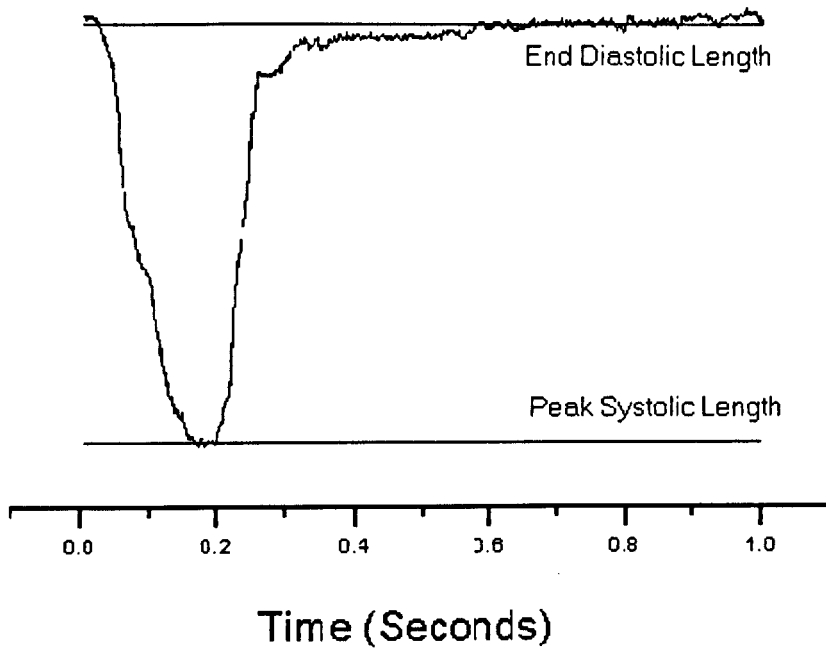


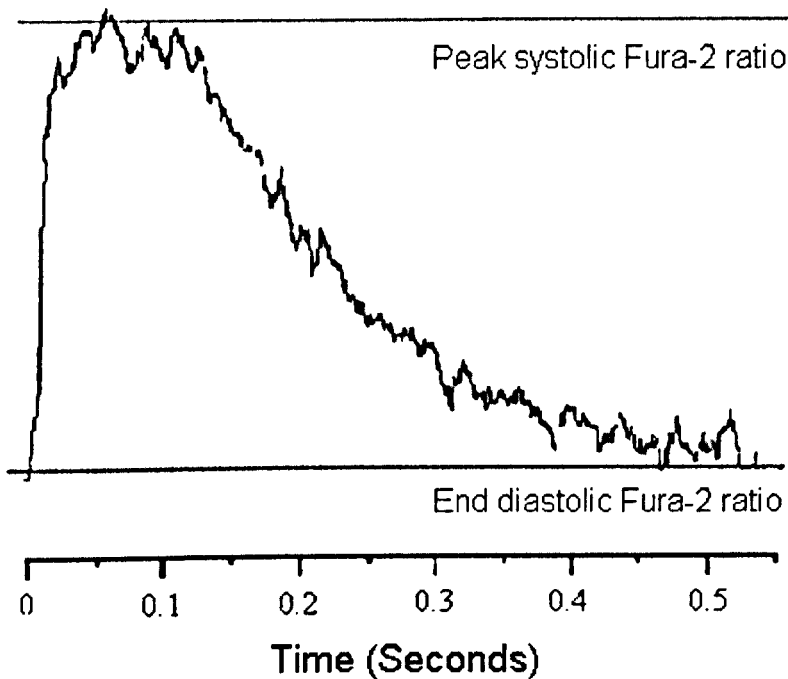
Figure 2.4 Schematic of the single cell shortening/ Ca^{2+} measurement set up. DM (dichroic mirror).

2.2.3 Data analysis

Data were analysed off line using the computer program WCP. Using this program, the last 8 Ca^{2+} transients and cell shortening measurements from periods of recording were averaged. Measurements were rejected if not worthy of analysis. Usually a trace was rejected if the signal to noise ratio was too high, although this was not a quantitative measurement. Data were exported to a computer graph program Origin (Microcal) and converted using a template (Prof. Godfrey Smith, Glasgow University) to Fura-2 ratio and cell length (μm). Fractional shortening was calculated and represented as relative changes in end systolic and end diastolic length whilst the Ca^{2+} content of the cell was represented by the relative changes in end diastolic and end systolic Fura-2 ratios. Figure 2.6 show how these parameters were defined; Figure 2.6a illustrates the parameters used for the measurement of fractional cell shortening, and Figure 2.6b for the measurement of Ca^{2+} transients.



A. Parameters measured to calculate contractility of isolated single cardiac myocytes. Percentage fractional shortening = (End systolic length / End diastolic length) x 100.



B. Ca²⁺ transient illustrating parameters measured.

Figure 2.5 The parameters used for measurement of single cell fractional shortening (A) and Ca²⁺ transients (B).

2.3 Statistical analysis

All statistical tests were performed using the DOS based computer program Instat. Individual tests are indicated at the relevant points in the text. The null hypothesis is a term that statisticians often use to indicate the statistical hypothesis tested. The purpose of most statistical tests is to determine if the results obtained provide a reason to reject the hypothesis that they are merely a product of chance factors. E.g. in an experiment in which two groups of randomly selected subjects have received different treatments and have yielded different means, it is always necessary to ask if the difference between the obtained means is among the differences that would be expected to occur by chance whenever two groups are randomly selected. So, if the null hypothesis is true, the P value is the chance that random selection of subjects would result in a difference as large (or larger) than observed in the study. If the null hypothesis is true, there is a 5% chance of randomly selecting subjects such that the trend is statistically significant.

2.3.1 Student's t-test

Paired and unpaired t-tests test the hypothesis that the mean value of a variable differs between 2 groups. The paired t-test is used when each data point in one group directly corresponds to a matching data point in the other group. The unpaired t-test compares the means of 2 groups. When there are 3 or more data sets to be compared multiple t-tests are not appropriate and the ANOVA (see below) should be used instead. In using the Student's t-test, the data are assumed to be continuous, with a normal distribution and equal variances in the two groups. However, t-test is robust to departures to the assumption of normality, but is more sensitive to unequal variances. Where a t-test was not appropriate for these reasons

the non-parametric equivalent test (Wilcoxon test) was used. Where multiple t-tests were applied a Bonferroni correction was also used.

2.3.2 ANOVA (Analysis of variance)

ANOVA is used to analyse data between 3 or more groups. One-way ANOVA tests the hypothesis that the mean value of a variable differs among groups. Post tests (Tukey) were also applied. The limitations of ANOVA are the same as those for the t-test (see above); if these are not satisfied non-parametric tests are available.

Chapter 3 - Methods of recording cardiac electrical activity

3.1 Development of methods used to record MAPs

In the clinical setting, there are several different methods that can be employed to investigate electrophysiological abnormalities in the heart. Monophasic action potential (MAP) recordings are one of the most recent developments in the recording of local myocardial activity, both in the normal and pathological state. MAP recordings are now commonly being used where no other technique is viable. There are several different methods used to record MAPs that will be discussed later. Firstly, attention shall be focused on other methods of recording repolarisation times.

3.1.1 Unipolar and bipolar recordings

Before the technique of MAP recording was developed, local myocardial electrical activity was recorded using biphasic or multiphasic deflections recorded by unipolar or bipolar contact electrodes. These electrodes detect activation well but provide little information concerning refractoriness and repolarisation. Activation and repolarisation are detected, but the membrane potential during the process between the two is not. Nevertheless, attempts to use these limited repolarisation transients obtained using the unipolar configuration have regularly appeared in the literature (Chinushi *et al*, 1998, Taggart *et al*, 2001) as “activation recovery interval” (ARI). Therefore, information regarding repolarisation times can be obtained by measuring the ARI. Activation is indicated by a sharp deflection in the trace whereas the recovery (repolarisation) is indicated by a small ‘bump’ in the trace. In this methodology, the interval between the activation complex and the repolarisation bump (analysed by dV/dt_{\max} and d^2V/dt^2 respectively) is used as a measure of repolarisation time. The ARI therefore indicates the time between the

activation complex and repolarisation, but gives no indication of what is occurring electrically during the repolarisation period. The advantages and disadvantages of unipolar and bipolar electrodes are shown in Table 3.1a and 3.1b respectively.

ADVANTAGES	DISADVANTAGES
Lack of directional sensitivity Less severe myocardial contact Definite criterion for detection of local activation – maximum negative dV/dt	Low amplitude local activity may be obscured

A. Advantages and disadvantages of the unipolar electrode.

ADVANTAGES	DISADVANTAGES
Detects low amplitude local activity well Amplified easier than unipolar recordings Easier to reduce noise	Requires close contact with the myocardium Various criteria adopted for the detection of local activity

B. Advantages and disadvantages of the bipolar electrode.

Table 3.1 The advantages and disadvantages of unipolar (A) and bipolar (B) electrode recording.

3.1.2 Transmembrane action potentials

The transmembrane action potential (TAP) may be considered the gold standard to which other methods of recording are compared. The TAP is recorded by insertion of a KCl filled glass microelectrode, with a tip diameter of approximately $0.5\mu\text{m}$, into a single myocyte. An extracellular ground electrode is placed near the cell membrane in the surrounding fluid contained in the tissue bath, this permits a potential difference to be recorded between the extracellular and intracellular voltages.

3.1.3 Monophasic action potentials

MAPs are extracellular wave forms which provide accurate information on the local activation time as well as representing the repolarisation time course of the local electrical activity of excitable myocardium. MAPs resemble the TAP both in configuration and duration (Franz, 1983; Levine *et al*, 1986; Runnals *et al*, 1987; Yuan *et al*, 1994). Whereas the MAP is recorded extracellularly, TAPs, which have been previously discussed, are recorded via the impalement of individual myocytes by a glass microelectrode and are therefore limited to *in vitro* applications. MAPs however can be recorded from the endocardial and epicardial surfaces of the *in vivo* and *in vitro* intact beating heart, including that of human subjects. This allows the utilisation of such a method in the clinical as well as experimental situation. The main applications of MAPs include: i) rate and rhythm dependent changes in MAP duration (restitution), ii) investigation of the effect of antiarrhythmic drugs, iii) triggered activity that may cause early- or delayed afterdepolarisations, iv) detection of myocardial ischaemia, v) measurement of dispersion of repolarisation/refractoriness, vi) measurement of activation times and

vii) the effect of mechanoelectrical feedback on arrhythmia formation (Yuan *et al*, 1994).

In comparative studies of the MAP and TAP recordings it has been concluded that MAPs are not absolute representations of TAPs (Franz *et al*, 1986; Runnals *et al*, 1987). Whilst the TAP is a recording from a single myocyte, the MAP electrode records from a number of cells. The cells over which the MAPs record from depolarise sequentially with time. This is thought to produce an action potential with a lower amplitude (10-50mV from a MAP recording compared to 120mV from a TAP recording (Franz, 1991)) and slower maximum upstroke velocity, V_{\max} (6.4V/s for the MAP compared to 200-300V/s for the TAP (Franz, 1991)) (Hoffman *et al*, 1959). Other factors influencing the MAP amplitude, as described by Hoffman *et al*, include; the magnitude and direction of local current flow; the degree of cellular coupling between the depolarised cells under the MAP electrode and the adjacent normal cells; and the electrical conductance in the extracellular and intracellular media surrounding the site of recording.

Monophasic action potentials have previously been used to characterise ventricular fibrillation (VF) (Swartz *et al*, 1993), an observation that is near impossible using the intracellular transmembrane method of recording. They characterised monomorphic ventricular tachycardia by a regular shaped action potential in the absence of electrical diastole. Ventricular fibrillation/polymorphic ventricular tachycardia was characterised as a random event where re-stimulation occurred prior to a resting membrane potential (i.e. incomplete repolarisation and an absence of resting membrane potential). Again, there was an absence of a diastolic interval.

In 1882, Burdon-Sanderson and Page recorded monophasic action currents (later termed potentials) from the frog heart by placing an electrode on uninjured, intact, epicardial tissue and another on an injured site; hitherto only multiphasic deflections had been used to record myocardial electrical activity. In 1951 Draper and Weidmann, in experiments on the chordae tendinae ('false tendons') of the dog heart, discovered that the transmembrane action potential was also monophasic. For many years it was thought that injuring the myocardium was the only method through which MAPs could be produced. The suction electrode method, devised in 1935 by Shultz (Franz, 1999), uses injury to generate MAP transients. Several years later (Korsgren *et al*, 1969) demonstrated the use of the suction electrode in recording electrical activity in the human subjects.

3.1.3.1 Suction electrode

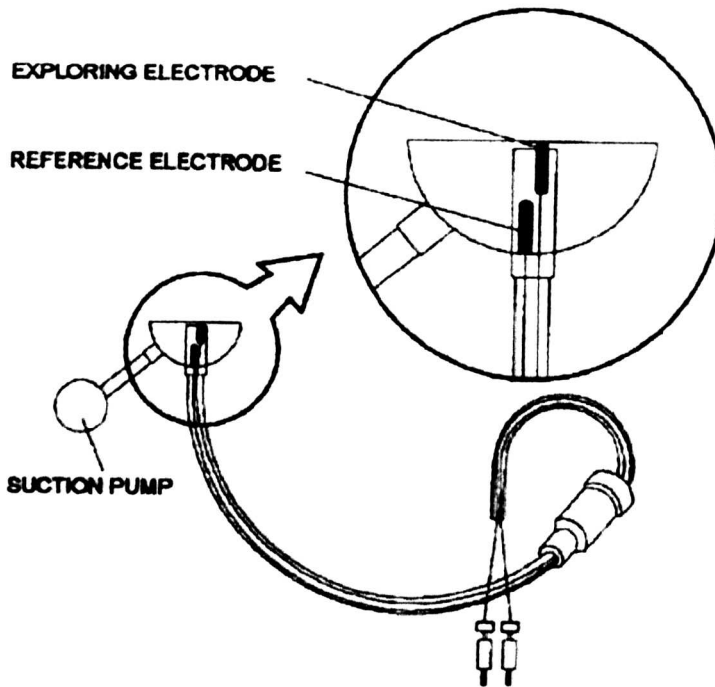
This technique is based on the principle that when contact is made with the myocardium, surface tissue is sucked into the tip of the catheter tubing, causing the cells in this tissue to become ischaemic, and after a short time, inexcitable. The electrode records the membrane potential difference between the still excitable cells adjacent to the tip of the electrode and the inexcitable cells beneath the electrode. A schematic drawing of a suction electrode is shown in Figure 3.1a. There are several disadvantages in using the suction electrode for MAP recording:

- a) Because of excessive injury that the electrode incurs to the myocardium at the site of the electrode, the application of such a technique is limited to periods of time less than approximately 2 minutes, after which localised ischaemia becomes prominent.
- b) The necessity for pumps, stop-cocks, and the physical size of the electrode itself makes the use of the suction electrode awkward.
- c) When recording from the artificially perfused heart, the mechanical movement of the heart tends to

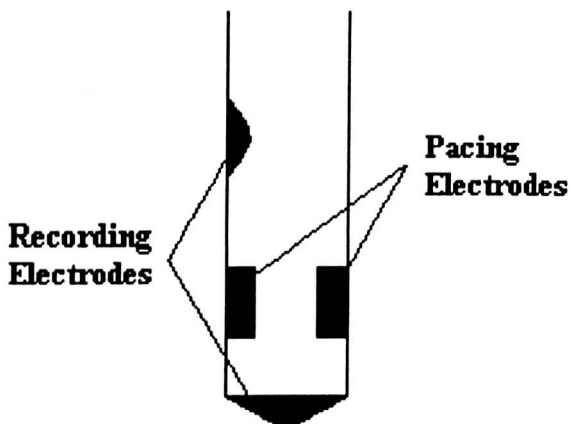
cause motion artefacts that distort the MAP. The existence of these limitations led, in part, to the development of the contact catheter electrode (which is a non-traumatic method of recording MAPs). A major disadvantage of the suction electrode, which is of special importance in this study, is the impracticalities (see above: size, time limitations, motion artefacts) of using it to make simultaneous recordings.

3.1.3.2 The contact catheter electrode

Franz developed the catheter electrode in 1983 and this is still the choice method for evaluating myocardial repolarisation times in the clinical setting today. This is primarily because it offers a less traumatic (in terms of tissue damage) way of recording MAPs. Using the catheter electrode to record MAPs involves pressing a non-polarisable Ag-AgCl electrode against viable myocardium (endo- or epicardium). Typical electrode tips have a diameter of approximately 1 to 2mm. The shape of a commonly used contact catheter electrode is shown in Figure 3.1b.



A. The epicardial suction electrode. Taken from Leimer and Cestari (1999).



B. Tip of a MAP Catheter Electrode.

Figure 3.1 Schematic drawings of the suction (A) and contact catheter (B) electrodes.

3.1.3.3 MAP genesis

In attempting to explain how his contact catheter works, Franz (1999) proposed the following mechanism. The force that the electrode tip exerts on the myocardium causes the cells subjacent to it to depolarise to a fixed voltage of between -20 and -30mV with respect to the diastolic extracellular reference potential. At this level, Na⁺ channels are inactive and hence cannot contribute to the action potentials occurring in the adjacent excitable cells. Assuming that electrical coupling is unaffected, an electrical gradient is formed between the inexcitable cells and the adjacent excitable cells, and electrical current is able to flow between the two. When the heart is electrically diastolic, the cells subjacent to the electrode tip act as a current sink; in systole, they act in the opposite way, as a current source. This produces electrical fields of opposing polarity. Figure 3.2 summarises this hypothesis.

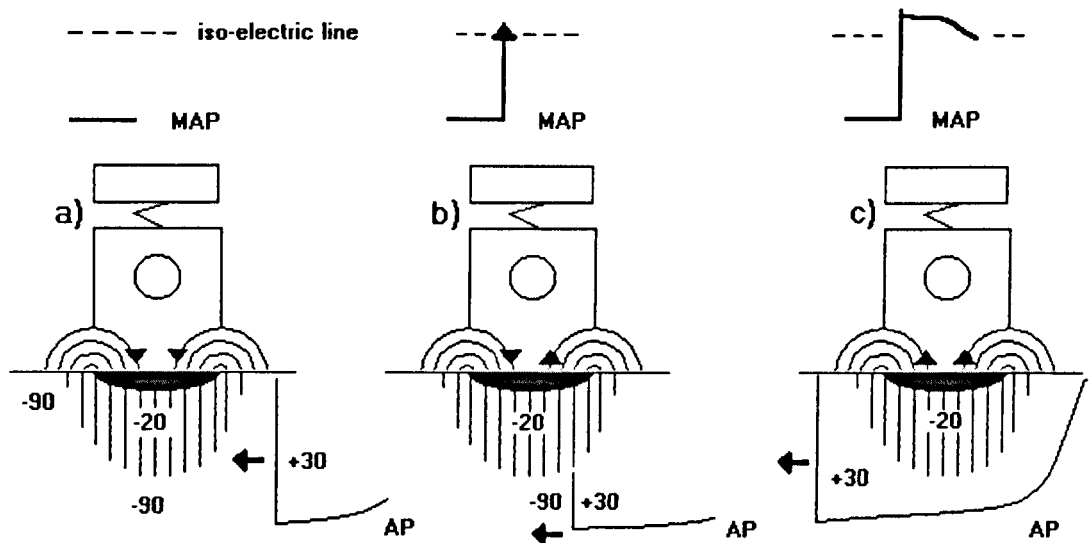


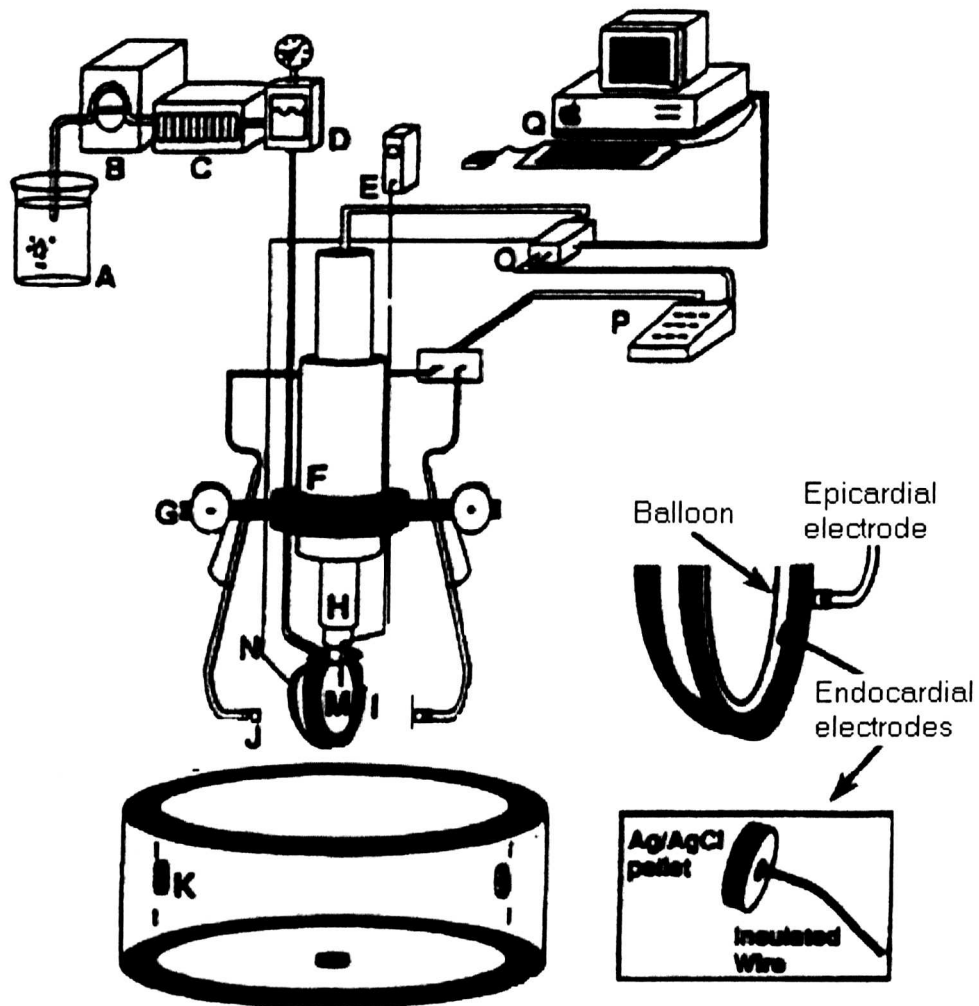
Figure 3.2 Diagram illustrating the hypothesis underlying the genesis of MAP recording by contact electrode (adapted from Franz, 1999). **(a)** Late electrical diastole. The cells are -90mV with respect to the outside. The cells subjacent to the electrode tip are depolarised to a fixed voltage of -20mV . The boundary gradient between the depolarised and surrounding excitable cells creates current flow (circular lines). Here the depolarised region is the current sink. The MAP recording (upper right) displays a steady negative potential. An arriving action potential arrives at the site (lower right). **(b)** Early electrical systole. An action potential arrives at the contact site. The boundary current and the field polarity potential are reversed. The MAP moves in the positive direction (upper right). **(c)** Mid electrical systole. The propagating action potential has completely encompassed the electrode site. The boundary gradients gradually diminish and the MAP shows repolarisation.

Because myocardial injury is less than with the suction electrode the contact electrode method allows stable MAP recordings to be made over longer periods of time (up to several hours). The ability of the contact electrode to record MAPs long term with no myocardial injury is one of the reasons why it has succeeded the suction electrode as the preferred method of recording in the clinical setting. This raises the question: can cells be depolarised by applying pressure without causing permanent injury? From preliminary experiments conducted as part of this study where MAPs were recorded under excessive pressure, the electrode removed and re-applied and MAPs recorded under light pressure, there is reason to believe that permanent injury does not occur, at least on relatively short time scales (seconds to minutes). However, in practice, several factors may militate against long term usage. Firstly, the difference in pressure between the electrode and the epicardium that is required to obtain sufficient depolarisation for a full amplitude MAP, and that which causes localised ischaemia, seems to be small. Secondly, when a MAP of acceptable amplitude is obtained where the electrode is very lightly touching the surface of the epicardium, it is very likely that the amplitude of the MAP will decline to the extent that analysis of durations becomes impossible or unreliable (after approximately 20-40 minutes). Within limits, increased contact pressure leads to an increase in the amplitude of the MAP. Even when contact pressure is constant, amplitude tends to increase initially. Over a longer time scale the MAP amplitude may a) stabilise at a maximum, b) decrease and stabilise or b) continue to decline until it is inseparable from the background noise. A continued decrease only usually occurs when the electrode has been left in place for an excessive amount of time.

The situation is further complicated by the changes in contact pressure caused by the contractions of the heart – a problem not so easily overcome. In addition, lateral movement of the electrode may cause artefacts on the recorded extracellular waveform. Because the electrode is not physically attached to the heart, contractions of the ventricle may move the electrode rhythmically, causing distortions of the MAP. In practice, these motion artefacts could be reduced to some extent by minimising heart motion in the Langendorff perfused set-up by using a concave cradle on which the heart rests. However, it is possible that contact pressure changes may produce transient alterations in the MAP amplitude are confused with true electrophysiological changes. Despite these disadvantages, the catheter electrode is relatively reliable in terms of a) obtaining usable MAPs and b) repeatability of MAP measurements. Patient setting up can yield high quality (see Franz, 1999, for the criteria of high quality) MAPs that may be recorded over long periods of time.

Simultaneous multiple MAP recording is a technique that allows an accurate measure of the dispersion of repolarisation to be obtained. Several groups have made an attempt to simultaneously MAP repolarisation in the whole heart. A multiple catheter electrode array was constructed by Franz (1992), based on a cantilever mechanism (Figure 3.3). The device held 6 extensions, 3 of which held cantilever arms attached to a coiled wire spring mechanism. Custom made Ag-AgCl bipolar contact MAP electrodes were mounted in the distal end of the cantilever arms. By adjusting the tension of these springs constant contact pressure between the electrodes and the heart was maintained. When considering how best to obtain multiple measurements from whole hearts in the present study, it was decided that the intricacies of such a mechanism and the difficulty in manipulating

the positions of the electrodes were impractical as a method of obtaining more than 3 simultaneous recordings using the contact catheter.



A.	Buffer Reservoir	I.	Heart
B.	Roller Pump	J.	MAP Electrode
C.	Heat Exchanger	K.	ECG Lead
D.	Air Trap/Manometer	M.	Intraventricular Balloon
E.	LV Pressure Recorder	N.	Epicardial Pacing Wires
F.	Linear Motor	O.	Analog/Digital Interface
G.	Cantilever Arm Ring	P.	9 Channel Amplifier
H.	Piston Pump	Q.	Macintosh II Computer

Figure 3.3 Experimental set-up used by Franz *et al* (1992) to simultaneously record 3 MAPs using a cantilever and spring mechanism. Taken directly from Franz, 1992.

3.2 The contact catheter electrode - preliminary investigations and limitations

3.2.1 Methods

Preliminary experiments were done to find out how long it takes for stable MAP recordings to be obtained. In this context stable MAP recordings may be defined as a state where no change in MAP duration is seen with time. A short protocol involving cycle length (CL) changes at 4 minute intervals was conducted. This involved pacing the heart at a constant CL of 350ms, followed by a change to 250ms, a return to 350ms, a change to 200ms, and a return to 350ms. Returning the basic CL to 350ms between changes in CL enabled determination of recovery of MAP duration following abrupt changes in CL.

The optimum contact pressure between the electrode and the myocardium was determined by applying the catheter to the epicardium at different pressures. The heart was paced at 350ms and perfused at 37°C with standard Tyrodes solution. Initially a very light contact pressure was maintained for 15 minutes. The electrode was then re-applied to the same location on the epicardium with firm pressure for a period of 15 minutes. The pressure applied to the myocardium was not quantified. MAPD₅₀, MAPD₉₀ and MAP amplitude were recorded. The ratio MAPD₅₀:MAPD₉₀ was calculated in order to reveal changes in MAP morphology, a decreasing ratio would indicate triangulation of the MAP. Triangulation of MAPs is associated with ischaemia.

3.2.2 Results

3.2.2.1 Time to steady state

A single experiment from a protocol carried out to determine the time taken for the MAPs to stabilise is shown in Figure 3.4. Recordings were made at cycle lengths of 350ms, 200ms, 350ms, 250ms and 350ms. Stabilisation is taken as time to observation of no changes in MAP duration. Here, $MAPD_{50}$ and $MAPD_{90}$ are plotted against time. From these data a minimum period of 3 minutes is required to allow stabilisation. From this it was concluded that a stabilisation period of 4 minutes should be allowed in subsequent experiments. $MAPD_{90}$ returns to its initial value on a return in pacing cycle length from a faster pace to the basic CL of 350ms. However, in this trace, a slight shortening of $MAPD_{50}$ was seen between the start and the end of the run. This change may indicate a slight 'run down' in this example, possibly due to mild ischaemia caused by slightly excessive contact pressure between the electrode and the myocardium.

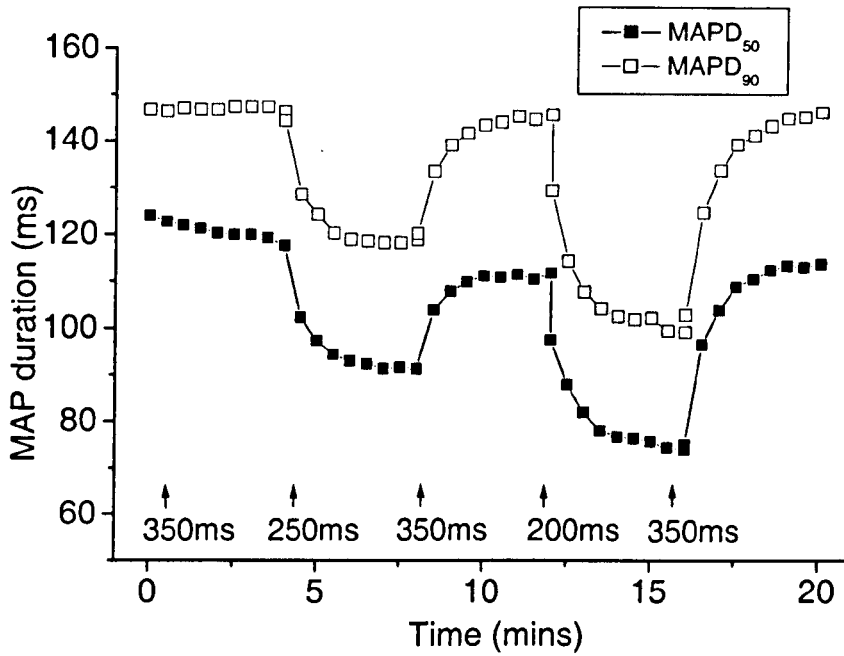
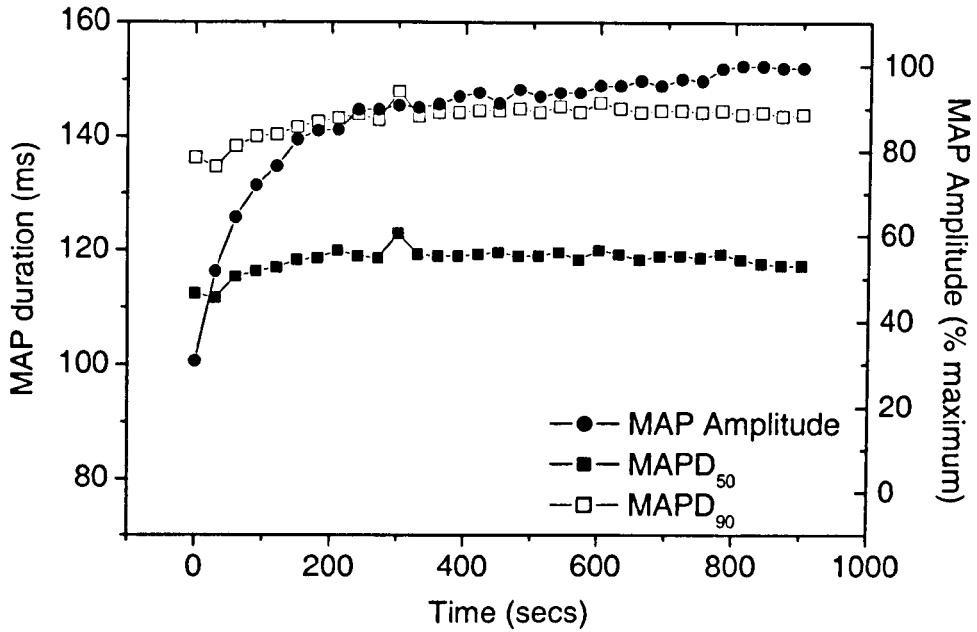


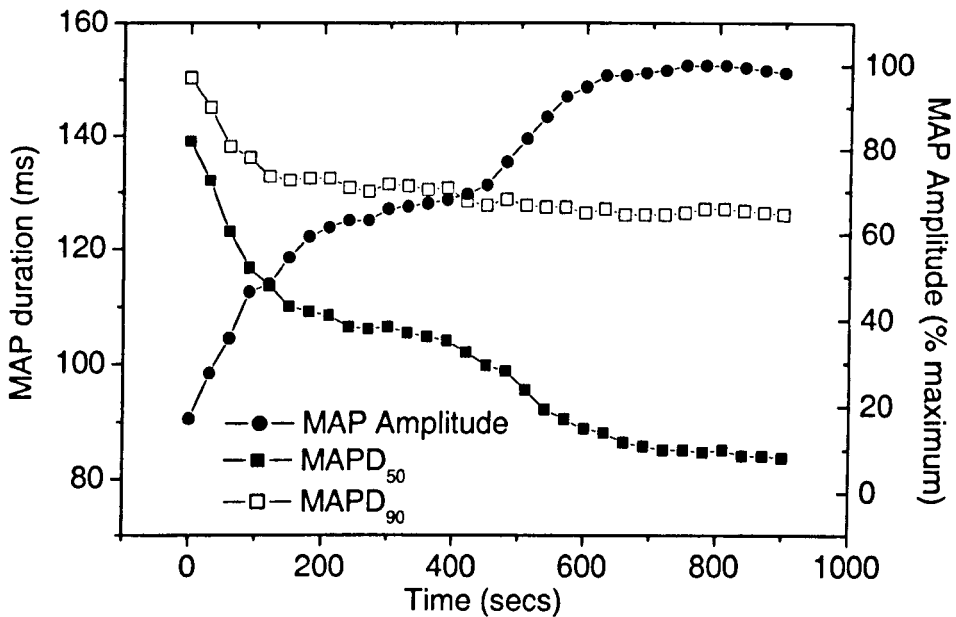
Figure 3.4 Typical experiment illustrating the time required to ensure stabilisation of MAP recordings. Both MAPD₅₀ and MAPD₉₀ are shown.

3.2.2.2 The effect of electrode contact pressure on MAP recordings

Figure 3.5 illustrates the effect of a light (A) and a heavy (B) electrode contact pressure on $MAPD_{50}$ and $MAPD_{90}$. Recordings were made at a steady state cycle length of 350ms. Light contact between the electrode and the epicardium results in a stable MAP recording where no increase or decrease is seen in $MAPD_{50}$ or $MAPD_{90}$ after the initial 4 minute stabilisation period. However, excessive pressure between the catheter and the epicardium was seen to cause a triangulation of the MAP. This is observed as a greater reduction in $MAPD_{50}$ relative to $MAPD_{90}$, and is illustrated in Figure 3.6 by a drop off in the ratio $MAPD_{50}:MAPD_{90}$. This drop off is not observed with light contact.

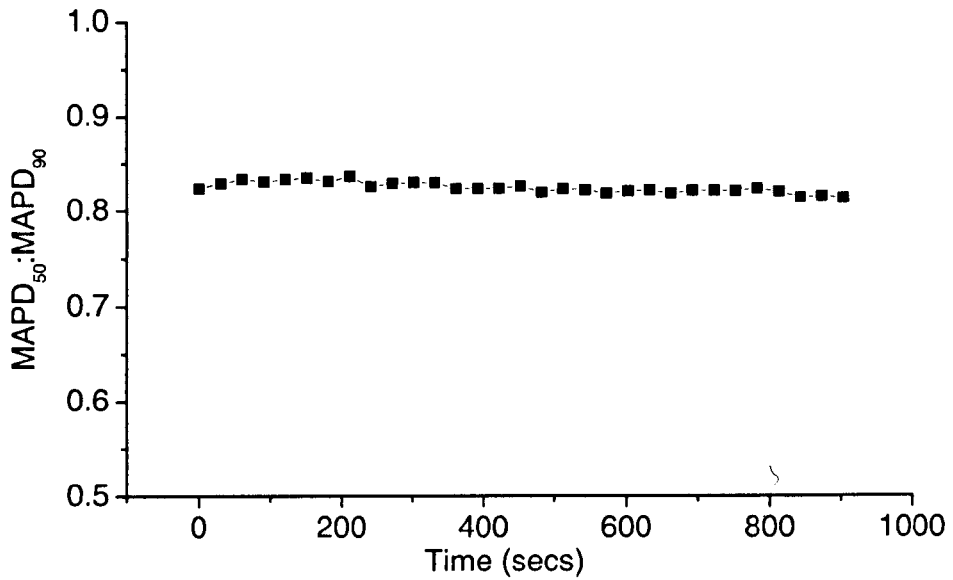


A. Light contact pressure between the electrode tip and the myocardium produces stable MAP durations.

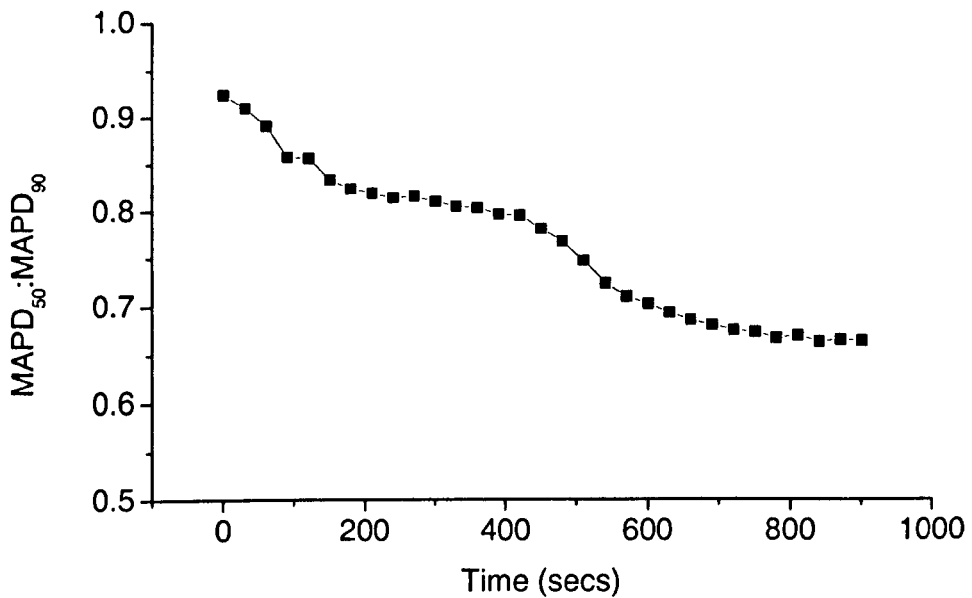


B. Excessive contact pressure between the electrode tip and the myocardium causes a decrease in MAP durations, this is more evident in MAPD₅₀.

Figure 3.5 The effect of contact pressure on MAP duration and amplitude.



A. MAPD₅₀:MAPD₉₀ under light contact pressure remains unchanged where there is light contact between the electrode and the surface of the epicardium indicating a MAP morphology is maintained.



B. MAPD₅₀:MAPD₉₀ under conditions of excessive electrode pressure decreases indicating a triangulation of MAP as part of a continuing change in MAP morphology.

Figure 3.6 The effect of contact pressure on the ratio MAPD₅₀:MAPD₉₀.

3.3 The syringe electrode – construction and preliminary investigations

3.3.1 Construction

The main objective of this part of the study was to develop a multiple MAP electrode array that could be used to simultaneously record up to 32 MAPs from the epicardial surface of the left ventricle. A unipolar electrode array had previously been developed by Dr. F. Burton (University of Glasgow). This array allowed the simultaneous recording of up to 256 unipolar electrograms from the epicardial surface of the left ventricle. This array consisted of Ag-AgCl wires embedded in a latex jacket (sheath). Developing a single syringe electrode on a spring mechanism (Figure 3.7) tested the feasibility of using a latex jacket electrode for the simultaneous recording of monophasic action potentials. MAP genesis by this method would arise through the same mechanisms as previously described. An electrode, the equivalent of the contact catheter electrode, would protrude through the latex and would impart to the myocardium the needed force for depolarisation of the myocardium. It was envisaged that other electrodes would be recessed into the latex to act as reference electrodes. To explore this possibility, a syringe was constructed with 3 of these reference electrodes to determine whether a configuration yielding recognisable MAPs could be obtained. The rationale of using 3 reference electrodes was that it might adequately approximate the ring with a wide field of view corresponding to the reference electrode in the Franz catheter (Figure 3.1b).

The syringe electrode consisted of a 2.5ml plastic syringe, a small circle of latex cut from a thin sheet, a metal spring and 4 pieces (for a 3 reference electrode

syringe) of insulated silver wire. The syringe was disassembled, and the plunger and plunger tip removed. The spring was placed over the plunger and the barrel of the syringe pulled on top to allow a spring action. The latex was moulded to allow one protruding depolarising electrode and 3 recessed electrodes to be added. The latex was fixed over the syringe using suture thread. The electrode terminals were made by melting the end of the Ag insulated wire with a small blow torch to form a 'ball' head. The more wire that was melted, the larger the terminal was, and possibly the more myocardial depolarisation incurred. 3 of the 4 wires are blown to a smaller size than the remaining 1 that is used as the protruding electrode (Figure 3.7).

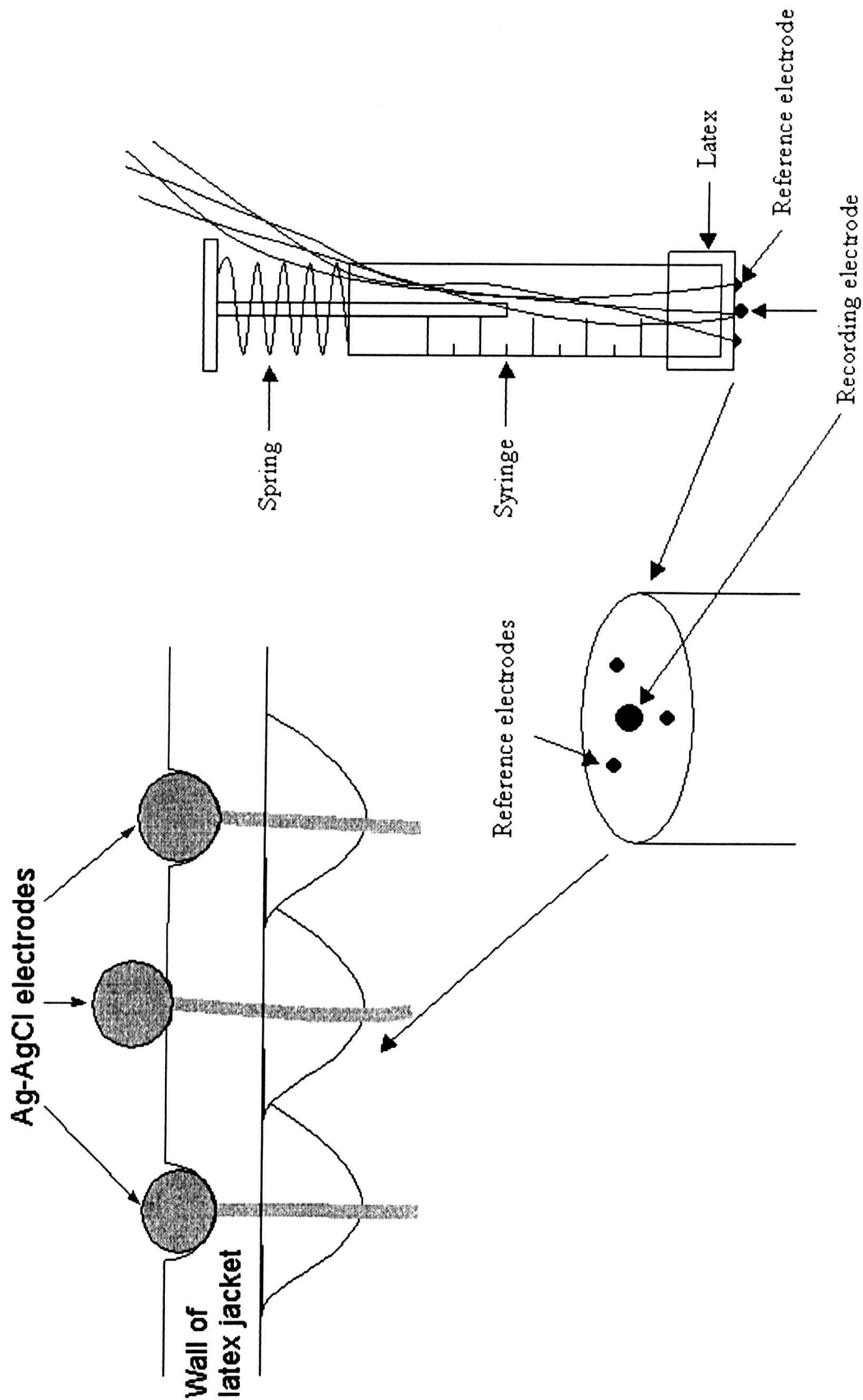


Figure 3.7 The syringe electrode including transverse section of the latex showing the recessed and protruding electrodes.

3.3.2 Methods

The syringe was held in place against the heart with a multi-hinged device (made from parts found around the lab) that allowed full movement of the electrode around the left ventricle. The spring mechanism enabled electrode contact with the myocardium despite cardiac movement. Once the electrode was positioned against the myocardium the heart was paced at a constant cycle length of 350ms for 4 minutes to allow stabilisation of MAP duration. During these preliminary stages steady state restitution protocols (to measure rate dependent changes in action potential duration) were performed as a test of the feasibility of the method. The AVN and SAN were ablated (refer to chapter 2, general methods) and the heart paced at 350ms for 4 minutes prior to the start of incremental changes in pacing rate. A range of cycle lengths was explored from a minimum of 150ms to the longest cycle length at which interference from intrinsic ventricular depolarisations did not occur.

3.3.3 Results

The syringe electrode produced excellent results when MAP quality was good. The restitution curve from a single experiment is shown in Figure 3.8. The results show the shape of a typical restitution curve and indicate a sound working electrode.

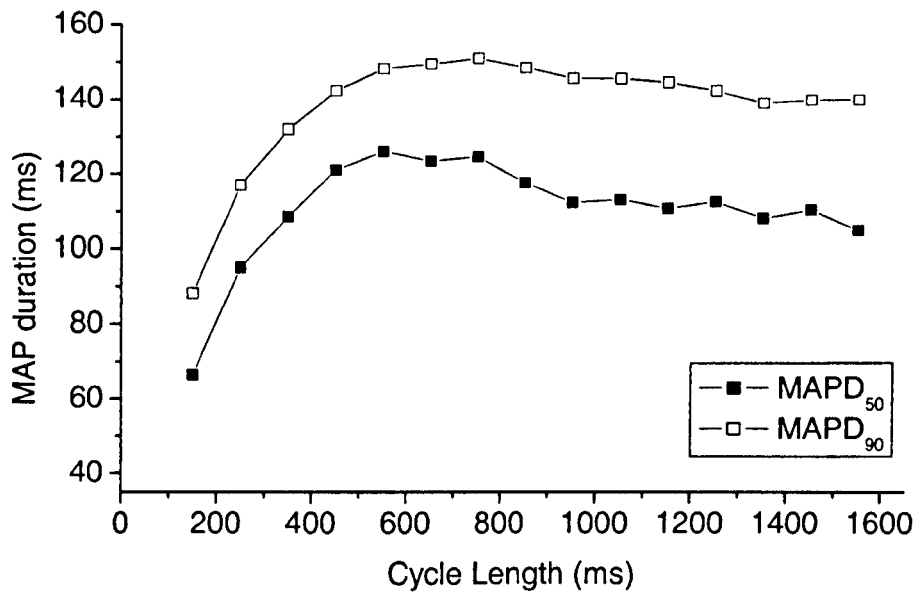


Figure 3.8 A typical restitution curve obtained from the epicardial surface of the left ventricle with the syringe electrode.

In general, and under good conditions, the syringe electrode yielded better shaped MAPs over a longer time period than the catheter electrode. However, the MAPs recorded using this method were of lower amplitude than those of the contact catheter. At low amplitudes contamination of the recordings by noise became problematic: as the amplitude decreases with time, the error in the MAP duration determination increases to the extent that the recordings can no longer be analysed.

On first contact with the epicardium, the MAPs obtained using the syringe electrode did not seem to show the initial increase in amplitude that is seen with the catheter electrode. Drift in baseline was also greater than with the catheter electrode. On initial contact with the epicardium, and on obtaining a recording, a considerable amount of drift is observed which, on the majority of occasions, stabilised over time but is seen reproducibly at the start of each experiment. This drift may be attributable to polarisation of the Ag as it becomes chlorided. This was not observed with the catheter electrode.

It was not possible to use the syringe electrode on small hearts due to its size. While the large area of the syringe end might have been expected to disperse the pressure over a larger area and hence lessen the likelihood of the onset of ischaemia it turned out to be unusable. This was because it caused the smaller hearts to compress to an unacceptable extent causing a decrease in left ventricular developed pressure (LVDP) and an increased perfusion pressure (PP) that was not observed with the catheter. The relative size of the tip of the syringe also makes precise location of the central electrode difficult, especially if the electrode is to be removed from the epicardium and later replaced at the same site.

The syringe incorporates a spring mechanism (see Figure 3.7) that allows a constant contact pressure to be maintained. This helps in overcoming problems of motion artefact. Nevertheless, support of the heart using the concave cradle was still essential when using the syringe. In the absence of the cradle the spring mechanism was defeated, because the unsupported heart was pushed away by the syringe. Furthermore, motion artefacts appeared and smaller amplitudes were obtained.

Following the success of the 3 reference electrode design, syringes incorporating 2 and 1 electrodes were built and tested. With 3 reference electrodes a consistent MAP could be recorded despite the rotational position of the electrode. In contrast, with only 1 reference electrode, only certain positions yielded a MAP like signal necessitating rotation of the syringe (Figure 3.9). A syringe electrode with 2 reference electrodes also required no rotation.

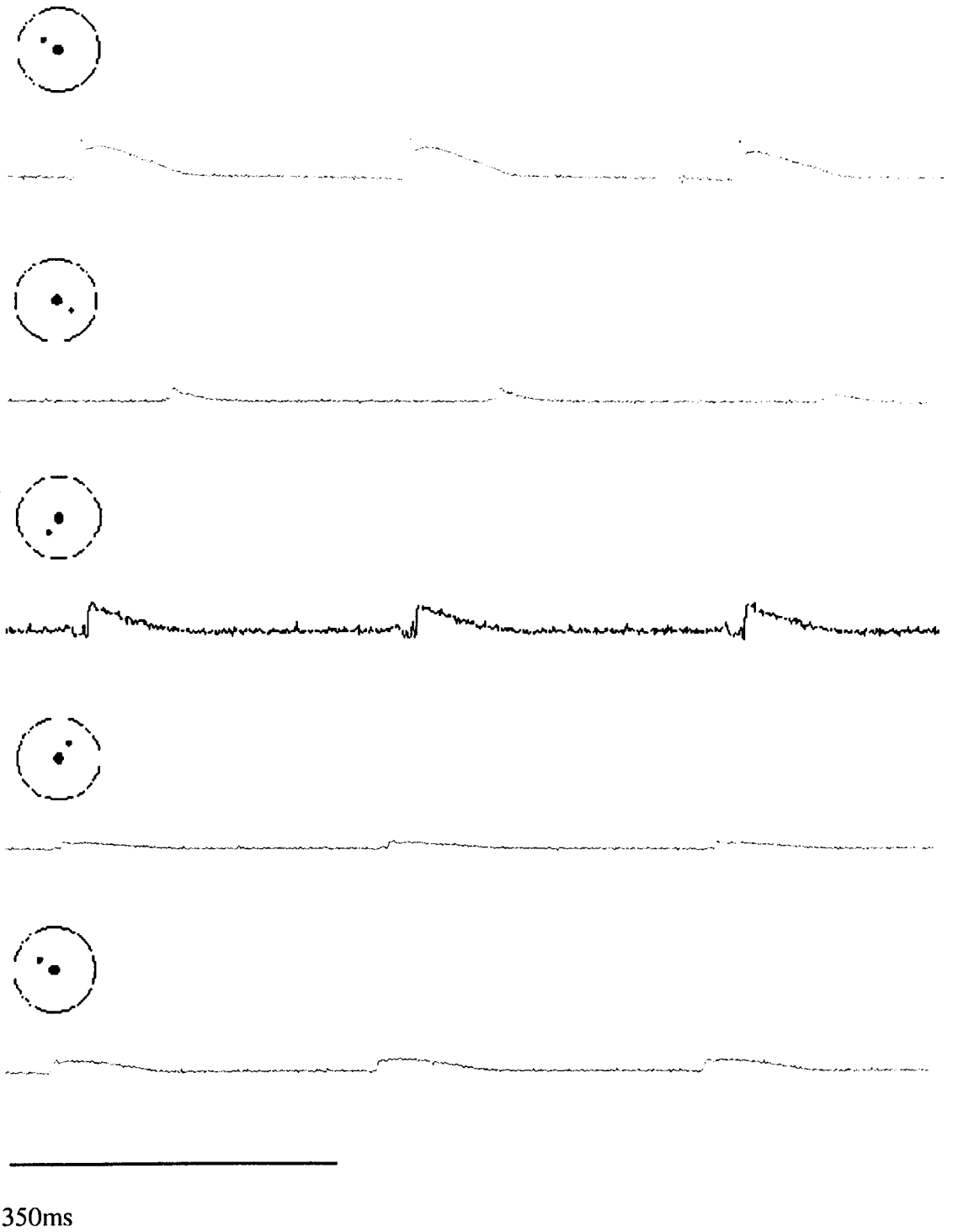


Figure 3.9 The effect of rotation of the syringe electrode. MAPs can not be produced at all electrode positions on rotating the single reference electrode syringe through 360°.

3.4 The jacket electrode – development, construction, and preliminary investigations

3.4.1 General construction of latex jackets and electrodes

Development of the jacket electrode array was driven by the desire to obtain simultaneous recording of multiple MAPs to enable accurate measurement of the dispersion of repolarisation across the epicardial surface of the left ventricle. The jacket MAP array was an extension of the syringe electrode design with the 3 reference electrodes, using the latex technology developed by Dr F.L. Burton (University of Glasgow). Initially a preserved heart was suspended in a container of Sylgard silicone which was allowed to set, producing a heart shaped mould. Liquid plaster was poured into the mould to make a plaster cast of the heart. After hardening this was further sculpted and surface imperfections removed. The cast was then painted with 2 coats of Hammerite to give a smooth finish. To produce the recessed areas of the latex into which the 3 indifferent electrodes fit, Ag-AgCl balls (also made by melting) were glued onto the ‘left ventricle’ of the cast at the appropriate positions. The cast could then be used to manufacture any number of latex jackets. The cast was dipped into liquid latex and air-dried, a process which was repeated 3 times or until the required thickness was obtained. The jacket was removed from the cast, the area corresponding to the right ventricle cut away and discarded, all remaining edges reinforced with latex, and a hole punched in the apex of the jacket to allow free drainage of the perfusate. Ag-AgCl electrodes were fed through the recessed areas and a central protruding electrode fed through the centre of the groups of 3 (exactly as described above, Figure 3.7). Ties (silk ligature) were then inserted into the cut open edges, one pair towards the apex and another towards the base of the jacket. These kept the jacket in position around the

heart and also allowed contact pressure between the electrodes and myocardium to be adjusted. The 2 pairs of ties were threaded through 2 short pieces of catheter tubing to allow the tightness of the jacket around the heart to be adjusted. In the early developmental stages, the electrodes were soldered to connecting pins and connected to an 8 channel amplifier. However on completion of a 16 electrode and full 32 MAP electrode the electrodes were soldered to 5 core wires that connected to a custom-built 32 channel MAP amplifier. Results obtained during the progression from 4, through 8 and 16, to 32 electrode arrays will be presented.

3.4.1.1 The 4 electrode array

The first step to building a 32 MAP electrode array was the 4 electrode array. This electrode array was not embedded in a latex jacket, the electrodes were embedded in to a strip of latex. This latex strip had 2 pins at either end that gripped in to the epicardium. This method of holding the array on to the myocardium was found to be unreliable as the strip would not maintain its position on the heart. Following this attempt, the 4 electrode array using the jacket design was constructed. The electrodes were arranged in a single line across the width of the jacket midway between the base and the apex.

3.4.1.1.1 Methods

Steady state restitution protocols (to determine rate dependent changes in action potential duration) were run to investigate the longer term viability of the 4 electrode array. For methods of the protocol refer to syringe electrodes methods. The protocol was terminated when the pacing cycle length exceeded the intrinsic cycle length.

3.4.1.1.2 Results

MAPs were analysed at 50% and 90% repolarisation and the results plotted against time. Figure 3.10 shows typical restitution curves from a single experiment where 3 MAPs have been obtained simultaneously using the 4 electrode array. A 4th MAP was not obtained. A 75% success rate (3/4 electrodes) was the maximum obtained at any one time.

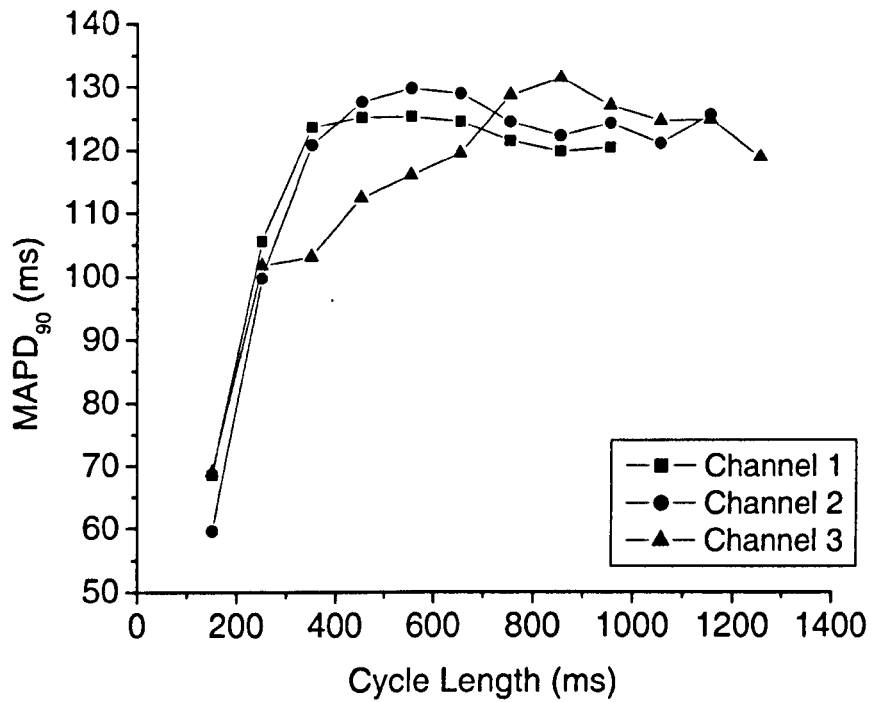


Figure 3.10 Simultaneously recorded MAPs obtained from the epicardial surface of the left ventricle by the 4 electrode array. MAPD₉₀ only is shown.

3.4.1.2 The 8 and 16 electrode arrays

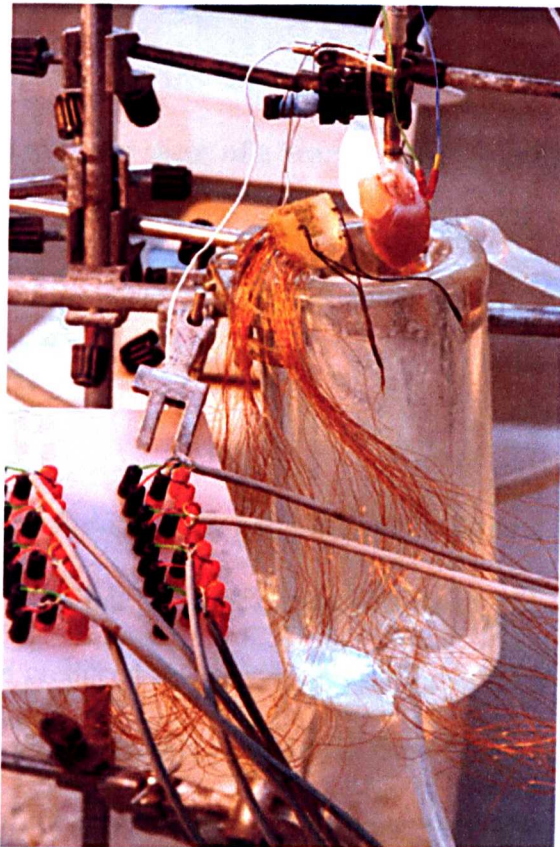
This stage of development was fairly rapid. The electrodes in these arrays were arranged in an almost triangular fashion, tapering towards the apex of the heart. The configurations of the electrodes from base to apex of the jacket were 4, 3, 1 for the 8 electrode array and 6, 5, 4, 1 for the 16 electrode array. On average only 50% of the electrodes yielded MAPs of quality sufficient enough to include in wavefront analysis of restitution. This relatively low success rate could be attributed to a gradient of MAP obtainability from base to apex. Basal areas tend to yield better quality MAPs, at a higher success rate, than apical regions. This point has been documented by Cowan *et al* (1987) in a study using a single MAP recording technique. Clearly, the horizontal arrangement of the 4 electrode array would preclude observation of such a gradient. Over this phase of development, the stimulus protocols were refined to overcome the tendency of amplitude (and ultimately the effective number) of the MAPs to decline over time.

3.4.1.3 The 32 electrode array

The 32 electrode array was constructed, from base to apex, with an 8, 7, 6, 5, 4, 2 electrode configuration. The 32 electrode array yielded good quality MAPs with a 25-50% success rate (i.e. 8-16 sites were usable). Figure 3.11 show photographs of the array both alone (A) and on the experimental set-up during an experiment (B).



A. The 32 electrode array showing apical and basal ties, intricacies of the electrodes and a perspective on size.



B. The electrode array being used during an experiment. The electrodes are connected via an intermediate plug board (at the left of the picture) to a 32 channel MAP amplifier.

Figure 3.11 The 32 electrode array.

The elastic property of the latex enables electrode contact with the epicardium to be maintained at all times when used with a heart that matches its shape and size. But, because every heart differs in shape and size one jacket is not optimal for all hearts. An inadequate fit may cause air to become trapped between the jacket and the epicardium. If the air bubble lies beneath an electrode that signal is effectively abolished. The ties permit a jacket to be used with a range of heart sizes by a degree of tightening. However, even with these a good fit is not guaranteed. As with the syringe electrode, the recorded MAPs are of lower amplitude than those obtained with the catheter, they tend to diminish with time, and there is a considerable amount of visible noise on analysis. A similar drift as seen with the syringe electrode is apparent on first application of the jacket. In addition, because the jacket is moulded to fit the shape of a heart, it is not possible to rotate the jacket without losing contact between the epicardial surface and (some of) the electrodes. Altering the position of the jacket more than a couple of millimetres can also cause air to become trapped.

Several problems arose during the progress towards making a 32 electrode jacket, some of which were overcome. One of the initial aims of this investigation was to study infarcted hearts produced by coronary artery ligation. It was found that the 32 electrode array yielded extremely poor results from failure hearts. This was not only due to the size of the infarct - severe infarctions may cover a large proportion of the left ventricle - but also because the shape and size of these hearts varies so much. The wide variation in the size of these hearts is due to the compensatory hypertrophy seen in the tissue remote from the infarct. This makes it impossible to construct a single jacket to work with all failure hearts. The stock hearts gave roughly a 50% success rate from a single experiment (i.e. 16 of 32 electrodes gave

good quality MAPs within minutes of setting up). However, the problem of obtaining a sustained MAP recording for any reasonable length of time (>1 hour) persisted, despite the remaking of electrodes, and jackets, of different sizes.

3.5 Discussion and conclusions

With all of the electrodes described in this chapter it was impossible to predict the quality of MAPs in advance. Apparent health and lack of surface abnormality was no predictor of individual MAP quality. For example, a stock or control heart may yield worse results, particularly when using the catheter electrode, in respect of quality of MAP than a severely infarcted heart. Sometimes the syringe electrode produced good quality MAPs that are sustained for a long period of time and are fully analysable, and the catheter produced MAPs that do not begin to show signs of ischaemia (as evident by triangulation of the MAP and reduction in $MAPD_{90}:MAPD_{50}$).

Another problem lies in the nature of the epicardial surface: severely infarcted hearts tend to have basally located fatty deposits that reduce the area over which MAPs may be obtained. This problem also occurred in the control hearts, although less often. MAPs were often not obtainable at one electrode site but were of very high quality at another despite a uniformly healthy-looking epicardium. The reason for this strange anomaly is unknown, but cannot be attributed to the electrode alone because the same electrode site might yield a good signal in another heart. Size of the protruding electrode which is known to affect the amplitude of the MAP may be a relevant factor.

Due to the progressive reduction in MAP amplitude that is observed with the jacket array, experiments must be devised which involve a much shorter protocol (less than 15 minutes) in order to obtain information on dispersion of repolarisation. Changes in cycle lengths and perfusion with uncoupling agents must be undertaken within this relatively short time scale. The extrastimulus technique for determining electrical restitution will provide an ideal means of recording dispersion of repolarisation.

In a study of the transmural dispersion of repolarisation in vivo and its relation to the development of Torsade de Pointes, Weissenburger *et al* (2000) proposed a radically different method of obtaining MAPs. They used a KCl inactivating electrode that was remote from the unipolar recording electrode. The degree of inactivation produced by this electrode was similar to that produced by the catheter electrode. The recording electrodes consisted of tungsten wire insulated up to the tip that can sit on the myocardium or be *plunged into it*. The recordings closely resemble MAPs obtained from the more conventional methods. Genesis of the MAP is assumed to involve the movement of current between the inactivated cells beneath the inactivating electrode and the surrounding active cells. At first glance, it would appear that they are recording the electrical activity of the area in contact with the reference electrode rather than that adjacent to the inactivating electrode. And yet they showed a variation in transmural MAP duration (24 ± 9 ms). This method promises a phenomenal increase in the number of sites which could be recorded simultaneously: tens to hundreds of MAP recordings could potentially be obtained from the surface of the left ventricle with relative ease. However, as the validity of this novel method remains to be proven the current project has therefore relied on the more conventional approach.

The use of voltage sensitive dyes has provided a new approach to mapping repolarisation and refractoriness in the whole heart (Dillon, 1991; Girouard *et al*, 1996; Horner *et al*, 1997; Efimov *et al*, 1998). Dyes (such as di-4-ANEPPS, WW781, and RH-421) bind to cell membranes and fluoresce with an intensity that varies proportionally with membrane potential. This fluorescence is captured and quantified by photodetector arrays or CCD cameras. Optical mapping allows multiple MAP recordings to be made simultaneously from hundreds of closely spaced sites. This new method is not a panacea however as motion artefacts are a serious problem. These may be suppressed partly or fully through the use of an electromechanical uncoupler such as 2,3-butanedione monoxime, BDM (Cheng *et al*, 1997) or cytochalasin-D (Wu *et al*, 1998). These agents have been found to have a reversibly negative inotropic affect on cardiac contraction but they also have side effects on ionic currents leading to changes (shortening) in MAP duration (Biermann *et al*, 1998). The utilisation of the electromechanical uncouplers means that this method cannot be employed in the *in vivo* human heart. Therefore, methods employing electrode arrays may still have a place in whole heart electrophysiology.

Table 3.2 summarises the techniques used to record the cardiac electrical activity that have previously been discussed.

Method	Location	In vivo and/or in vitro	Maximum simultaneous recordings
Intracellular microelectrode	Transmural (single cells)	In vitro	1
Suction Electrode	Surface, endocardial or epicardial	In vitro and in vivo	?
MAP electrode	Surface, endocardial or epicardial	In vitro and in vivo	~12
Optical Mapping	Superficial	In vitro	Hundreds to thousands

Table 3.2 Techniques for measuring repolarisation times.

**Chapter 4 – The effect of heart failure on whole heart
electrophysiology recorded by the Franz MAP catheter technique**

4.1 Introduction

Coronary heart disease often with previous myocardial infarction (MI) is the major cause of heart failure leading to sudden cardiac death in the industrialised world. Hundreds of thousands of lives are taken each year. MI is an irreversible condition where the cardiac muscle becomes necrosed due to prolonged ischaemia, as a result of coronary artery occlusion. Survivors of MI are at an increased risk of sudden cardiac death due to their predisposition to lethal cardiac arrhythmias such as ventricular tachycardia (VT) and ventricular fibrillation (VF).

There are many pathophysiological changes associated with heart failure. Ventricular arrhythmias are seen to be a common cause of sudden cardiac death in patients suffering from heart failure. The pathogenesis of lethal ventricular arrhythmias is not fully understood but it is thought that there are many underlying mechanisms (Pye and Cobbe,1992). It is known that electrophysiological abnormalities exist in heart failure, but current knowledge regarding electrical restitution, dispersion of repolarisation and ventricular fibrillation threshold is far from complete.

Abnormalities in repolarisation and refractoriness, such as those seen in heart failure, may increase the propensity for the heart to become arrhythmic. Most of the literature reports a lengthening of action potential duration and refractory period in heart failure (Tomaselli *et al*, 1994; Qin *et al*, 1996) although some report a shortening (Docherty and Cobbe, 1990). In addition, there is a switch in the epicardial to endocardial gradient of action potential duration; the epicardial action potential becomes significantly longer than that of the endocardial. These

electrophysiological changes associated with heart failure are heterogeneous and therefore create a dispersion of repolarisation and refractoriness that may cause re-entrant arrhythmias to occur.

Repolarisation abnormalities can be studied in a limited way using conventional external electrode techniques such as electrocardiography. However, the strength of this technique is as a diagnostic tool rather than a probe of mechanism. Invasive techniques, using the bipolar and unipolar electrodes, can detect local myocardial activation unambiguously but give limited information concerning refractoriness and the period of repolarisation. Monophasic action potentials (MAPs) however, whilst detecting both activation and recovery, also provide detailed information regarding the membrane potential between the two (i.e. the shape of the MAP between depolarisation and repolarisation).

MAPs can be recorded from epicardial and endocardial surfaces of the in situ beating heart, including that of human subjects, using a contact catheter electrode. Due to its non-destructive nature, MAP recording is therefore the chosen method of studying local myocardial electrophysiology, especially repolarisation, in the clinical setting. So MAPs have bridged the gap between basic and clinical electrophysiology in arrhythmia research.

This chapter presents the results obtained using the contact catheter electrode to record the electrical activity over the epicardial surface of the left ventricle. The aims were to investigate the changes in repolarisation and arrhythmogenesis due to heart failure. Specifically the following were examined:

- i) Regional and global cycle length dependent changes in MAPD₉₀.
- ii) Changes in sequentially recorded dispersion of repolarisation.
- iii) Changes in ventricular fibrillation threshold.

Data from normal, healthy, hearts were compared to those from failing hearts.

4.2 Methods

General methods concerning Langendorff perfusion, SAN removal and AVN ablation are described in chapter 2. MAPs were recorded from the epicardial surface of the left ventricle using a single MAP catheter electrode as described in chapter 3. 33 control hearts (ejection fraction (\pm SEM) = $74.5\pm 1.76\%$) and 29 failing hearts (ejection fraction (\pm SEM) = $50.29\pm 1.51\%$) were used in this study.

Steady state restitution protocols allow cycle length (CL) dependent changes in MAP duration to be investigated. This involves pacing the heart over a range of CLs. The CL is abruptly changed at intervals once stabilisation of MAP duration at the preceding CL has reached steady state. The protocol used in this investigation involved the heart initially being paced at a CL of 350ms for 4 minutes, following which incremental changes of 100ms were made at 4 minute intervals. Changes in CL covered a range from 150ms to 1250ms. The protocol was terminated and CL returned to 350ms if the pacing cycle length reached exceeded the intrinsic cycle length of the heart (this became evident as extra-systoles or extended periods of diastole), otherwise the full range of CLs were used. On each occasion the heart was finally paced again at 350ms for 4 minutes to observe recovery of MAP duration. In this chapter the steady state restitution protocol refers to the relationship between frequency and action potential duration at a steady state.

At the end of each experiment ventricular fibrillation (VF) was induced. Ventricular fibrillation thresholds have previously been used in laboratory investigations and human studies to assess the overall vulnerability to fibrillation. VF was induced by inserting a catheter electrode into the right ventricle via the opening made as a result removing the SAN. VF was induced by a stimulation protocol using gradually increasing current in to the base of the right ventricle via the catheter. The protocol consisted of a train of 16 basic S1 stimuli at 350ms intervals followed by a train of 40 stimuli at 10ms intervals then a 1000ms interval (square pulse, 2ms duration). Incremental increases of 5mA were made between each protocol until VF was induced. Conversion back to normal rhythm was with a small bolus of 1M KCl administered directly in to the perfusion line. Following each episode of VF the heart was perfused with Tyrodes for 4 minutes, paced at a CL of 350ms, to ensure that normal electrical activity returned.

To estimate the dispersion of repolarisation in these hearts, measured sequentially using a single catheter electrode, the heart was arbitrarily divided into 9 regions as shown in Figure 4.1. Dispersion from each heart was taken as the standard deviation of $MAPD_{90}$. Dispersion data from all hearts at a range of CLs was averaged to produce an overall mean dispersion of repolarisation.

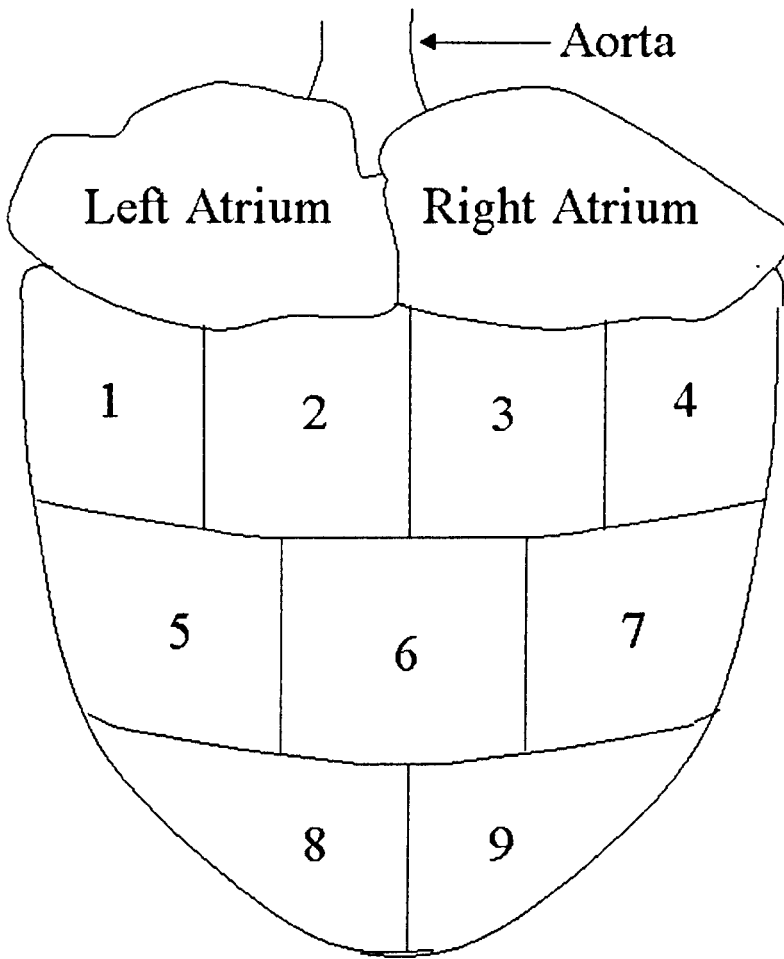


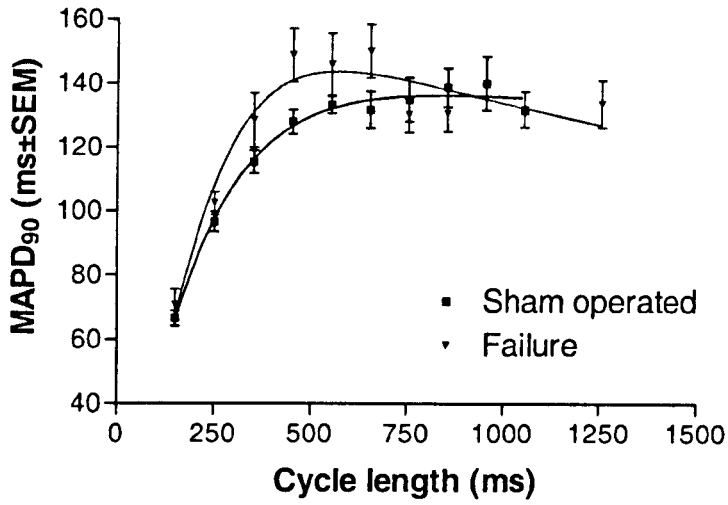
Figure 4.1 Schematic of the heart showing the division of the left ventricle for dispersion analysis. The left ventricular epicardial surface of the heart was arbitrarily divided into 9 areas to enable grouping of recordings for determination of dispersion.

4.3 Results

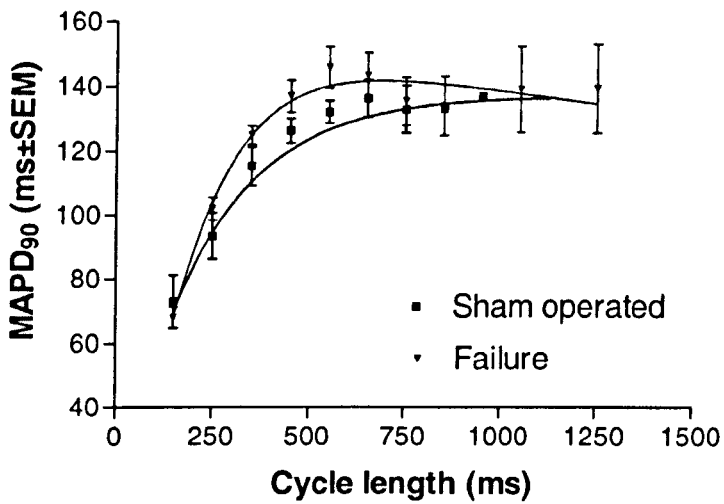
4.3.1 Cycle length dependent effects on MAP duration in sham operated and failure hearts

33 control hearts and 29 failing hearts were used to compare the steady state restitution properties of failing hearts with those of sham operated hearts. MAP duration (90% repolarisation) were plotted against cycle length (Figure 4.2). Each graph refers to one of the defined areas of the heart. Areas 8 and 9 are omitted due to the inability to obtain recordings over the area of infarction in failure hearts. The most obvious feature of these graphs is the general tendency for a prolongation of $MAPD_{90}$ in heart failure that is seen in 6 of 7 sites.

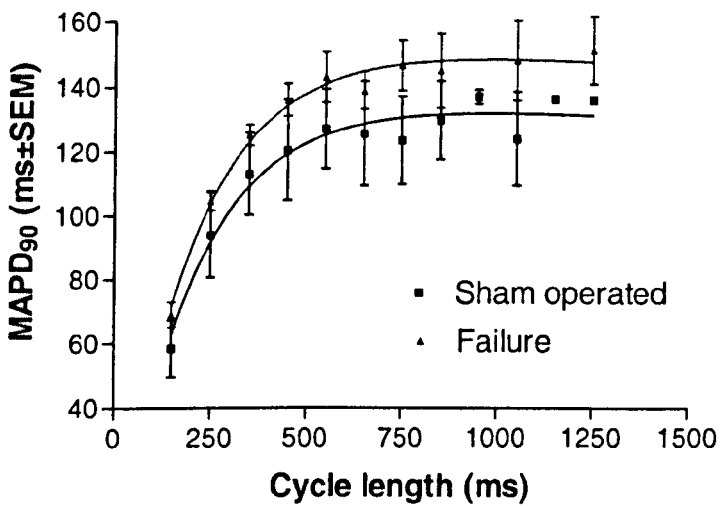
Data in Table 4.1 are absolute positive or negative changes in $MAPD_{90}$ from sham operated to failure heart data at a range of cycle lengths (150ms to 1250ms). This numerically represents the data shown graphically in Figure 4.2. The level of significance is indicated by asterisks. Numbers for each area at each cycle length are shown in brackets (sham, failure). All data (sham versus failure MAP duration at each cycle length) was analysed using an unpaired Student's t-test. The prolongation of MAP duration was only significant ($P < 0.05$) in data obtained from area 5, other areas did not show a prolongation of MAP duration. However on applying the Bonferroni correction, which adjusted the level of significance to < 0.005 , there was no significant prolongation in MAP duration in area 5.



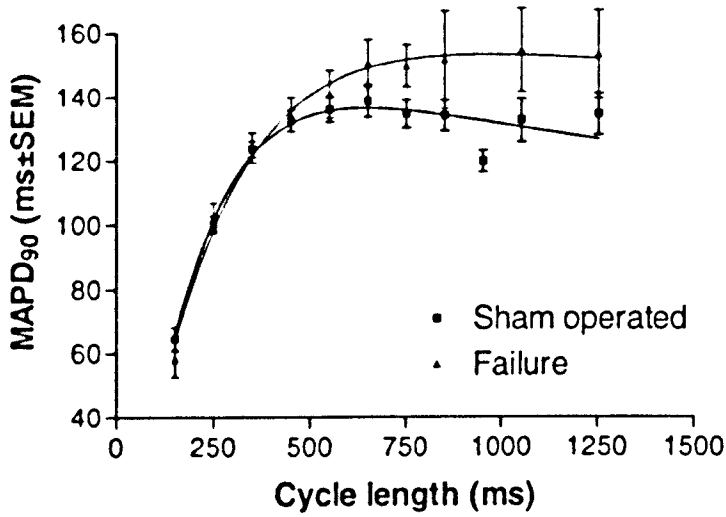
Area 1



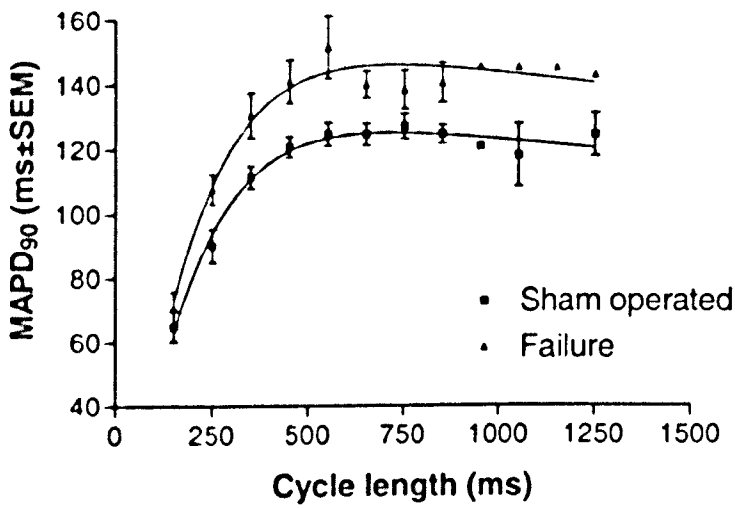
Area 2



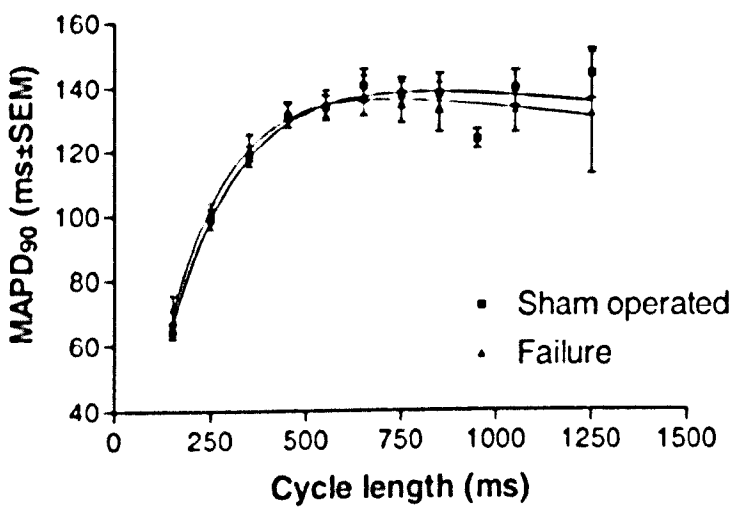
Area 3



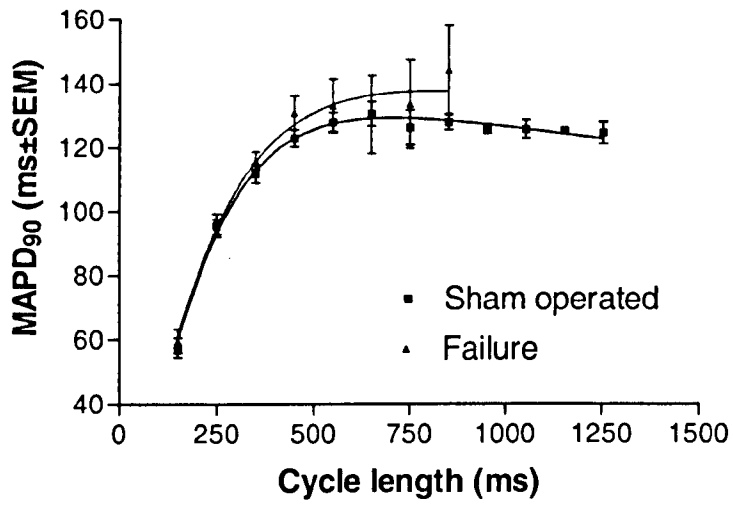
Area 4



Area 5



Area 6



Area 7

Figure 4.2 MAP duration v CL in failure hearts and sham operated hearts. All values are shown as mean ± SEM.

CL (ms)	Area						
	1	2	3	4	5	6	7
150	+4.27 (9,7)	-4.93 (7,9)	+8.42 (13,6)	-6.22 (10,7)	+5.68 (10,5)	+7.08 (10,6)	+2.12 (10,9)
250	+5.61 (9,10)	+8.56 (7,10)	+8.74 (13,10)	+2.42 (10,10)	+17.8* (10,10)	+0.96 (10,9)	-0.45 (10,10)
350	+13.16 (9,10)	+9.56 (7,10)	+9.1 (13,10)	+0.48 (10,10)	+19.23 (10,8)	+2.49 (10,8)	+4.21 (10,11)
450	+30.76 (8,8)	+10.72 (7,8)	+11.06 (13,8)	+1.94 (10,9)	+20.26* (9,8)	+0.13 (9,7)	+1.18 (10,11)
550	+12.57 (8,7)		+12.21 (13,6)	+4.71 (10,7)	+26.85* (8,8)	+1.44 (8,7)	+5.01 (9,7)
650	+18.3 (5,7)		+0.01 (8,5)	+15.31 (9,6)	-3.35* (9,5)	-3.05 (9,5)	-0.32 (7,3)
750	-4.81 (4,5)	+2.4 (5,4)	+11.62 (9,3)	+15.09 (9,3)	+11.23* (8,5)	-2.82 (7,5)	+7.3 (6,3)
850	-8.27 (3,5)	+0.72 (3,4)	+10.44 (10,2)	+17.44 (10,2)	+15.83* (4,3)	-4.67 (6,4)	+16.35 (4,2)
1050	----	----	+14.9 (7,2)	+22 (7,2)	-6.41 (4,4)	-6.74 (4,4)	----
1250	----	----	-14.5 (4,2)	+18.5 (4,2)			

Table 4.1 The effect of heart failure on MAPD₉₀. Positive or negative change in MAPD₉₀ from sham operated to failure hearts. Perfusion with Tyrodes. n-number in brackets (sham operated hearts, failure hearts). *P<0.05, unpaired Student's t-test (uncorrected).

4.3.2 Global differences in MAP duration between heart failure and sham operated hearts

In Figure 4.3 all the area data from both the sham operated and failure hearts have been pooled together to give a mean overall global MAP duration. The graphs show that in failure there is a global increase in MAP duration at all cycle lengths, although this increase appears to be more prominent at intermediate cycle lengths. In heart failure there was significant ($P < 0.05$, unpaired Student's t-test) increase in MAP duration, between cycle lengths of 250ms and 650ms, as compared to sham. Data were also statistically compared using a two way ANOVA which showed that failure significantly increases MAP duration at a level $P < 0.0001$.

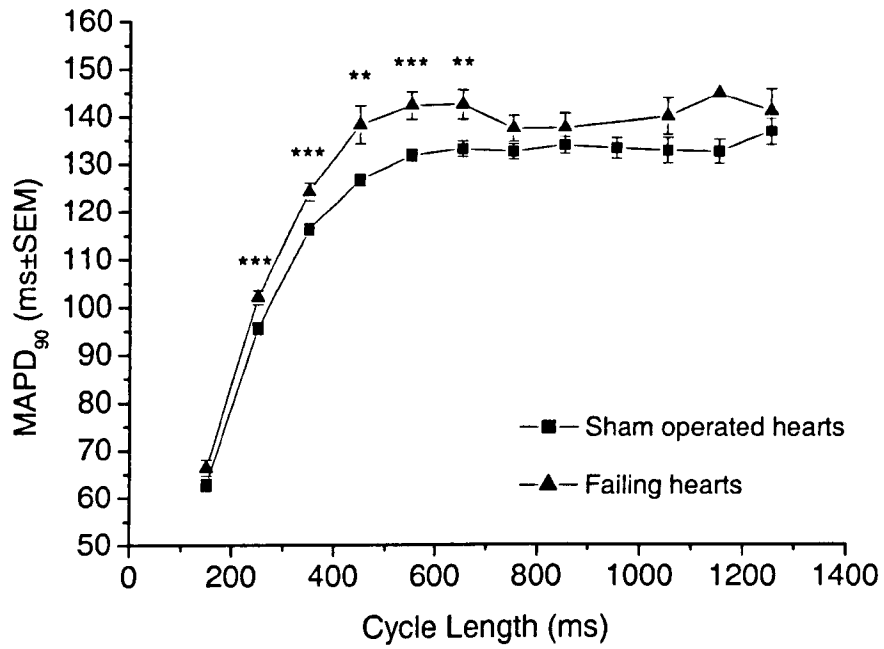
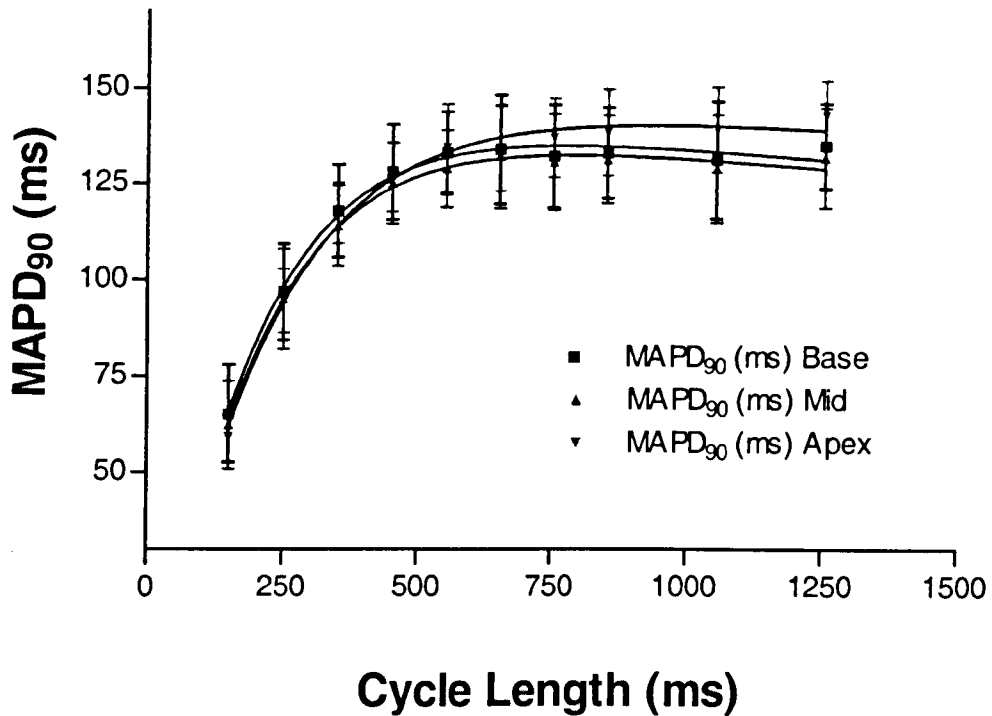


Figure 4.3 The effect of heart failure on global MAPD₉₀. Data points are shown \pm SEM. **P<0.01, ***P<0.001, unpaired Student's t-test. P<0.0001 by two way ANOVA.

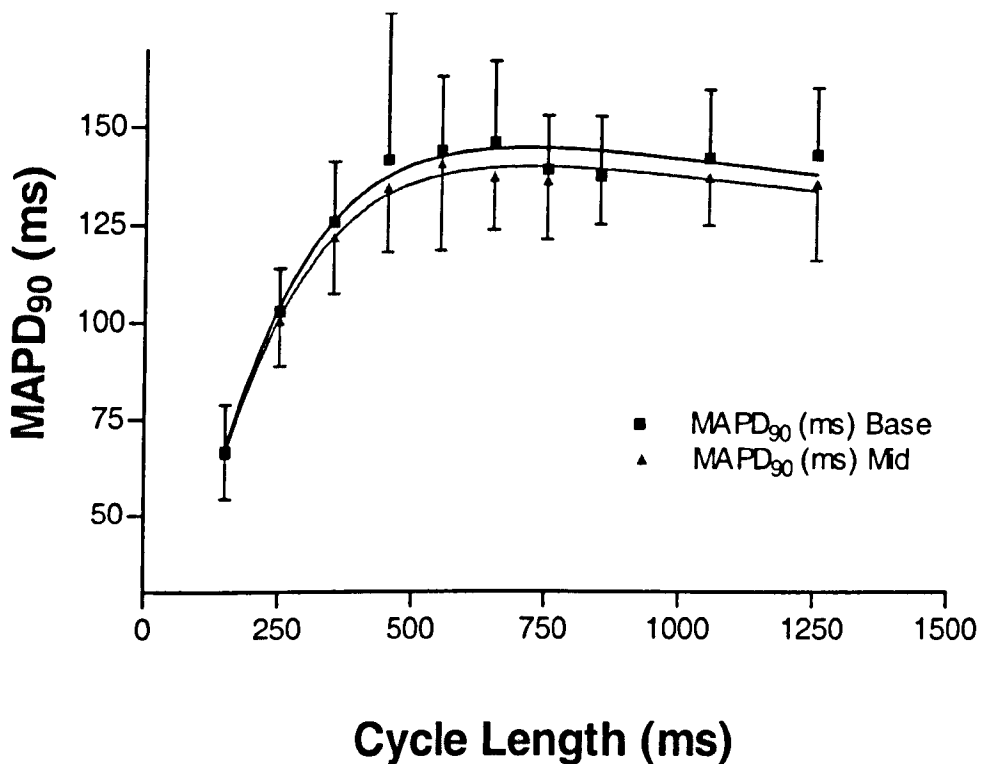
4.3.3 Base to apex differences between sham operated and failing hearts

Figures 4.4 illustrates the dispersion of repolarisation from basal to apical regions of the heart in sham operated (A) and failure (B) hearts. The base encompasses areas 1 to 4, mid areas 5 to 7, and apex areas 8 and 9. Apical regions (area 8 and 9) are omitted in comparisons with failing hearts due to the area of infarction. The graphs show that there is a slight, but non-consistent difference in MAP duration between regions of the heart. Areas were compared using a one-way ANOVA test in the case of the sham-operated data (base, mid, apical), and an unpaired Student's t-test in the case of the failure data (base and mid). Regions were compared to each other at each cycle length. The tests showed that MAP duration does not alter differences between regions.



A. Base to apex differences in MAP duration in sham operated hearts.

Values shown \pm SD.



B. Base to apex differences in MAP duration in failing hearts. Values

shown \pm SD.

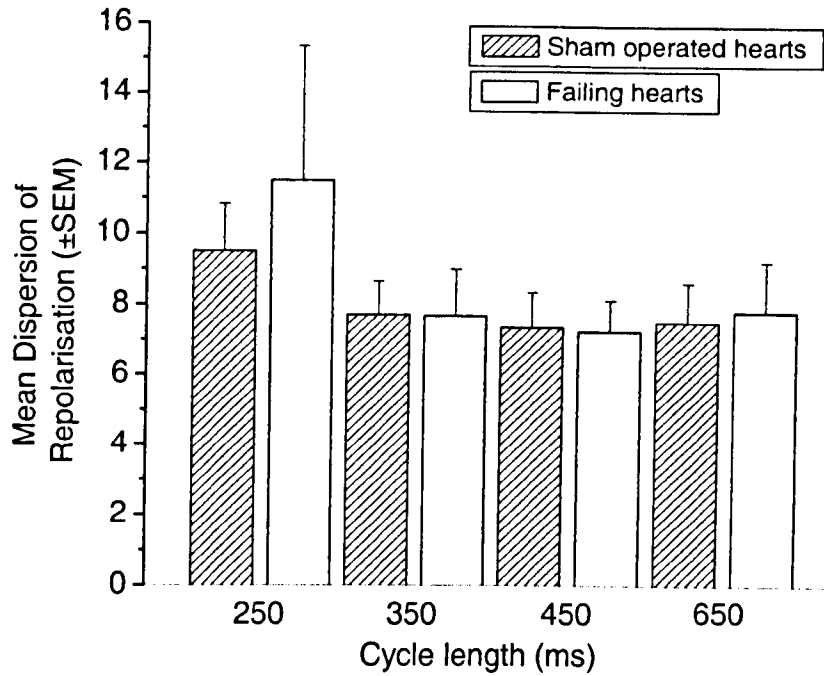
Figure 4.4 Base to apex differences in MAP duration.

4.3.4 The effect of failure on dispersion of repolarisation

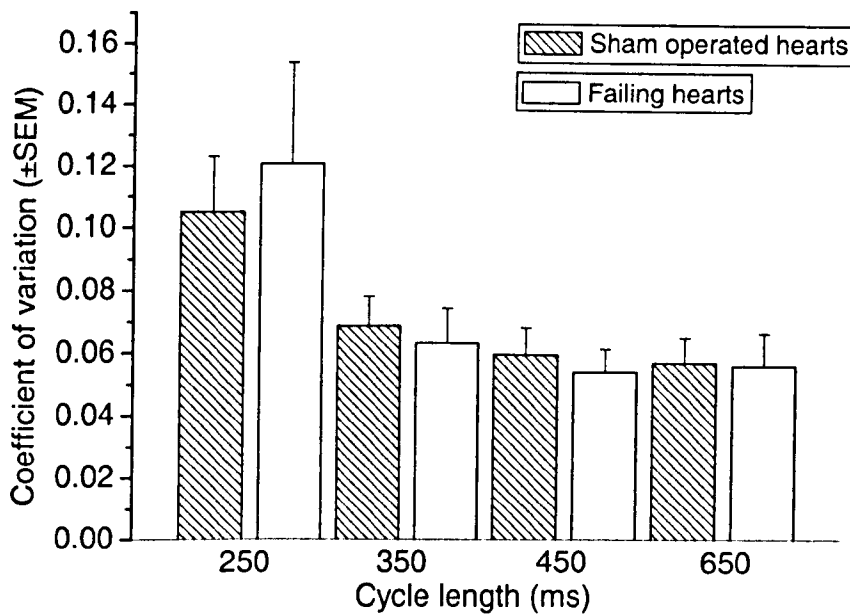
Dispersion of repolarisation was calculated for a range of CLs: 250ms, 350ms, 450ms, and 650ms. These specific intervals were chosen on the basis that the quantity of data obtained for each was sufficient for statistical comparison. The results in Figure 4.5a show no change in the mean dispersion of repolarisation between normal and failing hearts over a wide range of cycle lengths (as compared using an unpaired Student's t-test). Figure 4.5b represents the data as coefficient of variation. Absolute values of the mean dispersion of repolarisation are shown in Table 4.2.

Cycle Length	DOR Sham (\pm SEM)	n hearts	DOR Failure (\pm SEM)	n hearts
250	9.49 \pm 1.33	25	11.49 \pm 3.84	10
350	7.71 \pm 0.93	26	7.68 \pm 1.33	26
450	7.36 \pm 0.97	25	7.24 \pm 0.88	21
650	7.50 \pm 1.10	21	7.79 \pm 1.42	17

Table 4.2 Absolute changes in mean dispersion of repolarisation.
(DOR=dispersion of repolarisation).



A. Dispersion of repolarisation



B. Coefficient of variation.

Figure 4.5 The effect of failure on dispersion of repolarisation at a range of cycle lengths. Failure does not alter the sequentially recorded dispersion of repolarisation ($P > 0.05$, unpaired Student's t-test).

4.3.5 Ventricular fibrillation thresholds

Figure 4.6 shows an experimental trace where VF was induced in Tyrodes solution. The recording shows left ventricular developed pressure as recorded by the intraventricular balloon. To the left of the trace the heart was being paced at 350ms intervals, following this a train of stimuli was applied followed by an extended diastolic interval. The train of stimuli was repeated at an increasing current (5mA increases) until VF was induced (the ventricular fibrillation threshold). The uncoordinated events to the right of the trace is VF. VFT in this case was 30mA. The box and whisker plot in Figure 4.7 illustrates the difference in ventricular fibrillation threshold (VFT) between sham-operated and failure hearts. Mean threshold decreased from 34.58 ± 8.54 mA in sham operated hearts (n=12) to 26.16 ± 3.89 mA in failure hearts (n=43) (mean \pm SEM). This difference was not significant ($P > 0.05$).

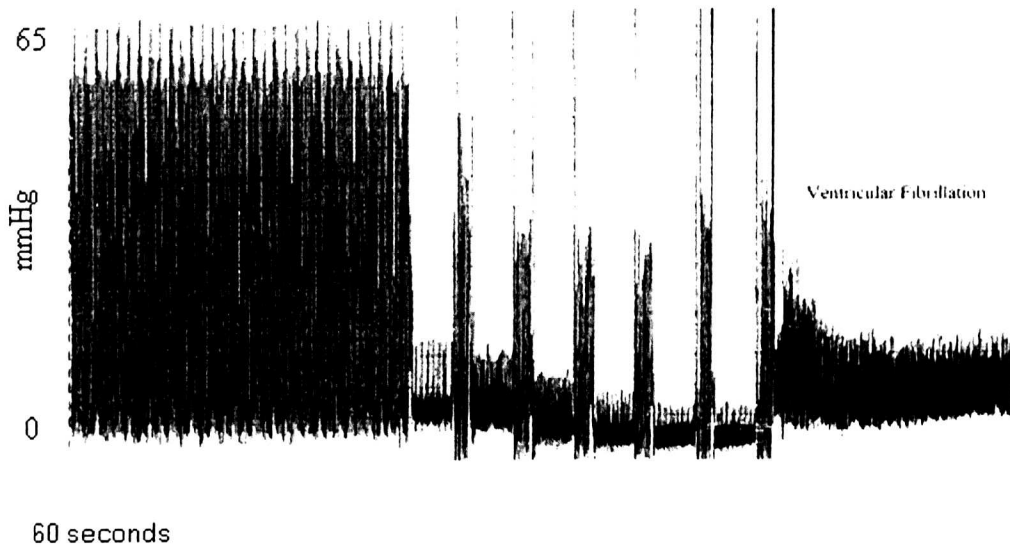


Figure 4.6 Experimental trace showing ventricular fibrillation induction.

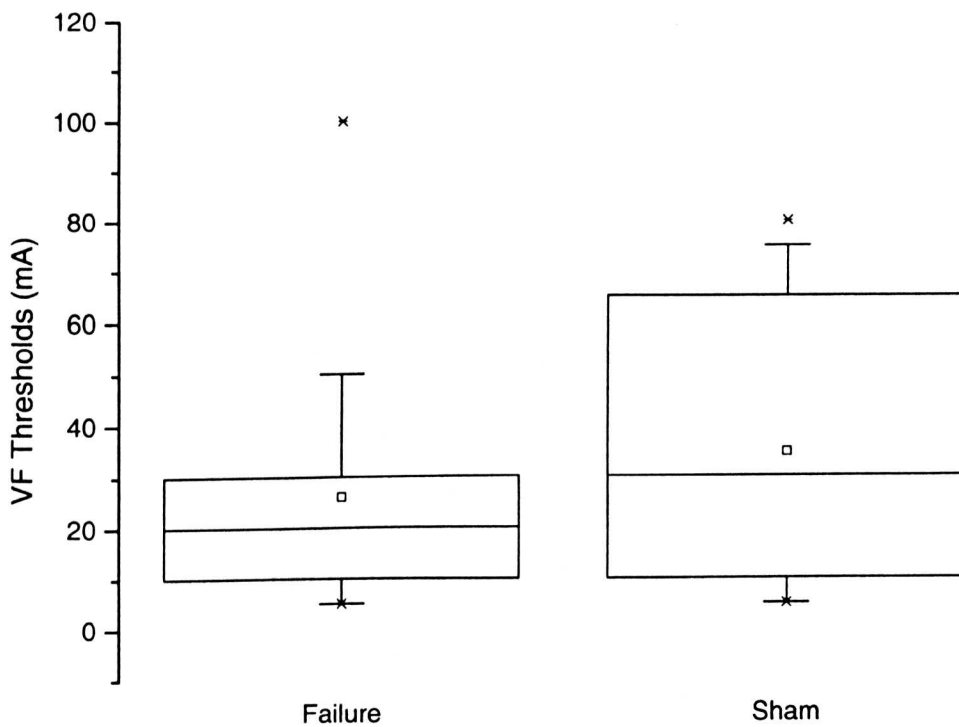


Figure 4.7 The effect of heart failure on ventricular fibrillation threshold. Failure causes a small decrease in VFT.

4.4 Discussion

The main reported electrophysiological abnormalities in heart failure are action potential duration prolongation and an increased dispersion of repolarisation/refractoriness as a result of electrical remodelling (reviewed in Wolk *et al* 1997). On theoretical grounds, one would expect to associate an increase in dispersion of repolarisation with a decreased ventricular fibrillation threshold. Our data indicates that heart failure does not change the dispersion of repolarisation nor does it change ventricular fibrillation threshold.

4.4.1 Ionic basis of action potential duration prolongation in heart failure

Although there was no change in MAP duration in individual areas, this study saw a global increase in MAP duration in ligated hearts across a wide range of stimulation frequencies with significant results being obtained at stimulation frequencies up to 650ms. Much work has been done to attempt to explain the ionic basis for the prolongation in action potential duration seen in heart failure. In humans, a prolongation of the action potential plateau may be due to reduced repolarising outward currents or a net increase in depolarising inward currents, or both (Pye & Cobbe, 1992). Na^+ - Ca^{2+} exchange is the primary mechanism by which Ca^{2+} is expelled from the myocyte. This generates an inward current that may effect repolarisation time. Changes in this current may cause action potential duration changes and an increase in arrhythmogenesis in hypertrophied hearts.

Several studies have investigated the effect of heart failure in human subjects. Jongasma (1999) stated that the increase in action potential duration seen in failing hearts is attributable to the decrease in expression of I_{to} . Hart (1994) also suggested that changes in K^+ (inward rectifier, I_{K1} , and the transient outward, I_{to1}) currents

might play a role in the prolongation of the action potential duration in hypertrophied hearts. Beuckelmann *et al* (1993) also attributed action potential duration prolongation in severe heart failure to a reduction in the inward rectifier K^+ current and of the transient outward K^+ current. It was also thought that the L-type Ca^{2+} current could cause action potential duration prolongation by its delayed inactivation, although at that time controversy existed as other workers had found no change (Pye and Cobbe, 1992). However, in 1999 Jongsma reported that action potential duration prolongation seen in heart failure (not end-stage) is attributed, in part, to an increase in the L-type Ca^{2+} current.

In a rabbit model of heart failure, Ng (1998) found that the time to peak of the MAP recorded using the suction electrode technique, was significantly longer in failing hearts than healthy hearts with the difference being maintained throughout the rest of the signal. However, the time course of these signals were timed from the start of upstroke of the action potential to various points of repolarisation whereas those in this study were analysed from the maximum slope of the upstroke (dv/dt_{max}). It was suggested that prolongation of the action potential in heart failure occurs mainly in the earlier phases and that this may be a result of a reduced outward current, increased inward current, or both.

4.4.2 Base to apex differences

Transmural heterogeneity in action potential duration is an area that has been comprehensively researched both in the normal heart (Li *et al*, 1999) and the failing heart (McIntosh, 1998). However base to apex differences in action potential duration have been somewhat neglected. In this particular study there was no change in the MAP duration between the basal and apical regions of the left

ventricle in both the normal and the failing heart. However, this is in conflict with the evidence of trans-epicardial differences found by other groups.

Cheng *et al* (1999) investigated base to apex differences in action potential duration and the E-4031-sensitive component (I_{Kr}) and in sensitive component (I_{Ks}) of the delayed rectifier, I_K , in isolated myocytes from the left ventricle of the rabbit heart using whole-cell patch clamping. They showed that action potentials obtained at 1Hz were substantially shorter in the base than the apex. They attributed this disparity in action potential duration to a higher density of expression of I_{Kr} in the apex than the base of the rabbit left ventricle. Similar gradients have been reported in other species. For example, Brahmajothi *et al* (1996) who showed that ERG, the gene that encodes the protein responsible for I_{Kr} is expressed more abundantly in all areas of the epicardium of the ferret ventricle, except in the base.

In contrast to the results found by these groups who showed a trans-epicardial dispersion of repolarisation, but in correlation with our results, a group from Breithardt's laboratory in Münster, Germany found no significant dispersion (personal communication). They recorded MAPs from the left and right ventricle of the rabbit heart using a cantilever system. This system allowed 2 MAPs to be recorded from the base, 2 from the mid, and 2 from the apex of the heart. In this personal communication, they commented that they did not observe base to apex differences (compared only between left and right ventricle).

Dean and Lab (1990), in a study using the *in situ* pig heart, found that increasing the left ventricular systolic pressure by aortic clamping caused a reduction in mean effective refractory period that was associated with a decrease in action potential

duration. The changes seen in this study were heterogeneous, with a larger change occurring at the apex than the base. Heterogeneity of repolarisation is potentially arrhythmogenic. Hence the findings of Dean and Lab suggest that increased ventricular load, as seen in heart failure, may be arrhythmogenic (see below).

An interesting study by VanTyn and MacLean (1961) on the important factors in determining ventricular fibrillation threshold indicated that there is also a base to apex dispersion of ventricular fibrillation threshold in the left ventricle in the canine heart.

4.4.3 Dispersion of repolarisation/refractoriness and ventricular fibrillation threshold

An increase in dispersion of refractoriness has been associated with a decrease in ventricular fibrillation threshold (Han and Moe, 1964; Janse and Wit, 1989; reviewed in Burton and Cobbe, 2001). The results of our study showed heart failure does not cause an increase in the dispersion of repolarisation nor does it change ventricular fibrillation threshold. There may be several reasons for our apparent lack of increased dispersion of repolarisation and decreased ventricular fibrillation threshold in heart failure. One possible explanation may be that the severity of heart failure in this study was too mild to show a significant difference. However, previous results in this lab (Burton *et al*, 1998), obtained from the same rabbit model of heart failure, showed that VFT was significantly lower in a severe left ventricular dysfunction (LVD) group compared to controls. Burton *et al* (1998) found that left ventricular ejection fraction was <45%. Using the intervals between local activations during VF to measure local refractoriness they also found that dispersion of refractoriness was greater in the severe LVD group than the

control. Although ventricular dilatation decreased VFT in normal hearts, it did not cause any further decrease in VFT in hearts with severe LVD. Latent inhomogeneities in the local dispersion of refractoriness in the normal myocardium of the LVD group were however apparent. Despite no observed increase in dispersion of epicardial MAP duration in failing hearts, Bryant *et al* (1997) concluded that the differences in action potential duration between sub-endocardial and sub-epicardial myocytes in normal hearts is lost in hypertrophy (in guinea pig hearts with mild cardiac hypertrophy induced by aortic constriction).

An interesting special communication by Cha *et al* (1993) delved in to the hypothesis that ventricular fibrillation threshold testing is a probability function. They tested ventricular fibrillation threshold in open chested dogs using the single premature stimulus or the train of stimuli method with increasing current strengths. They showed that there was a wide spread of stimulus strengths associated with a 0% and 100% probability of ventricular fibrillation induction, which they concluded indicated that an all or none threshold for ventricular fibrillation is absent. So taking this in to consideration, how accurate a measure of arrhythmia inducibility is ventricular fibrillation threshold testing?

A further reason for an apparent lack of difference between control and LVD hearts in dispersion of repolarisation or ventricular fibrillation threshold in this study could be that Langendorff perfused hearts show less of a difference compared to working hearts due to the difference in loading conditions. Although the effect of heart failure on dispersion and ventricular fibrillation threshold has little been studied, many groups have investigated the effect of increased ventricular load on dispersion of refractoriness and its consequent effects on ventricular fibrillation and

arrhythmia inducibility. Since pressure overload or ventricular dilatation leads to hypertrophy, which is a compensatory mechanism seen in heart failure, it is fair to discuss such experiments in relation to heart failure itself.

Reiter *et al* (1988) linked dilatation of the left ventricle in the isolated rabbit heart to an increase in dispersion of refractoriness. In a later study Reiter, along with co-workers Jalal *et al* (1992), investigated the effect of acute ventricular dilatation on refractoriness and fibrillation threshold, again in the isolated rabbit heart. They showed that ventricular dilatation (of either ventricle) consistently decreased ventricular fibrillation threshold and that this decrease was highly and linearly correlated with the decrease in local refractoriness. Calkins *et al* (1989a) found that, in the isolated blood perfused infarcted canine heart, an increase in left ventricular end diastolic volume increased the inducibility of arrhythmia. This increase in inducibility was, again, associated with shortening of refractoriness. In contrast, in the *normal* isolated blood perfused canine heart, later work by Calkins and co-workers (1989b), found no change in ventricular fibrillation threshold or inducibility of arrhythmias on increased volume load in the ventricles. They suggested that in the normal blood perfused mammalian heart under steady state conditions, volume load is not a significant electrophysiological factor. Loading conditions may be of greater significance in the infarcted heart in both an electrophysiological and pro-arrhythmic sense.

A final reason that may explain the absence of a decreased ventricular fibrillation threshold in failing hearts is the method used to induce VF. The animal model of heart failure used in this study produces an apical infarct in the left ventricle that may extend into the apex of the right ventricle. Since the VF induction catheter is

inserted in to the right ventricle and rests in the apex it is entirely possible that the infarcted region restricts the induction of VF and hence increases the overall mean threshold for induction.

4.4.4 Conduction delay

Although this part of the investigation did not involve measurements of conduction delay or indeed conduction velocity it is a parameter that is measured in work that will be discussed later. Left ventricular hypertrophy has been associated with changes in cell to cell electrical coupling (Cooklin, 1997; Jongsma 1999). Cooklin *et al* (1997) used a guinea pig model of myocardial hypertrophy where the aorta was constricted for 150 days. They found an increase in intercellular resistance that was attributable to an increase in junctional impedance between adjacent cells. As mentioned, electrical conductance via connexins can be mediated by i) a fall in intracellular pH or Ca^{2+} concentration, or ii) an alteration of the number, distribution or type of connexin subtype. Cooklin *et al* suggested that conductance is altered in myocardial hypertrophy by the latter of the above mentioned options. This was concluded as an intracellular acidosis of 0.19 pH units that accompanies left ventricular hypertrophy in the model they used would only decrease conductance by approximately 4%. Also, pH buffering is greater in hypertrophied hearts than normal hearts. Cooklin *et al* also discussed the importance of the effect of an increase in intercellular resistance on a reduction in conduction velocity of the action potential. If conduction velocity were to decrease equally in all dimensions (longitudinally and transversely) during hypertrophy there may be an increased propensity for the occurrence of re-entrant circuits to develop. The effect of intercellular resistance is an important aspect of altered conduction velocity. A change in conduction velocity may be implicated in arrhythmogenesis in the failing

heart. Pharmacological interventions that alter intercellular resistance are a focus of the remainder of this study.

**Chapter 5 – The effect of 1-heptanol on whole heart
electrophysiology in normal and failing hearts recorded by the
Franz MAP catheter technique**

5.1 Introduction

5.1.1 Gap junction uncoupling and 1-heptanol

Gap junctional conductance (g_j) is regulated by numerous mechanisms such as the phosphorylation state of connexins (Bastide *et al*, 1995), transjunctional voltage, $[H^+]_i$, $[Ca^{2+}]_i$, [ATP] and cellular fatty acid composition (Bastiaanse *et al*, 1993; Jongasma and Wilders, 2000). Many substances have been found to reduce g_j including lipophilic agents such as halothane (He and Burt, 2000), aliphatic alcohols such as heptanol and octanol (Zhang *et al*, 1996), and stearic acid derivatives (Takens-Kwak *et al*, 1992). The focus of this study is however the effects of 1-heptanol.

The Takens-Kwak group correctly supposed the decrease in g_j must be as a result of either a reduction in the number of gap junction channels, a reduction in the conductance of individual channels or a reduction in the duration each channel is open. They suggested that heptanol does not remove gap junctions, or decrease the conductance of the individual gap junction. If heptanol removed gap junction channels a change in junctional current (I_j) would be expected. However there was no change in I_j before uncoupling with heptanol and following washout of the agent. Single channel conductances were also collected and no change shown between the perfused and undisturbed cells, indicating that heptanol does not uncouple cells by decreasing the conductance of single channels. It was however, by process of elimination, assumed that heptanol changes the gap junction protein conformation by altering the membrane and therefore decreases the gap junction open probability. This hypothesis was also suggested by Lars Bastiananse *et al* (1993). A direct interaction of heptanol with a membrane component is also

suggested due to the speed at which electrical uncoupling occurs (2mM completely uncouples cardiomyocyte pairs in less than 200 seconds). The speed at which this occurs suggests that removal of gap junctions from the membrane is not likely.

5.1.2 Mechanisms of action of 1-heptanol

Several hypotheses have been proposed for the possible mechanism of action of heptanol. These are i) an alteration of the lipid environment around the channel leading indirectly to alterations in the gap junctional protein conformation, ii) a direct effect on the channel by binding to the protein, and iii) an indirect mechanism mediated through an increase in intracellular Ca^{2+} concentration, or a change in intracellular pH. The first hypothesis suggests that the uncoupling action of heptanol, and other lipophilic molecules, is a result of alterations in the lipid component of the membrane bilayer. This has been noted as the most likely mechanism of heptanol induced uncoupling. Evidence to support this hypothesis is discussed below. The second hypothesis assumes a direct interaction with the channel protein, and is difficult to distinguish from the first proposed mechanism. The third hypothesis suggests an effect of changes in pH and Ca^{2+} concentration on cellular uncoupling. Buffering Ca^{2+} however, has been shown not to have an effect on heptanol induced uncoupling in cardiac myocytes from guinea pigs and rats (Rudisuli, 1989; Takens-Kwak, 1992). Rudisuli (1989) showed no change in the single channel current upon moderate elevation of $[\text{Ca}^{2+}]$ by weak intracellular Ca^{2+} buffering (EGTA, 0.1mM, no added CaCl_2) as compared to experiments using strongly buffered (EGTA 10mM, CaCl_2 1mM) solution.

Lars Bastiaanse *et al* (1993) did a comprehensive investigation, using neonatal rat myocytes in a combined fluorescence anisotropy and electrophysiological study. They investigated the effect of heptanol on the fluidity of the membrane cholesterol rich domains. Knowing that gap junction channels are embedded in cholesterol rich domains of the membrane, this group attempted to assess the effect of heptanol and another lipophilic agent 2-(methoxyethoxy)ethyl 8-(cis-2-*n*-octylcyclopropyl)-octanoate (A₂C) on the fluidity of the membrane. They did this by measuring junctional and non-junctional membrane currents and steady state anisotropy (r_{ss}), which decreases as membrane fluidity increases, in different membrane domains. They found that both A₂C and heptanol increased bulk membrane (sarcolemmal) fluidity. However, while A₂C does not affect g_j , heptanol decreases it indicating that sarcolemmal fluidity is not a determinant for gap junctional conductance, and that the increase seen with heptanol is not responsible for its uncoupling effect.

In whole cell voltage clamp experiments on pairs of cells, heptanol was found to completely uncouple the cell pairs whilst A₂C did not. Using dehydroergosterol (DHE) to specifically assess the fluidity of the cholesterol rich domains it was found that heptanol decreased fluidity whereas A₂C had no effect. Increasing cholesterol content of the cells decreased the gap junctional uncoupling effect of heptanol whilst non-junctional conductance remained unaltered, highlighting the relative importance of changes in the fluidity of the cholesterol rich domain rather than merely the bulk membrane fluidity.

The effect of heptanol on dispersion of repolarisation has not been widely studied. The effect of heptanol on arrhythmia inducibility has however been relatively

widely studied (Boersma et al, 1994; Callans *et al*, 1998). This part of the study concentrates on the effect of heptanol on mechanical and electrical activity, including dispersion of repolarisation and ventricular fibrillation threshold, in normal and failing hearts.

5.2 Methods

MAPs were measured using a single catheter electrode (as described in chapter 3) from the epicardial surface of the left ventricle. MAPs were measured from 9 areas of the epicardial surface of the left ventricle (Figure 4.1). The heart was initially perfused with Tyrode's solution and paced at a basic cycle length (CL) of 350ms via bipolar pacing electrodes at the base of the right ventricle. A settling period of approximately 20 minutes was allowed to allow the heart to physiologically stabilise in the artificial system.

Once a good quality MAP recording was obtained the following protocol was performed. The heart was initially perfused with Tyrode's solution and paced at 350ms for 4 minutes, prior to making incremental CL changes. CL was increased in increments of 100ms starting with 150ms, proceeding until pacing cycle length exceeded the intrinsic cycle length, or 1250ms was reached. Each cycle length was maintained for 4 minutes prior to change. CL was then returned to the basic CL of 350ms for 4 minutes. In this chapter the steady state restitution protocol as described refers to the relationship between frequency and action potential duration at a steady state.

Perfusion was then changed to 0.3mM heptanol (Sigma, Poole, UK) solution via the 2-way switch incorporated in to the perfusion lines. Because of the lipophilic nature of heptanol it is insoluble in water so it was dissolved in ethanol before adding to Tyrode's solution. Keevil *et al* (2000) reported that heptanol is soluble in aqueous solution up to a concentration of 9mM, however this was found not to be the case in this study as 0.3mM heptanol would not dissolve in an aqueous solution. The final concentration of ethanol in the solution was 0.005%. The heart was perfused with 0.3mM heptanol at the basic CL of 350ms for 5 minutes prior to running through the same protocol as described above for Tyrode perfusion.

In any single experiment several runs of the same protocol were made. At the end of a protocol, the catheter electrode was removed and placed on a different area of the epicardial surface of the left ventricle and the protocol run through again. This allowed acquisition of sequential data to quantify dispersion of repolarisation.

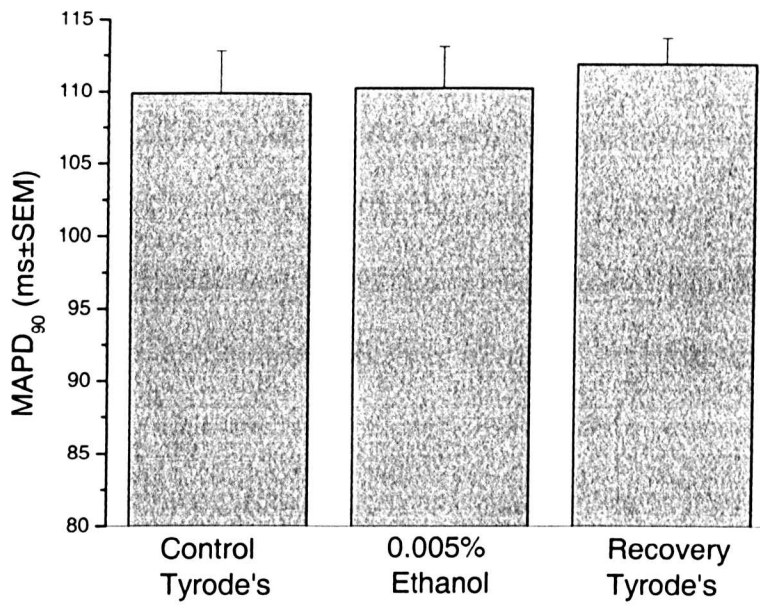
Ventricular fibrillation (VF) was induced at the end of each experiment, both in Tyrode's solution and 0.3mM heptanol. Refer to chapter 4 methods for details of VF induction.

MAPs were analysed at each CL to obtain MAPD₅₀, MAPD₉₀, and conduction delay (CD). Stimulus artefact was not observed in all cases, and hence in these cases CD could not be measured. Results were entered into an Excel database (Microsoft) and graphed in Origin (Microcal). One way ANOVA and paired or unpaired Student's t-tests depending on the data analysed. Refer chapter 2 general methods for details of statistical tests.

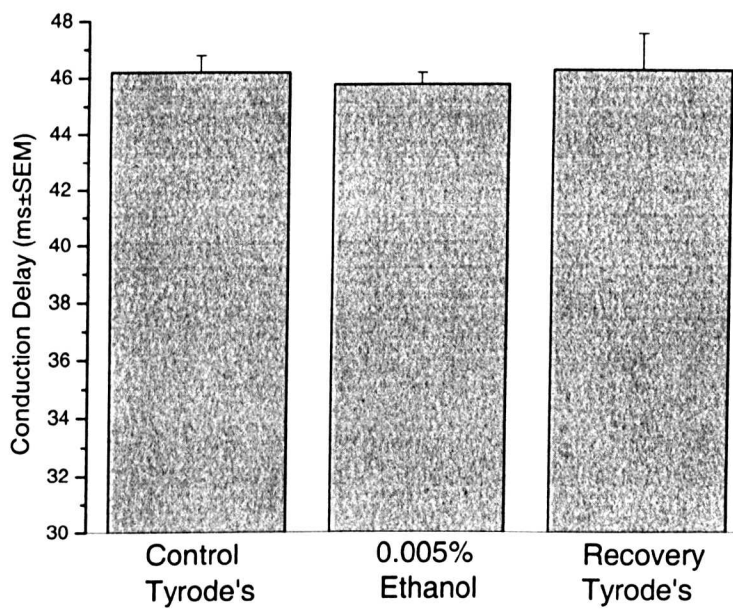
5.3 Results

5.3.1 The effect of ethanol on whole heart electrophysiology

Control experiments were done to ensure that the ethanol used to dissolve heptanol does not effect the electrophysiology of the whole heart. 4 control hearts were used in this study. Figure 5.1 illustrates the effect of 0.005% ethanol on MAP duration, at 90% repolarisation, and conduction delay. The heart was paced at 350ms for 4 minutes in normal Tyrode solution followed by 15 minutes perfusion with Tyrode's solution containing ethanol (0.005% final concentration). Ethanol was washed out for a further 15 minutes with normal Tyrode's solution. The results show that ethanol has no effect on MAP duration or conduction delay.



A. MAPD₉₀.



B. Conduction delay.

Figure 5.1 The effect of 0.005% ethanol on MAPD₉₀ (A) and conduction delay (B). n=4 hearts.

5.3.2 1-Heptanol dose response curve

Preliminary experiments were done to determine a suitable concentration of heptanol for study of gap junction uncoupling effects. Heptanol has previously been observed to have a considerable negative inotropic effect on the working myocardium. Reduction in contractility was used as the criteria for determining a suitable heptanol concentration. The heart was perfused with a range of heptanol concentrations (0.1 to 0.5mM), and the difference in peak systolic and end diastolic pressures calculated from chart recorder traces. The graph in Figure 5.2 shows the marked decline in left ventricular developed pressure (LVDP) with increasing heptanol concentration. From these plots, it was decided that a concentration of 0.3mM heptanol would be used for subsequent electrophysiological measurements.

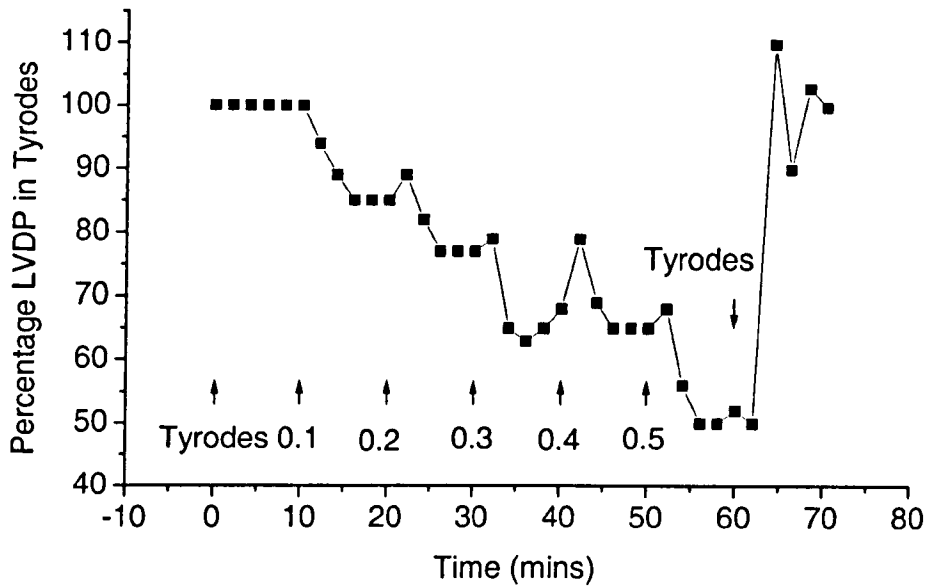


Figure 5.2 The effect of increasing heptanol (mM) concentration on left ventricular developed pressure (LVDP). Data is expressed as percentage of stable pressure in Tyrode's solution. Basic CL=350ms. Sham operated heart.

5.3.3 1-Heptanol reversibly modifies the mechanical activity in the whole heart

A typical experiment illustrating the changes in LVDP prior to, during, and after perfusion with 0.3mM heptanol is shown in Figure 5.3. The heart was perfused with Tyrode's solution for a period of 20 minutes prior to a period of 30 minutes perfusion with 0.3mM heptanol, followed by a period of 30 minutes reperfusion/washout with Tyrode's solution. The experiment shows that the negative inotropic effect of 0.3mM heptanol is completely reversible. The time lag of approximately 2 minutes prior to observation of pressure decline is due to the time taken for the new solution to reach the heart. The recovery of LVDP (approximately 12 minutes) on reperfusion with Tyrode, is slower than the decline (approximately 5 minutes) caused by perfusion with 0.3mM heptanol.

Figure 5.4 shows scanned traces of the LVDP recorded from a single experiment where the effect of 0.3mM heptanol on LVDP was investigated. The heart was initially perfused with Tyrode's followed by a 30 minute perfusion with 0.3mM heptanol solution. The negative inotropic effect of heptanol is illustrated in Figure 5.4a, and its reversibility by reperfusion with Tyrode's solution in Figure 5.4b.

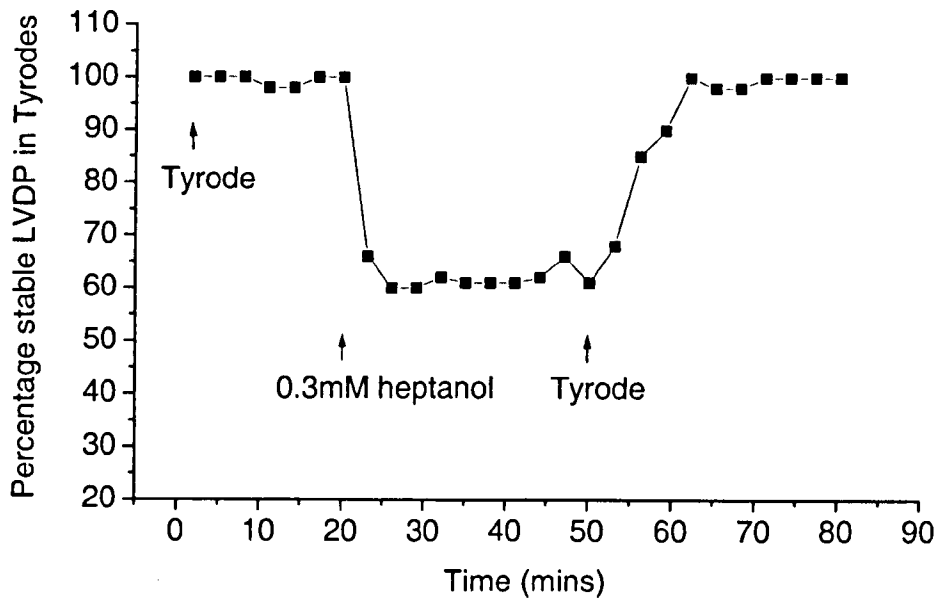
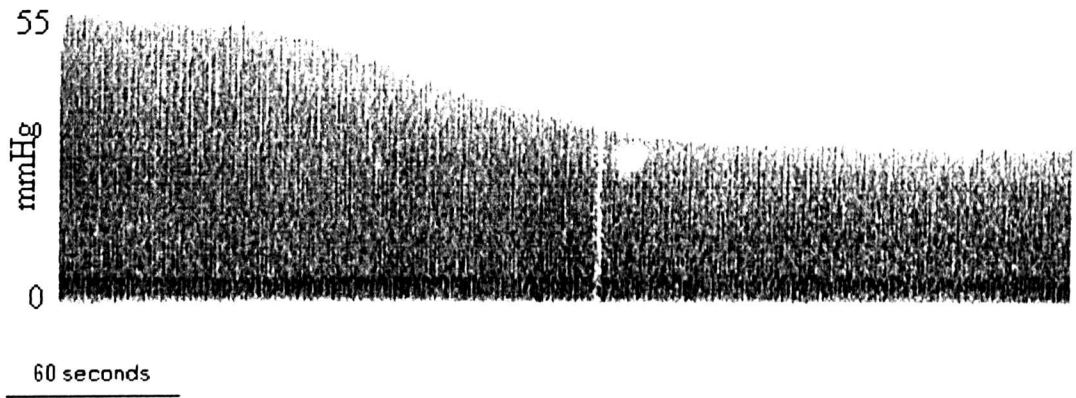


Figure 5.3 Reversible effect of perfusion with 0.3mM 1-heptanol on LVDP. Data are expressed as changes in the percentage stable pressure in Tyrode's. BCL=350ms. Sham operated heart.



A. The effect of 0.3mM 1-heptanol on LVDP.



B. The effect of 0.3mM 1-heptanol on LVDP is completely reversible.

Figure 5.4 The effect of 0.3mM 1-heptanol on LVDP as illustrated by experimental traces.

5.3.4 1-Heptanol reversibly modifies the electrical activity of the whole heart

A typical experiment illustrating the changes in MAPD₉₀ prior to, during, and after perfusion with 0.3mM heptanol is shown in Figure 5.5. The heart was perfused with Tyrode's solution for a period of 20 minutes prior to a period of 20 minutes perfusion with 0.3mM heptanol, followed by a period of 30 minutes reperfusion with Tyrode's solution. The effect of 0.3mM heptanol on MAP duration is reversible. A similar time lag to that described above can be seen. The recovery of MAP duration, on reperfusion with Tyrode's, is slower (15 minutes) than the observed decline (2 minutes) in MAP duration on perfusion with 0.3mM heptanol. Figure 5.6 shows a control MAP obtained in Tyrodes solution with a MAP obtained after perfusion with 0.3mM heptanol.

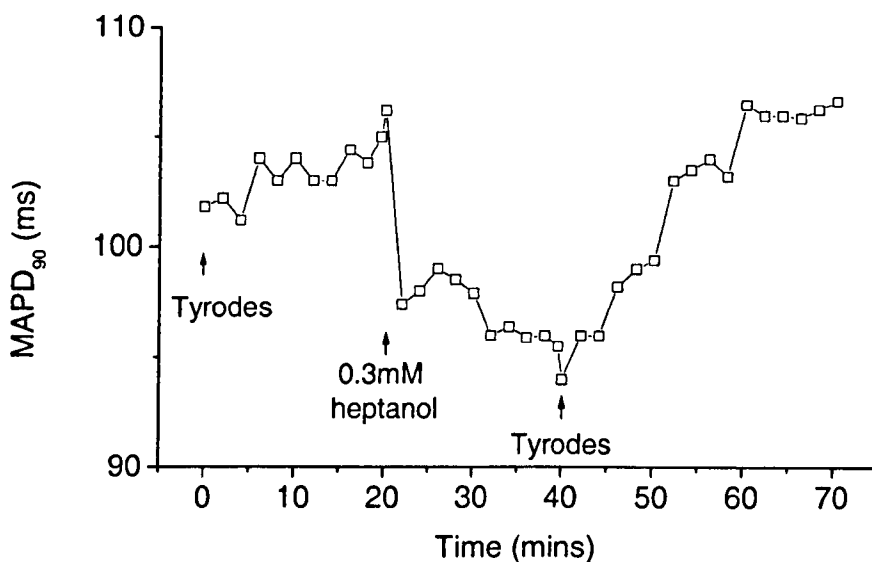


Figure 5.5 Reversible effect of perfusion with 0.3mM 1-heptanol on MAPD₉₀. BCL=350ms. Sham operated heart.

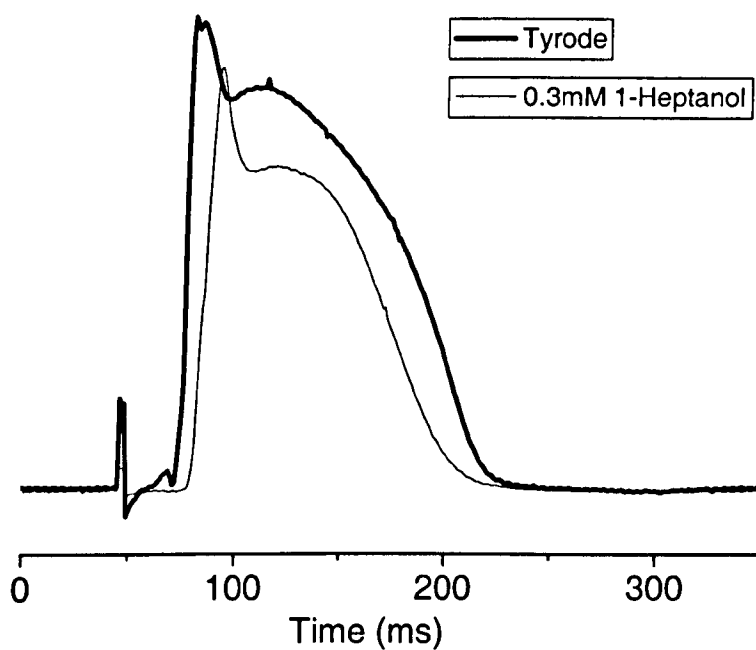


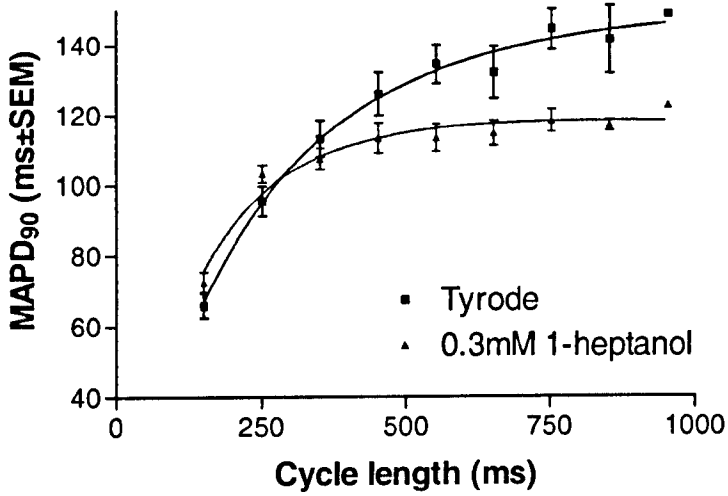
Figure 5.6 The effect of 0.3mM 1-Heptanol on single MAPs. Heptanol decreases MAP duration.

5.3.5 The effect of 0.3mM 1-heptanol on electrical activity in sham operated hearts

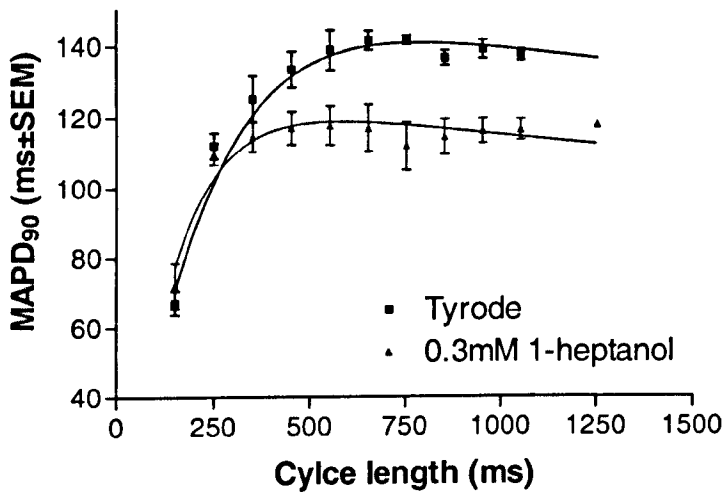
26 control rabbits (ejection fraction (\pm SEM) = $73\pm 2.76\%$) were used to investigate the effect of heptanol on MAPD₉₀ in the 9 designated areas of the LV using the CL protocol as previously described. Table 5.1 shows the positive or negative changes in MAPD₉₀ caused by the effects of heptanol. At short CLs (150ms and 250ms) the majority of the changes are positive ($P>0.05$), whilst at longer CLs (above 250ms) changes are negative (some significant). Area 5 showed no significant changes at any CL. On using a multiple test correction (Bonferroni correction) the level of significance changed from $P<0.05$ to: <0.0051 for 10 tests, <0.0057 for 9 tests and <0.0063 for 8 tests. Values still significant following correction are indicated in bold in Table 5.1.

Figure 5.7 shows all 9 area graphs (mean \pm SEM). In all areas, a greater difference in MAP duration between Tyrode's perfused and 0.3mM heptanol perfused hearts, was seen at longer CLs where 0.3mM heptanol reduced repolarisation duration. Small positive differences are observed at shorter CLs. Area 5 shows the least significance between values.

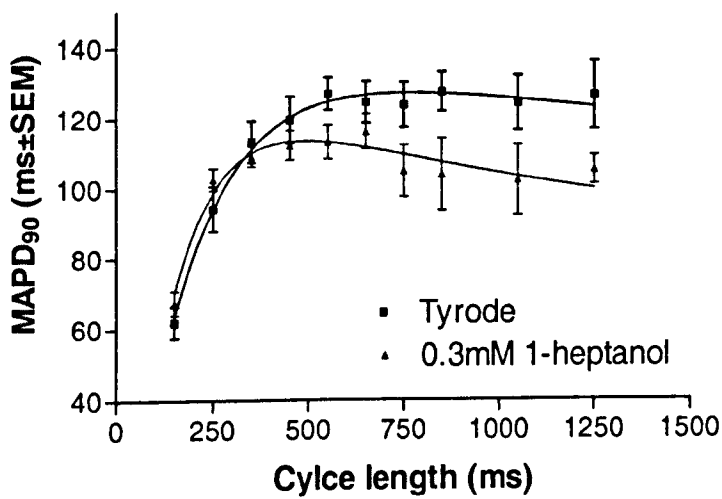
To assess the possibility of a global dispersion of repolarisation over the LV, a statistical comparison of MAPD₉₀ between areas was performed using a one way ANOVA. At a range of CLs (150ms to 1250ms) there was no change ($P>0.05$) between area 1 to 9 of sham operated hearts.



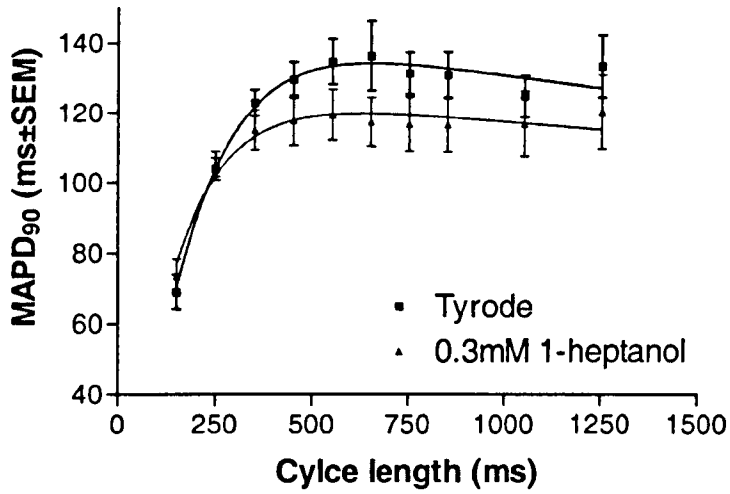
Area 1



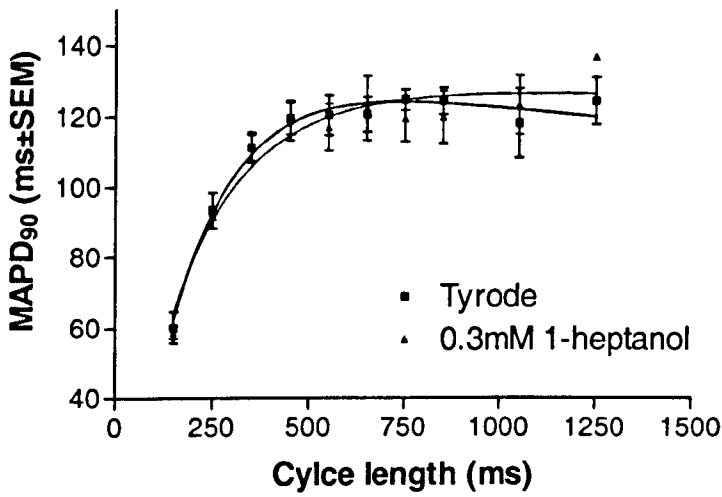
Area 2



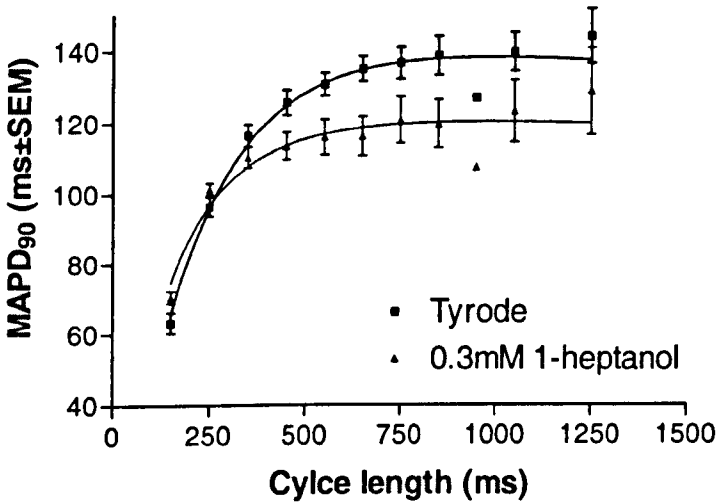
Area 3



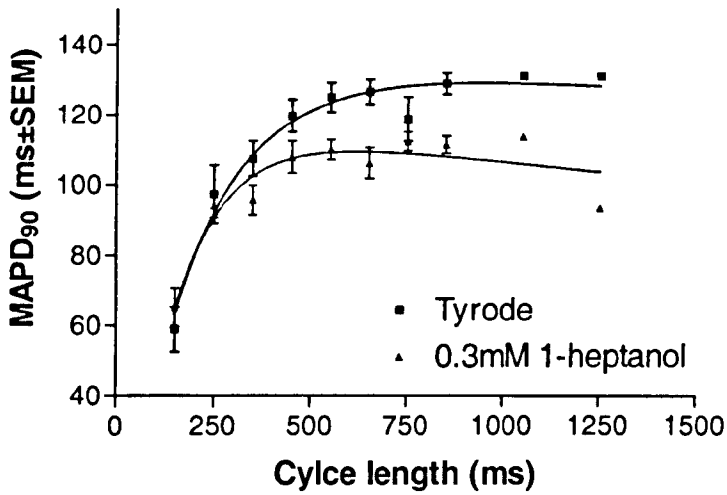
Area 4



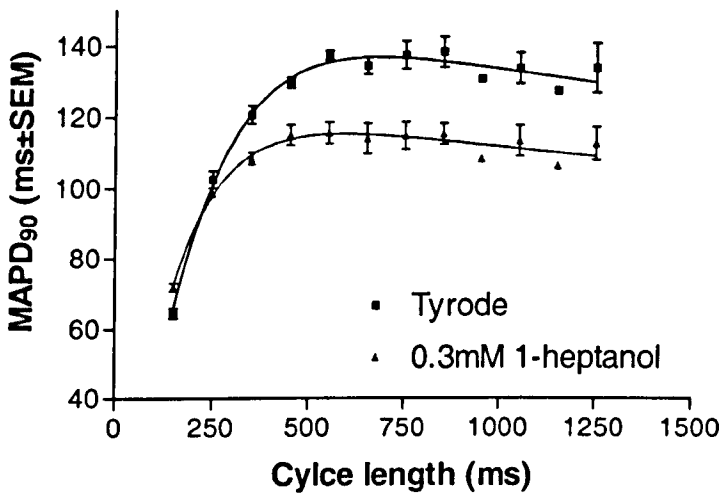
Area 5



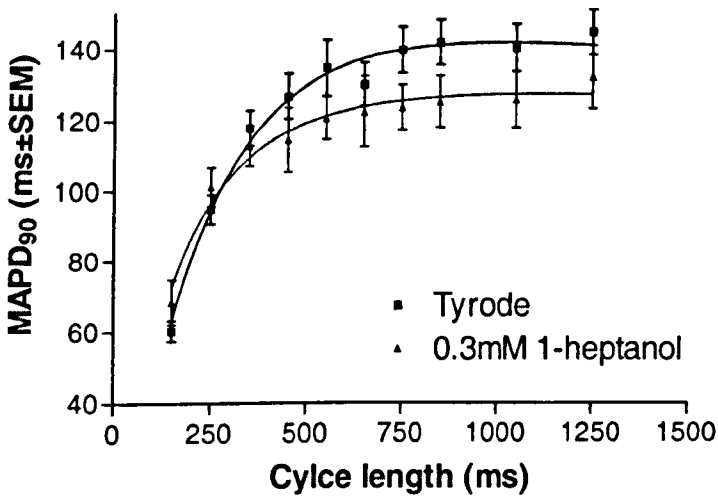
Area 6



Area 7



Area 8



Area 9

Figure 5.7 Graphs illustrating the effect of 0.3mM 1-heptanol on stable state restitution in sham-operated hearts.

CL (ms)	Area								
	1	2	3	4	5	6	7	8	9
150	+6.6 (5)	+9.9 (4)	+5.8 (7)	+7.5 (5)	-1.4 (4)	+6.6 (6)	+6.2 (4)	+7.3 (3)	+2.8 (4)
250	+7.8 (5)	-2.0 (5)	+8.3 (7)	+1.4 (6)	-0.6 (4)	+5.0 (6)	-3.2 (4)	-4.1 (3)	+6.52 (5)
350	-5.8 (5)	-9.6 (4)	-4.2 (7)	-7.8 (4)	0.0 (4)	6.0 (6)	-11.8 (4)	-16.3* (3)	-4.9 (5)
450	-13.1 (5)	-15.2 (5)	-7.2 (7)	-11.7 (6)	-0.7 (4)	-12.2 (6)	-11.7 (4)	-14.6 (3)	-12.2 (5)
550	-21.8** (5)	-19.4 (5)	-13.5** (7)	-15.2*** (6)	-3.8 (4)	-14.7* (6)	-14.8* (3)	-21.7* (3)	-14.0* (5)
650	-17.7 (5)	-22.3 (5)	-10.62 (7)	-17.3*** (6)	+6.3 (4)	-18.7* (6)	-20.3 (3)	-18.2 (2)	-12.1* (4)
750	-23.6 (2)	-26.8* (2)	-20.7** (4)	-14.6* (6)	-2.7 (3)	-15.8** (5)	-6.3 (3)	-17.6** (3)	-16.0** (4)
850	-23.8 (2)	-20.9** (2)	-23.3* (3)	-14.3* (6)	-4.5 (3)	-18.9*** (5)	-15.0 (2)	-23* (3)	-16.6* (5)
1050			-21.8* (3)	-8.0 (5)	+5.2 (3)	-16.5* (4)			-14.4* (5)
1250			-20.9 (2)	-19.7* (3)	+12.4 (2)	-16.3 (3)		-21.2 (2)	-8 (3)

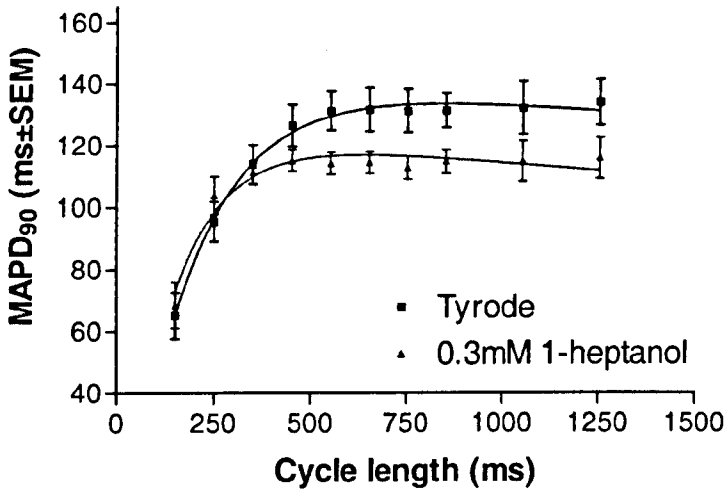
Table 5.1 The effect of 0.3mM 1-heptanol on MAPD₉₀ in sham operated hearts. Positive or negative change in MAPD₉₀ on perfusion with 0.3mM heptanol, as compared to Tyrode perfused hearts. n-number in brackets. * P<0.05, ** P<0.01, *** P<0.001 (paired Student's t-test). Bold indicating significance following Bonferroni correction.

5.3.6 The effect of 0.3mM 1-heptanol on electrical activity in failure hearts

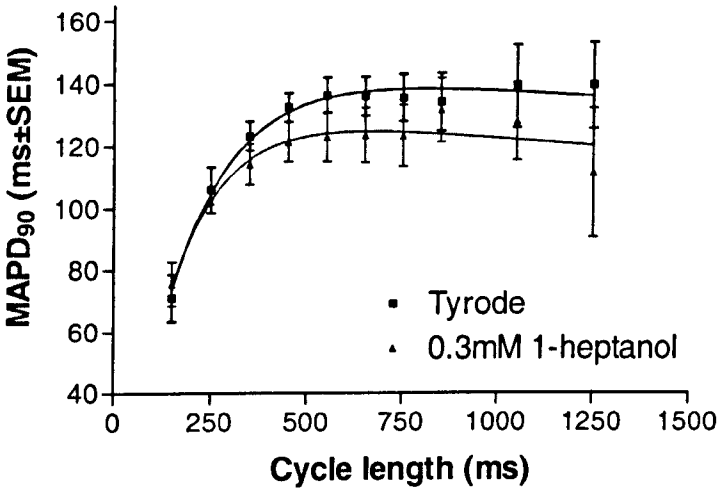
25 failure hearts (ejection fraction (\pm SEM) = $48.91 \pm 1.01\%$) were used to investigate the effect of heptanol on MAPD₉₀ in areas 1 to 7 of the LV using the steady state restitution protocol as previously described. Areas 8 and 9 were always affected by a region of infarction, and hence MAP duration recording from these areas was not possible. Table 5.2 shows the positive or negative changes in MAPD₉₀ caused by heptanol. Apart from the absence of data from areas 8 and 9, the results were broadly comparable to those in sham hearts. At 150ms the majority of the changes are positive ($P > 0.05$), whilst at CLs above 150ms changes are negative (some significant). Area 5 is again the only region that shows no significant changes at any CL. On using a multiple test correction (Bonferroni correction) the level of significance changed from < 0.05 to: < 0.0051 for 10 tests, < 0.0057 for 9 tests and < 0.0063 for 8 tests. Values still significant following correction are indicated in bold in Table 5.2.

Figure 5.8 shows all 9 area graphs (mean \pm SEM). In all areas, a greater difference in MAP duration between Tyrode perfused and 0.3mM heptanol perfused hearts, is seen at longer CLs where 0.3mM heptanol reduces repolarisation duration. Small positive differences are observed at a CL of 150ms. Area 5 shows no significant difference between values.

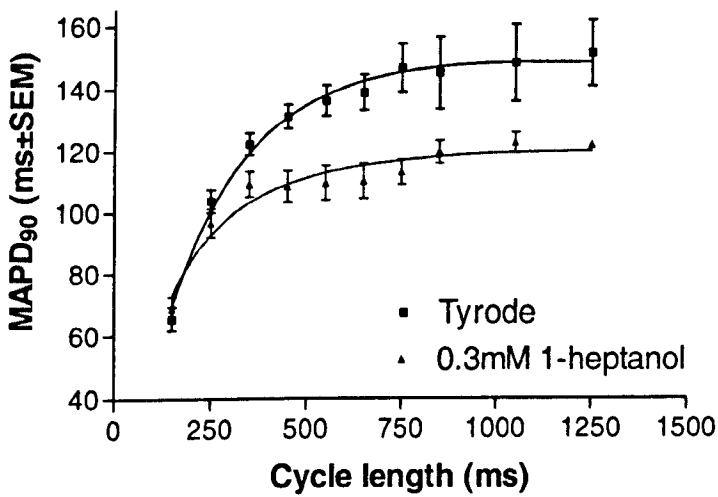
Analysis of variance of MAPD₉₀ between areas again showed that, at a range of CLs (150ms to 1250ms) there was no change between area 1 to 7 of failure hearts.



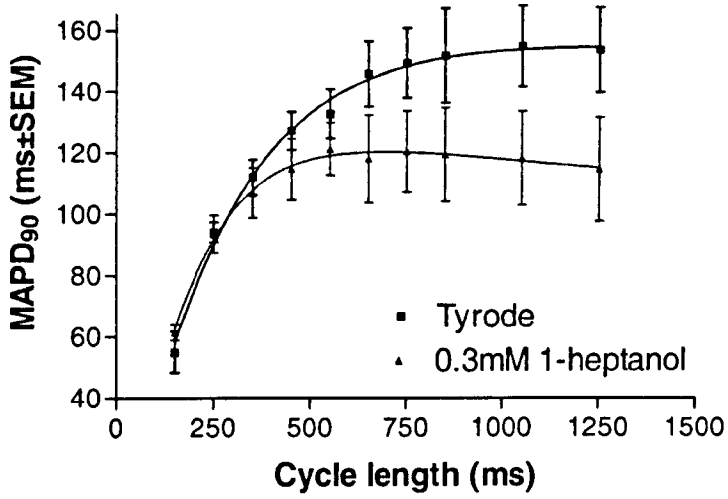
Area 1



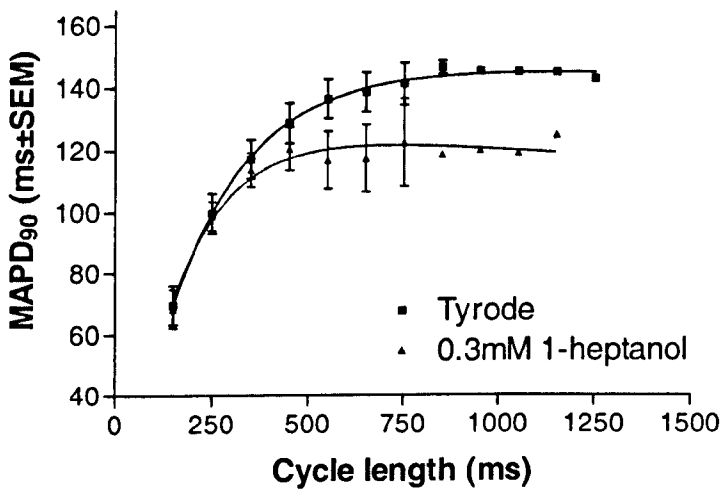
Area 2



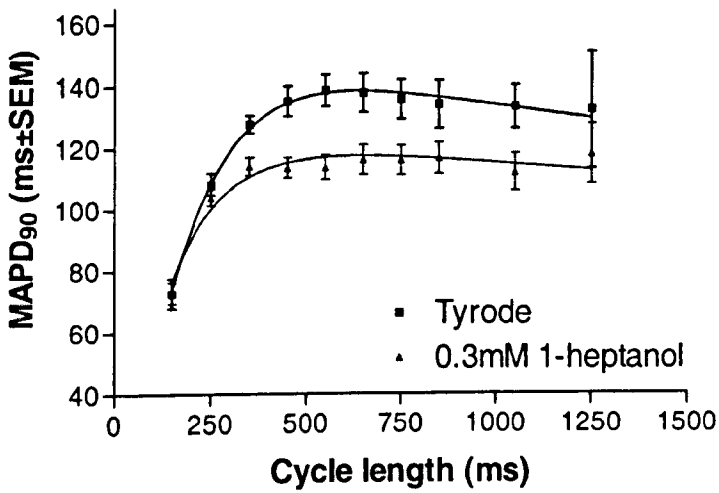
Area 3



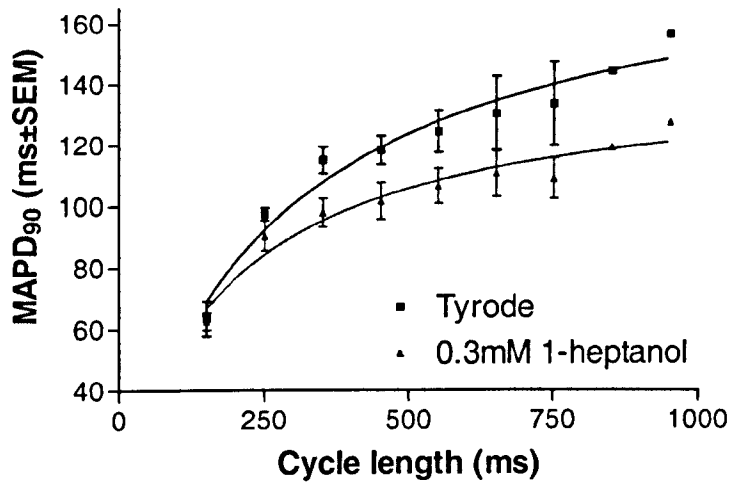
Area 4



Area 5



Area 6



Area 7

Figure 5.8 Graphs illustrating the effect of 0.3mM 1-heptanol on stable state restitution in failure hearts.

CL (ms)	Area						
	1	2	3	4	5	6	7
150	+3.3 (5)	+4.5 (4)	+3.9 (4)	+6.4 (5)	-1.16 (4)	+0.16 (5)	-2.6 (4)
250	+8.45 (4)	-3.8 (4)	-6.97 (5)	-0.68 (5)	-0.9 (4)	-4.4 (5)	-4.99 (6)
350	-2.4 (4)	-9.05** (4)	-13.09 (5)	-5.12 (5)	-3.4 (4)	-13.52** (5)	-14.67* (6)
450	-11.35 (4)	-11.1 (4)	-22.75 (5)	-12.6 (4)	-8.2 (4)	-21.32** (5)	-14.76* (6)
550	-16.95* (4)	-13.35 (4)	-26.69** (5)	-11.4* (4)	-19.5 (4)	-24.64** (5)	-14.46* (5)
650	-17.1* (4)	-12.4* (4)	-28.59** (5)	-16.1 (2)	-12.6 (4)	-21.32* (5)	-16.97* (3)
750	-18.5* (4)	-12.1* (4)	-30.73* (3)	-20.2 (2)	-15.4 (3)	-19.36* (5)	-22.14* (4)
850	-16.55* (4)	-7.33 (3)	-25 (2)	-24.6 (2)		-18.6* (4)	-25.1 (2)
1050	-17.2* (3)	-11.2 (3)	-25.4 (2)	-27 (2)		-14.76* (4)	
1250	-18** (3)	-16.2 (2)	-29.1 (2)	-29.5 (2)		-16.4 (2)	

Table 5.2 The effect of 0.3mM 1-heptanol on MAPD₉₀ in failure hearts. Positive or negative change in MAPD₉₀ on perfusion with 0.3mM heptanol, as compared to Tyrode perfused hearts. n-number in brackets. * P<0.05, **P<0.01, *** P<0.001 (paired Student's t-test). Bold indicating significance following Bonferroni correction.

5.3.7 The effect of 0.3mM 1-Heptanol on sham hearts v failure hearts

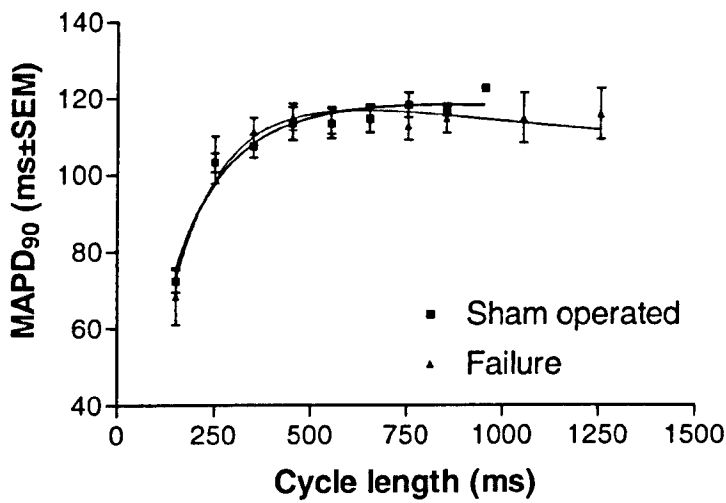
Graphs from all 7 regions illustrating the difference between heptanol perfused sham-operated and failure hearts are shown in Figure 5.9. No changes between sham operated and failure hearts were found at a MAP duration of 90%. Unpaired Student's t-tests ($P < 0.05$ considered significant) were used to statistically compare sham operated and failure hearts perfused with 0.3mM heptanol (omitting areas 8 and 9 from tests due to the region of infarction). The numbers of observations are as follows:

		Area													
		1		2		3		4		5		6		7	
CL															
(ms)	S	F	S	F	S	F	S	F	S	F	S	F	S	F	
150	5	5	4	4	7	4	5	5	4	4	6	5	4	4	
250	5	4	5	4	7	5	6	5	4	4	6	5	4	6	
350	5	4	4	4	7	5	4	5	4	4	6	5	4	6	
450	5	4	5	4	7	5	6	4	4	4	6	5	4	6	
550	5	4	5	4	7	5	6	4	4	4	6	5	3	5	
650	5	4	5	4	7	5	6	2	4	4	6	5	3	3	
750	2	4	2	4	4	3	6	2	3	3	5	5	3	4	
850	2	4	2	3	3	2	6	2	3		5	4	2	2	
1050		3		3	3	2	5	2	3		4	4	5		
1250		3		2	2	2	3	2	2		3	2			

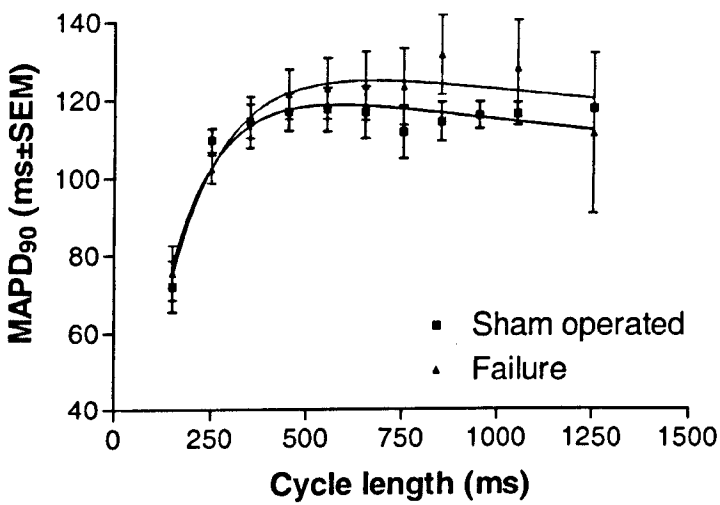
Table 5.3 Sham and failure n-numbers.

S – Sham operated hearts

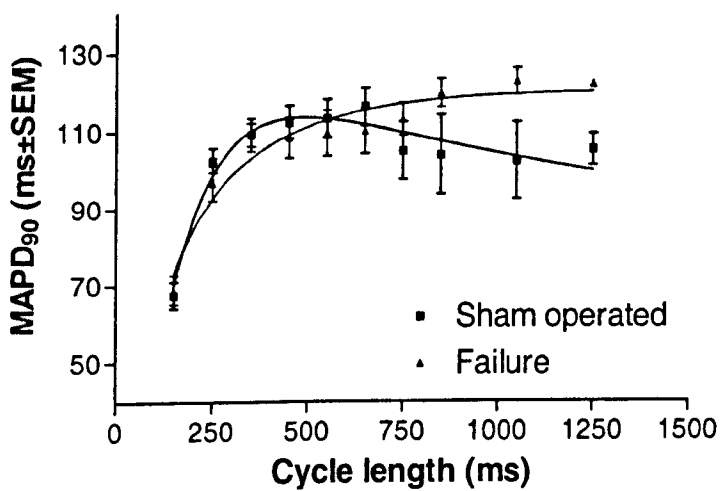
F – Failure hearts



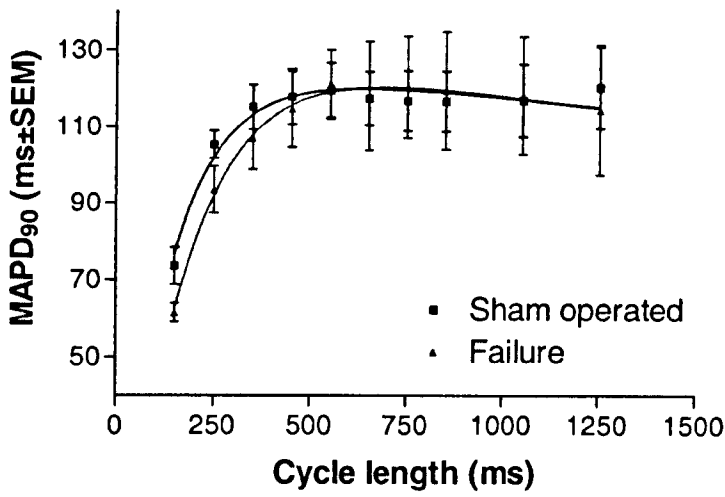
Area 1



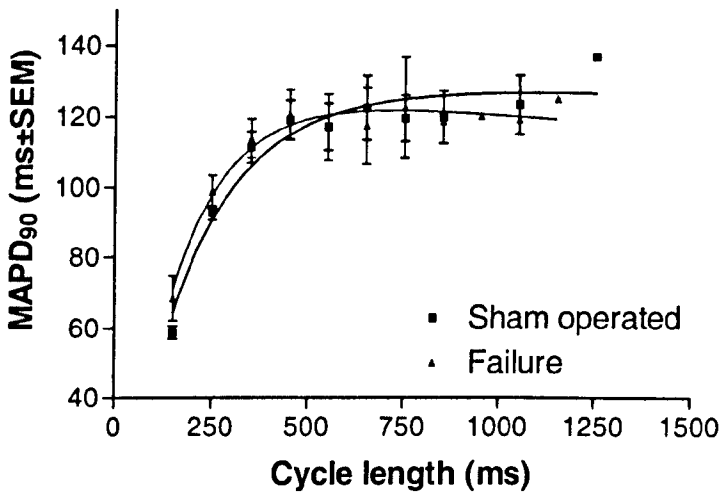
Area 2



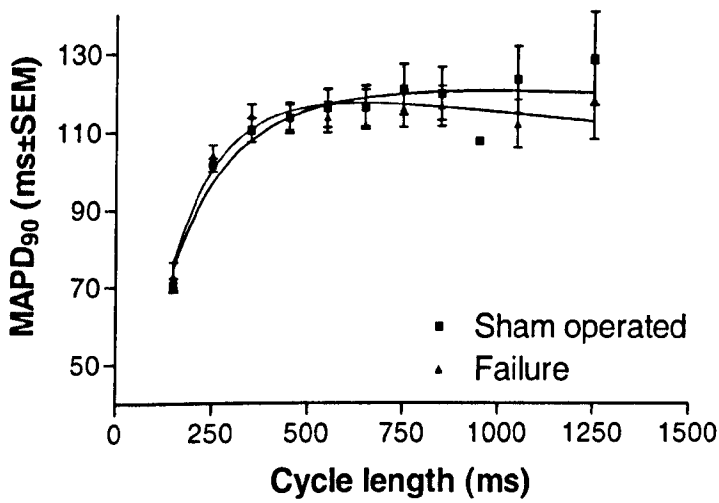
Area 3



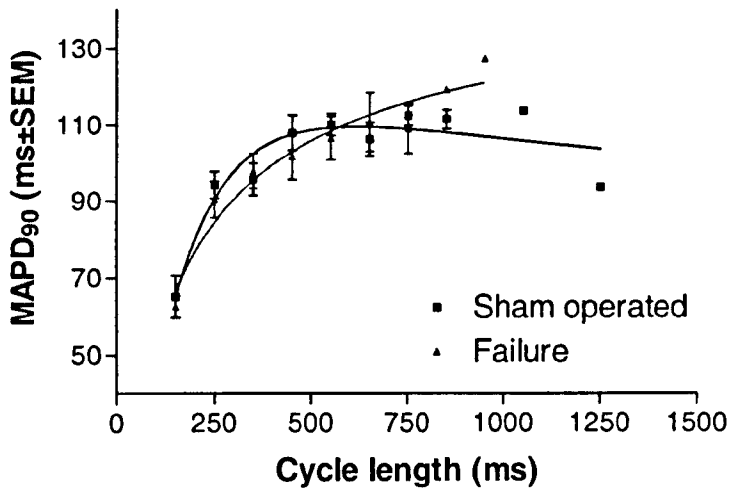
Area 4



Area 5



Area 6



Area 7

Figure 5.9 Graphs illustrating the effect of 0.3mM 1-heptanol on stable state restitution in sham-operated v failure hearts.

5.3.8 The global effect of 0.3mM 1-heptanol on MAP duration in sham operated hearts

Figure 5.10 shows the overall effect of perfusing the heart with 0.3mM heptanol on MAPD₉₀. Data from all 9 areas have been pooled together to give a global value. 0.3mM heptanol significantly ($P < 0.05$) induces an increase in MAPD₉₀ at a cycle length of 150ms and a significant decrease in average MAP duration in sham operated hearts at cycle lengths greater than 350ms.

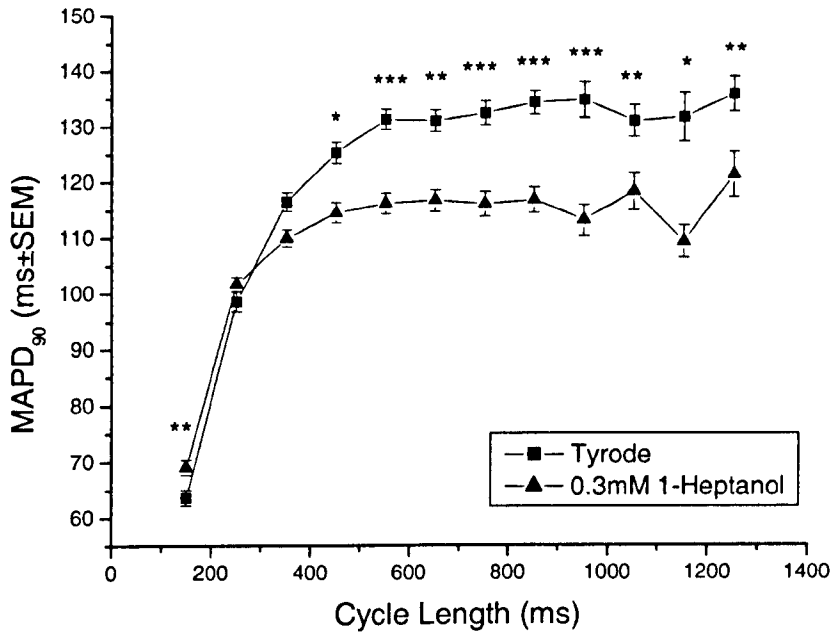


Figure 5.10 The effect of 0.3mM 1-heptanol on MAPD₉₀ in sham operated hearts. Data shown mean±SEM. Paired Student t-test, * = P < 0.05. ** = P < 0.01. *** = P < 0.0001.

5.3.9 The global effect of 0.3mM 1-heptanol on MAP duration in failure hearts

Figure 5.11 shows the overall effect of perfusing the heart with 0.3mM heptanol on MAPD₉₀. All data from all 7 areas have been pooled to give a global value at each cycle length. 0.3mM heptanol induces a significant ($P < 0.05$) decrease in average MAP duration in failure hearts at cycle lengths greater than 350ms.

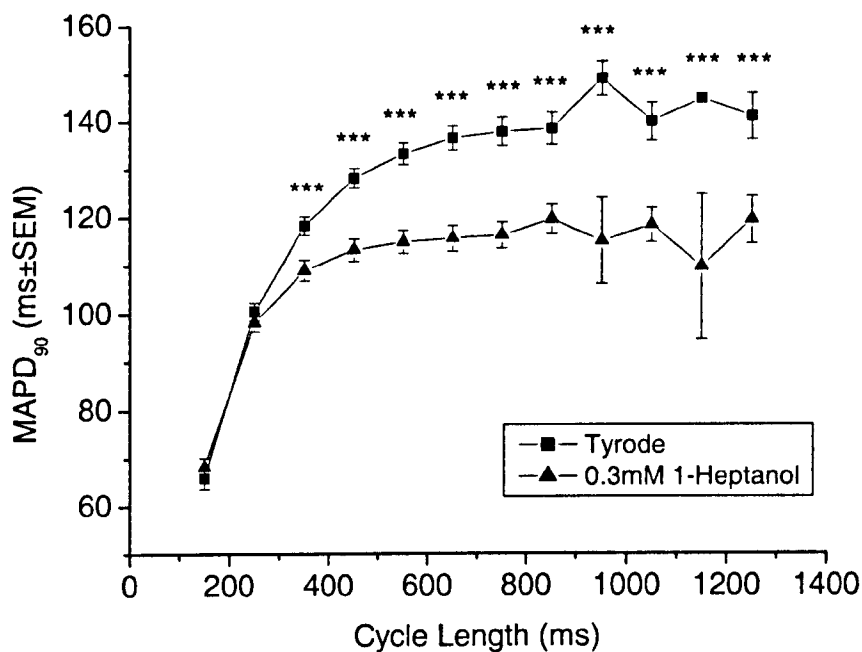


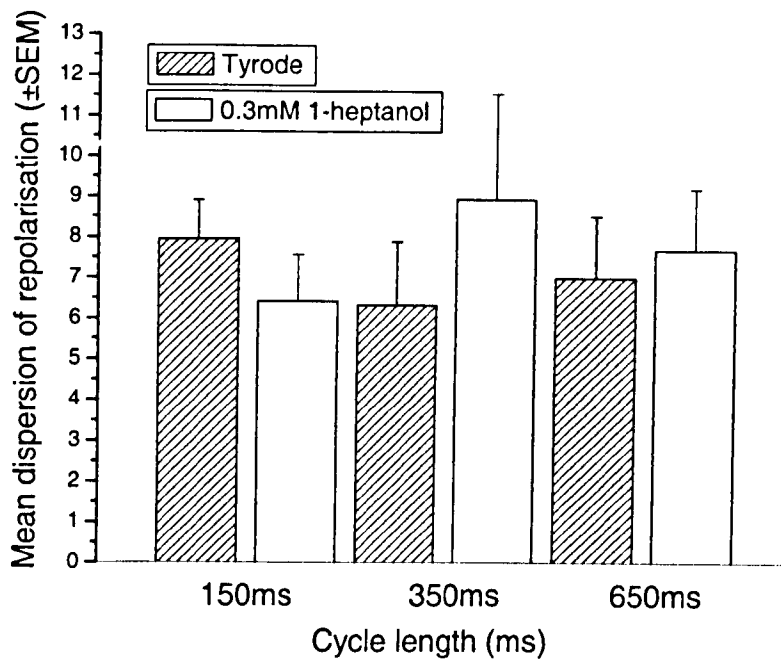
Figure 5.11 The effect of 0.3mM 1-heptanol on MAPD₉₀ in failure hearts. Data shown mean±SEM. ***=P<0.001.

5.3.10 The effect of 0.3mM 1-heptanol on dispersion of repolarisation in sham operated hearts

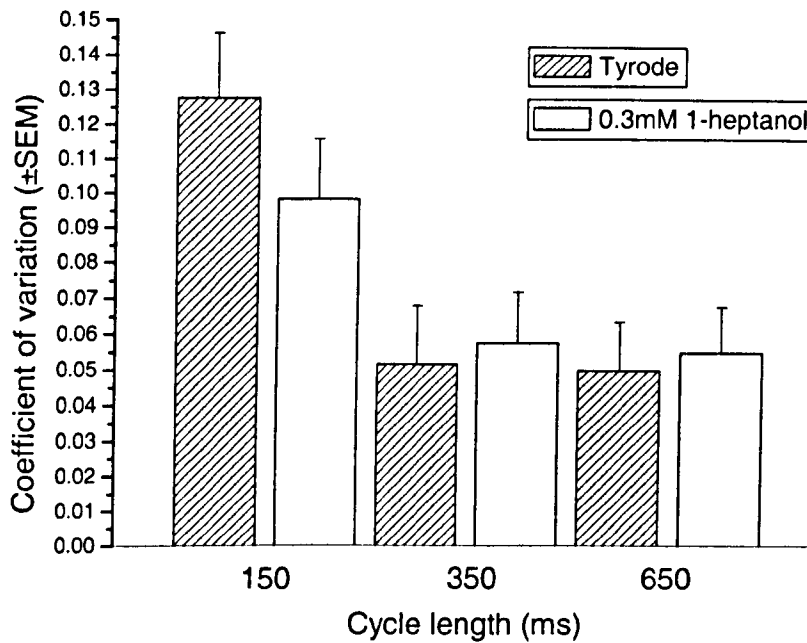
The mean dispersion of repolarisation as calculated as the average of the standard deviation of MAPD₉₀ within each heart, for Tyrode's solution (red bar) and 0.3mM heptanol (grey bar) is illustrated in Figure 5.12a. 0.3mM heptanol induces no increase ($p>0.05$) in dispersion of repolarisation at a CL of 350ms and 650ms only. The data are represented as coefficient of variation in Figure 5.12b. Table 5.4 indicates the dispersion of repolarisation at cycle lengths of 150ms, 350ms and 650ms.

	Dispersion of repolarisation (ms±SEM)		
	150ms	350ms	650ms
Tyrode	7.94±0.56	6.32±1.56	7.00±1.53
0.3mM 1-heptanol	6.60±1.15	8.94±2.61	7.69±1.52

Table 5.4 Dispersion of repolarisation in sham operated hearts.



A. Dispersion of repolarisation.



B. Coefficient of variation.

Figure 5.12 The effect of 0.3mM 1-heptanol on dispersion of repolarisation in sham operated hearts. 0.3mM heptanol does not increase dispersion of repolarisation ($P > 0.05$, paired Student's t-test) at 350ms and 650ms only. $n = 11$ hearts.

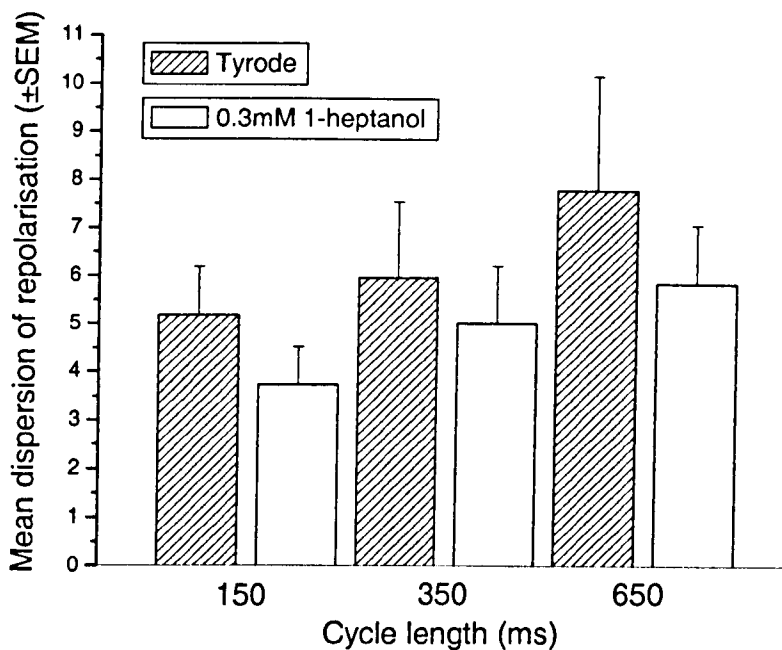
5.3.11 The effect of 0.3mM 1-heptanol on dispersion of repolarisation in failure hearts

In failing hearts 0.3mM heptanol causes a non-significant *decrease* in mean dispersion of repolarisation at a cycle lengths of 150ms, 350ms and 650ms. Statistical comparisons were made using a paired Student's t-test. The results are illustrated in Figure 5.13a and b as dispersion of repolarisation and coefficient of variation respectively. Dispersion of repolarisation results are also tabulated in Table 5.5.

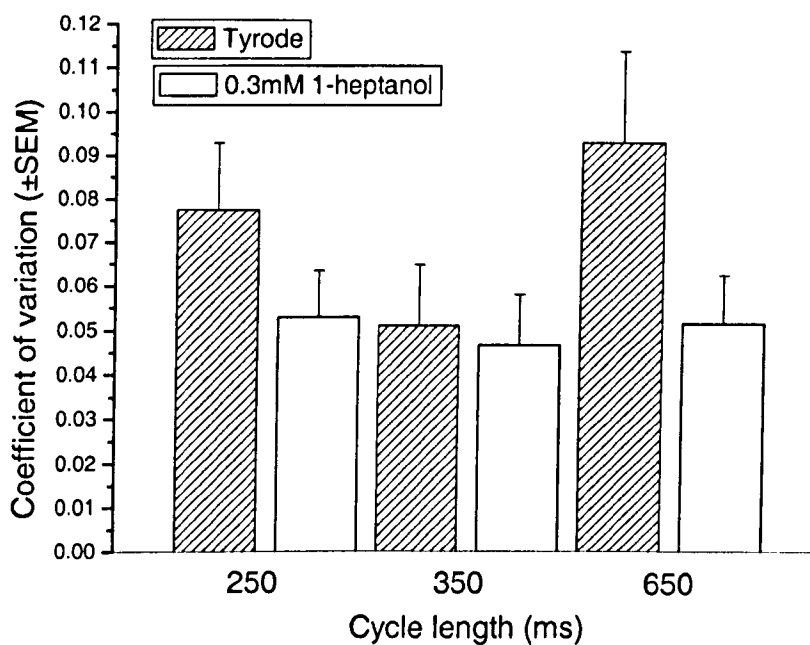
	Dispersion of repolarisation (ms±SEM)		
	150ms	350ms	650ms
Tyrode	5.18±1.01	5.95±1.59	7.79±2.39
0.3mM 1-heptanol	3.73±0.79	5.02±1.19	5.84±1.22

Table 5.5 Dispersion of repolarisation in failure hearts.

Figures 5.14a and b compares mean dispersion of repolarisation and coefficient of variation respectively in failing and sham operated hearts. Dispersion is measured at a cycle length of 150ms, 350ms and 650ms. Failure *decreases* dispersion of repolarisation at all cycle lengths ($P>0.05$). Statistical comparisons were made using an unpaired Student's t-test.

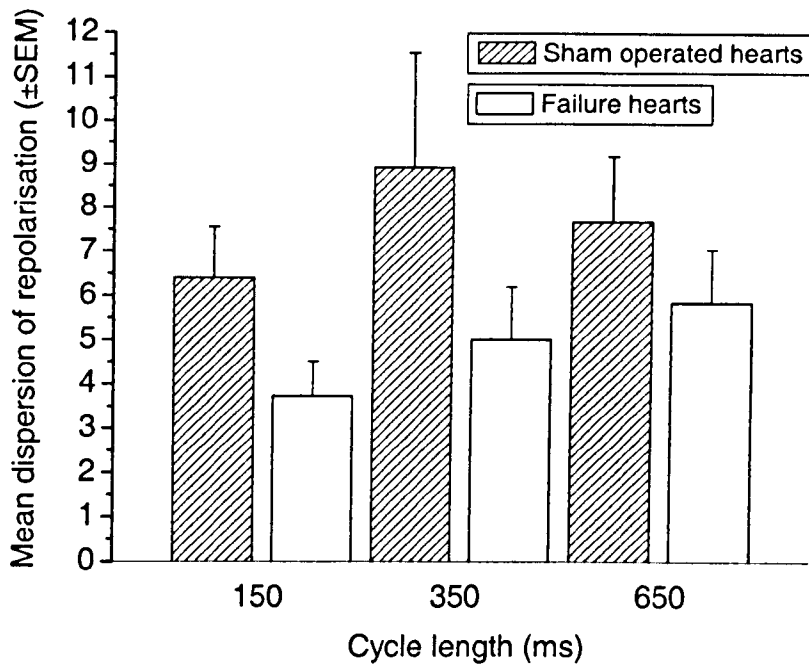


A. Dispersion of repolarisation.

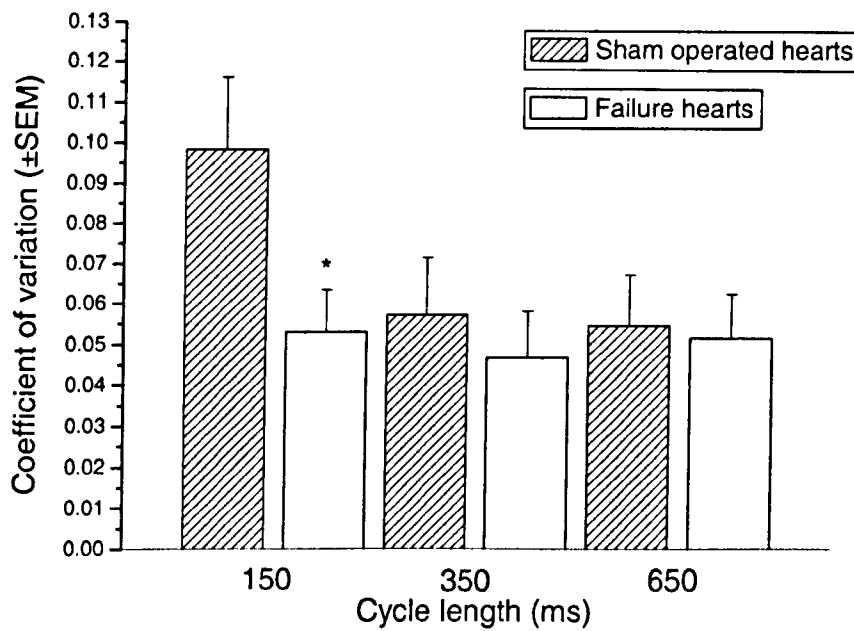


A. Coefficient of variation.

Figure 5.13 The effect of 0.3mM 1-heptanol on dispersion of repolarisation in failing hearts. 0.3mM heptanol causes does not decrease dispersion of repolarisation ($P > 0.05$, paired Student's t-test). $n = 13$ hearts.



A. Dispersion of repolarisation.

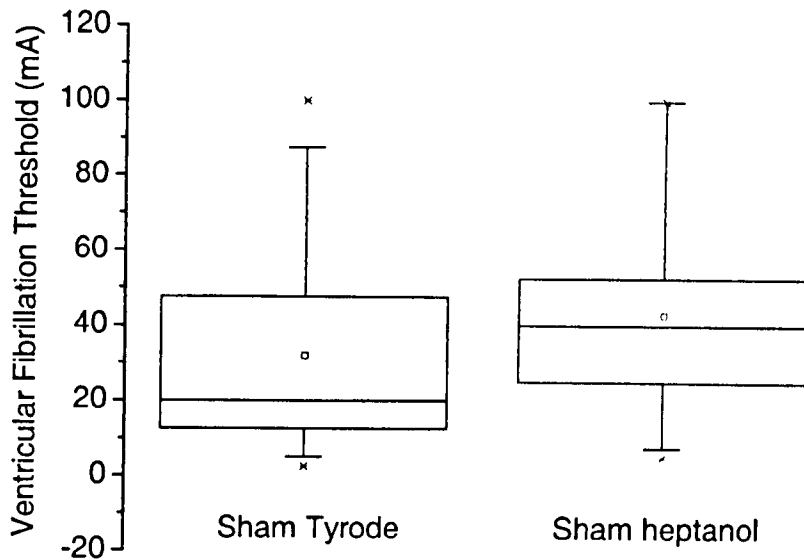


B. Coefficient of variation.

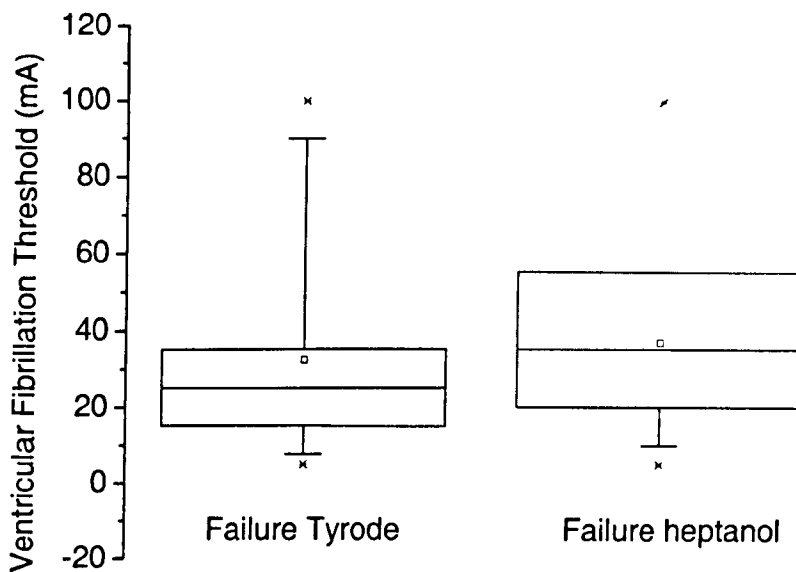
Figure 5.14 The effect of failure on the dispersion of repolarisation in the 0.3mM 1-heptanol perfused heart. Failure causes a significant decrease in dispersion of repolarisation at 150ms only ($P < 0.05$, unpaired Student's t-test). $n = 11$ sham operated hearts, 13 failure hearts.

5.3.12 The effect of 0.3mM 1-heptanol on ventricular fibrillation threshold

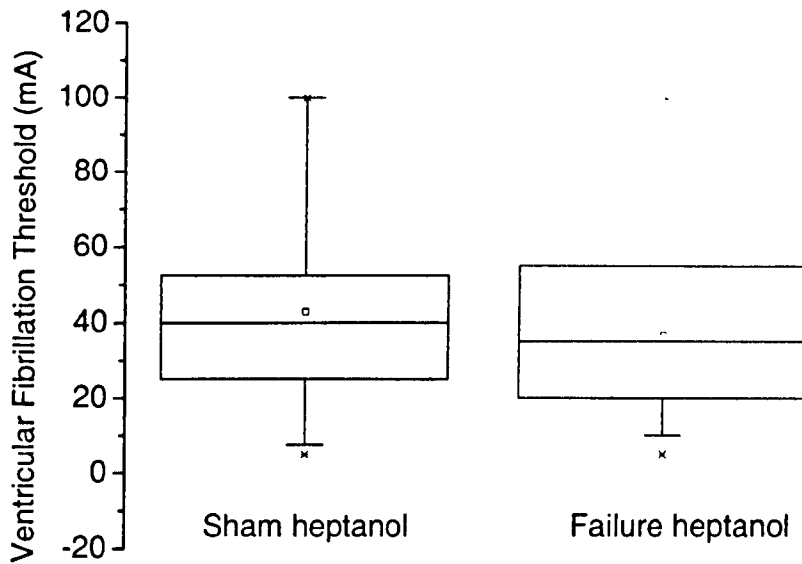
Figures 5.15a and 5.15b show the effect on ventricular fibrillation threshold of 0.3mM heptanol on sham operated hearts and failure hearts respectively. Heptanol causes an increase in ventricular fibrillation threshold of (mean±SEM) 31.88±4.27mA to 42.76±5.41mA in the sham hearts ($P>0.05$) and 32.16±3.90mA to 36.67±6.24mA ($P>0.05$) in the failure hearts. Neither of these effects was significant. The box and whisker plot in Figure 4.7 illustrates the difference in ventricular fibrillation threshold between sham-operated and failure hearts on perfusion with normal Tyrode's solution. Mean ventricular fibrillation threshold was decreased ($P>0.05$) in failing hearts. Furthermore, as illustrated in Figure 5.15c failure caused a decrease in ventricular fibrillation threshold of 6.09mA, a decrease from (mean±SEM) 42.76±5.41mA to 36.67±6.24mA ($P>0.05$) in heptanol perfused hearts



A. The effect of 0.3mM 1-heptanol on ventricular fibrillation threshold in sham operated hearts. Heptanol causes an increase ($P>0.05$, unpaired Student's t-test) in ventricular fibrillation threshold. (n=44 and 29 hearts respectively)



B. The effect of 0.3mM 1-heptanol on ventricular fibrillation threshold in failure hearts. Heptanol causes an increase ($P>0.05$, unpaired Student's t-test) in ventricular fibrillation threshold. (n=37 and 15 hearts respectively)



C. The effect of heart failure on ventricular fibrillation threshold in 0.3mM 1-heptanol perfused hearts. Heptanol causes a decrease ($P>0.05$, unpaired Student's t-test) in ventricular fibrillation threshold. ($n=29$ and 15 hearts respectively)

Figure 5.15 The effect of 0.3mM 1-heptanol on ventricular fibrillation thresholds.

5.5 Discussion

In this study, at 0.3mM, 1-heptanol significantly decreased contractility and MAP duration but did not have any effect on sequentially recorded dispersion of repolarisation or ventricular fibrillation threshold. The effect of heptanol on the first two confirms results from previous studies (see below). However the effect of heptanol on dispersion of repolarisation is a poorly researched area.

5.5.1 Effect on contractility

Keevil *et al* (2000) studied the effect of heptanol on contractile function in the isolated, perfused rabbit heart. Using similar methods to those used in this study, they found that heptanol inhibited pressure generation as measured by the insertion of a latex water filled balloon in to the left ventricle. Left ventricular developed pressure (LVDP) was calculated as the difference between peak systolic pressure and end diastolic pressure. Keevil *et al* showed that LVDP was abolished by perfusion with 1mM or higher heptanol. A lower concentration (0.3mM) was used in this study which led to approximately 50-60% reduction in LVDP. This effect was seen to be completely reversible, in both studies, upon perfusion with normal Tyrode's solution.

A reduction in junctional conductance may lead to a negative inotropic effect due to increased asynchrony of force development across the syncytium. Synchronisation of force development depends on a properly timed sequence of ventricular depolarisation. This is reflected in a certain delay between the earliest and latest activations in this sequence. As intracellular resistance increases, the conduction velocity decreases, synchronisation of force development is delayed,

and overall contractility is reduced. However, isolated cell studies suggest an alternative explanation for the negative inotropic effect of heptanol. It is thought that this is due to the inhibition of I_{Ca} . Heptanol is able to enter the myocyte due to its lipophilic properties and therefore may affect the sarcoplasmic reticulum Ca^{2+} release and re-uptake channels. The slow recovery of LVDP after perfusion with heptanol (Keevil *et al*, 2000) could be due to the time taken to fully washout heptanol from the intracellular compartments.

Shaw and Rudy (1997) stated that a non-membrane change such as decreased intercellular coupling could cause the L-type Ca^{2+} current to become more important than the Na^+ current as the major ionic current supporting conduction.

5.5.2 Reduction in action potential duration

In both normal and failing hearts it was shown that 0.3mM heptanol caused a significant decrease in MAP duration especially at longer stimulation intervals (over approximately 250ms). Keevil *et al* (2000), in their work with heptanol on the isolated perfused (healthy) rabbit heart, showed that heptanol over a wide range of concentrations (0.001-1mM) decreased repolarisation duration as recorded by the activation recovery intervals of bipolar electrogram recordings. The size of the effect varied from approximately 98% to 70% in the epicardium and 95% to 55% in the endocardium. Activation recovery intervals are an unreliable index of repolarisation duration compared to MAP recording, especially under ischaemic conditions where S-T segment changes occur. In the same study Keevil *et al* also recorded the effect of heptanol (0.001-0.56mM) using a MAP electrode. They found that heptanol acts in a dose dependent manner to decrease repolarisation as

measured by MAPD₇₀. They also investigated the effect of heptanol on the latency between stimulus and left ventricular activation. Low concentrations of heptanol (less than 0.3mM) were found to induce a gradual but significant increase whilst higher concentrations (0.3mM-1.0mM) produced a sharp increase in latency. These values were consistent with a reduction in conduction velocity.

A non-uniform reduction in repolarisation would result in a dispersion that may facilitate arrhythmogenesis (Kuo *et al*; 1983; Surawicz, 1997). Consequently the effect of heptanol on the dispersion of repolarisation and arrhythmia inducibility as measured by ventricular fibrillation threshold (VFT) was investigated, in normal and failing hearts.

5.5.3 Dispersion of repolarisation and effect on arrhythmogenesis

Heptanol has previously been used to study the electrophysiological consequences of the disruption of cellular uncoupling and its relevance to the induction of re-entrant arrhythmias (Callans *et al*, 1996). The disturbance of intercellular coupling has been thought to have an effect on arrhythmogenesis. Lesh *et al* (1989) investigated the ability of alterations in cellular coupling to mask or unmask intrinsic differences in action potential duration in a sheet of ventricular myocardium. They found that normal low resistance coupling masked dispersion of repolarisation whilst increased axial resistance unmasked dispersion. If a cell with a shorter intrinsic action potential is well coupled to a neighbouring cell with longer action potential, electrotonic flow between them will produce synchronised repolarisation, but if intercellular coupling is disturbed re-entry may be facilitated.

This study showed that 0.3mM heptanol caused no change in dispersion of repolarisation. It must be remembered though that dispersion in this study was recorded sequentially rather than with the more reliable method of simultaneous MAP recording which is dealt with in the chapter 6. In fact this concentration of heptanol actually caused a slight decrease in dispersion of repolarisation in failing hearts. Furthermore, no changes in VFT were observed. This contrasts with the results found when Callans *et al* (1996) investigated the effect of heptanol on conduction and ventricular arrhythmias in infarcted canine myocardium. They found that heptanol has a bimodal effect on susceptibility to inducible ventricular tachycardia (VT) in infarcted canine hearts. Low doses (0.5mM) of heptanol reproducibly induced VT whilst high doses (1.0mM) had an antiarrhythmic effect. This also contrasts to earlier studies that investigated the effect of heptanol in normal myocardium, where 0.5mM heptanol had little effect and 1.0mM facilitated the induction of VT.

Keevil *et al* (2000), during premature stimulation protocols, found that lower concentrations of heptanol (0.1-0.3mM) caused a higher incidence of arrhythmias than higher concentrations (>0.3mM) in the normal heart. They suggested that there might be a critical range of slowed conduction in which re-entrant arrhythmias could develop, although changes in repolarisation duration may contribute to this pro-arrhythmic effect. This illustrates the point that heptanol can be both pro-arrhythmic and antiarrhythmic depending on the concentration and the state of intercellular coupling prior to heptanol perfusion.

Evidence from the above mentioned study by Callans *et al* suggests that 0.3mM heptanol should be pro-arrhythmic. However, in this study there is very little

change in ventricular fibrillation threshold on perfusion with 0.3mM heptanol. It may be that under the conditions of this study the concentration of heptanol used may be at a point intermediate between pro- and anti-arrhythmic effects. Spontaneous arrhythmias however did occasionally occur although not in any consistent way with heptanol. Failure hearts understandably showed the highest incidence of spontaneous arrhythmia but on a small number of occasions sham operated hearts became tachycardic.

**Chapter 6 – The effect of the gap junction uncoupler 1-heptanol on
the electrophysiology of the whole heart as recorded by the 32
MAP electrode array**

6.1 Introduction

Cellular uncoupling has been demonstrated in the later phases of ischaemia and various types of injury. As cells become progressively uncoupled (gap junctional resistance increases and gap junctional conductance decreases), conduction velocity decreases monotonically (Rudy and Shaw, 1997). Reduced coupling between cells causes longer delays in propagation across gap junctions and hence reduces the conduction velocity. One of the prerequisites for re-entry is unidirectional conduction block. Altered cell coupling leading to alterations in the electrophysiological properties of the tissue may result in unidirectional block and hence arrhythmia. Shaw and Rudy stated that non-sustained re-entry can be transformed to sustained re-entry by a uniform, or non-uniform, reduction of cellular coupling by gap junctions. In the case of severe gap junction uncoupling, propagation cannot be sustained and conduction block occurs. Conduction block has been discussed as a pre-requisite to arrhythmia in the general introduction (chapter 1).

The importance of tissue refractoriness in arrhythmogenesis has long been known. Increasingly restitution (the rate dependent alterations of action potential duration) is being recognized as a factor for determining the ease with which re-entrant arrhythmias are initiated and maintained. Generally, action potential duration is a monotonic function of the coupling interval. However, restitution of action potential duration has been found to be biphasic (Morgan *et al*, 1992; Bass 1975). With increasing coupling interval action potential duration initially increased to a local maximum, then decreases to a local minimum, and then increases to reach a steady action potential duration. This biphasic relationship is particularly evident

in the human ventricle (Bass 1975; Franz *et al*, 1988). It is expected that biphasic restitution and steep gradient (>1) of the ascending slope would predispose the heart to the development of complex dynamic behaviour. Watanabe *et al* (1976) developed an analytical model to determine how biphasic restitution gives rise to this behaviour.

The effect of heptanol on electrical restitution and the implications for arrhythmogenesis are unknown and were therefore studied as part of this investigation. The effect of heptanol on dispersion of repolarisation has already been discussed as a poorly studied area. Sequential recording of dispersion (chapter 5) provided inconclusive evidence concerning the effect of 0.3mM heptanol on the dispersion of repolarisation. An improved method of MAP recording that potentially allows the simultaneous recording of 32 MAPs from the epicardial surface of the left ventricle (chapter 3) was used in this study to obtain more reliable dispersion results.

The 32 electrode array imposes a time limit to the period of recording that produces reasonable, and analysable, MAPs. MAP quality and quantity declined rapidly with time to the extent that the 32 MAP array could not produce good quality MAPs for the time period required for a stable state restitution protocol (protocol as previously described for single MAP recording). The 32 MAP electrode array is discussed in detail in chapter 3. Due to the time limitations imposed by the electrode array an extrastimulus protocol was used to measure restitution. In the clinical setting, drive trains consisting of 8 S1 stimuli followed by the premature stimulus S2 are used. However, preliminary experiments suggested that such a short protocol may not always produce stabilization of MAP duration by the end of

the S1 pulse train. (8 beat S1 trains are usually used in such investigations (Leerssen *et al*, 1994) but uncertainty in this study was with the stability of such a short protocol.) Therefore a series of experiments was conducted to compare protocols with 8 and 16 S1 stimuli. Conduction delay as an indicator of gap junction uncoupling was also studied.

6.2 Methods

Multiple MAPs were simultaneously recorded from the epicardial surface of the intact left ventricle with the 32 electrode array. The construction of and the theory concerning this method of recording are described in detail in chapter 3. This series of experiments were performed exclusively using normal control hearts.

6.2.1 Protocols

General methods are described in chapter 2. The heart was perfused in Langendorff mode with normal Tyrode's solution and with solution containing 0.3mM heptanol. Upon cannulation of the heart, adjustment of perfusion rate, removal of the right atrium and ablation of the atrio-ventricular node, a 20 minute stabilisation period was allowed. During the stabilisation period the heart was paced at a constant pacing cycle length (CL) of 350ms. The electrode array was positioned around the heart and adjusted so that the maximum number of MAPs were obtained. A 4 minute MAP stabilisation period in normal Tyrode's solution was then allowed. Stimulation protocols were then carried out under normal Tyrode perfusion and also after a switch to 0.3mM heptanol solution. The solution switch took place 2 minutes prior to the end of the extrastimulus protocol in Tyrode's - the time required for the solution to travel from the stock solution to the

heart. A further 4 minute period elapsed to allow stabilisation of MAP duration and left ventricular developed pressure (LVDP). The extrastimulus protocol was then performed under perfusion with 0.3mM heptanol solution. The protocol is shown diagrammatically in Figure 6.1.

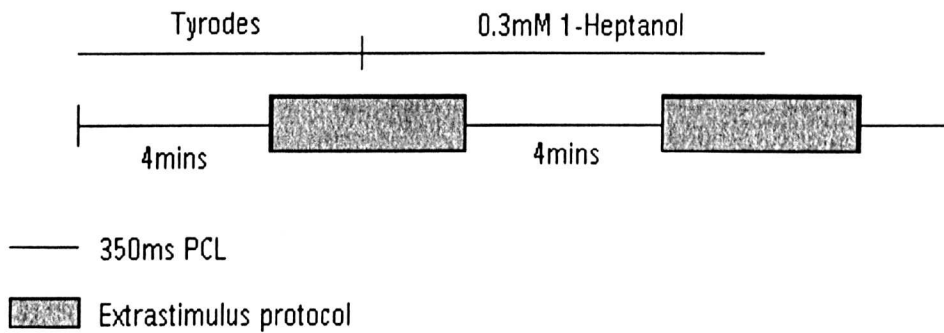
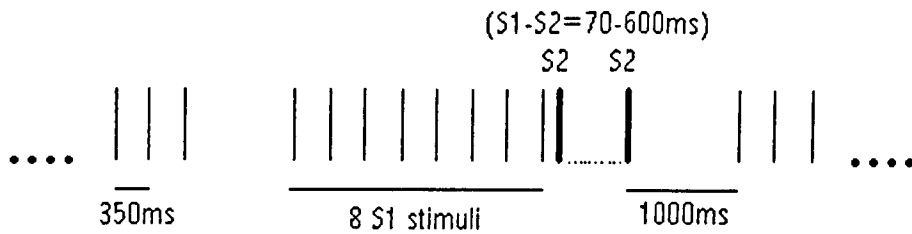
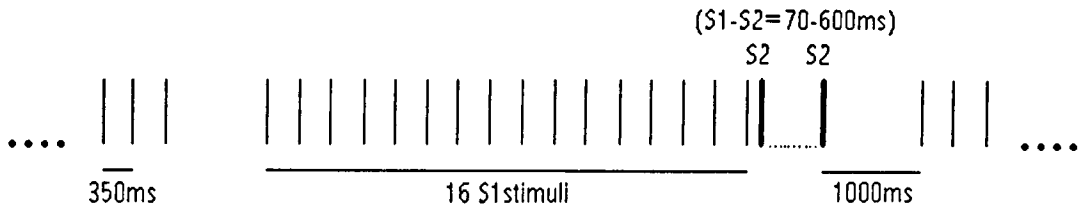


Figure 6.1 Whole heart perfusion protocol, including stabilisation times (solid thin lines), extrastimulus protocols (grey solid boxes), and solution changes.

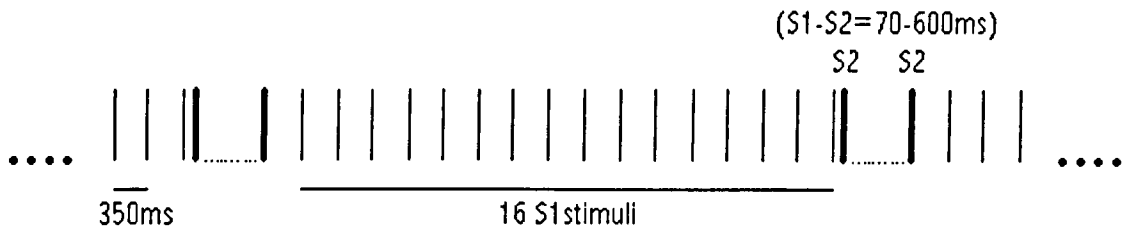
Three different extrastimulus protocols were used to investigate the restitution properties of the heart: 8 S1 stimuli plus 1000ms diastole; 16 S1 stimuli plus 1000ms diastole; 16 S1 stimuli with 1000ms diastole omitted. All protocols involved 8 or 16 basic S1 stimuli of 350ms intervals followed by an extrastimulus S2. The S2 followed the last S1 of the train by between 70ms and 600ms and is the S1-S2 interval. The intervals were increased from 70ms to 600ms in increments of 5ms between 70ms and 150ms, 10ms between 150ms and 350ms, and 50ms between 350ms and 600ms. In two of the protocols a 1000ms diastolic period followed the S2 stimuli. The 8 S1 and 16 S1 protocols were performed in different hearts. These protocols are shown diagrammatically in Figure 6.2.



A. 8 S1 stimuli with 1000ms gap.



B. 16 S1 stimuli with 1000ms gap.



C. 16 S1 stimuli.

Figure 6.2 Whole heart extrastimulus protocols. For clarity S1 stimuli are shown in thin lines whilst S2 stimuli (minimum and maximum) are shown in bold lines. **A.** initial protocol used involves an 8 S1 stimuli with 1000ms diastole. **B.** second protocol used involves a 16 S1 stimuli with 1000ms diastole. **C.** as B but without 1000ms pause.

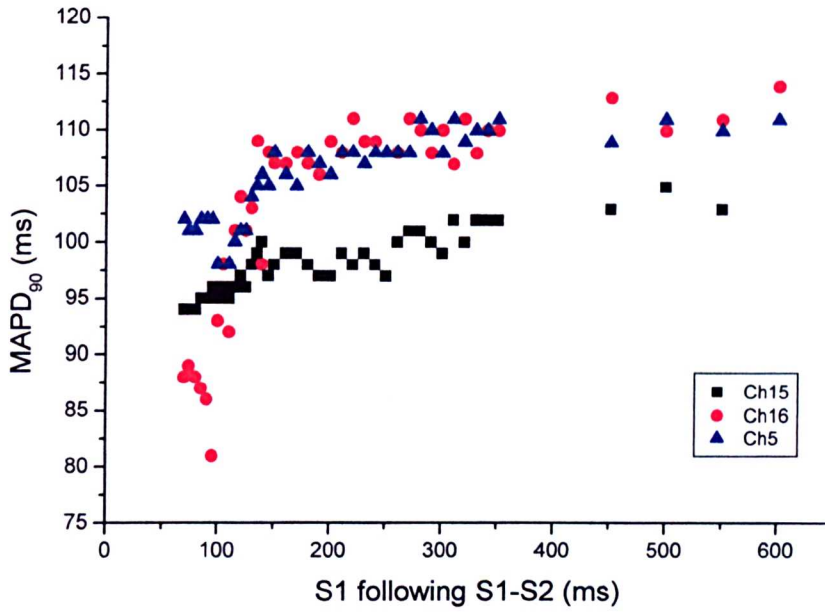
6.2.2 Data acquisition and analysis

Full details of data acquisition and MAP analysis are described in chapter 2. MAP signals were digitally recorded and stored on to hard disk for off-line analysis using Acq (Dr. F.L. Burton, University of Glasgow). MAPs were analysed to obtain estimations of MAPD₅₀, MAPD₉₀ and conduction delay (CD) using NMAP (Dr. F.L. Burton, University of Glasgow). The data was saved in to Excel 97 spreadsheets (Microsoft) and graphs were created in Origin 6.1 (Microcal). Due to the time restriction imposed by the 32 electrode array on MAP recording, the majority of data collected was from the 16 S1 extrastimulus protocol with 1000ms pause omitted, hence data was extrapolated from these experiments only. This protocol allowed stable S1 MAPs to be obtained prior to the extrastimulus S2. Data was then analysed to look at:

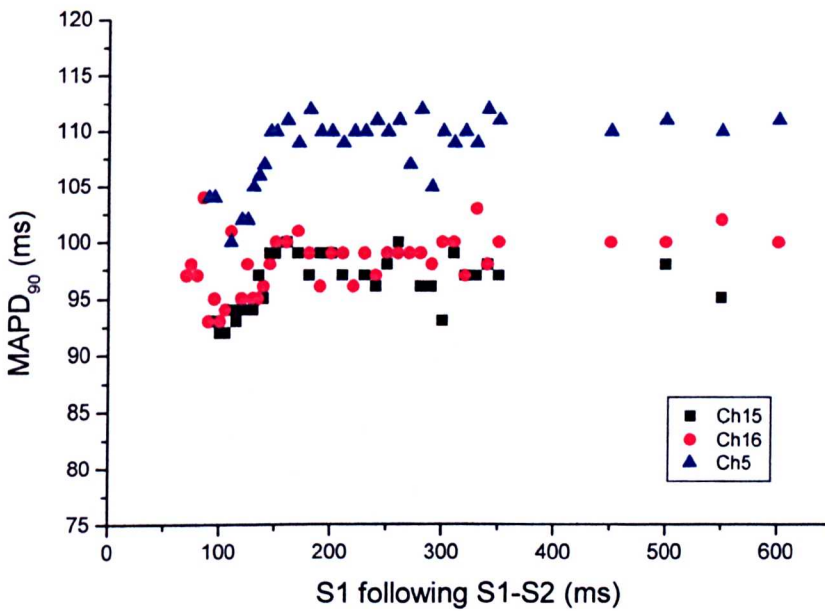
- i) stability of the extrastimulus protocol.
- ii) dispersion of repolarisation within hearts, compared between perfusion conditions (paired Student's t-test).
- iii) conduction delay, compared between perfusion conditions (paired Student's t-test) .
- iv) the negative slope of each individual restitution curve obtained, compared between perfusion conditions (paired Student's t-test)

6.3.1 Stabilisation of the basic S1 MAPs *prior* to the extrastimulus

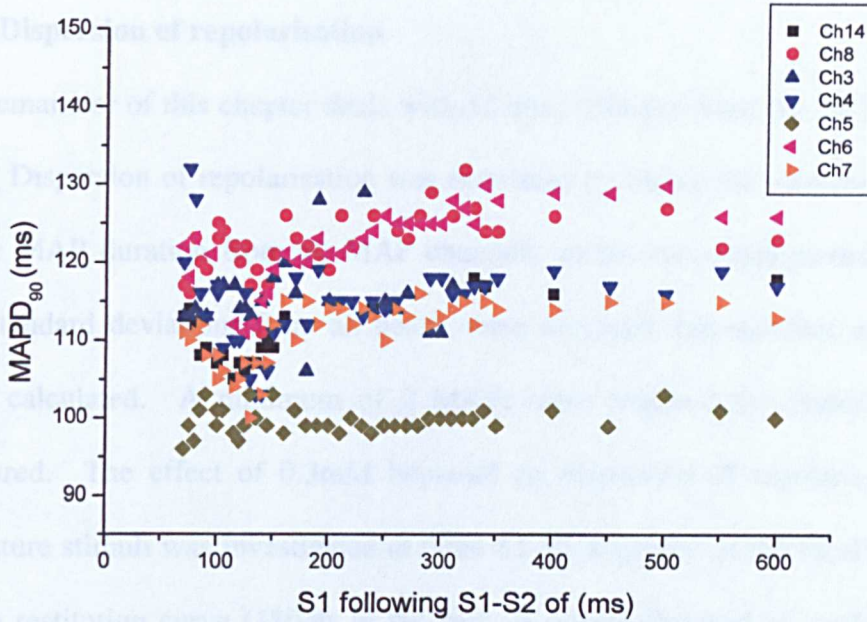
This section (6.3.1) is devoted to the stabilisation of restitution protocols and refers to the last S1 MAP of a train following the S2 extrastimulus and *not* the S1-S2 restitution curve. In order to check that the S2 stimulus was delivered to a heart that had reached steady state, the last S1 MAP in the 8 or 16 stimuli train following each extrastimulus was plotted against the previous S1-S2 interval, which was progressively increased in sequence (from 70ms up to 600ms). Graphs from individual experiments using the 8 and 16 S1 protocol both in Tyrode's and heptanol are shown in Figure 6.3. On perfusion with both Tyrode's and heptanol, the resulting graph from 8 S1 stimuli data resembled a restitution curve in so far as the curve had a local maximum and a plateau (Figure 6.3a and b). In contrast, the same graphs for the 16 S1 stimuli protocols were flat (Figure 6.3c and d). This indicates that 8 S1 stimuli is not sufficient to produce a stable MAP duration. However, the 16 S1 produces a stable MAP duration and therefore is the chosen protocol to use for the remainder of this study.



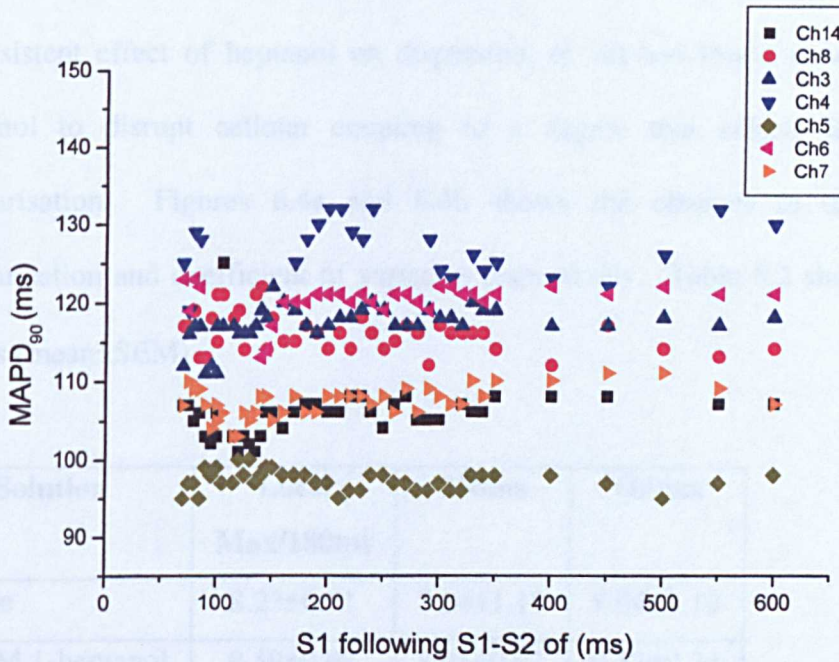
A. 8 S1 protocol, heart perfused with Tyrode's solution.



B. 8 S1 protocol, heptanol perfused heart.



C. 16 S1 protocol, Tyrode perfused heart.



D. 16 S1 protocol, heptanol perfused heart.

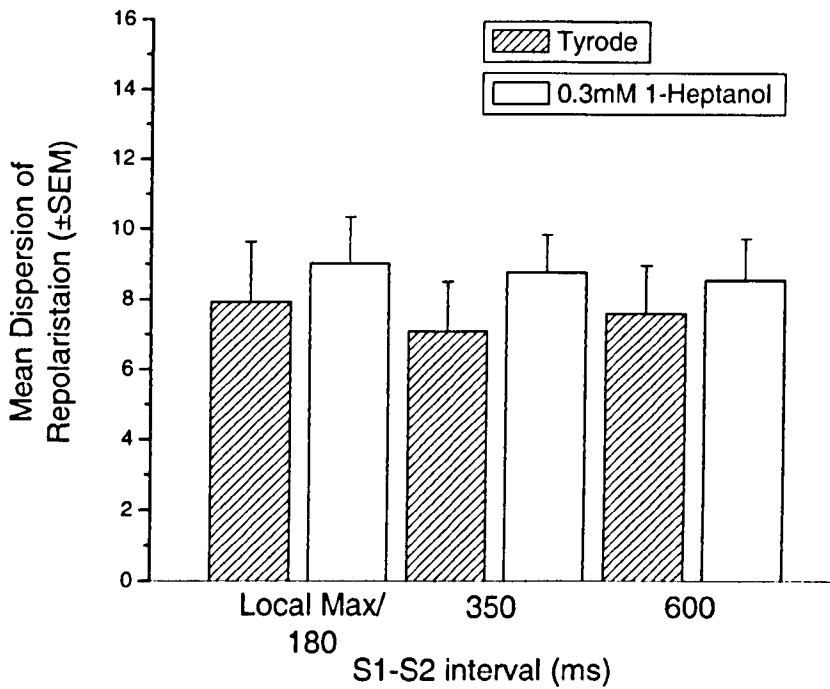
Figure 6.3 Typical experiments showing the stability of the S1 MAP on giving 8 S1 (A and B, 3 MAPs obtained simultaneously) and 16 S1 (C and D, 7 MAPs obtained simultaneously). Stimulation in Tyrodes (A and C) and heptanol (B and D) perfused hearts.

6.3.2 Dispersion of repolarisation

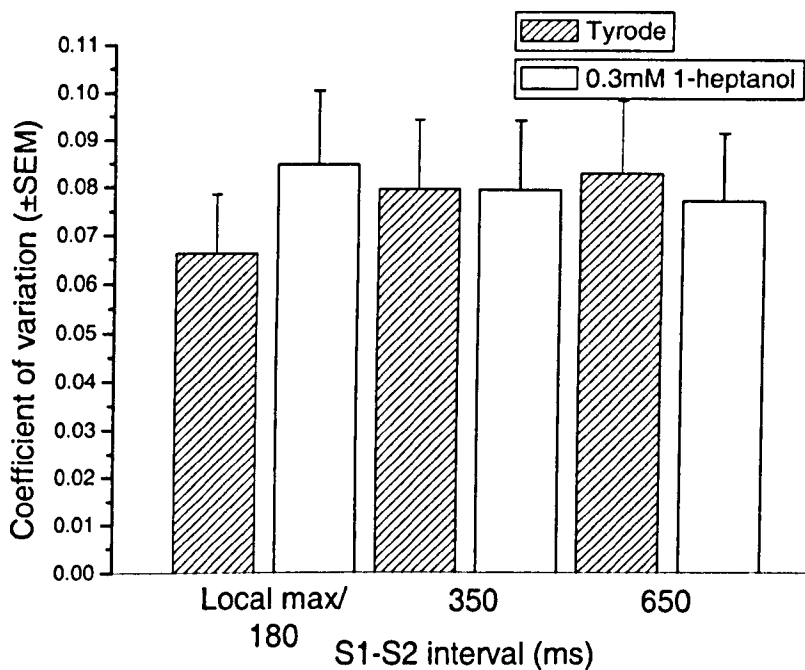
The remainder of this chapter deals with *S2 data* obtained from the *16 S1 protocol only*. Dispersion of repolarisation was estimated by taking the standard deviation of the MAP duration from all MAP channels within one experimental protocol. The standard deviations from all hearts were averaged and standard error of the mean calculated. A minimum of 2 MAPs were required for dispersion to be measured. The effect of 0.3mM heptanol on dispersion of repolarisation after premature stimuli was investigated at three S1-S2 intervals: at the local maximum on the restitution curve (180ms in the case of results obtained on perfusion with Tyrode), at 350ms and at 600ms. 0.3mM heptanol caused a small but non-significant (paired Student's t-test, $P>0.05$) increase in dispersion of repolarisation. This non-significant result may be due to i) variability in the data, ii) the inconsistent effect of heptanol on dispersion, or iii) too low a concentration of heptanol to disrupt cellular coupling to a degree that effects dispersion of repolarisation. Figures 6.4a and 6.4b shows the changes in dispersion of repolarisation and coefficient of variation respectively. Table 6.2 shows absolute values (mean \pm SEM).

Solution	Local Max/180ms	350ms	600ms
Tyrode	8.23 \pm 0.71	7.34 \pm 1.19	8.04 \pm 1.19
0.3mM 1-heptanol	8.59 \pm 0.98	8.91 \pm 0.93	9.52 \pm 0.74

Table 6.1 The effect of 0.3mM 1-heptanol on dispersion of S2 repolarisation. $P>0.05$, paired Student's t-test.



A. Dispersion of repolarisation.



B. Coefficient of variation.

Figure 6.4 Effect of 0.3mM 1-heptanol on dispersion of repolarisation in S2 MAPs, represented by SD (A) and coefficient of variation (B). 0.3mM 1-heptanol does not cause a change in dispersion of MAPD₉₀ repolarisation. n=9 hearts, 28 data sets.

6.3.3 Conduction delay

Conduction delay was measured as the time (ms) between the stimulus artefact and the upstroke of the MAP (V_{max}). Conduction delay varied depending on the position of the electrode in relation to the stimulus. Conduction delay was averaged from each MAP channel and the Tyrode data compared to the 0.3mM heptanol data by a paired Student's t-test. 0.3mM heptanol significantly increased conduction delay from (mean \pm SEM) 44.2 \pm 0.82ms to 49.2 \pm 0.87ms ($P < 0.0001$). Figure 6.5 represents these results.

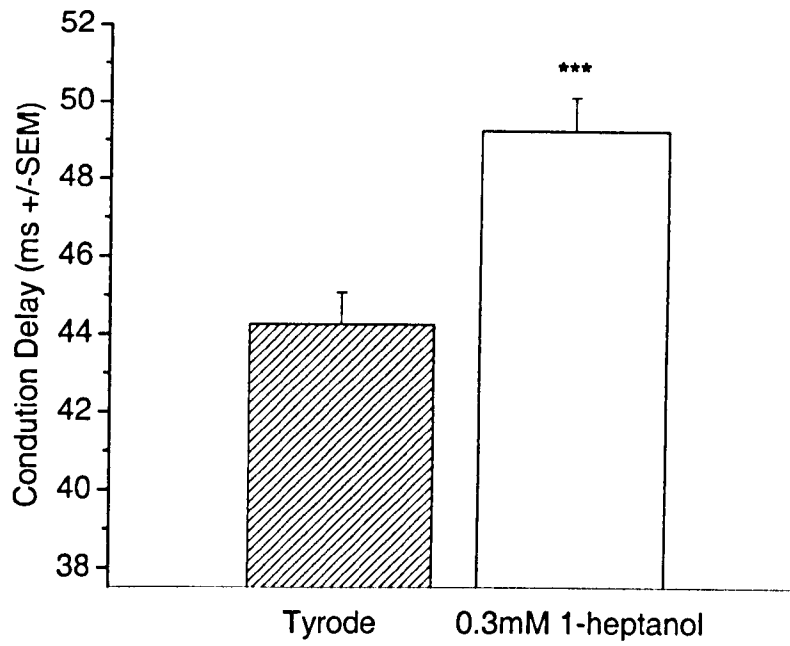
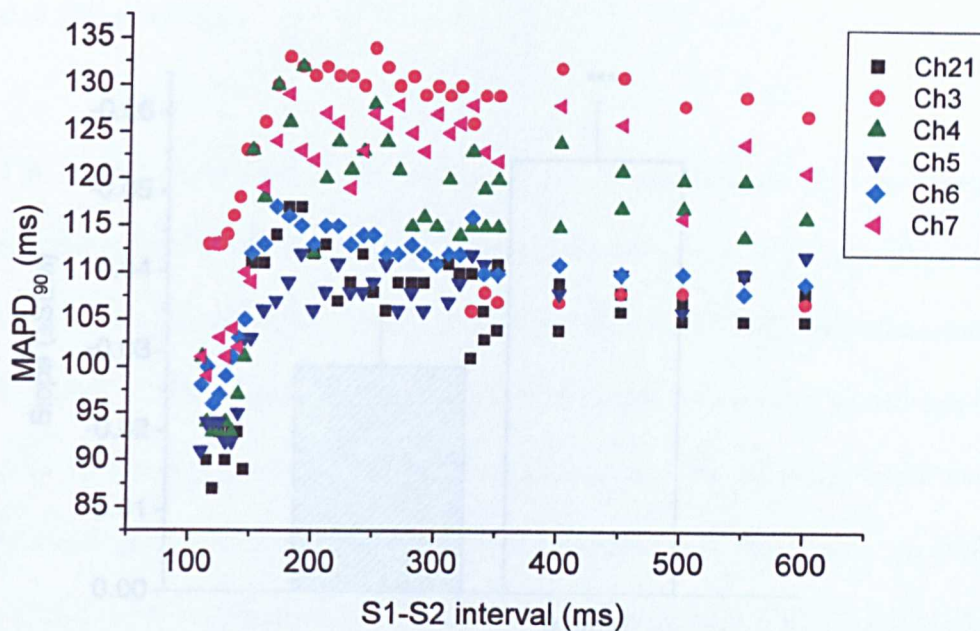


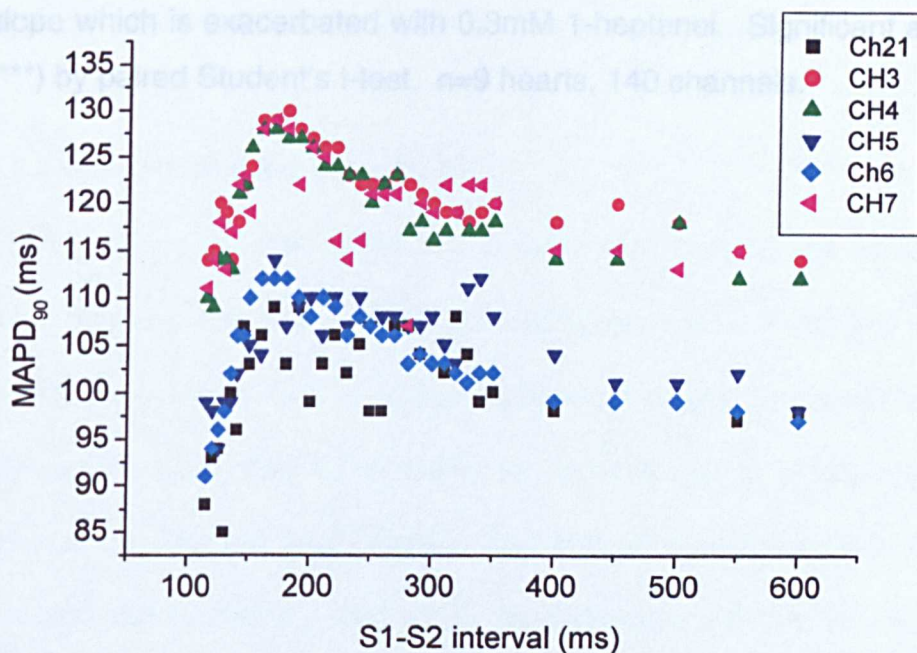
Figure 6.5 Effect of 0.3mM 1-heptanol on conduction delay. 0.3mM heptanol increases conduction delay significantly ($P < 0.001$ (***) by paired Student's t-test). $n=9$ hearts, 148 channels

6.3.4 The negative slope

Restitution curves from one typical experiment where 6 MAPs have been obtained simultaneously are shown in Figure 6.6. The most obvious effect of 0.3mM heptanol was to change the gradient of the slope between the local maximum on the restitution curve and S1-S2 interval of 350ms. This biphasic restitution curve was analysed between S1-S2 values of 180ms and 350ms in Tyrode perfused hearts, or between the local maximum on the restitution curve and 350ms in 0.3mM heptanol perfused hearts. These criteria were used due to the absence of a maximum in restitution curve of Tyrode perfused hearts and 180ms is a close approximation to the local maximum in the heptanol perfused hearts. Resulting slopes of the restitution curves were compared. 0.3mM heptanol significantly exacerbates the negative slope between the local maximum and 350ms. Figure 6.6a represents data obtained on perfusion with Tyrode's solution whilst Figure 6.6b illustrates the induction of a negative slope in the curve by 0.3mM heptanol. The averaged results of all experiments are illustrated in Figure 6.7. The gradient of the slope was significantly (paired Student's t-test, $P < 0.001$) altered by 0.3mM heptanol from (mean \pm SEM) -0.031 ± 0.004 in Tyrode's to -0.063 ± 0.005 .



A. Perfusion with Tyrode's solution.



B. Perfusion with 0.3mM heptanol solution.

Figure 6.6 Restitution data obtained from a single experiment where 6 MAPs have been obtained simultaneously.

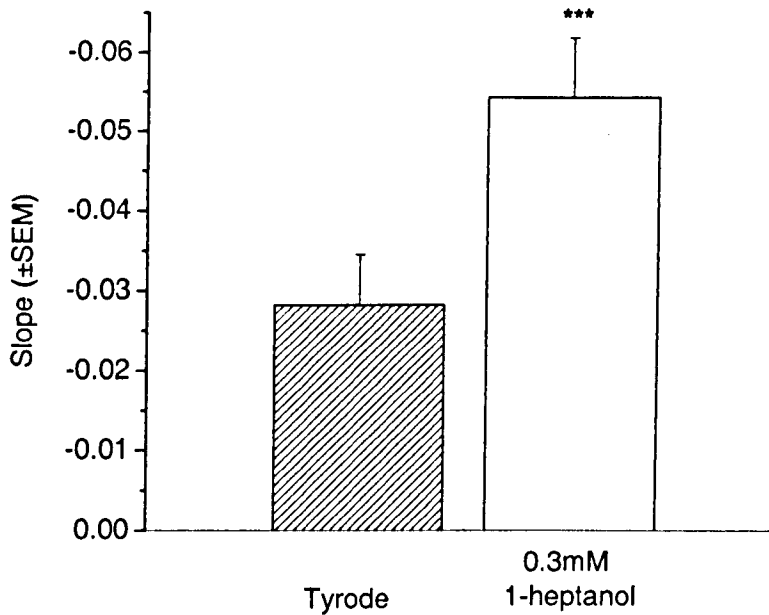


Figure 6.7 The effect of 0.3mM 1-heptanol on the slope of the restitution curve between 180ms (Tyrode, hashed) or the local maximum (0.3mM 1-heptanol, blank) and 350ms. Tyrode shows a slight negative slope which is exacerbated with 0.3mM 1-heptanol. Significant at $P < 0.001$ (***) by paired Student's t-test. $n=9$ hearts, 140 channels.

6.4 Discussion

The results show that MAP duration is not in steady-state prior to applying the extrastimulus S2 when a train of 8 S1 pulses are given. The resulting restitution curve looks plausible, but clearly it does not represent S1-S2 restitution accurately. The train of 8 S1 stimuli are not sufficient to enable recovery of membrane currents prior to the application of the next extrastimulus. On the other hand, the 16 S1 protocol produced stable S1 MAPs and therefore was the chosen protocol from which to extrapolate results. It is usually standard practice both clinically (Morady, 1988) and experimentally (Ramza, 1990) to use an 8 or 10 beat S1 stimuli train. Extrastimulus protocols are commonly used in humans and animals to measure refractory periods. Hence the finding of instability in MAP duration on application of an 8 S1 stimuli after an extrastimulus may be of importance.

6.4.1 Conduction delay and velocity

The significant increase in conduction delay seen with 0.3mM heptanol in this study suggests that gap junction uncoupling occurred. Spear and co-workers (1990) have shown that in normal anisotropic canine ventricular epicardium, heptanol causes a slowing of conduction velocity due to a relatively selective decrease in gap junctional conductance without significantly affecting action potential depolarisation. This effect on conduction velocity is greater in the transverse direction than the longitudinal direction due to the anatomical distribution of cardiac gap junctions and the greater effective axial resistance in the transverse direction. Gap junction channels are found mainly at the cell poles with only a few located at the lateral cell borders, thus contributing to the anisotropy of

the cardiac tissue. It has also been noted by this group that conduction block induced by heptanol occurs firstly in the transverse direction.

Delmar *et al* (1987) investigated the effects of increased intercellular resistance on transverse and longitudinal propagation in sheep epicardial muscle. They superfused thin square pieces of sheep epicardial muscle with 1.5mM heptanol whilst recording TAPs at opposite corners of the preparation and alternately stimulating in the longitudinal or transverse directions. It was concluded that, on impaired intercellular coupling by heptanol, transverse propagation is more vulnerable to block, and this is not dependent on changes in V_{max} . However, dispersion of action potential duration as an indicator of the arrhythmogenic effects of heptanol was not determined.

In the work of Spear *et al* (1990) on infarcted canine myocardium it was hypothesised that an abnormally high intercellular coupling resistance between surviving cells caused slowed conduction. Low concentrations (<0.5mM) of heptanol that had been shown to have a minimal effect on conduction in normal myocardium, induced local conduction block in infarcted myocardium which already showed abnormal conduction. This selective conduction block in infarcted regions may give the impression that a low concentration of heptanol improves conduction. They proposed that heptanol might 'electrically unload' a pathway to allow conduction to occur by causing uncoupling in an adjacent region. The ability of heptanol to abolish abnormal conduction in infarcted myocardium may lead a way to finding an agent with the uncoupling effect of heptanol (but much less toxic properties) that could have anti-arrhythmic properties in infarction.

Keevil *et al* (2000) investigated the effect of a range of heptanol concentrations on the electrogram latency in Langendorff perfused rabbit hearts. By taking the reciprocal of the electrogram latency and estimated inhibition of gap junctions they gave an accurate measurement of the conduction velocity. Heptanol did not change the shape of the electrogram recordings, indicating that the activation wavefront was moving in a similar direction with and without heptanol. They therefore suggested that the increase in latency seen with heptanol is due to a decrease in conduction velocity. In their study, 0.1mM heptanol decreased conduction velocity by 8% whilst 1mM heptanol decreased it by 65% and was not pro-arrhythmic. The decrease in conduction velocity seen on perfusion with heptanol is a global effect as opposed to the more local effect seen in myocardial infarction. It is however clear that changes in conduction velocity may have implications in arrhythmogenesis.

6.4.2 Dispersion of repolarisation

In contrast to theory and hypothesis, the gap junction uncoupler heptanol at a concentration of 0.3mM did not cause a consistent significant increase in dispersion of repolarisation. A significant increase in dispersion of repolarisation was observed at an S1-S2 interval of 600ms only.

In the normal heart regional differences in action potential duration are seen, and this is a completely physiological occurrence (base to apex, and transmural differences in action potential duration are discussed in the general introduction (chapter 1)). Action potentials tend to be longer at earlier activation sites and shorter at later activation sites to ensure that recovery is homogenous. The electrotonic interaction between cells is thought to mask the intrinsic dispersion of

repolarisation (differences between individual cells) (Joyner, 1986) and enables this homogenous recovery to occur. Single cells are therefore able to express their intrinsic action potential duration in the absence of electrotonic interactions. Therefore, uncoupling cells (i.e. as with heptanol) should lead to an increase in heterogeneity of repolarisation which may favour re-entry (Janse and Wit, 1989).

Lesh *et al* (1989) hypothesised (and tested via a computer simulation model) that when cells are well coupled, local differences in intrinsic action potential duration are not apparent but as axial resistivity increases, local variation in action potential duration become evident. They showed that changes in axial resistivity can modulate how spatial dispersion of intrinsic action potential duration is manifest (i.e. uncoupling increases dispersion of repolarisation). These findings may be important in understanding the mechanism of re-entrant arrhythmia initiation in infarctions where evidence suggests that abnormal cellular coupling is the primary electrophysiological derangement.

6.4.3 The negative slope in the restitution curve

The induction of a negative slope by 0.3mM heptanol is a phenomenon that was observed, but was not a result initially expected. The single catheter results showed that heptanol decreases MAP duration. The 32 MAP electrode array results indicated that there is indeed a decrease in MAP duration, but this decrease is more substantial at intermediate S1-S2 intervals, between the local maximum and S1-S2 interval of 350ms. The cause of the induction of the negative slope by heptanol will be discussed in the final discussion and conclusion (chapter 10), where further work will also be addressed.

Considering heptanol has previously been described as a non-specific gap junction uncoupler (Rudisuli and Weingart, 1989), a natural progression in this study was to investigate the effect of heptanol on single cells. This manifested itself as an investigation in to whether the negative slope in the restitution curve is a gap junction uncoupling phenomenon or whether it is caused by a disruption in E-C coupling.

**Chapter 7 - The effect of 1-heptanol and nifedipine on single cell
fractional shortening and calcium handling**

7.1 Introduction

This chapter deals primarily with the effect of heptanol on single cell contractility, Ca^{2+} transient, and SR Ca^{2+} content in isolated epicardial left ventricular myocytes. As reviewed in chapters 5 and 6, heptanol is known to affect gap junctions at relatively high (approximately 1-3mM) concentrations. At these concentrations heptanol seems also to effect several other cellular processes. Takens-Kwak *et al* (1992) used cultured neonatal rat cells to investigate the effect of 1mM heptanol on non-junctional membranes. They found that both the inward rectifying K^+ current (I_{K1}), the delayed rectifying current (I_K), the inward Na^+ current (I_{Na}), and the L-type Ca^{2+} current (I_{CaL}) were all reduced. In work on the effects of general anaesthetics on current flow across membranes in guinea pig myocytes (Niggli *et al*, 1989), found that n-alkanols (heptanol, octanol) and halothane caused a decreased amplitude and an accelerated inactivation of I_{CaL} . These, and other studies (Burt and Spray, 1989; Niggli *et al*, 1989; Rudisuli and Weingart, 1989) used isolated guinea pig myocytes. No detailed study on the effects of heptanol in the rabbit has appeared in the literature.

This study has shown that, in the whole rabbit heart, heptanol caused a marked decrease in contractility (as measured by LVDP, refer to chapter 5 section 5.3.2.1). Although a reduction in gap junction coupling may in itself lead to a less synchronised spread of conduction and therefore decrease contractility, this cannot account for (all) the reduction in LVDP. Based on previously published work a more likely explanation for the reduction in contractility is an effect of heptanol on E-C coupling of individual myocytes. In particular, there is evidence (Niggli *et al*,

1989; Takens-Kwak *et al*, 1992) to suggest that it may have a direct effect on the L-type Ca^{2+} channel.

Due to the speculation concerning the effect of heptanol on the L-type Ca^{2+} channel the effect of nifedipine, an L-type Ca^{2+} blocker, was investigated in single cells and subsequently the whole heart. Nifedipine is a specific L-type Ca^{2+} channel antagonist that binds to the L-type Ca^{2+} channel (dihydropyridine receptor) in a voltage dependent manner. The aim of this investigation was to relate the negative inotropic effect of heptanol in the single cell, to a concentration of nifedipine that produces the equivalent negative inotropic effect on contractility in the single cells. This would give an approximate concentration of nifedipine that could then be used on the Langendorff perfused rabbit heart to investigate the effect of partial L-type Ca^{2+} channel blockade on the gradient of the slope of the electrical restitution curve.

7.2 Methods

Details of cell isolation and the measurements of single cell fractional shortening, Ca^{2+} transient, and SR Ca^{2+} content was given in chapter 2. Left ventricular *epicardial* myocytes from stock and sham-operated rabbit hearts were used to allow comparison with previous measurements from the epicardial surface of the whole heart. Cells were pipetted into the perfusion bath and allowed to settle for approximately 5 minutes prior to switching on perfusion. This settling period allowed enough cells to stick to the glass bottom of the bath, which could then be superfused without being dislodged. Perfusion was initially with normal Krebs solution at 37°C.

7.2.1 Fractional shortening and Ca^{2+} measurement stimulation protocols

The stimulation protocol for fractional cell shortening measurements is illustrated in Figure 7.1a. The stimulation protocol was initially recorded on perfusion with 0.03mM heptanol and then repeated, at both stimulation frequencies, with 0.1mM and 0.3mM heptanol. Finally, re-perfusion with Krebs allowed reversibility to be measured. Solution changes were made via a custom made 4-way solution changer. In the preliminary investigations using nifedipine, various concentrations of nifedipine solution were tried with the aim of determining a concentration of nifedipine that caused a similar degree of inhibition of fractional cell shortening compared to heptanol (see results). These experiments indicated that inhibition of shortening comparable to that seen with heptanol was obtained on perfusion with 0.15 μ M nifedipine.

Initially it was planned that fractional cell shortening and Ca^{2+} measurements be obtained simultaneously. However, due to technical difficulties complicating the process of simultaneous recording separate experiments were required. Fura-2 seemed to reduce the contractility of the cell to a degree at which single cell shortening measurements were difficult to maintain. Fractional cell shortening was calculated from end-diastolic and end-systolic cell lengths, and Ca^{2+} measurements from end-diastolic and end-systolic Fura-2 ratios (refer to chapter 2 general methods).

7.2.2 Caffeine induced sarcoplasmic reticulum Ca^{2+} release stimulation protocols

To investigate the effect of heptanol and also nifedipine on SR Ca^{2+} content, rapid perfusion with caffeine (20mM) was performed. This causes a rapid release of Ca^{2+} from the SR. Many studies have used the amplitude of caffeine induced release as an indicator of the SR Ca^{2+} content (e.g. Denvir *et al*, 1998; Davies *et al*, 2000). Cells were initially perfused with Krebs at 37°C and paced at 1Hz for 60 seconds. Stimulation was briefly stopped as perfusion was switched from Krebs to a rapid application of 20mM caffeine. Following the caffeine response stimulation at 1Hz was resumed with Krebs perfusion. Stimulation was stopped for a maximum of 5 seconds. The protocol was repeated with either 0.1mM heptanol or 0.15 μM nifedipine solution. The caffeine protocol is shown schematically in Figure 7.1b.

7.2.3 Statistical analysis

The majority of the measurements made within this section were compared to an individual control (Krebs), therefore it was necessary to make statistical comparisons using a paired Student's's t-test rather than a repeated measures ANOVA.

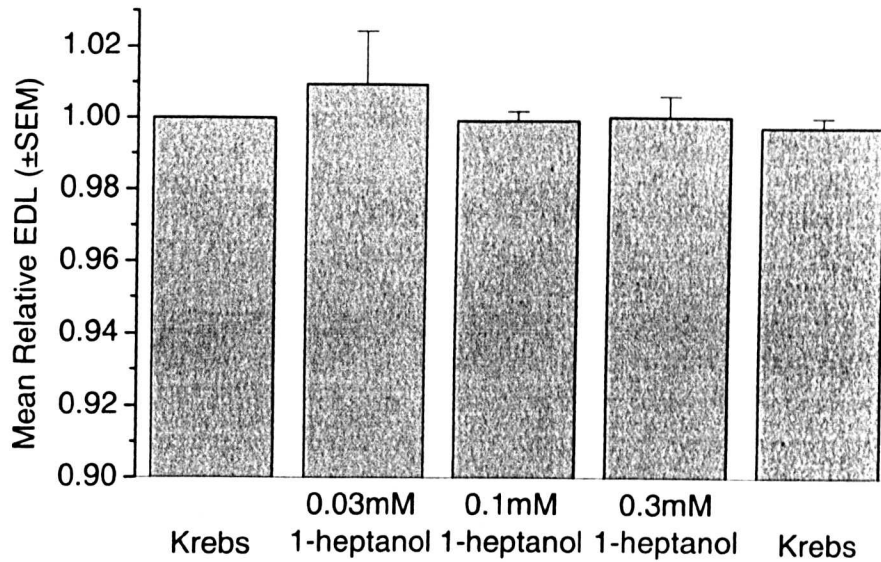
7.3 Results

7.3.1 Relative end-diastolic lengths

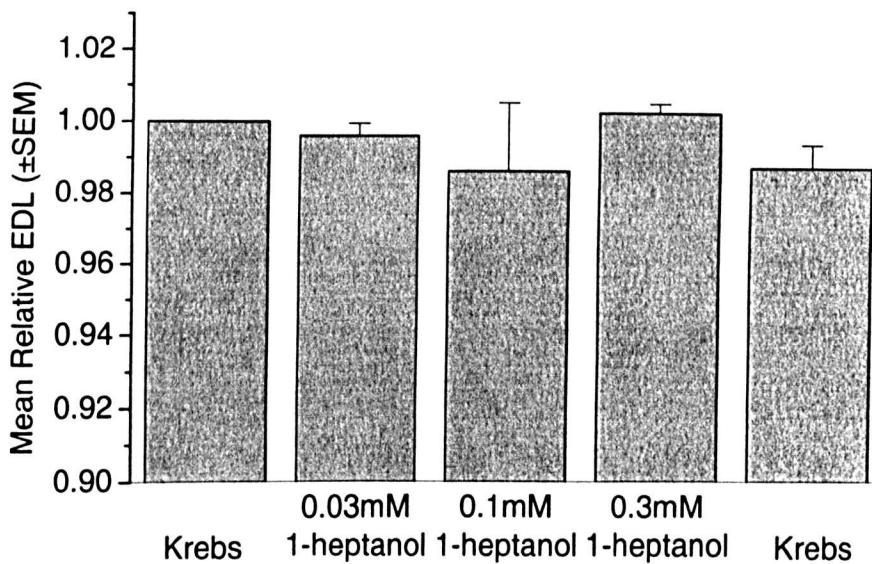
End diastolic length (EDL) was measured during perfusion with Krebs, 0.03mM, 0.1mM and 0.3mM heptanol and on reperfusion with Krebs. Data were normalised to the baseline value in Krebs, and expressed as relative EDL. In a second set of experiments EDLs were recorded on perfusion with 0.1 μ M, 0.15 μ M and 0.2 μ M nifedipine.

The effect of heptanol over a range of concentrations on relative EDL is illustrated in Figure 7.2. Heptanol, at all concentrations and at both 1Hz and 3Hz stimulation rates, did not have any effect on the EDL.

Figure 7.3 illustrates the relative EDL values obtained on perfusion with the nifedipine concentration range at 1Hz. It is evident that nifedipine also does not effect EDL in the range of concentrations studied.



A. Stimulation at 1Hz. n=11 heart, 46 cells.



B. Stimulation at 3Hz. n=9 hearts, 24 cells.

Figure 7.2 The effect of 1-heptanol on end diastolic length. Heptanol is normalised to the value on Krebs prior to exposure to heptanol.

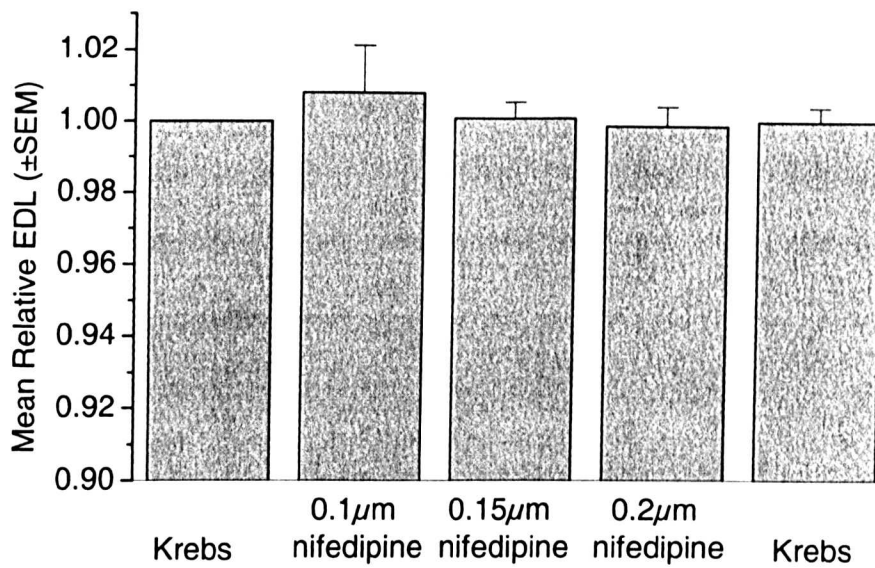


Figure 7.3 The effect of 0.1 μM, 0.15 μM and 0.2 μM nifedipine on relative end diastolic length. n=4 hearts, 24 cells. Nifedipine is normalised to the value on Krebs prior to exposure to heptanol.

7.3.2 Fractional shortening

Changes in percentage fractional shortening on perfusion with heptanol or nifedipine solution were used to indicate changes in cell contractility. Fractional cell shortening is calculated as follows:

$$\text{Fractional cell shortening (\%)} = 100 - (\text{ESL}/\text{EDL}) \times 100$$

where ESL=end systolic length and EDL=end diastolic length

To allow the average effect of heptanol to be calculated, data were further analysed and graphically illustrated as the relative fractional cell shortening. This is fractional shortening (see above) normalised to the standard conditions (stimulation in Krebs solution).

Relative fractional cell shortening is calculated, for each concentration of heptanol and nifedipine as follows (heptanol appears in the equation but may be substituted for nifedipine):

$$\text{Relative fractional cell shortening (RFS)} = (\text{Heptanol FS}/\text{Krebs FS})$$

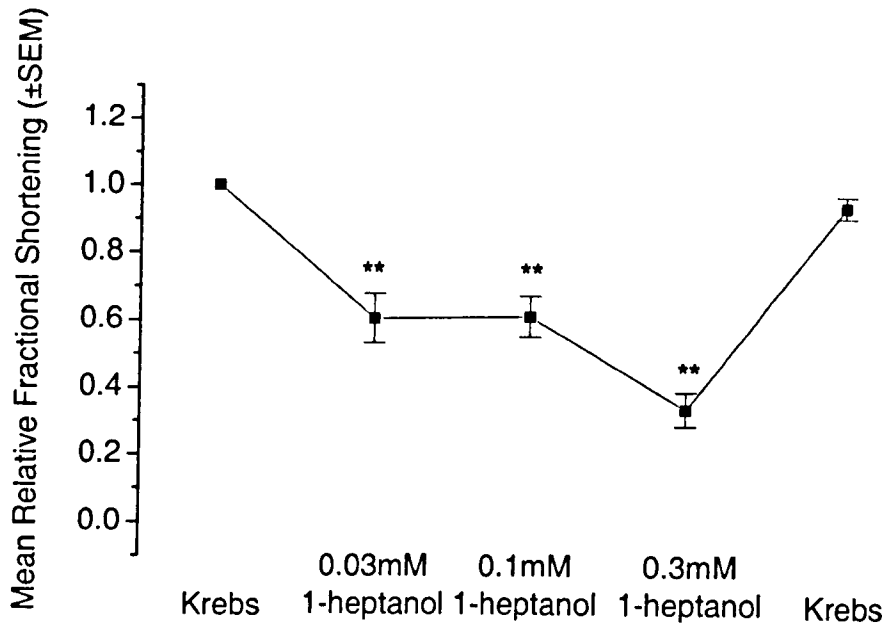
0.03mM, 0.1mM and 0.3mM heptanol induced a significant decrease in fractional cell shortening. Contractility is fully recovered on reperfusion with normal Krebs solution. Comparable results were obtained at 1Hz and 3Hz. Figures 7.4a and 7.4b illustrate the effect of 0.03mM, 0.1mM and 0.3mM 1-Heptanol on relative fractional shortening, from cells stimulated at 1Hz and 3Hz respectively. The experimental trace in Figure 7.5 shows a typical result where contractility was significantly reduced on perfusion with 0.1mM heptanol (stimulation at 1Hz).

Contractility was fully recovered on reperfusion with Krebs. Data are also shown in Table 7.1 as absolute values.

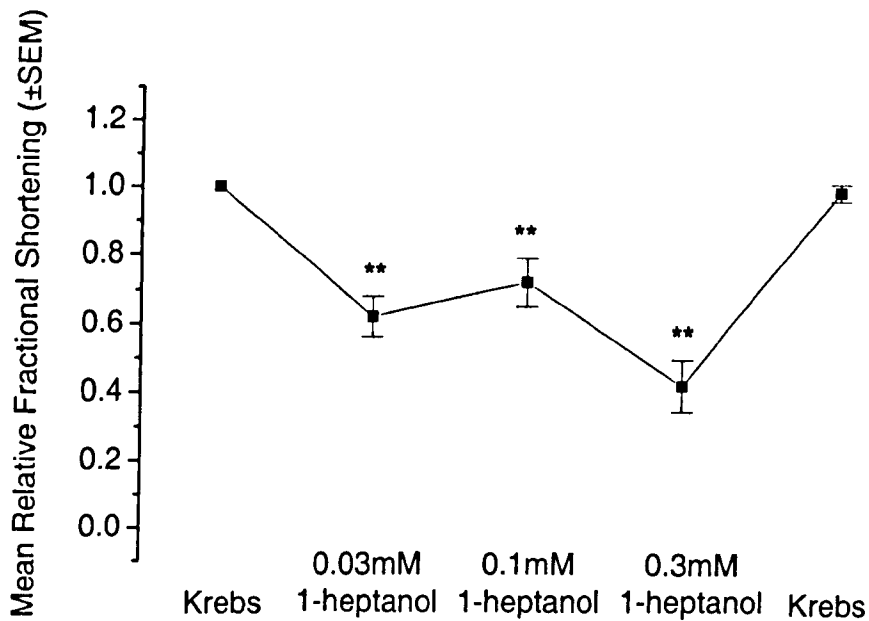
Figure 7.6 illustrates the changes in relative fractional cell shortening caused by perfusion with the 3 nifedipine concentrations at 1Hz only. Nifedipine also decreases fractional cell shortening. This effect was significant at 0.15 μ M and 0.2 μ M but not at 0.1 μ M nifedipine. The experimental trace in Figure 7.7 illustrates a typical result from an experiment where 0.15 μ M nifedipine decreases single cell contractility. Data is also shown in Table 7.1 as absolute values.

	Mean Fractional Cell Shortening (%) (\pm SEM)				
	Krebs	0.03mM heptanol	0.1mM heptanol	0.3mM heptanol	Krebs
1Hz	9.3 \pm 0.8	5.7 \pm 0.7**	5.6 \pm 0.9**	3.2 \pm 0.8**	7.7 \pm 0.8
3Hz	10.6 \pm 0.8	6.5 \pm 1.4**	7.7 \pm 1.4**	4.7 \pm 1.5**	10.9 \pm 1.3
		0.1 μ M nifedipine	0.15 μ M nifedipine	0.2 μ M nifedipine	
1Hz	8.9 \pm 0.7	5.8 \pm 0.7	3.4 \pm 0.9***	0.8 \pm 0.2***	9.2 \pm 1.4

Table 7.1 The effect of 1-heptanol at 1Hz and 3Hz, and nifedipine at 1Hz, and on mean fractional cell shortening. Heptanol and nifedipine significantly decrease fractional cell shortening (unpaired Student's t-test **= P <0.01, ***= P <0.001).



A. Stimulation at 1Hz. n=11 heart, 46 cells.



B. Stimulation at 3Hz. n=9 hearts, 24 cells.

Figure 7.4 The effect of 1-heptanol on relative fractional cell shortening. **A.** Stimulation at 1Hz and **B.** Stimulation at 3Hz on perfusion with 0.03mM, 0.1mM and 0.3mM heptanol. Unpaired Student's t-test **= $P < 0.01$, ***= $P < 0.001$.

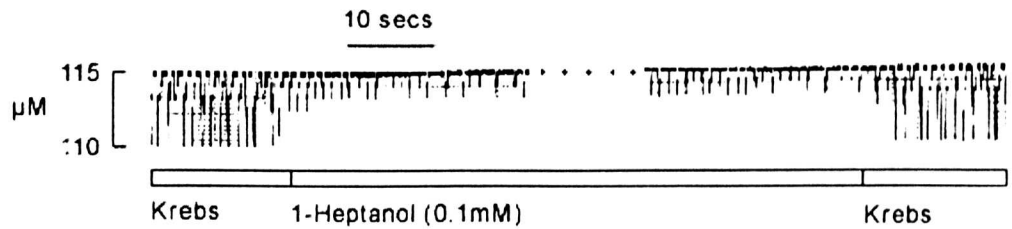


Figure 7.5 Trace showing the effect of 0.1mM 1-heptanol on single cell shortening. A typical experimental trace showing that perfusion with 0.1mM heptanol significantly reduces contractility, but is fully reversible. Stimulation is at 1Hz. The length of the cell (μM) is shown to the left of the trace.

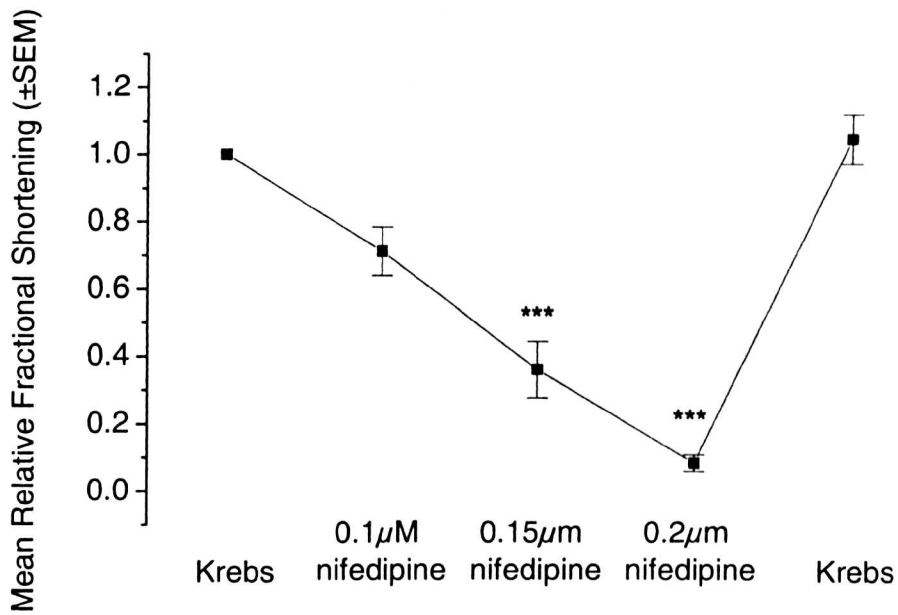


Figure 7.6 The effect of 0.1 μM, 0.15 μM and 0.2 μM nifedipine on relative fractional shortening.

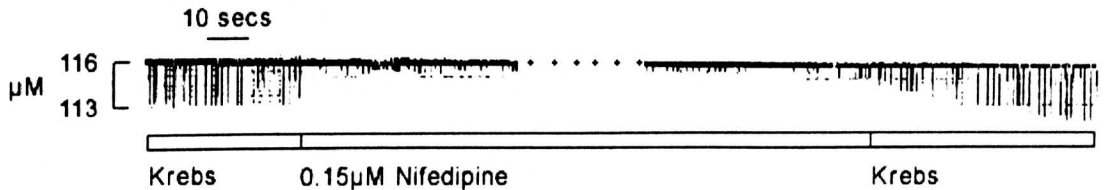
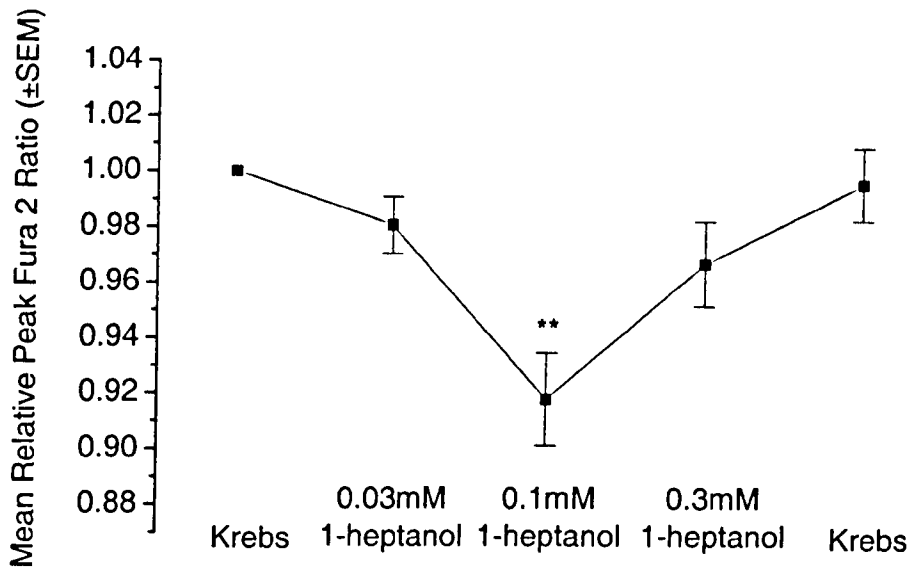


Figure 7.7 Experimental trace illustrating the effect of 0.15 μM nifedipine on single cell contractility. Nifedipine significantly decreases single cell contractility but, as with heptanol, the effect is fully recoverable. Stimulation is at 1 Hz. The length of the cell (μM) is shown to the left of the trace.

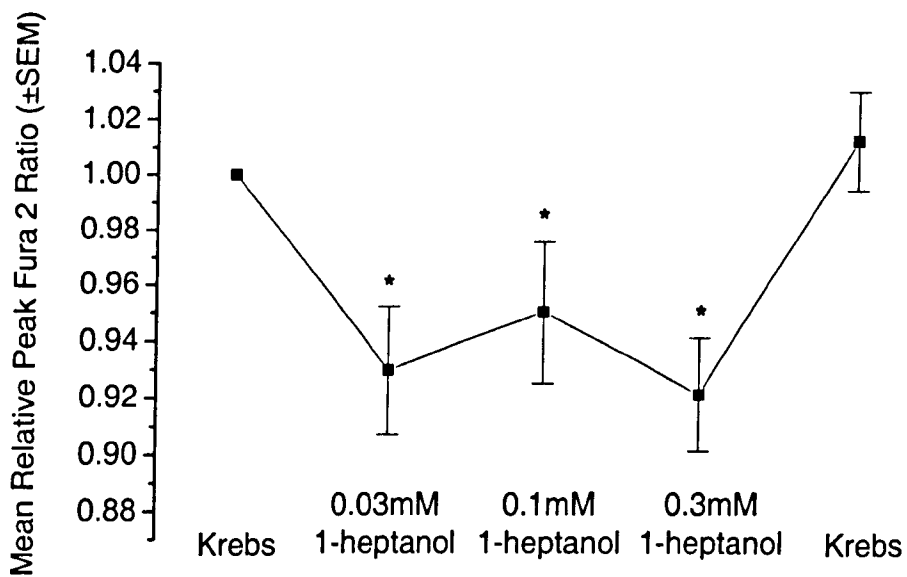
7.3.3 Calcium handling

Ca^{2+} measurements were obtained to attempt to relate the reduction in single cell fractional shortening to changes in single cell intracellular Ca^{2+} concentration. Calcium transients were quantified in terms of end diastolic Fura-2 ratio and peak systolic Fura-2 ratio.

Figures 7.8a and 7.8b illustrate the effect of heptanol on peak Fura-2 results for cells stimulated at 1Hz and 3Hz respectively. 0.03mM, 0.1mM and 0.3mM heptanol decreased peak Fura-2 ratio. This effect was statistically significant with 0.1mM heptanol at 1Hz but at all concentrations at 3Hz ($P < 0.05$, unpaired Student's t-test). The heptanol results contrast, in significance, to the results found with 0.1 μM , 0.15 μM and 0.2 μM nifedipine whose effect on peak Fura-2 ratio was found to be statistically significant at 1 Hz across the concentration range (Figure 7.9). Figure 7.10 and 7.11 are examples of experimental traces that illustrate the effect of 0.1mM heptanol and 0.15 μM nifedipine on the Ca^{2+} (Fura-2) transients. The amplitude of the Ca^{2+} transients recovered on reperfusion with normal Krebs solution at both 1Hz and 3Hz after perfusion with heptanol and nifedipine. End diastolic results are not shown but no change was detected.



A. Stimulation at 1Hz. n=5 heart, 15 cells.



B. Stimulation at 3Hz. n=7 hearts, 15 cells.

Figure 7.8 The effect of 1-heptanol on relative peak Fura-2 ratios. Perfusion with Krebs, 0.03mM, 0.1mM and 0.3mM heptanol. Student's unpaired t-test *= $P < 0.05$, ** $P < 0.01$.

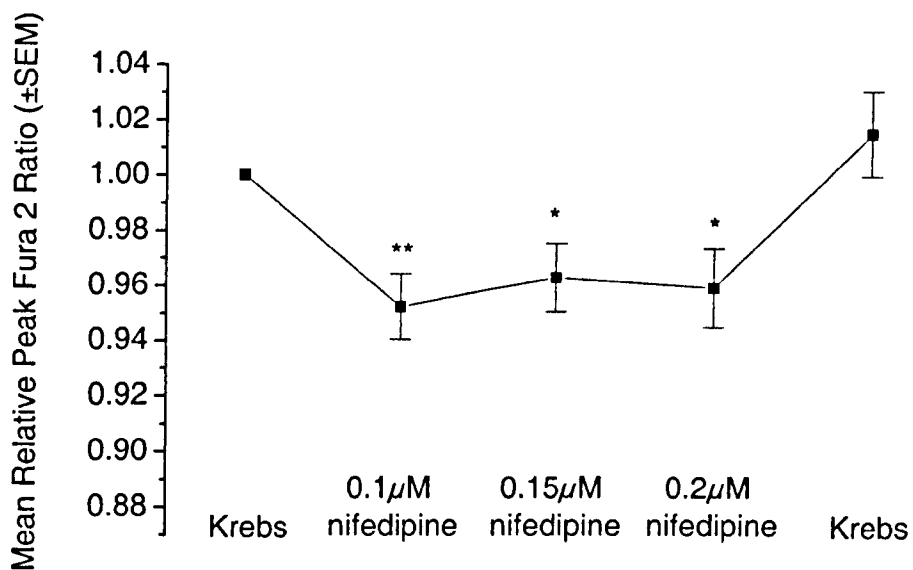


Figure 7.9 The effect of 0.1 μ M, 0.15 μ M and 0.2 μ M nifedipine on relative peak Fura-2 ratio. n=3 hearts, 9 cells. Unpaired Student's t-test *=P<0.05, **=P<0.01.

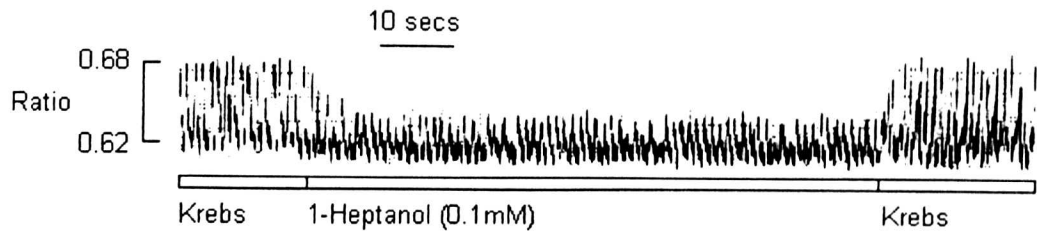


Figure 7.10 Experimental trace showing the effect of 0.1mM 1-heptanol on single cell Fura-2 ratio.

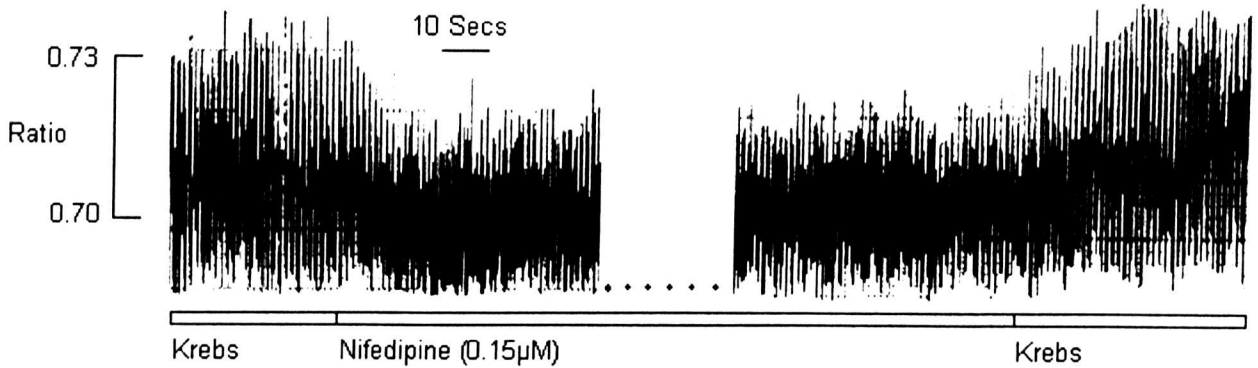


Figure 7.11 Experimental trace showing the effect of 0.15µM nifedipine on Fura-2 ratio.

7.3.4 Sarcoplasmic reticulum Ca^{2+} content

SR Ca^{2+} content was assessed by applying a bolus of 20mM caffeine to cells that had previously been stimulated at 1Hz. Stimulation was stopped momentarily for the caffeine to be pulsed. Baseline (stimulation at 1Hz), and caffeine peak Fura-2 ratios were measured from cells perfused with Krebs solution and 0.1mM heptanol and 0.15 μ M nifedipine solution.

The effect of 0.1mM heptanol on peak systolic SR Ca^{2+} content (as measured by Fura-2 ratios) is illustrated in Figure 7.12. Figure 7.12 shows that 0.1mM heptanol caused a decrease ($P>0.05$) in SR Ca^{2+} release but did not effect SR Ca^{2+} content. Figure 7.13 shows experimental traces illustrating the changes in SR Ca^{2+} content with 0.1mM heptanol.

Nifedipine similarly induced a decrease ($P>0.05$) in SR Ca^{2+} release. It also reduced ($P<0.05$) SR Ca^{2+} content, as compared to control Krebs. (Figure 7.14). Figure 7.15 shows experimental traces that illustrate the effect of 0.15 μ M on SR Ca^{2+} content.

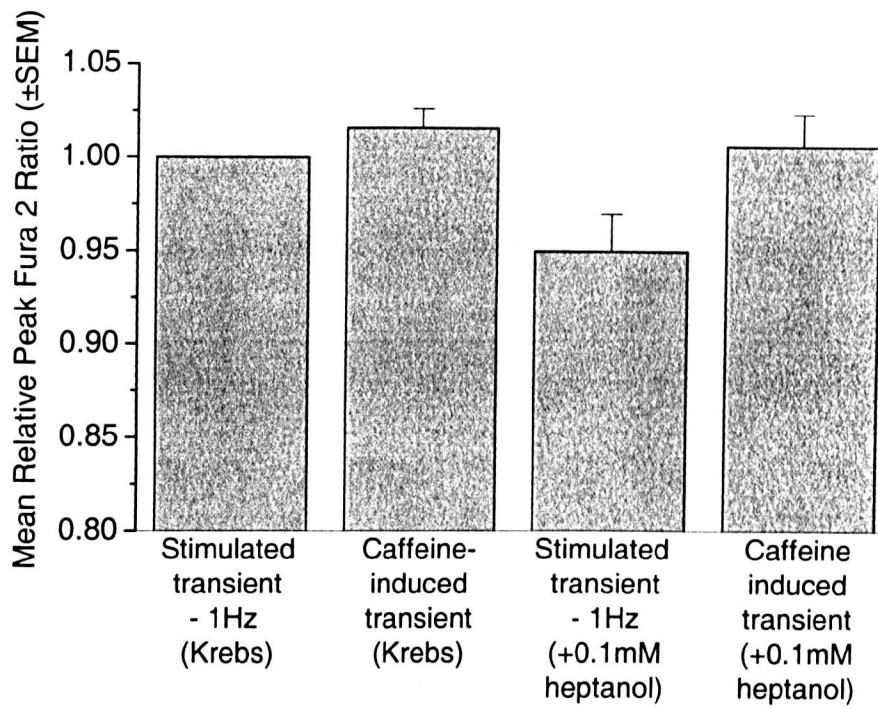
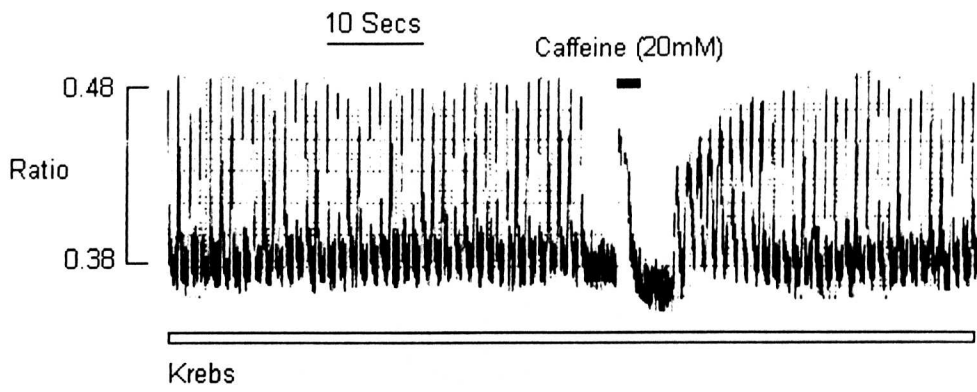
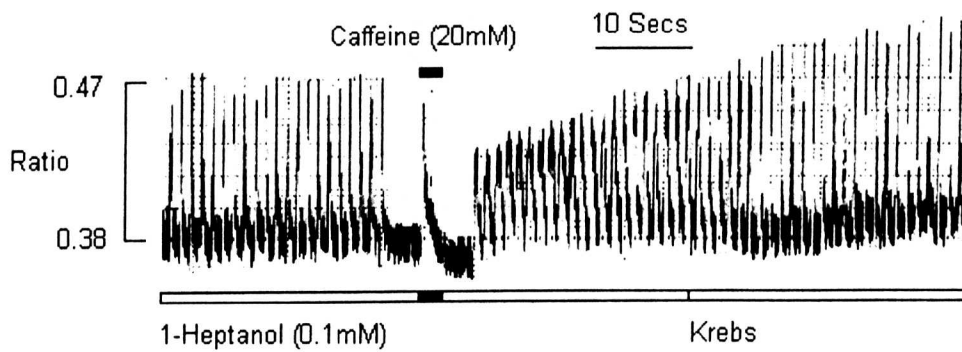


Figure 7.12 The effect of 0.1mM 1-heptanol on sarcoplasmic reticulum Ca^{2+} content. n=3 hearts, 11 cells.



A. Experimental trace showing the SR Ca^{2+} content by application of 20mM caffeine.



B. Experimental trace showing the effect of 0.1mM 1-heptanol on SR Ca^{2+} content by application of 20mM caffeine.

Figure 7.13 The effect of 1-heptanol on SR Ca^{2+} content: experimental traces. Ratios are indicated to the left of the traces.

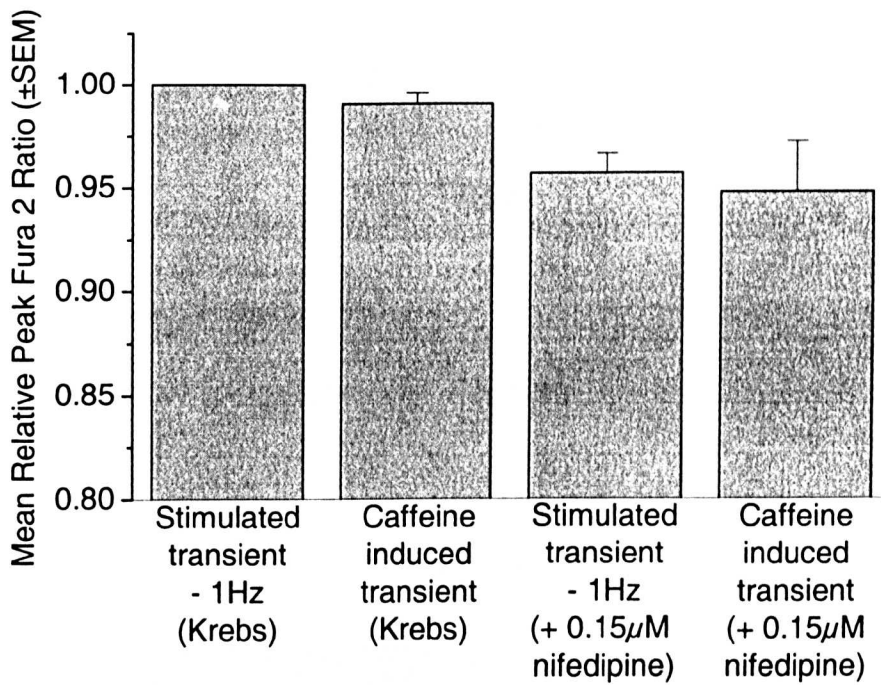
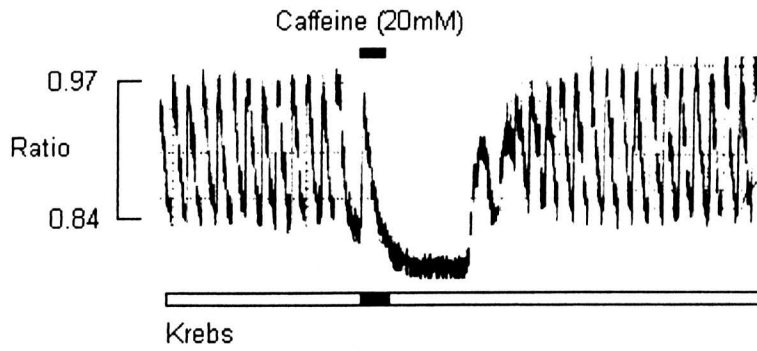
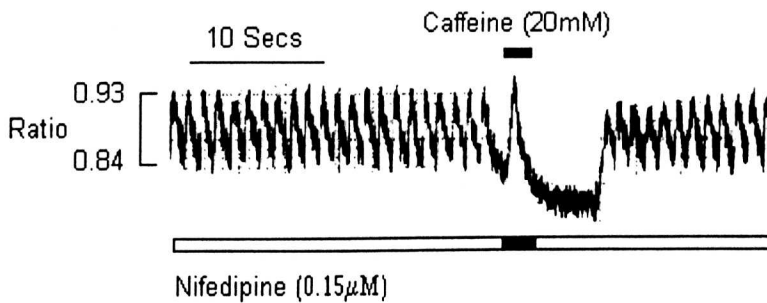


Figure 7.14 The effect of 0.15µM nifedipine on SR Ca²⁺ content. n= 3 hearts, 22 cells.



A. Experimental trace showing SR Ca^{2+} content by application of 20mM caffeine.



B. Experimental trace showing the effect of 0.15µM nifedipine on SR Ca^{2+} content.

Figure 7.15 Experimental traces showing the effect of nifedipine on SR Ca^{2+} content. Ratios are shown to the left of the traces.

7.4 Discussion

The results in this chapter show that at a concentration known to cause gap junction uncoupling, heptanol also has significant depressive effects on E-C coupling. In this investigation the initial studies on cell shortening indicate that, at both 1Hz and 3Hz stimulation rates, 0.1mM heptanol decreased fractional shortening to approximately 50% of control values. Higher concentrations of heptanol are required to produce comparable depressions of contractility in whole hearts. As shown in chapter 5, 0.3mM heptanol was required to produce an approximate 50% reduction in contractility. The reason for this disparity is unknown although one possible factor may be the different forms of contractility recorded in the two experiments. Single cell shortening occurs unrestrained and therefore represents an isotonic measurement, whilst LVDP represents the pressure the myocardium can generate under practically isometric conditions. A more relevant single cell measurement would therefore have been isometric tension development, but this would require that the ends of the single cells be fixed which is technically difficult to perform.

The effect on cell shortening suggests that heptanol may reduce the size of the Ca^{2+} transients, and/or the ability of Ca^{2+} to generate force/shortening. The measurement of Ca^{2+} transients using Fura-2 was used to discriminate between these two options. The effect of heptanol on the Ca^{2+} transient on stimulation at 1Hz was complex. 0.1mM heptanol caused a decrease in Ca^{2+} transient amplitude, whilst at 0.3mM the Ca^{2+} transient was not different from control. At 3Hz stimulation rate, heptanol caused a decrease in Ca^{2+} transient amplitude at 0.1mM and 0.3mM. These results suggest that part of the effect of heptanol on E-C

coupling is via a reduced amplitude of the Ca^{2+} transient, and partly may be due to reduced Ca^{2+} sensitivity of the myofilaments. The latter however is favoured, given that 0.3mM heptanol has a greater negative inotropic effect than 0.1mM heptanol. The reduced Ca^{2+} transient amplitude may be due to either the effects on the L-type Ca^{2+} channel or SR Ca^{2+} release and uptake.

On the basis of the work by Takens-Kwak *et al* (1992) in neonatal rat myocytes it seems more likely that heptanol inhibits the L-type Ca^{2+} channel. Bastide *et al* (1995) on studying cultured rat myocytes reported that the intracellular Ca^{2+} concentration is not involved in the rapid and reversible uncoupling action of heptanol. They ruled out the contribution of H^+ , cyclic nucleotides and protein kinase C to the rapidity of uncoupling, and suggested that this was consistent with a direct effect of the alcohol on membrane components (junctional proteins or their lipid environment). An effect directly on the sarcolemma would be consistent with an effect on the L-type Ca^{2+} channel.

It has previously been reported that the inhibition of the slow inward Ca^{2+} current by nifedipine reduces action potential duration and produces a dose dependent negative inotropic effect (Segawa *et al*, 1999). This reduction in contractility is due to a reduced inward movement of Ca^{2+} during the action potential plateau phase (due to inhibition of the L-type Ca^{2+} channel). The effects of nifedipine on action potential duration and contractility correlate well with those found in this study with heptanol.

In this study it was found that nifedipine decreased the amplitude of the Ca^{2+} transient and the caffeine induced Ca^{2+} release transient (ryanodine receptor).

However, the caffeine induced Ca^{2+} release was unaffected by heptanol. Nifedipine would be expected to reduce both Ca^{2+} transient and caffeine induced release since lowered Ca^{2+} influx via the L-type Ca^{2+} channel would lower SR Ca^{2+} content (Frampton *et al*, 1991). In contrast, heptanol did not reduce caffeine induced Ca^{2+} release, suggesting that heptanol reduces the Ca^{2+} transient in rabbit myocytes by reducing the efficacy of the link between the L-type Ca^{2+} channel and SR Ca^{2+} release. Further study is required to determine the exact nature of this link.

**Chapter 8 – The effect of the L-Type calcium channel blocker
nifedipine on the negative slope of the restitution curve in the
whole heart**

8.1 Introduction

The last chapter described comparable effects of heptanol and nifedipine on single cell contractility and intracellular Ca^{2+} . Nifedipine, in the concentration range 0.1-0.2 μM , induced a decrease in fractional cell shortening and SR Ca^{2+} release that is of an equivalent magnitude to 0.03-0.3mM heptanol. It is conceivable that the negative slope phenomenon seen in the whole heart with heptanol is a product of the effect of heptanol on the L-type Ca^{2+} channel and not a direct effect of gap junction uncoupling. For this reason, it was logical to study the effect of nifedipine on whole heart electrophysiology, and more specifically the effect on the slope of the restitution curve.

The series of experiments described have attempted to relate any changes caused by nifedipine to those seen with heptanol (i.e. induction of an increased negative slope between the local maximum on the restitution curve and an S1-S2 interval of 350ms). Additionally data concerning dispersion of repolarisation and conduction delay were also obtained.

8.2 Methods

Multiple MAPs were simultaneously recorded from the epicardial surface of the intact left ventricle of stock and sham-operated rabbit hearts with the 32 electrode array, and using stimulation protocols described in chapter 6. The 16 S1 protocol was used exclusively in all experiments using nifedipine. The protocol was repeated several times within one experiment (a single heart) to obtain replicate data concerning the effect of 0.1 μ M, 0.15 μ M and 0.2 μ M nifedipine on the restitution curve. Between the perfusion of each concentration of nifedipine there was a 15 minute washout with Tyrode (cycle length = 350ms) prior to perfusion with the next concentration of nifedipine. The electrode array remained positioned around the heart for the duration each protocol, being removed only between protocols.

8.3 Results

8.3.1 The effect of nifedipine on LVDP

Figure 8.1 illustrates the effect of nifedipine on left ventricular developed pressure (LVDP). 0.1 μ M, 0.15 μ M and 0.2 μ M nifedipine caused a significant decrease in LVDP from 100% to (mean \pm SEM): 59.65 \pm 2.95% (0.1 μ M) P<0.05; 51.15 \pm 4.85% (0.15 μ M) P<0.05; 55.38 \pm 6.44% (0.2 μ M) P<0.001 (paired Student's t-test). Recovery in Tyrode's solution was to 105.86 \pm 6.11% of control.

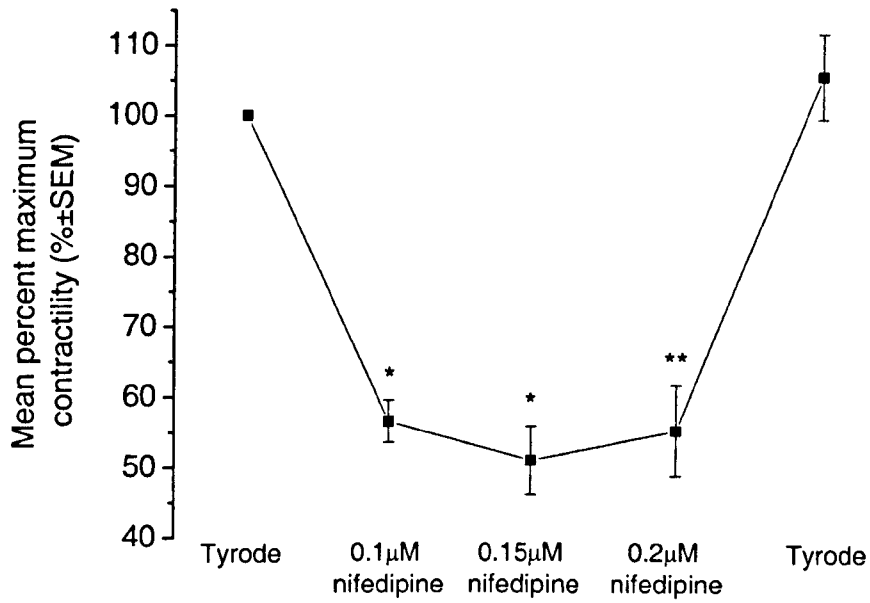


Figure 8.1 The effect of nifedipine on LVDP. Nifedipine significantly decreases LVDP (paired Student's t-test *=P<0.05, **=P<0.01).

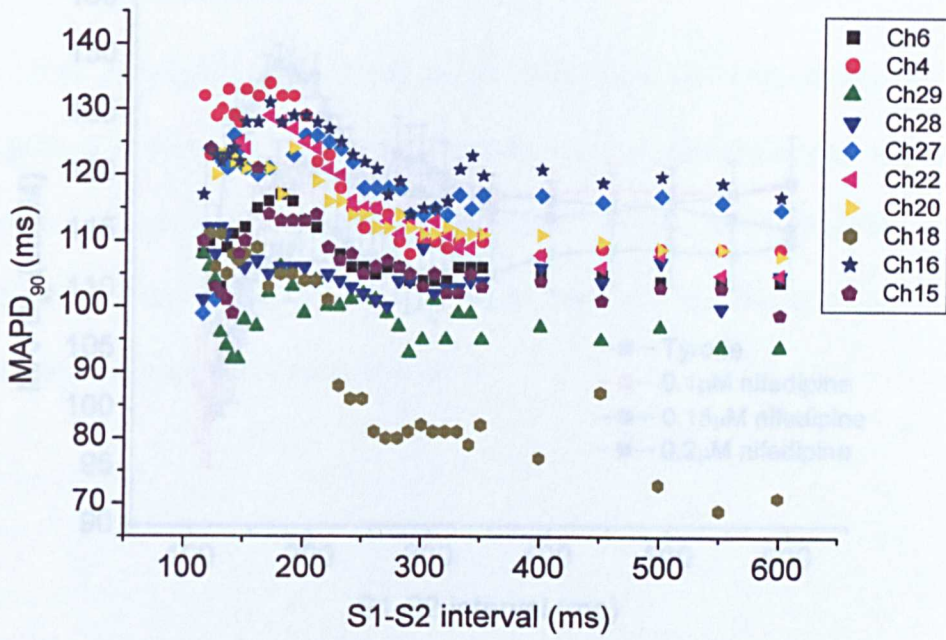
8.3.2 The negative slope

The graphs in Figure 8.2 show typical results from a single experiment where the heart has been perfused with $0.1\mu\text{M}$ nifedipine, 10 MAPs have been obtained simultaneously. 3 normal rabbit hearts were used with 3 to 10 MAPs being obtained simultaneously from each of these. The restitution curve obtained on perfusion with nifedipine showed an ascending slope similar to that of the control (Tyrode) or of heptanol. This involved a rapid increase in MAP duration with increasing S1-S2 interval. Over the range of concentrations used, nifedipine made the slope of the restitution curve less negative (in contrast to heptanol). If the restitution curve showed a biphasic relationship, the slope was analysed between an S1-S2 interval of the local maximum on the curve and an S1-S2 interval of 350ms. If the curve was a typical restitution curve, i.e. it showed a monotonic increase in MAP duration with S1-S2 interval, the slope was determined between S1-S2 intervals of 180ms and 350ms.

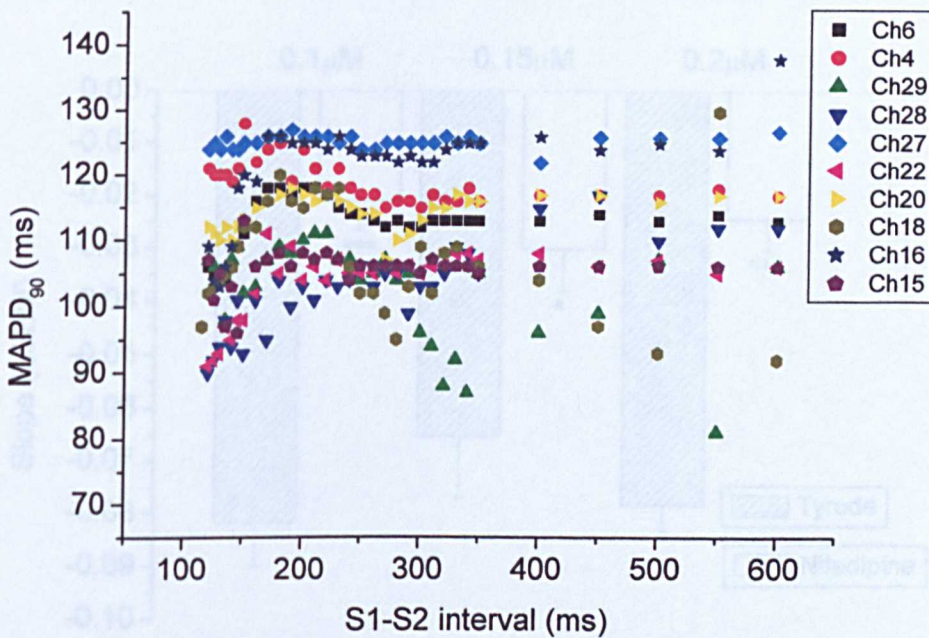
Figure 8.3 illustrates the significant effect that nifedipine has on flattening the slope of the restitution curve whilst Figure 8.4 summarises this. Table 8.1 contains the absolute values for the slope of the graphs (average of all results).

	Slope (\pm SEM) at nifedipine concentration of (μM)		
	0.1	0.15	0.2
Tyrode	-0.082 ± 0.0082	-0.0654 ± 0.0019	-0.0784 ± 0.0053
Nifedipine	$-0.021\pm 0.0056^{***}$	$-0.0303\pm 0.0080^*$	$-0.0245\pm 0.0061^{***}$

Table 8.1 The effect of nifedipine on the gradient of the slope of the restitution curve. n=3 hearts, 27 channels ($0.1\mu\text{M}$ nifedipine) $P<0.001$; n=3 hearts, 19 channels ($0.15\mu\text{M}$ nifedipine) $P<0.05$; n=3 hearts, 20 channels ($0.2\mu\text{M}$ nifedipine) $P<0.001$.



A. Tyrode perfusion.



B. 0.1µM nifedipine perfusion.

Figure 8.2 Restitution curves from a typical experiment where the heart was perfused with normal Tyrode's solution (A) followed by 0.1µM nifedipine solution (B).

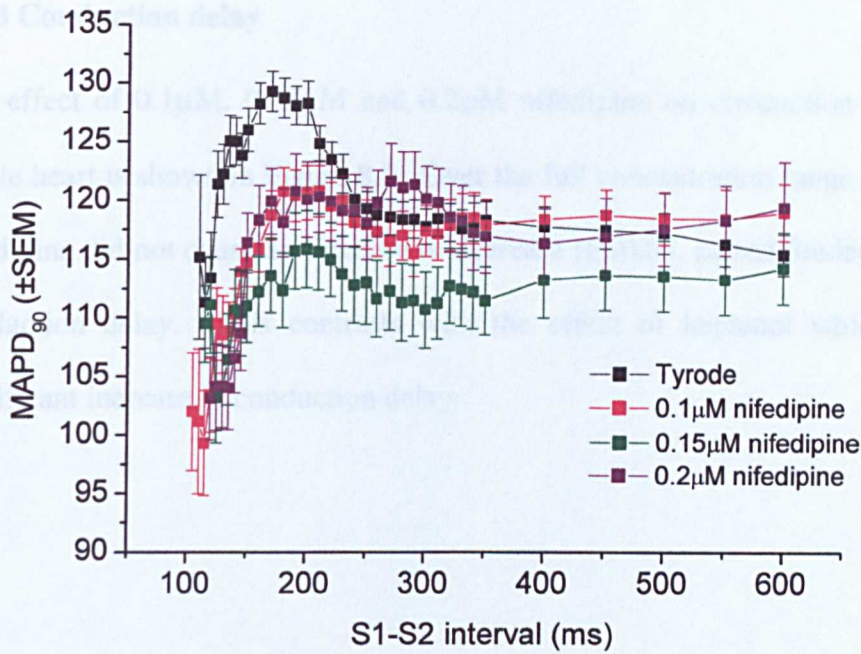


Figure 8.3 The global effect of nifedipine on electrical restitution

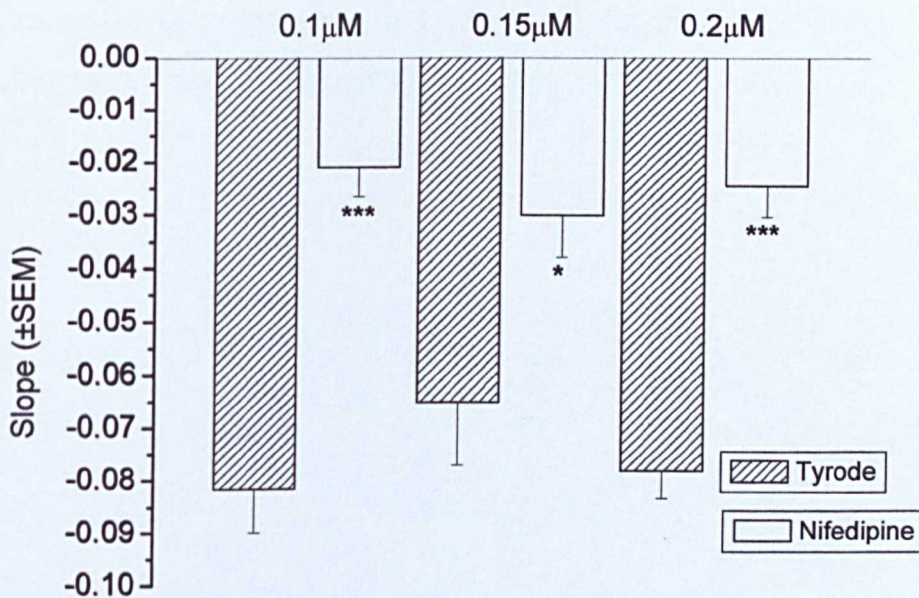


Figure 8.4 The effect of nifedipine on the gradient of the slope of the restitution curve. $n=3$ hearts, 27 channels ($0.1\mu\text{M}$ nifedipine) $P<0.001$; $n=3$ hearts, 19 channels ($0.15\mu\text{M}$ nifedipine) $P<0.05$; $n=3$ hearts, 20 channels ($0.2\mu\text{M}$ nifedipine) $P<0.0001$ (paired Student's t-test).

8.3.3 Conduction delay

The effect of 0.1 μ M, 0.15 μ M and 0.2 μ M nifedipine on conduction delay in the whole heart is shown in Figure 8.5. Over the full concentration range investigated, nifedipine did not cause an increase or decrease ($P>0.05$, paired Student's t-test) in conduction delay. This contrasts with the effect of heptanol which caused a significant increase in conduction delay.

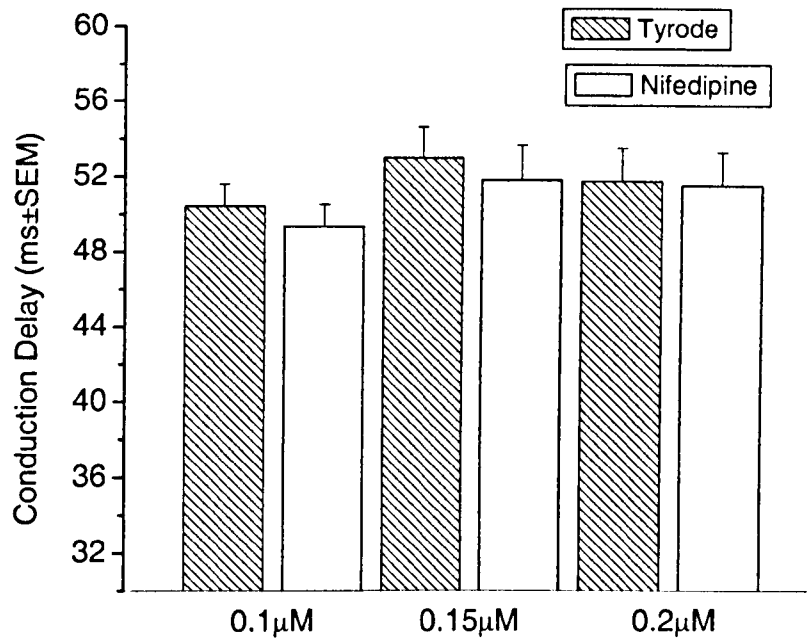
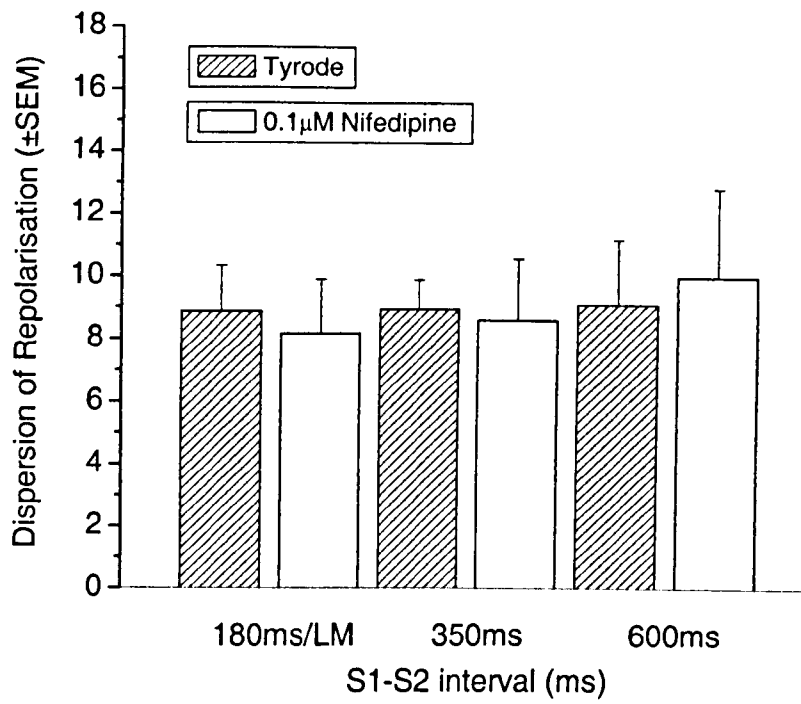


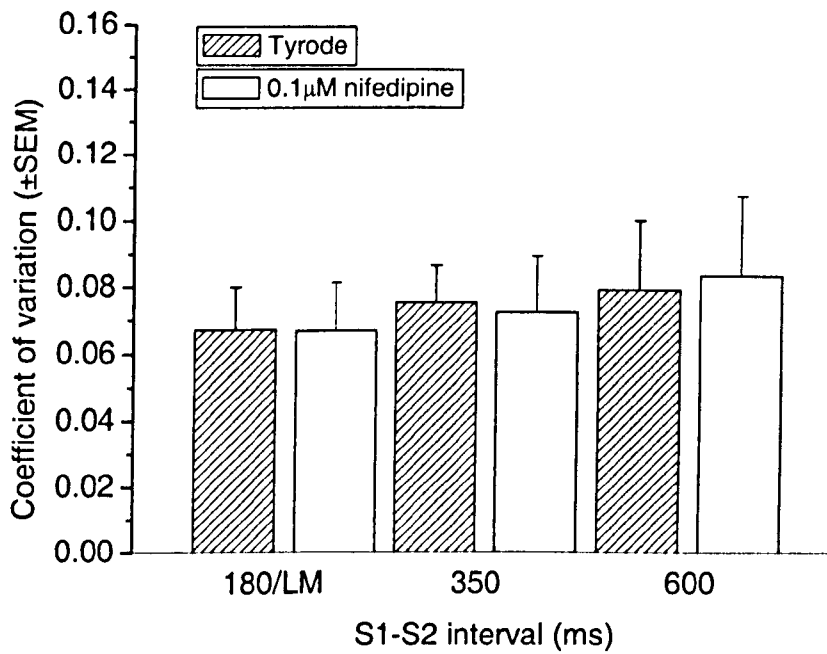
Figure 8.5 The effect of nifedipine on conduction delay. n=3 hearts, 27 channels (0.1µM nifedipine); n=3 hearts, 19 channels (0.15µM nifedipine); n=3 hearts, 20 channels (0.2µM nifedipine).

8.3.3 Dispersion of repolarisation

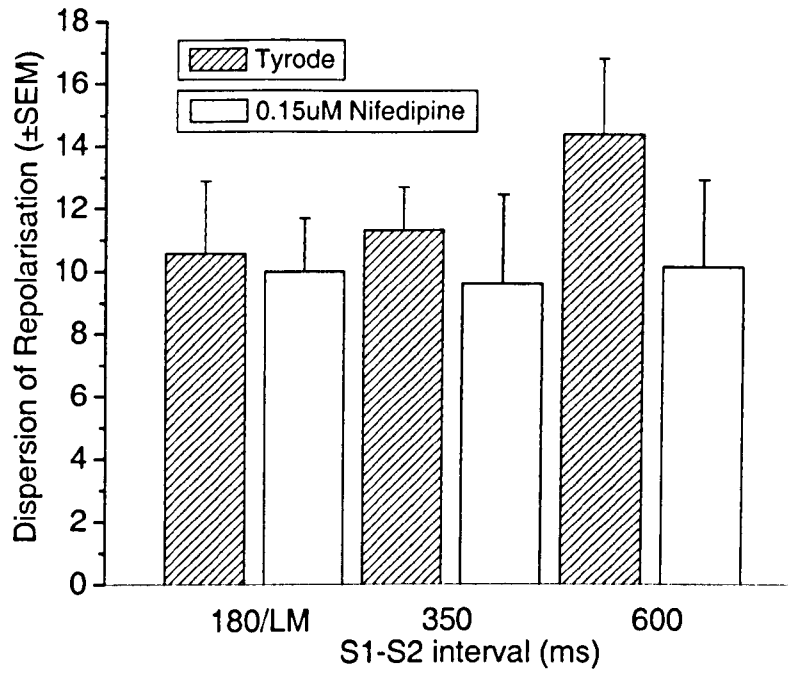
The effect of 0.1 μ M, 0.15 μ M and 0.2 μ M nifedipine on S2 dispersion of repolarisation at S1-S2 intervals of the local maximum (nifedipine)/180ms (Tyrodes), 350ms and 600ms was investigated. The results are illustrated in Figure 8.6a-f as dispersion of repolarisation and coefficient of variation. Dispersion of repolarisation is not consistently increased or decreased at the concentrations studied. However, at an S1-S2 interval of 600ms 0.15 μ M nifedipine caused a decrease ($P>0.05$, paired Student's t-test) in dispersion, and 0.2 μ M nifedipine increased ($P>0.05$, paired Student's t-test) dispersion.



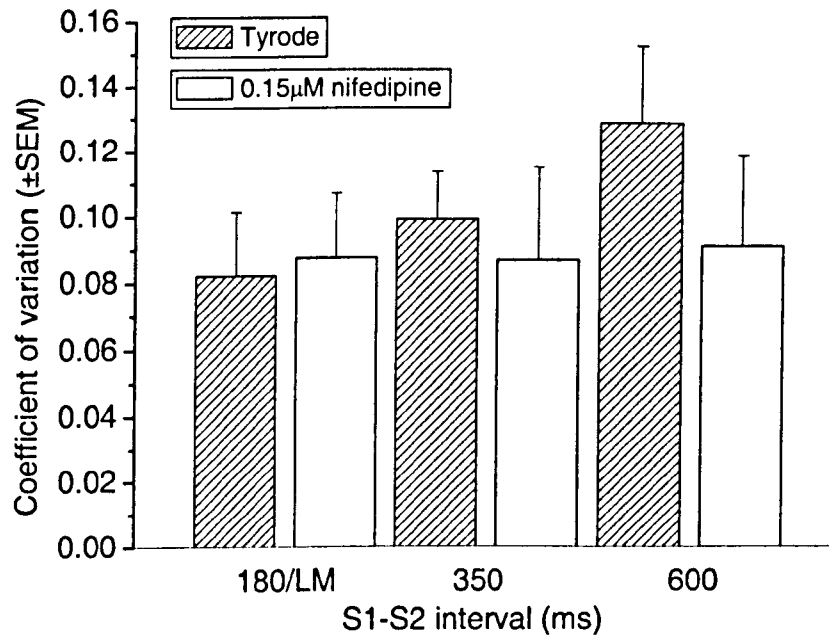
A. The effect of 0.1 µM Nifedipine on dispersion of repolarisation.



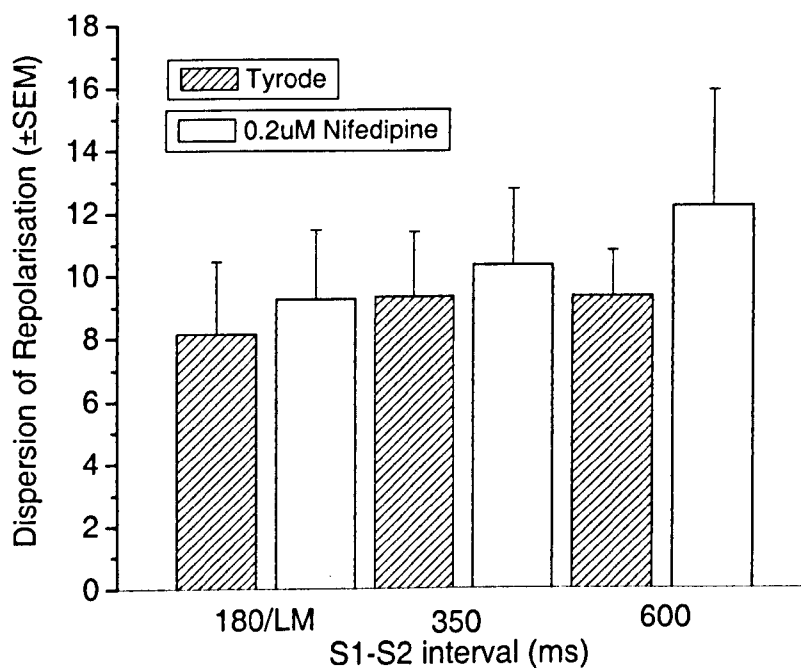
B. The effect of 0.1 µM Nifedipine on dispersion as represented by the coefficient of variation.



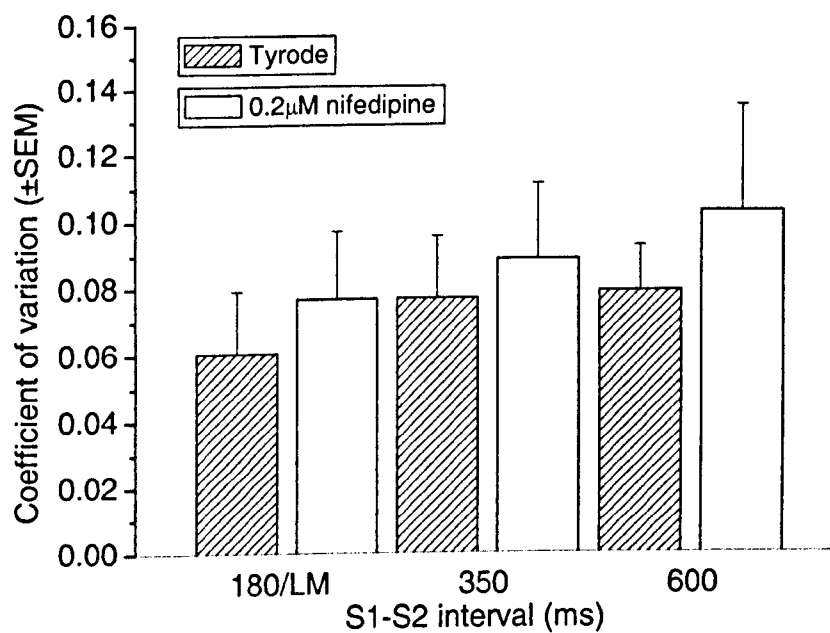
C. The effect of 0.15 μ M nifedipine on dispersion of repolarisation.



D. The effect of 0.15 μ M nifedipine on dispersion as represented by coefficient of variation.



E. The effect of 0.2 μ M nifedipine on dispersion of repolarisation.



F. The effect of 0.2 μ M nifedipine on dispersion as represented by coefficient of variation.

Figure 8.6 The effect of nifedipine on dispersion of repolarisation.

8.4 Discussion

Although the aim of this study was solely to establish the effect of nifedipine on the gradient of the slope of the restitution curve between the local maximum (or $S1-S2=180\text{ms}$), conduction delay and dispersion of repolarisation were also analysed. This enabled a direct comparison with the results obtained with heptanol. It was shown that nifedipine does not induce an increase in conduction delay in the left ventricle of the intact rabbit heart nor does it cause a significant dispersion of repolarisation.

In contrast to the study investigating the effect of heptanol as a gap junction uncoupler, the primary aim of these experiments was to investigate the L-type Ca^{2+} channel blockers effect on the slope of the restitution curve. The appearance of a negative slope by heptanol is a phenomenon observed during whole heart experiments. Single cell experiments revealed that heptanol has affects in addition to gap junction uncoupling, specifically the reduction in SR Ca^{2+} release and fractional cell shortening. In this study the effect of heptanol on E-C coupling was mimicked by nifedipine. The effect of nifedipine on single cell Ca^{2+} handling was investigated and a concentration ($0.15\mu\text{M}$) found that reduces cell shortening to a similar degree as 0.3mM heptanol. Therefore a possible cause of the negative slope is altered action potential characteristics as an indirect result of the effect of heptanol on E-C coupling.

As previously discussed in this study, the relationship between the action potential duration and preceding diastolic interval is known as a restitution relation. Alternations of action potential duration often occur on alteration of this relation.

Riccio *et al* (1999) described the implications of the slope of the restitution relation to arrhythmogenesis. Electrical alternans is known to develop if the slope of the restitution relation is greater or equal to 1, and if this is the case then rapid pacing may induce fibrillation. However, if the slope of the restitution relation is less than 1 then neither alternans nor fibrillation occurs. This would imply that if a steep slope in the restitution relation is a prerequisite for ventricular fibrillation then a reduction in the slope might prevent it.

In a recent publication by Fox *et al* (2002) the role of I_{Ca} in electrical alternans in an ionic model based on canine myocyte data was discussed. In the control model after short paced cycle lengths, and only partial recovery of I_{Ca} , there was a shortening of action potential duration followed by a longer diastolic interval. Assuming fast pacing at the shorter cycle length is maintained, a self-perpetuating alternans is established. However, decreasing the permeability of the L-type Ca^{2+} channel decreased the magnitude of I_{Ca} which shifted the balance between I_{Ca} and K^+ currents to the repolarising currents. This resulted in a longer diastolic interval and a complete recovery of I_{Ca} . At shorter cycle lengths the recovery of I_{Ca} was incomplete. Because of the reduced magnitude of I_{Ca} and the rate dependent accumulation of incompletely deactivated K^+ current, the action potentials remained short as the dependence on I_{Ca} was minimal. This mechanism is similar to that that describes the attenuation of alternans, at short cycle lengths, in the control model used. This may implicate I_{Ca} as the current primarily responsible for beat to beat variations in action potential duration. These findings strengthened the decision to focus on Ca^{2+} related mechanisms rather than K^+ as the origin of the negative slope.

The effect of nifedipine on whole heart electrophysiology was investigated using the same protocols as those for heptanol. It was found that nifedipine flattened the slope of the restitution curve between the S1-S2 interval of the local maximum on the restitution curve and 350ms. This suggests that nifedipine may have an opposite effect to heptanol on the membrane currents responsible for the negative slope phenomenon.

The fact that partial blockade of E-C coupling by inhibition of the L-type Ca^{2+} channel is not associated with a negative slope in the restitution curve rules out the idea that the L-type Ca^{2+} channel may be responsible for the negative slope.

**Chapter 9 – The effects of gap junction uncoupler carbenoxolone
on whole heart electrophysiology and single cell contractility and
calcium handling**

9.1 Introduction

Carbenoxolone is a mineralocorticoid that is used to promote healing in the treatment of gastric and mouth/oral ulcers. It is thought to work by stimulating the production of mucus that forms a protective coating over the stomach's lining, acting as an antacid. At $\text{pH} < 4$, carbenoxolone polymerises to a gel that binds to and covers ulcers – it acts as a "bandage" on the ulceration, preventing further exposure to gastric acid and, thus, further erosion and damage to the mucosa. Experimentally, work with carbenoxolone has previously been largely restricted to neurological investigations where it has been found to reversibly abolish gap junction-mediated intercellular coupling (rat sympathetic preganglionic neurones) (Leslie *et al*, 1998). However, its effect on cardiac gap junction uncoupling has not been widely studied. One study, reported in a poster at the American Heart Association conference 1999 (de Groot *et al*), concluded that carbenoxolone is a specific gap junction uncoupler. $50\mu\text{M}$ and $100\mu\text{M}$ carbenoxolone were found to delay conduction in isolated cell pairs and caused localised conduction slowing and block which indicated gap junction uncoupling. However, it did not influence action potential characteristics, nor did it influence transmembrane currents indicating that carbenoxolone is specific to gap junction uncoupling. Due to the reported apparent specificity of carbenoxolone, it was an obvious choice of substance for comparison with the relative unspecific effects of heptanol.

Since several of the effects of heptanol on MAP recording cannot easily be attributed to gap junction uncoupling, it was of interest to investigate the effects of a specific agent on the same parameters. The primary aim of these experiments was to test whether carbenoxolone i) induced a negative slope in the restitution

curve, similar to that seen with heptanol, ii) unmasked any dispersion of repolarisation, and iii) caused an increase in conduction delay. Despite the preliminary evidence from de Groot *et al* that carbenoxolone has no effect on transmembrane currents, a single cell study was also carried out to investigate the effect of carbenoxolone on single cell fractional shortening and intracellular Ca^{2+} measurements.

9.2 Methods

MAPs were simultaneously recorded from the epicardial surface of the left ventricle of the Langendorff perfused rabbit heart using the 32 electrode monophasic action potential array. Stock and sham hearts were used throughout.

9.2.1 Whole heart experiments

The 16 S1 extrastimulus protocol was used for all whole heart carbenoxolone experiments (n=4 hearts, 24 MAP channels). The heart was paced at a CL of 350ms on perfusion with normal Tyrode's solution for 4 minutes before starting the 16 S1 extra-stimulus protocol. This protocol was then repeated following regular pacing for 4 minutes in the presence of 50 μ M carbenoxolone.

A suitable concentration of carbenoxolone was found by looking at the dose dependent effects of carbenoxolone on whole heart electrophysiology and perfusion/left ventricular pressures. A concentration range of 10 μ M to 100 μ M carbenoxolone was studied. It was found that <50 μ M carbenoxolone had little effect on any of the target parameters to be studied. However, >60 μ M

carbenoxolone had dramatic and irreversible toxic effects on the heart, namely: an increase in perfusion pressure, and an increase in end diastolic and end systolic pressures. Therefore the maximum concentration of carbenoxolone that could be used in this study is 50 μ M, a value that would allow comparison to the work done by de Groot *et al* (2000). Due to the irreversible nature of its effects, only one episode of perfusion with carbenoxolone was attempted.

9.2.2 Single cell experiments

Left ventricular epicardial myocytes were used for all carbenoxolone experiments. Perfusion protocols were carried out firstly at 1Hz and then 3Hz. The cells were perfused initially with Krebs for 60 seconds followed by 50 μ M carbenoxolone for 60 seconds. Carbenoxolone was washed out with a Krebs for 60 seconds. SR Ca²⁺ content was investigated by application of 20mM caffeine to cells stimulated at 1Hz. Based on results from whole heart experiments, only the effect of 50 μ M carbenoxolone was studied.

9.3 Results – Whole heart

9.3.1 Monophasic action potential duration

The effect of 50 μ M carbenoxolone on MAPD₉₀ was analysed. Mean S2 MAPD₉₀ was taken from the S2 at the S1-S2 interval of the local maximum on the curve, 350ms, and 600ms. 90ms was omitted, as it was rare that capture occurred at this coupling interval. Figure 9.1 illustrates the effect of 50 μ M carbenoxolone on MAPD₉₀. S1 MAP duration was reduced by 7%. S2 MAP duration was reduced but the reduction is not uniform over the test intervals. S2 MAPD₉₀ is longer at the shorter S1-S2 interval, although the reductions in duration appear to be of roughly equal magnitude. Absolute changes in MAPD₉₀ are shown in Table 9.1.

Figure 9.2 shows a control MAP recording and a recording under perfusion with 50 μ M carbenoxolone.

		MAPD ₉₀ (ms) (\pm SEM) at S1-S2 Interval of		
		180ms/ Local max	350ms	600ms
S2	Tyrode	115.17 \pm 4.23	105.00 \pm 2.21	104.53 \pm 2.37
	50 μ M carbenoxolone	104.58 \pm 2.32*	96.75 \pm 2.53**	98.00 \pm 2.90

Table 9.1 The effect of 50 μ M carbenoxolone on the mean MAPD₉₀ of S1 and S2 MAPS. Paired Student's t-test *= P <0.05, **= P <0.01.

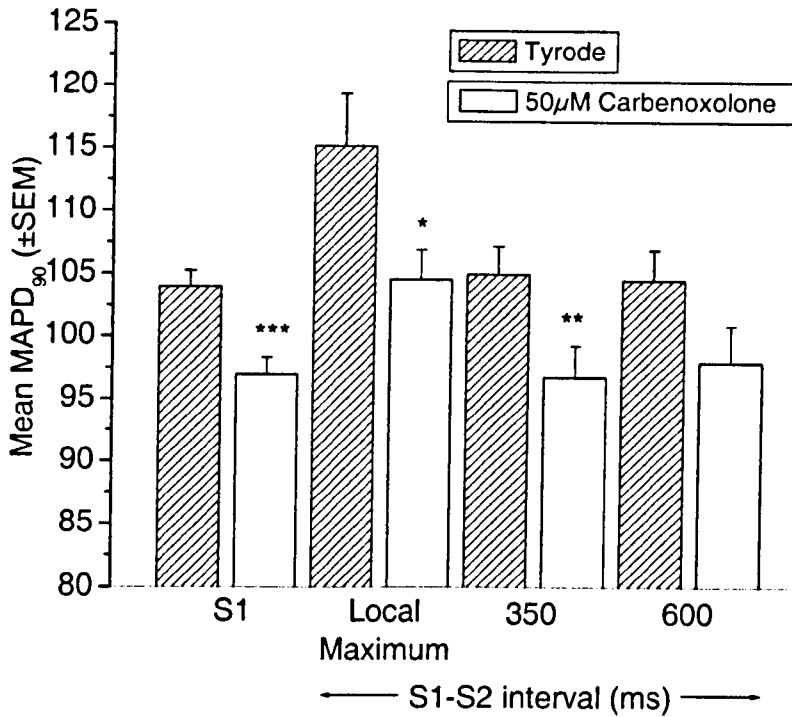


Figure 9.1 The effect of carbenoxolone on MAPD₉₀. Carbenoxolone significantly ($P < 0.001$ ***, $P < 0.01$ **, $P < 0.05$ *, paired Student's t-test) decreases S1 and S2 MAPD₉₀ at the S1-S2 intervals as shown.

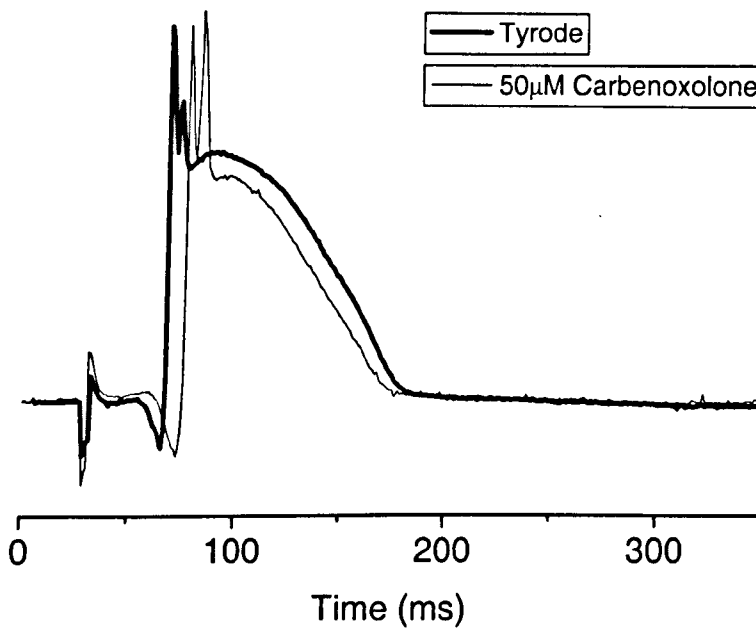


Figure 9.2 MAP recordings showing the effect of perfusion with 50µM carbenoxolone on MAP duration and morphology.

9.3.2 Conduction delay

Conduction delay, the time interval between the stimulus artefact and the upstroke of the MAP, was increased significantly by 50 μ M carbenoxolone. Conduction delay was increased from (mean \pm SEM) 45.50 \pm 2.12ms in Tyrode to 55.11 \pm 2.82ms in carbenoxolone (P <0.001, paired Student's t-test) (Figure 9.3). The effect of 50 μ M carbenoxolone on conduction delay can also be seen in Figure 9.2. For comparison, the increase in 0.3mM heptanol was from (mean \pm SEM) 44.23 \pm 9.98ms to 49.25 \pm 10.57ms (P <0.001, paired Student's t-test), see Figure 6.7. The 'control' conduction delay as observed in Tyrode's solution is equivalent both prior to heptanol and prior to carbenoxolone. Carbenoxolone does however increase conduction delay to 121% of control compared to 111% with 0.3mM heptanol.

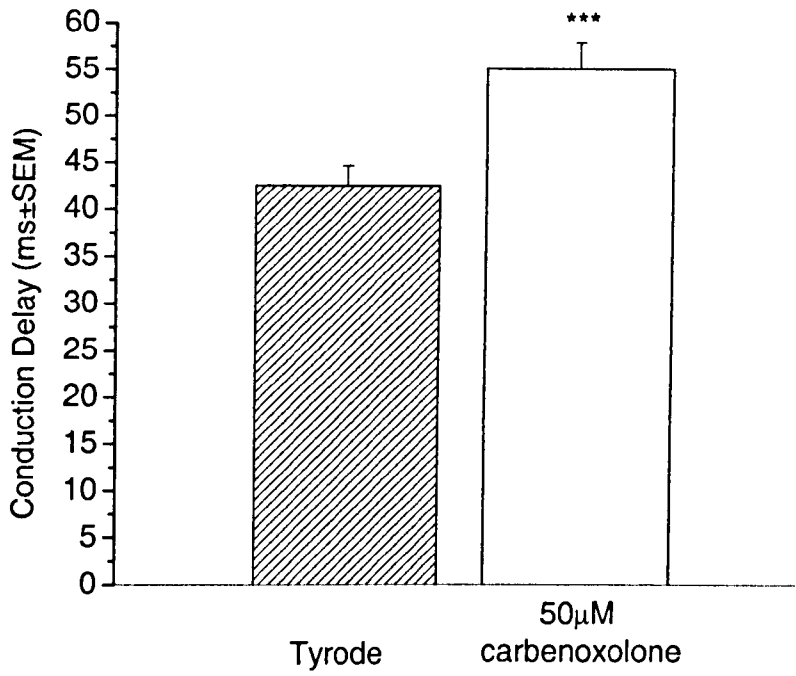


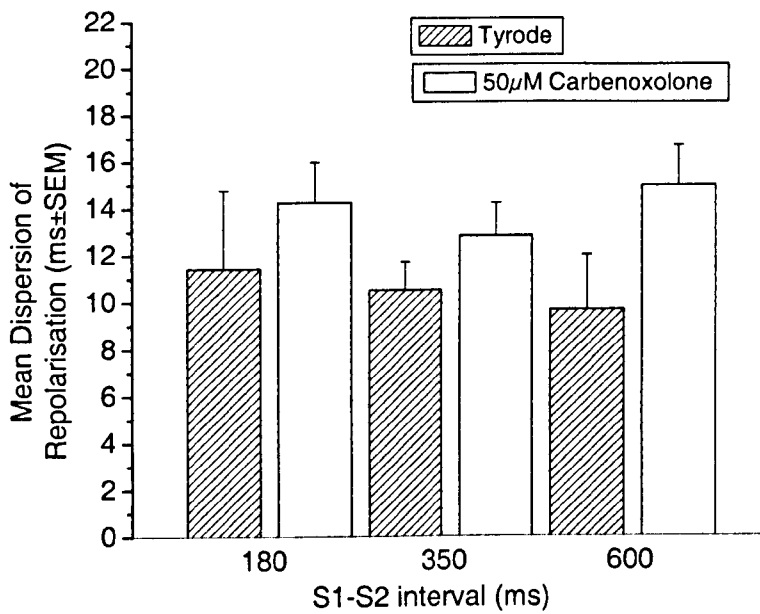
Figure 9.3 The effect of 50µM carbenoxolone on conduction delay. Carbenoxolone (grey bar) significantly increases conduction delay ($P < 0.001$ ***, paired Student's t-test). $n = 4$ hearts, 24 channels.

9.3.3 Dispersion of repolarisation

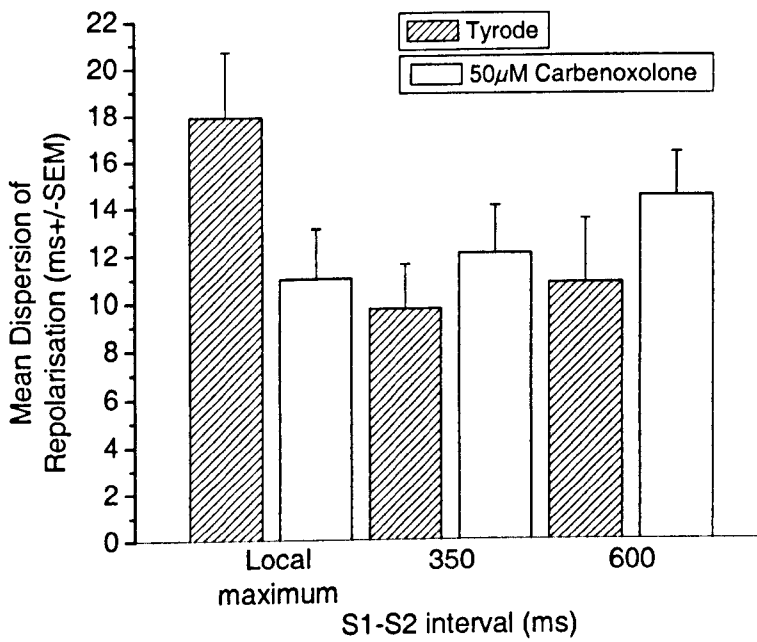
Dispersion of repolarisation over the epicardial surface of the left ventricle was estimated as the standard deviation of repolarisation (MAPD_{90}) from each heart. Mean dispersion was measured from the last S1 MAP of the 16 S1 train and also the S2 extrastimulus MAP at S1-S2 intervals of 90ms (S1 only), 180ms (S1) or the local maximum (S2), 350ms and 600ms. The S1-S2 interval in the case of the S1 MAPs is taken as the S1 MAP preceding the S1-S2 interval of x. In both the S1 and S2 MAPs 50 μ M carbenoxolone was associated an increase ($P>0.05$, paired Student's t-test) in dispersion of repolarisation at longer S1-S2 intervals only, except at the S2 local maximum. The data are summarised in the Table 9.2 and illustrated in Figure 9.4a and 9.4b (S1 and S2 respectively).

Protocol		Dispersion (ms \pm SEM) at S1-S2 Interval of		
		Local max/ 180ms	350ms	600ms
S1	Tyrode	11.4 \pm 3.3	10.5 \pm 1.2	9.2 \pm 2.3
	carbenoxolone	14.2 \pm 1.7	12.8 \pm 1.4	15.0 \pm 1.7
S2	Tyrode	17.9 \pm 2.8	9.7 \pm 1.9	10.8 \pm 2.7
	carbenoxolone	11.0 \pm 2.1	12.0 \pm 2.1	14.5 \pm 1.9

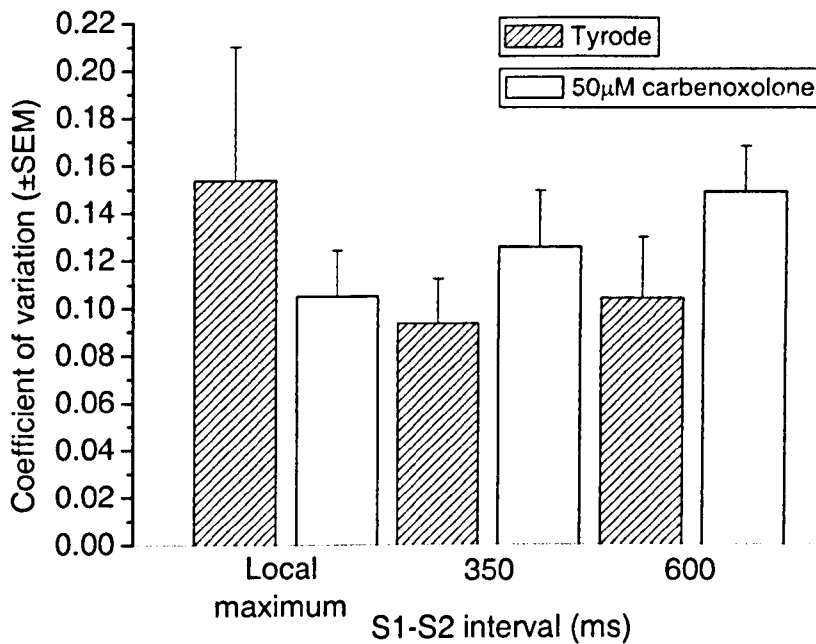
Table 9.2 The effect of 50 μ M carbenoxolone on dispersion of repolarisation. n=4 hearts, 24 channels.



A. The effect of 50µM carbenoxolone on S1 dispersion of repolarisation.



B. The effect of 50µM carbenoxolone on S2 dispersion of repolarisation.



C. The effect of 50µM carbenoxolone on S2 dispersion as represented by the coefficient of variation.

Figure 9.4 The effect of 50µM carbenoxolone on dispersion of S1 (A) and S2 (B and C) repolarisation. Carbenoxolone an increase ($P>0.05$, paired Student's t-test) in S2 dispersion at longer S1-S2 intervals only (350ms and 600ms).

9.3.4 The negative slope

The gradient of the slope of the restitution curve was measured between local maximum on the curve and an S1-S2 interval of 350ms. 50 μ M carbenoxolone did not alter ($P>0.05$) the gradient of the slope between the local maximum on the restitution curve and an S1-S2 interval of 350ms. The values were (mean \pm SEM) -0.063 \pm 0.020 in Tyrode and -0.050 \pm 0.011 in 50 μ M carbenoxolone. The results are illustrated in Figure 9.5.

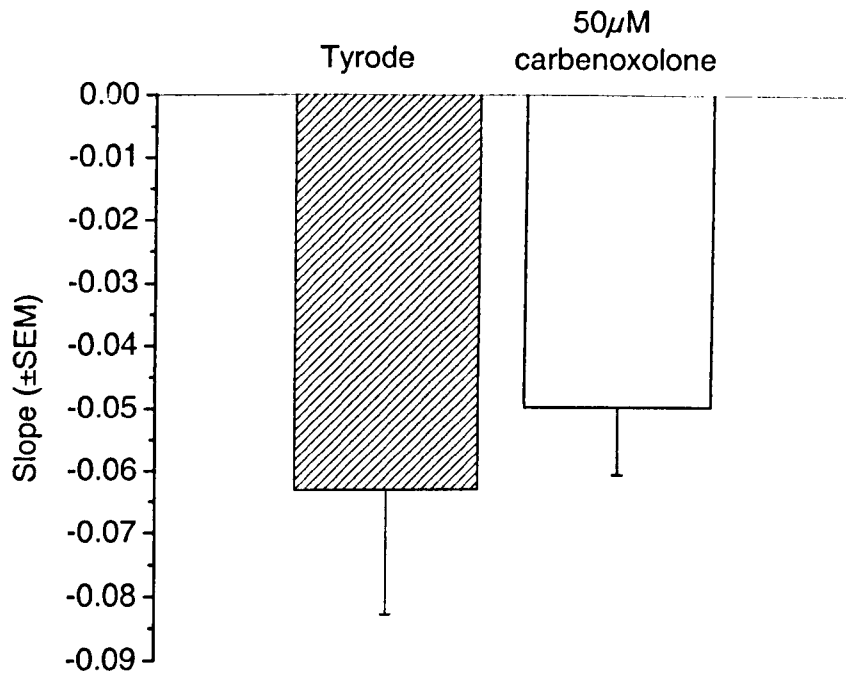


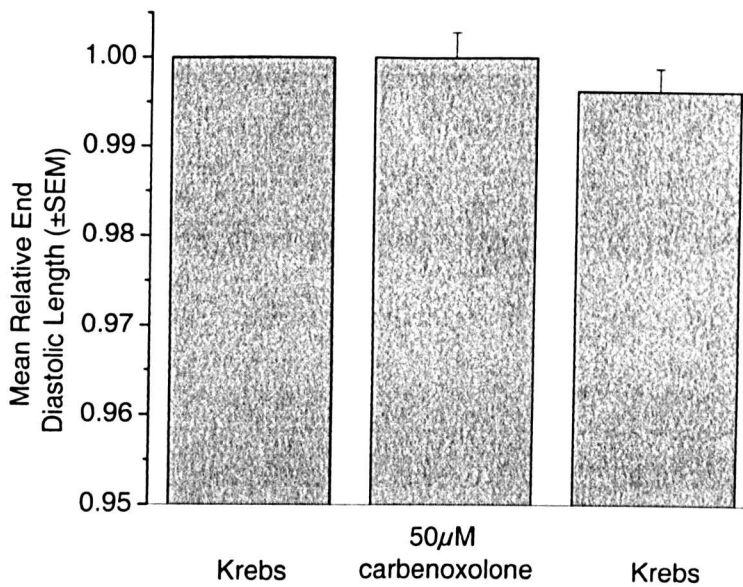
Figure 9.5 The effect of 50µM carbenoxolone on the gradient of the slope of the restitution curve between the local maximum on the curve and an S1-S2 interval of 350ms. Carbenoxolone does not decrease ($P>0.05$, paired Student's t-test) the gradient of the slope. $n=4$ hearts, 24 channels.

9.4 Results – Single Cells

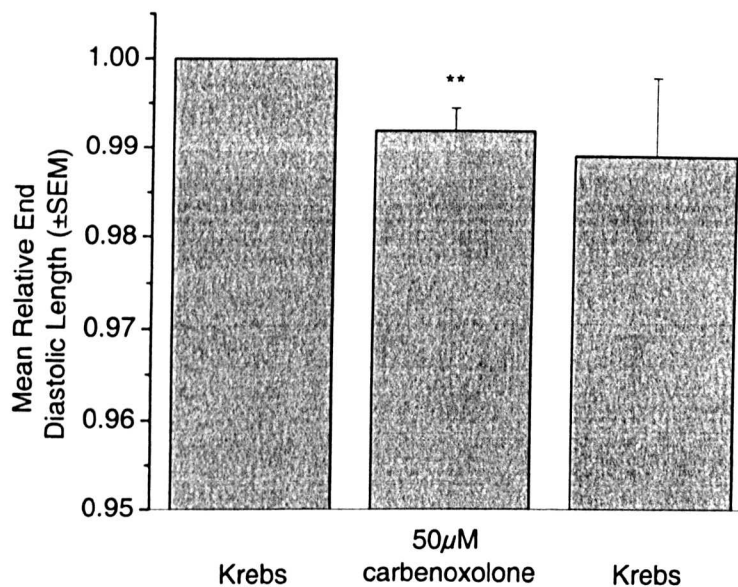
9.4.1 Relative end diastolic lengths

The relative end diastolic lengths were calculated to determine the effect of carbenoxolone on resting cell length. EDLs were measured firstly on perfusion with Krebs superfusate, after 50 μ M carbenoxolone, and also after a washout with Krebs superfusate. The cells were stimulated at 1Hz and 3Hz, under each perfusion condition, for 60 seconds. Stimulation protocols are described in chapter 6 methods.

At a stimulation frequency of 1Hz, 50 μ M carbenoxolone did not have a significant effect on the end diastolic cell length (Figure 9.6a). However, at 3Hz, 50 μ M carbenoxolone significantly decreased EDL from (mean \pm SEM) 126.32 \pm 4.67 μ M to 125.21 \pm 4.50 μ M, $P < 0.01$. EDL did not recover on reperfusion with Krebs superfusate (Figure 9.6b).



A. The effect of 50µM carbenoxolone on the end diastolic length of cells paced at 1Hz. Carbenoxolone does not change end diastolic cell length ($P>0.05$, paired Student's t-test). $n=4$ hearts, 19 cells.

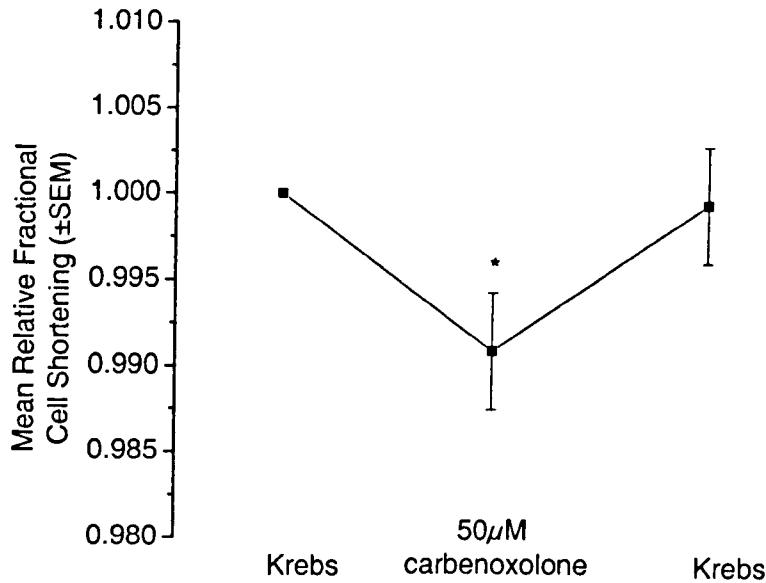


B. The effect of 50µM carbenoxolone on the end diastolic length of cells paced at 3Hz. Carbenoxolone significantly ($P<0.01$, paired Student's t-test) decreases end diastolic cell length. The effect is not reversible. $n=4$ hearts, 17 cells.

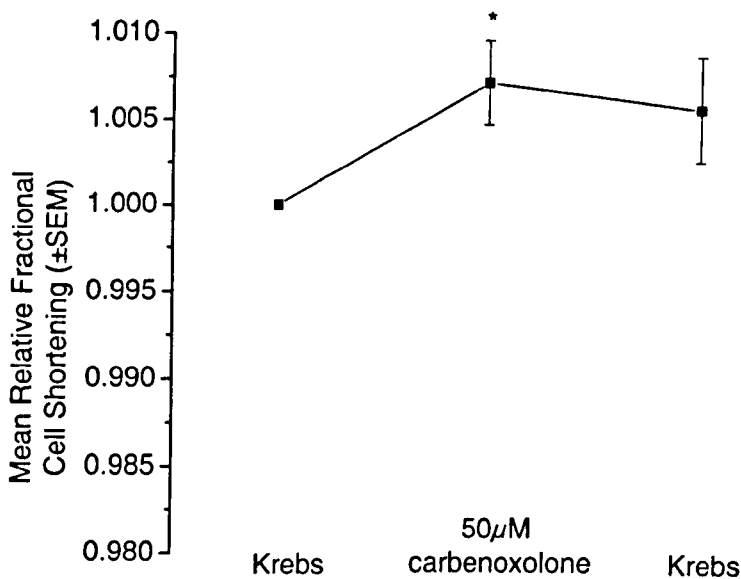
Figure 9.6 The effect of 50µM carbenoxolone on end diastolic length.

9.4.2 Relative fractional cell shortening

Relative fractional shortening was measured on perfusion with 50 μ M carbenoxolone at 1Hz and 3Hz. At 1Hz 50 μ M carbenoxolone significantly increased the mean fractional cell shortening from 9.82 \pm 0.009% to 10.762 \pm 0.008% in 50 μ M carbenoxolone (mean \pm SEM), P<0.05. Contractility was fully recovered on reperfusion with Krebs. However, at 3Hz, 50 μ M carbenoxolone was seen to significantly *decrease* mean relative fractional shortening from 10.89 \pm 0.01% to 10.24 \pm 0.01% (mean \pm SEM), P<0.05. Contractility was not fully recovered on reperfusion with Krebs. Figure 9.7a and 9.7b illustrate the effect of 50 μ M carbenoxolone on relative fractional cell shortening at 1Hz and 3Hz.



A. The effect of 50µM carbenoxolone on fractional cell shortening on stimulation at 1Hz. Carbenoxolone significantly ($P < 0.05$, paired Student's t-test) reduced fractional cell shortening. $n = 4$ hearts, 19 cells.



B. The effect of 50µM carbenoxolone on fractional cell shortening on stimulation at 3Hz. Carbenoxolone significantly ($P < 0.05$, paired Student's t-test) increase relative fractional shortening. This effect is not fully reversible. $n = 4$ hearts, 17 cells.

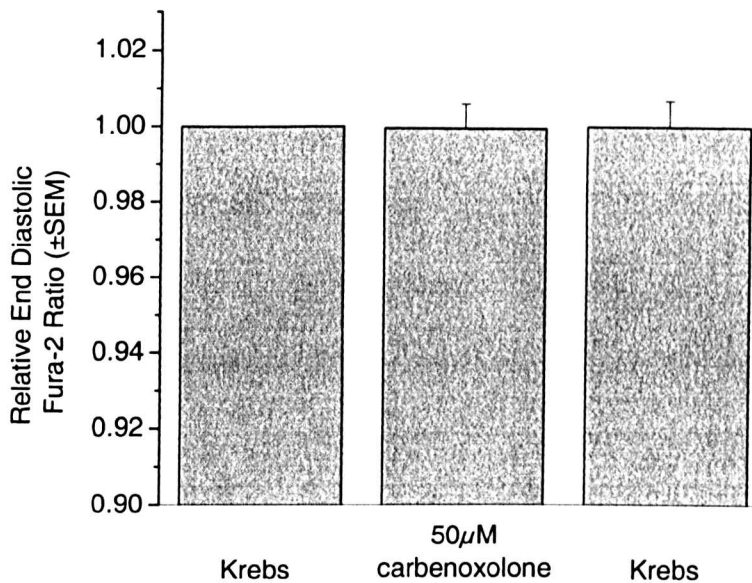
Figure 9.7 The effect of 50µM carbenoxolone on fractional cell shortening.

9.4.3 Calcium handling

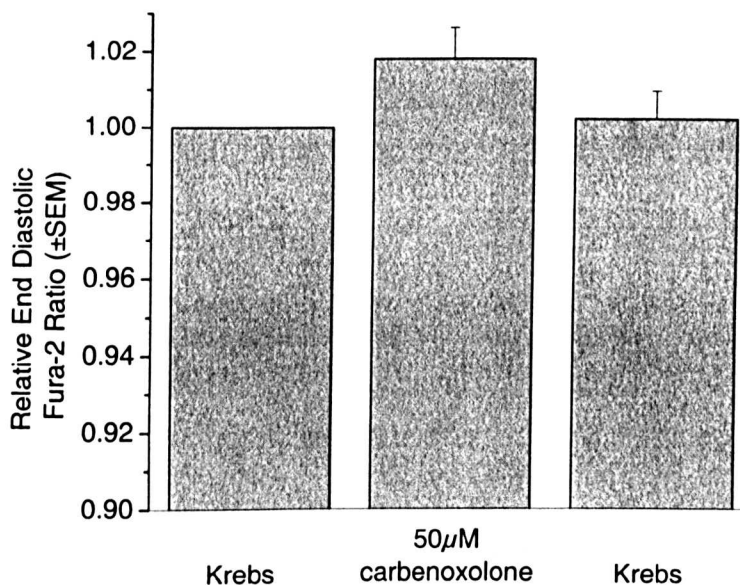
Due to the inconsistency of fractional shortening results obtained at 1Hz and 3Hz (i.e. a decrease at 1Hz and an increase at 3Hz) and also to the observed effects on the end diastolic cell lengths, it was necessary to analyse all data for Ca^{2+} measurements. As before, results are expressed in terms of the Fura-2 ratio rather than absolute Ca^{2+} concentration.

At 1Hz, 50 μM carbenoxolone did not lead to any discernible change in end diastolic Fura-2 ratio (Figure 9.8a) which corresponds with the shortening data obtained (see above). However, at 3 Hz there was a slight increase in end diastolic Fura-2 ratio (0.840 ± 0.018 to 0.855 ± 0.021 , mean \pm SEM) which was fully reversible on reperfusion with Krebs (Figure 9.8b). This data is consistent with shortening data obtained at 3Hz where there was a non-reversible increase in contractility.

Relative end systolic Fura-2 ratios as measured at 1Hz and 3Hz upon perfusion with Krebs and 50 μM carbenoxolone correspond with the end diastolic ratios. At 1Hz 50 μM carbenoxolone does not affect ($P > 0.05$, paired Student's t-test) Fura-2 ratio (Figure 9.9a), whilst at 3Hz there is a reversible, significant increase in Fura-2 ratio (Figure 9.9b), $P < 0.05$ (paired Student's t-test).

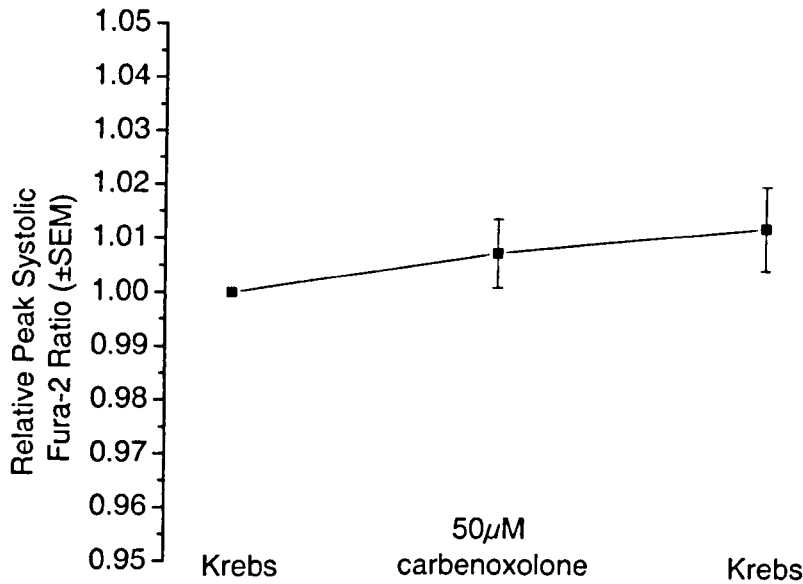


A. The effect of 50µM carbenoxolone on relative end diastolic Fura-2 ratio on stimulation at 1Hz. Carbenoxolone does not alter end diastolic Ca^{2+} concentration. $n=4$ hearts, 18 cells.

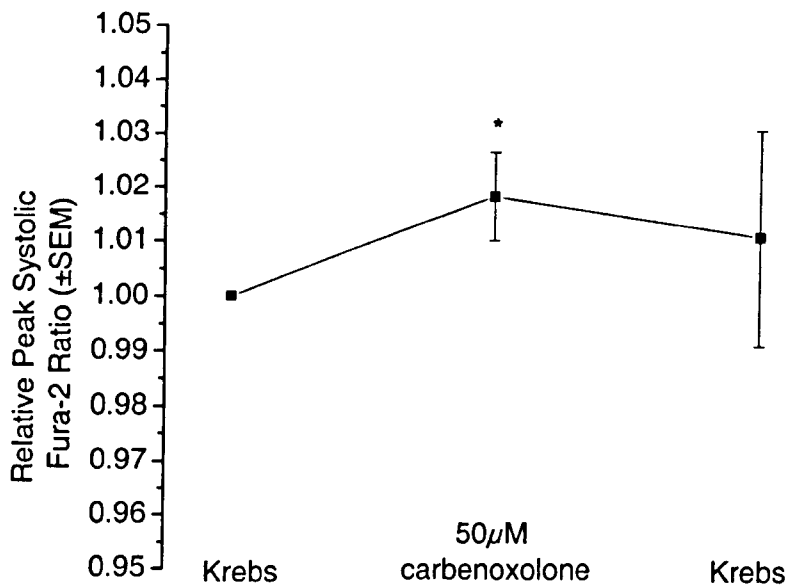


B. The effect of 50µM carbenoxolone on relative end diastolic Fura-2 ratio on stimulation at 3Hz. Carbenoxolone increases ($P>0.05$, paired Student's t-test) end diastolic Ca^{2+} concentration. The effect is fully reversible. $n=4$ hearts, 15 cells.

Figure 9.8 The effect of 50µM carbenoxolone on end diastolic Fura-2 ratio.



A. The effect of 50 μ M carbenoxolone on relative peak Fura-2 ratio on stimulation at 1Hz. Carbenoxolone does not change ($P > 0.05$, paired Student's t-test) peak systolic Ca^{2+} concentration. $n = 4$ hearts, 18 cells.



B. The effect of 50 μ M carbenoxolone on relative peak Fura-2 ratio on stimulation at 3Hz. Carbenoxolone induces a significant ($P < 0.05$, paired Student's t-test) increase in systolic Ca^{2+} concentration. $n = 4$ hearts, 15 cells.

Figure 9.9 The effect of 50 μ M carbenoxolone on relative peak Fura-2 ratio.

9.4.4 Sarcoplasmic reticulum Ca^{2+} release kinetics

The effect of $50\mu\text{M}$ carbenoxolone on the kinetics of SR Ca^{2+} transients were analysed. The time to 10% and 90% decay of the transient was analysed at both 1Hz and 3Hz (Figure 9.10). The difference between the 2 values was calculated and the results shown in Figure 9.11a and 9.11b (1Hz and 3Hz respectively). $50\mu\text{M}$ carbenoxolone does not alter the time to 90% and 50% decay at either 1Hz or 3Hz stimulation rates.

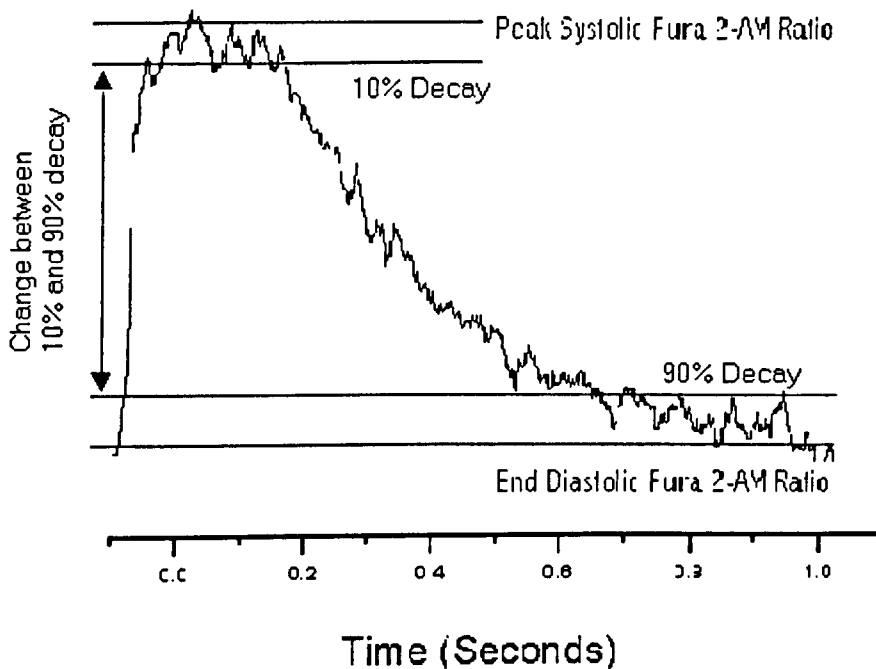
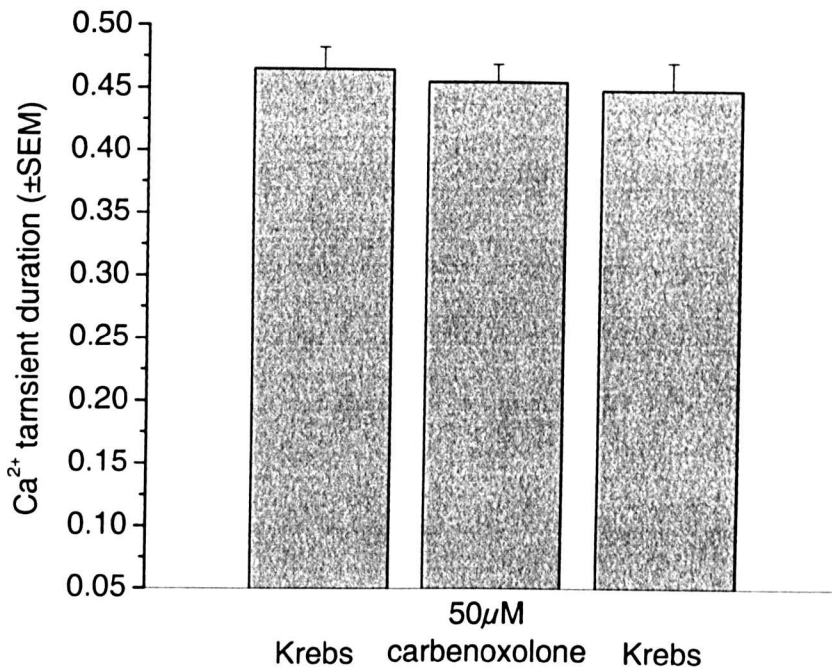
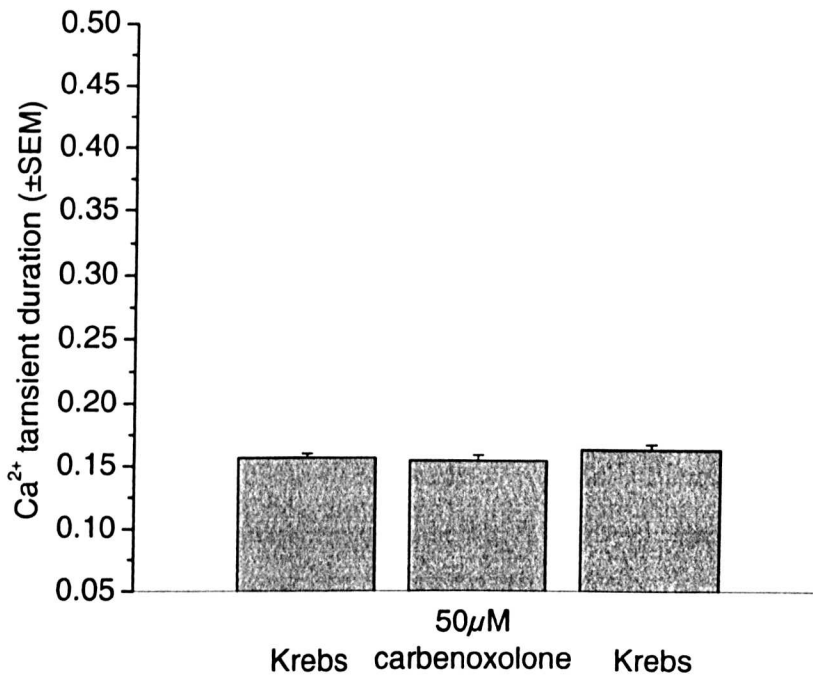


Figure 9.10 Analysis of Ca^{2+} transient kinetics.



A. Stimulation at 1Hz.



B. Stimulation at 3Hz.

Figure 9.11 The effect of 50 μM carbenoxolone on the kinetics of Ca^{2+} decay at 1Hz (A) and 3Hz (B) as measured by Fura-2. 50 μM carbenoxolone does affect ($P > 0.05$, paired Student's t-test) the kinetics of decay.

9.4.5 Sarcoplasmic reticulum Ca^{2+} content

The SR Ca^{2+} content was measured by applying a bolus of 20mM caffeine to the cells. The effect of 50 μM carbenoxolone on peak systolic Fura-2 ratio and SR Ca^{2+} content as measured by Fura-2 ratio is shown in Figure 9.12. The results of these experiments show that 50 μM carbenoxolone does not decrease SR Ca^{2+} release, nor does it alter the SR Ca^{2+} content.

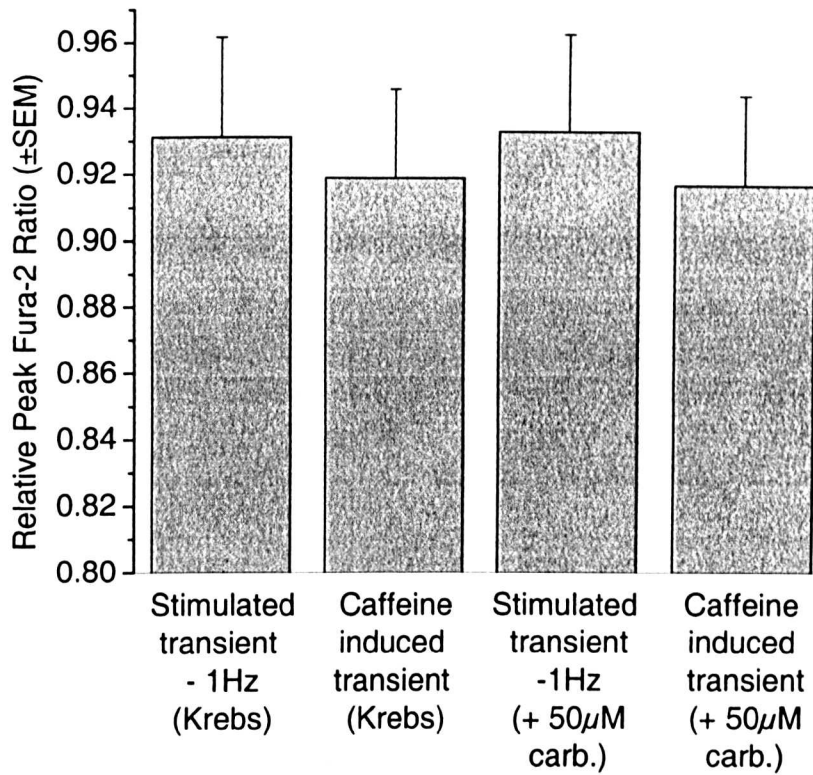


Figure 9.12 The effect of 50µM carbenoxolone on SR Ca²⁺ content. Carbenoxolone did not appear to cause a significant ($P > 0.05$, paired Student's t-test) change in SR Ca²⁺ content.

9.5 Discussion

Carbenoxolone has only recently been reported as a cardiac gap junction uncoupler. De Groot *et al* (1999) reported carbenoxolone as a novel specific gap junction uncoupler. In their investigations they used Langendorff perfused rabbit hearts perfused with Tyrode's solution and paced at twice diastolic threshold. Following electrical stabilisation they changed the perfusate to 50 μ M or 100 μ M carbenoxolone for 5 minutes. They did not examine the effect of the agent on cardiac electrical restitution although they did find that carbenoxolone: i) *slightly* decreases APD₂₀ and APD₅₀ although *slightly* increases MAPD₉₀ with no alteration in membrane currents in isolated myocytes, ii) alters cell to cell coupling via gap junctions in cell pairs as evident by delayed conduction, and iii) causes reversible, localised conduction slowing and block in the intact heart.

In the present study it was found that 50 μ M carbenoxolone did increase ($P>0.05$) dispersion of repolarisation, which is comparable to the non-significant effect of heptanol on dispersion of repolarisation. This was evident more so in the S1 MAPs than the S2 MAPs. There was however, a decrease in S2 dispersion at the local maximum on the restitution curve. Despite carbenoxolone seemingly acting as a gap junction uncoupler (as was assumed by its effect on increasing conduction delay and dispersion of repolarisation), it did not induce (or exacerbate) a negative slope in the restitution curve. This suggests that the negative slope seen with heptanol is not a phenomenon that can be attributed to gap junction uncoupling.

Both this study and that of de Groot *et al* conclude that carbenoxolone delays conduction. However, there was a major discrepancy between the 2 studies in respect of the effect of carbenoxolone on MAP configuration. De Groot *et al*

demonstrated that carbenoxolone at both 50 μ M and 100 μ M concentrations does not effect ventricular action potential characteristics (as evident by no change in action potential duration at 90% repolarisation). This study has shown that 50 μ M carbenoxolone *decreases* ventricular action potential characteristics as measured by the MAP duration at 90% repolarisation. This suggests that carbenoxolone either influences transmembrane currents directly, or indirectly by causing the heart to become ischaemic.

Furthermore, the data presented in this chapter suggests that the agent has small but significant effects on the Ca²⁺ transient. This further supports the non-specific effects of this agent. However, in contrast with the results obtained with 0.1mM heptanol there was no change in SR Ca²⁺ content. The effect of carbenoxolone on MAP duration and Ca²⁺ transient suggests that this agent has effects on cardiac E-C coupling unrelated to the effect on gap junction channels. This complicates the interpretation of the results of dispersion of repolarisation.

At 3Hz 50 μ M carbenoxolone irreversibly, and significantly, decreased the end diastolic cell length. This may confirm the toxic, and also irreversible, effect of carbenoxolone that is seen in the whole heart. At 1Hz, however this effect was not observed (end diastolic length remained relatively stable). At 3Hz the end diastolic Fura-2 ratio increased on application of 50 μ M carbenoxolone, this was not an observation that was made at 1Hz where end Fura-2 ratio also remained relatively stable. It is possible that this effect may be a time dependent effect of carbenoxolone on SR Ca²⁺ uptake (decay of the Ca²⁺ transient). At 1Hz there may be sufficient time between consecutive stimuli (Ca²⁺ transients) for Ca²⁺ to return to its initial concentration (i.e. uptake back in to the SR is complete). At 3Hz

however, there may not be sufficient time for the re-uptake back in to the SR, so that the end diastolic Fura-2 ratio may appear to be raised. Arguing against this mechanism, however, was the finding that 50 μ M carbenoxolone did not effect the kinetics of Ca²⁺ transient decay, as evident by no change in the time between 10% and 90% decay of the transient.

Chapter 10 – Summary and conclusions

10.1 Summary

This thesis deals with the effects of gap junction uncoupling on:

- i) whole heart electrophysiology and mechanical properties, and
- ii) single cell shortening and intracellular Ca^{2+} .

In the intact Langendorff perfused rabbit heart left ventricular epicardial repolarisation was measured using both a single MAP catheter electrode and also a custom made 32 MAP electrode array. These were used to assess heterogeneity of repolarisation following cellular uncoupling with gap junction uncoupling agents. The direct effects of these agents on E-C coupling were studied using single cell preparations.

10.2 Electrophysiological abnormalities associated with heart failure

Initially the single MAP electrode was used to investigate electrophysiological abnormalities (which may increase the propensity of the heart to become arrhythmic) associated with heart failure. The main reported electrophysiological abnormalities in heart failure are action potential duration prolongation and an increased dispersion of repolarisation/refractoriness as a result of electrical remodeling (reviewed in Wolk *et al* 1997). This thesis showed that in a rabbit model of heart failure there was a significant increase in MAP duration. The sequentially recorded dispersion of repolarisation however was not affected. This correlated well with the non-significant change in ventricular fibrillation threshold. The absence of any change in VF threshold and dispersion could be due to:

- i) the lack of severity of failure in the hearts used in the current study,

- ii) the high variability in the measurement of ventricular fibrillation threshold testing,
- iii) the impingement of the apical infarct in to the right ventricle where the ventricular fibrillation induction catheter is placed,
- iv) the sequential recording of MAPs to assess dispersion.

10.3 Simultaneous recording of cardiac electrical activity

One of the first aims of this study was to design and construct a method of simultaneously recording monophasic action potentials (MAPs) from the epicardial surface of the left ventricle in the intact rabbit heart. Simultaneous recording from multiple sites is superior to sequential recording with a single electrode from multiple sites in the experimental setting. Sequential recording requires multiple recordings to be made one at a time and hence requires a considerable amount of time to complete the measurements. During this time, the electrical properties of the heart may change due to prolonged perfusion with Tyrode solution.

10.3.1 The 32 MAP electrode array

The construction of a 32 MAP electrode array was an extremely delicate operation that required considerable of manual dexterity and a substantial amount of time and patience. As with many techniques used in cardiac electrophysiology, the application of the technique wasn't without its difficulties and drawbacks. It was originally hoped that the electrode array could be used to simultaneously record up to 32 MAPs from normal and failing hearts. However, it soon became apparent that the 32 electrode array worked poorly with infarcted hearts, mainly because of

the variability in the size of infarcted hearts. This meant that the use of the MAP jacket apparatus was restricted to normal hearts only. Although the array was not 100% successful (i.e. yielded at most 16/32 MAPs) it is a significant advancement on previous attempts to simultaneously record MAPs (e.g. Franz *et al*, 1992).

In order to mimic the electrical uncoupling that is believed to occur in hypertrophic myocardium, agents reported to disrupt cellular electrical coupling were investigated using the multiple MAP apparatus.

10.4 Gap junction uncoupling

1-Heptanol and carbenoxolone have previously been used to study the electrophysiological consequences of the disruption of cell to cell coupling in cardiac muscle, but their effects on dispersion of repolarisation and electrical restitution has been poorly studied.

Using the 32 MAP electrode array in normal hearts it was found that 0.3mM heptanol non-significantly increases dispersion of repolarisation, which was consistent with the non-significant decrease in ventricular fibrillation threshold that was also observed. The concentration of heptanol used in this study is comparable to that used by others (Callans *et al* 1996; Keevil *et al*, 2000). In previous studies, concentrations below 0.3mM have been noted as causing a higher incidence of arrhythmias than at higher concentrations. This may explain the minimal effects of the 'intermediate' concentration of 0.3mM heptanol that was used in this study. It was also observed that heptanol causes a dramatic decrease in left

ventricular developed pressure. The direct effect of heptanol on E-C coupling was investigated later in this study (refer to section 10.5.2.2).

Electrical uncoupling, which is seen in cardiac hypertrophy, is thought to contribute to enhance the substrate for arrhythmias. As previously discussed, changes in electrical restitution may serve as a positive indicator for arrhythmogenesis where abnormalities are seen in the restitution curve, i.e. where there is biphasic restitution. As heptanol has an effect on MAP duration, and since it is a poorly studied area, the effect of cellular uncoupling on electrical restitution was investigated.

10.5 Restitution

10.5.1 Measurement of restitution

A large proportion of the whole heart simultaneous recording studies were conducted using extrastimulus restitution protocols. One important question arising from these experiments was: *How many S1 beats are required to obtain steady state MAP durations prior to the S2 extrastimulus?* Initially 8 S1 stimuli train protocols were used which is a protocol used both clinically and experimentally. However, analysis of the last S1 MAP in the 8 beat train showed that 8 stimuli prior to the S2 extrastimulus was not sufficient enough to produce a stable final S1 MAP. Plotting MAP duration versus cycle length from the last S1 stimuli yielded restitution like curves. As a result, the S2 restitution curves were unreliable despite looking plausible. However, using a 16 S1 stimuli protocol S1 stability was ensured as was evident by a flat S1 graph.

10.5.2 The negative slope in the restitution curve

An interesting but unexpected effect of heptanol, which later became the focus of this study, was the induction of a negative slope in the restitution curve by 0.3mM heptanol. In normal hearts perfused with physiological saline, the restitution curve showed a monotonic relationship – a steep increase in MAP duration with increasing S1-S2 interval followed by a plateau at longer S1-S2 intervals. Heptanol however caused a biphasic relationship where a decrease in MAP duration was observed through intermediate S1-S2 intervals. This raised the questions: *Is the induction of a negative slope in the restitution curve a gap junction uncoupling phenomenon or, given the negative inotropic properties of heptanol, is it a product of the disruption of E-C coupling?*

10.5.2.1 Phenomena related to gap junction uncoupling

If the negative slope is a gap junction uncoupling phenomenon then it would be expected that other gap junction uncouplers (preferably with few non-specific effects) would also induce a negative slope. Carbenoxolone was reported as a specific gap junction uncoupler by De Groot *et al* (1999) and was used in this study in the whole heart. It was found that carbenoxolone did not induce a negative slope in the restitution curve, indicating that the negative slope is not a gap junction uncoupling property. However in contrast to the results obtained by De Groot *et al*, it was found that carbenoxolone significantly decreases MAP duration, in addition to slightly increasing dispersion ($P>0.05$). In single cells it was also seen that carbenoxolone causes a decrease in SR Ca^{2+} release, raising doubts about the claimed selectivity of the uncoupler.

10.5.2.2 Disruption of E-C uncoupling

The effects of heptanol on single cell shortening and SR Ca^{2+} release and content in left ventricular epicardial myocytes from healthy hearts was studied with a view to answering the question concerning the selectivity of heptanol as a gap junction uncoupler. At 1Hz and 3Hz heptanol decreased fractional cell shortening to a similar degree as seen in the whole heart (~50-60%) but at a lower concentration (0.1mM). This disparity may have arisen from the different type of force measurements in single cells and the whole heart (isotonic versus isometric). It was also observed that heptanol decreased SR Ca^{2+} release but had no effect on SR Ca^{2+} content. This effect may be via a reduction in Ca^{2+} transient amplitude, and/or a reduced Ca^{2+} sensitivity of the myofilaments. Hence the reduction of Ca^{2+} transient amplitude may be due to either the effects on the L-type Ca^{2+} channel or SR Ca^{2+} release and uptake.

Possible effects of heptanol on the L-type Ca^{2+} channel suggested the involvement of this channel in the negative slope of the restitution curve. The L-type Ca^{2+} channel blocker nifedipine was used in single cells to attempt to mimic the effect of heptanol on contractility and Ca^{2+} measurements. It was also used to determine a concentration that produces equivalent effects on contractility and Ca^{2+} that could be used in the whole heart to investigate the effects of L-type Ca^{2+} channel blockade on the negative slope of the restitution curve. In fact, $0.15\mu\text{M}$ nifedipine in fact had the opposite effect of heptanol on the slope of the restitution curve – it was flattened. This result ruled out the idea that the L-type Ca^{2+} channel is associated with the negative slope.

10.6 Tried but failed

Following the success of heptanol and carbenoxolone in the whole heart, an attempt to investigate the effect of other gap junction uncouplers on the electrophysiology of the whole heart was made. Dhein *et al* (1999) investigated the effect of the gap junction uncoupler palmitoleic acid on the activation wavefronts and repolarisation in the rabbit heart using a 256 unipolar electrode array. They noted a dramatic increase in the dispersion of epicardial repolarisation (as measured by activation recovery intervals). On attempting to use palmitoleic acid it was found that keeping the agent in solution was problematic. Oleic acid and linoleic acid were also tried but the same precipitation problem was encountered.

10.7 Future directions

The question *What causes the induction of the negative slope in the restitution curve of the intact rabbit heart on perfusion with heptanol?* still needs to be answered. The most direct way to tackle this problem would be to perform voltage clamp experiments on isolated cells. This would permit dissection of the current(s) involved in the phenomenon. Because the negative slope occurs between approximately 180ms and 350ms S1-S2 intervals, likely initial candidates to investigate would be the K^+ current.

Optical mapping using voltage sensitive dyes is a newer technique that is becoming popular to use for mapping the electrical activity in the intact heart. It affords higher spatial resolution than contact electrode techniques. It also appears to allow

recording from infarcted hearts. However, this method of simultaneously recording requires the use E-C uncouplers to reduce motion artefact. E-C uncouplers are not without direct electrophysiological effects. It is also necessary to have a flat epicardial surface from which to record. This is obtained by holding the heart in a chamber to ensure that the tissue under investigation is held flat against a glass surface. Because of this, records can only be made from a limited and (to some extent) distorted area, which contrasts to the 32 electrode array where the heart is not physically distorted and E-C uncouplers are not used. Thus optical mapping is no panacea; some questions may be better addressed using electrode array techniques.

References

- Allessie, M.A., Bonke, F.I.M., and Schopman, F.J.G. (1976) Circus movement in rabbit atrial muscle as a mechanism of tachycardia. II. The role of non-uniform recovery of excitability in the occurrence of unidirectional block as studied with multiple microelectrodes. *Circulation Research* **39**:168-177.
- Allessie, M.A., Bonke, F.I.M., and Schopman, F.J.G. (1977). Circus movement in rabbit atrial muscle as a mechanism of tachycardia. III. The “leading circle” concept: A new model of circus movement in cardiac tissue without the involvement of an anatomical obstacle. *Circulation Research* **41**(1):9-18.
- Antzelevitch, C.A., Sicouri, S., Litovsky, S.H., Lukus, A., Krishnan, S.C., Di Diego J.M., Ginant G.A., and Lui D. (1991) Heterogeneity within the ventricular wall. Electrophysiology and pharmacology of epicardial, endocardial and M cells. *Circulation Research* **69**(6):1427-1449.
- Anyukhovskiy, E.P., Sosunov, E.A., and Rosen, M.R. (1996) Regional differences in electrophysiological properties of epicardium, midmyocardium, and endocardium. In vitro and in vivo correlations. *Circulation* **8**:1981-1988.
- Bass, B.G. (1975) Restitution of the action potential in the cat papillary muscle. *American Journal of Physiology* **228**(6):1717-1724.
- Bastide B., Herve J.C., Cronier L., and Deleze J. (1995) Rapid onset and calcium independence of the gap junction uncoupling induced by heptanol in cultured heart cells. *Pflugers Archives - European Journal of Physiology* **429**:386-393.
- Behrens, S., Li, C., Fabritz, L., Kirchhof, P.S., and Franz, M.R. (1997) Shock-induced dispersion of ventricular repolarization: Implications for the induction of ventricular fibrillation and the upper limit of vulnerability. *Journal of Cardiovascular Electrophysiology* **8**(9):998-1008.

- Bers, D.M (2001) Excitation-contraction coupling and cardiac contractile force. 2nd Edition. Eds: Kluwer, Academic Publishers
- Beuckelmann, DJ., Nabauer, M., and Erdmann, E. (1993) Alterations of K⁺ currents in isolated human ventricular myocytes from patients with terminal heart failure. *Circulation Research*. **73(2)**:379-85.
- Biermann, M., Rubart, M., Moreno, A., Wu, J., Josiah-Durant, A., and Zipes D.P. (1998) Differential effects of cytochalasin D and 2,3 butanedione monoxime on isometric twitch force and transmembrane action potential in isolated ventricular muscle: implications for optical measurements of cardiac repolarization. *Journal of Cardiovascular Electrophysiology* **9(12)**:1348-57
- Boersma, L., Brugada, J., Abdollah, H., Kirchhof, C., and Allessie, M. (1994) Effects of Heptanol, Class Ic, and Class III drugs on reentrant ventricular tachycardia. Importance of the excitable gap for the inducibility of double-wave reentry. *Circulation* **90**:1012-1022.
- Boyett, M.R., and Jewell, B.R. (1978) A study of the factors responsible for rate-dependent shortening of the action potential in mammalian ventricular muscle. *Journal of Physiology* **285**:359-380.
- Boyett, M.R., and Jewell, B.R. (1980) Analysis of the effects of changes in rate and rhythm upon electrical activity in the heart. *Progress in Biophysical and Molecular Biology* **36**:1-52.
- Brahmajothi, M.V., Morales, M.J., Reimer, K.A., and Strauss, H.C. (1996) Regional localization of ERG, the channel protein responsible for the rapid component of the delayed rectifier, K⁺ current in the ferret heart. *Circulation Research* **81**:128-135.
- Bryant, S.M., Shipsey, S.J., and Hart, G. (1996) Regional differences in electrical and mechanical properties of myocytes from guinea-pig hearts with mild left ventricular hypertrophy. *Cardiovascular Research* **35**:315-323.

Burdon-Sanderson, J. and Page, F.J.M. (1882) On the time-relations of the excitatory process in the ventricle of the heart of the frog. *Journal of Physiology* **2**:385-412.

Burton, F.L. and Cobbe, S.M. (1998) Effect of sustained stretch on dispersion of ventricular fibrillation intervals in normal rabbit hearts. *Cardiovascular Research* **39**:351-359.

Burton, F.L., McPhaden, A.R., and Cobbe, S.M. (2000) Ventricular fibrillation threshold and local dispersion of refractoriness in isolated rabbit hearts with left ventricular dysfunction. *Basic Research Cardiology* **95**(5):359-67.

Burton, F.L. and Cobbe, S.M. (2001) Dispersion of ventricular repolarisation and refractory period. *Cardiovascular Research* **50**:10-23.

Calkins, H., Maughan, W.L., Weisman, H.F., Sugiura, S., Sagawa, K., and Levine, J.L. (1989a) Effect of acute volume load on refractoriness and arrhythmia development in isolated, chronically infarcted canine hearts. *Circulation* **79**(3):687-696.

Calkins, H. Maughan, W.L., Kass, D.A., Sagawa, K., and Levine, J.H. (1989b) Electrophysiological effect of volume load in isolated canine hearts. *American Journal of Physiology* **256**:H1697-H1706.

Callans D.J., Moore E.N., and Spear J.F. (1996) Effect of coronary perfusion of heptanol on conduction and ventricular arrhythmias in infarcted canine myocardium. *Journal of Cardiovascular Electrophysiology* **7**:1159-1171.

Cha, Y-M., Peters, B.B., Birgersdotter-Green, U., and Chen, P-S. (1993) A reappraisal of ventricular fibrillation threshold testing. *American Journal of Physiology* **264**:H1005-1010 (Special communication).

Cheng, Y., Mowrey, K., Efimov, I.G., Van Wagoner, D.R., Tchou, P.J., and Mazgalev, T.N. (1997) Effects of 2,3-Butanedione Monoxime on atrial-atrioventricular nodal conduction in isolated rabbit heart. *Journal of Cardiovascular Research* **8**:790-802.

Cheng, J., Kamiya, K., Liu, W., Tsuji, Y., Toyama, J., and Kodama, I. (1999) Heterogeneous distribution of the two components of delayed rectifier K⁺ current: a potential mechanism of the pro-arrhythmic effects of methanesulfanilide class III agents. *Cardiovascular Research* **43**:135-147.

Chinushi, M., Restivo, M., Caref, EB., and El-Sherif, N. (1998) Electrophysiological basis of arrhythmogenicity of QT/T alternans in the long-QT syndrome: tridimensional analysis of the kinetics of cardiac repolarisation. [Journal Article] *Circulation Research*. **83**(6):614-28.

Cook, S.J., Chamunorwa, J.P., Lancaster M.K., and O'Neill, S.C. (1997) Regional differences in the regulation of intracellular sodium and in action potential configuration in rabbit left ventricle. *Pflugers Archives - European Journal of Physiology* **433**:515-522.

Cooklin, M., Wallis, W.R.J., Sheriden, D.J., and Fry, C.H. (1997) Changes in cell-to-cell electrical coupling associated with left ventricular hypertrophy. *Circulation Research* **80**:765-771.

Coraboeuf, E. and Nargeot, J. (1993) Electrophysiology of human cardiac cells. *Cardiovascular Research* **27**:1713-1725.

Coronel, R., Opthof, T., Taggart, P., Tytgat, J., and Veldkamp, M. (1997) Differential electrophysiology of repolarisation from clone to clinic. *Cardiovascular research* **33**:503-517.

Cowan, J.C., Griffiths, C.J., Hilton, C.J., Tansuphaswadikul, S., Murray, A., and Campbell, R.W.F. (1987) Epicardial repolarisation mapping in man. *European Heart Journal* **8**:952-964.

- Davies, L.A., Gibson, C.N., Boyett, M.R., Hopkins, P.M., and Harrison, S.M. (2000) Effects of isoflurane, sevoflurane, and halothane on myofilament sensitivity and sarcoplasmic reticulum Ca^{2+} release in rat ventricular myocytes. *Anesthesiology* **93**(4):1034-1044.
- Dean, J.W. and Lab, M.J. (1990) Regional changes in ventricular excitability during load manipulation of the *in situ* pig heart. *Journal of Physiology* **429**:387-400.
- de Bakker, J.M.T., van Capelle, F.J.L., Janse, M.J., Tasseron, S., Vermuelen, J.T., de Jonge, N., and Lahpor, J.R. (1993) Slow conduction in the infarcted human heart. 'zigzag' course of activation. *Circulation* **88**(3):915-926.
- De Groot, J.R., Verkerk, A.O., Veenstra, T., Smits, J.P.P., Verheijck, E.E., and Coronel, R. (1999) Carbenoxolone, a novel specific gap junction uncoupler. *Circulation* **100**(20):I-839.
- Delmar, M., Michaels, D.C., Johnson, T., and Jalife, J. (1987) Effects of increasing intercellular resistance on transverse and longitudinal propagation in sheep epicardial muscle. *Circulation Research* **60**:780-785.
- Delmar, M. (2000) Gap junctions as active signaling molecules for synchronous cardiac function. *Journal of Cardiovascular Electrophysiology* **11**:118-120.
- Denvir, M.A., MacFarlane, N.G., Cobbe, S.M., and Miller, D.J. (1998) Sarcoplasmic reticulum Ca^{2+} loading in rabbits 8 and 15 weeks after coronary artery ligation. *Pflugers Archive* **436**(3):436-42.
- Dhein, S., Kruzmann, A., Schaefer, T. (1999) Effects of the gap junction uncoupler palmitoleic acid on the activation and repolarization wavefronts in isolated rabbit hearts. *British Journal of Pharmacology* **128**(7):1375-84.

- Dillon, S.M. (1991) Optical recordings in the rabbit heart show that defibrillation strength shocks prolong the duration of depolarisation and the refractory period. *Circulation Research* **69**:842-856.
- Docherty, J.D. and Cobbe, S.M. (1990) Electrophysiological changes in an animal model of heart failure. *Cardiovascular Research* **24**:309-316.
- Drouin, E., Charpentier, F., Gauthier, C., Laurent, K., and Le Marec, H. (1995) Electrophysiologic characteristics of cells spanning the left ventricular wall of human heart: Evidence for the presence of M cells. *Journal of the American College of Cardiology* **26**:185-192.
- Eddlestone, G.T., Zygmunt, A.C., and Antzelavitch, C. (1996) Larger late sodium current contributes to the longer action potential duration of the M cell in canine ventricular myocardium. *Pacing Clinical Electrophysiology* **19**:II-569 (Abstract)
- Efimov, I.G., Huang, D.T., Rendt, J.M., and Salama, G. (1994) Optical mapping of repolarisation and refractoriness from intact hearts. *Circulation* **90**:1469-1480.
- Efimov, I.G., Biermann, M., and Zipes, D. (2001 in press) Fast fluorescent mapping of electrical activity in the heart: Practical guide to experimental design and applications. *In: Cardiac Mapping*. 2nd edition. Futura Publishing Co.
- Elharrar, V. and Surawicz, B. (1983) Cycle length restitution of action potential duration in cardiac dog fibres. *American Journal of Physiology* **244**:H782-H792.
- Fedida, D. and Giles, W.R. (1991) Regional variations in action potentials and transient outward current in myocytes isolated from rabbit left ventricle. *Journal of Physiology*. **442**:191-209.
- Fox, J.J., McHarg, J.L., and Gilmour Jr, R.F. (2002) Ionic mechanisms of electrical alternans. *American Journal Hear Circulation Research* **282**:H516-H530.

- Frampton, J.E., Orchard, C.H., and Boyett, M.R. (1991) Diastolic, systolic and sarcoplasmic reticulum [Ca^{2+}] during inotropic interventions in isolated rat myocytes. *Journal of Physiology*. **437**:351-75.
- Franz, M.R. (1983) Long term recording of MAPs from human endocardium. *American Journal of Cardiology* **51**:1629-1634.
- Franz, M.R. (1991) Method and theory of MAP recording. *Progress in Cardiovascular Disease*. **33**:347-348.
- Franz, M.R. (1999) Current status of the monophasic action potential recording: Theories, measurements and interpretations. *Cardiovascular Research* **41**:25-40.
- Franz, M.R., Burkhoff, D., Spurgeon, H., Weisfeldt, M.L., and Lakatta, E.G. (1986) *In vitro* validation of a new cardiac catheter technique for recording monophasic action potentials. *European Heart Journal* **7**:34-41.
- Franz, M.R., Curia, R., Wang, D., Profitt, D., and Kurz, R. (1992) Electrophysiological effects of myocardial stretch on mechanical determinants of stretch activated arrhythmias. *Circulation* **86**:968-978.
- Franz, M.R., Swerdlow, C.D., Liem, L.B., and Schaefer J. (1988) Cycle length dependence of human action potential duration in vivo. Effects of single extrastimulus, sudden sustained rate acceleration and deceleration, and different steady-state frequencies. *Journal of Clinical investigation* **82**:972-979.
- Gilmour, R.F. Jr., Chialvo, D.R. (1999) Electrical restitution, critical mass, and the riddle of fibrillation. *Journal of Cardiovascular Electrophysiology*. **10**(8):1087-9.
- Girouard, S., Laurita, K.R., and Rosenbaum D.S. (1996) Unique properties of cardiac action potentials recorded with voltage sensitive dyes. *Journal of Cardiovascular Electrophysiology* **7**(11):1024-1038.

- Gros, DB. and Jongsma, HJ. (1996) Connexins in mammalian heart function. *Bioassays* **18**(9):719-30.
- Han, J. (1969) Mechanisms of ventricular arrhythmia associated with myocardial infarction. *American Journal of Cardiology* **14**:516-24.
- Han, J. and Moe, G.K. (1964) Non-uniform recovery of excitability in ventricular muscles. *Circulation Research* **XIV** 14-44.
- Han, J., Garcia DeJalaon, P.D., and Moe, G.K. (1964) Adrenergic effects on ventricular vulnerability. *Circulation Research* **14**:516-524.
- Hart, G. (1994) Cellular electrophysiology in cardiac hypertrophy and failure. *Cardiovascular Research* **28**:933-946.
- He, D.S. and Burt, J.M. (2000) Mechanisms and selectivity of the effects of halothane on gap junction channel function. *Circulation Research* **86**:104-109.
- Hiraoka, M. and Kawano, S. (1987) Mechanisms of increased amplitude and duration of the plateau with sudden shortening of diastolic intervals in rabbit ventricular cells. *Circulation* **60**:14-26.
- Hoffman, B.F., Cranefield, P.F., Lipeschkin, E., Surawicz, B., and Herrlich, H.C. (1959) Comparison of cardiac monophasic action potentials recorded by intracellular and suction electrodes. *American Journal of Physiology* **196**(6):1297-1301.
- Horner, S.M., Vespalcova, Z., and Lab, M.J. (1997) Electrode for recording direction of activation, conduction velocity, and monophasic action potential of myocardium. *American Journal of Physiology* **272**:H1919-H1927.
- Huxley, H.E. (1969) The mechanism of muscle contraction. *Science* **164**:1356-1365.

Jalal, S., Williams, G.R., Mann, D.E., and Reiter, M.J. (1992) Effect of acute dilatation on fibrillation thresholds in the isolated rabbit heart. *American Journal of Physiology* **263**:H1306-H1310.

Jalife, J., Delmar, M., Davidenko, J.M., and Anumonwo, J.M.B. (1999) In: Basic cardiac electrophysiology for the clinician.

Janse, M.J. and Wit, L.A. (1989) Electrophysiological mechanisms of ventricular arrhythmias resulting from myocardial ischaemia and infarction. *Physiological Reviews* **69**(4):1049-1169.

Jauch, W., Hicks, M.N., and Cobbe, S.M. (1994) Effects of contraction-excitation feedback on electrophysiological and arrhythmogenesis in rabbits with experimental left ventricular hypertrophy. *Cardiovascular Research* **28**:1390-1396.

Jongsma, H.J. (1997) Gap junction channels and cardiac conduction. In: *Discontinuous conduction in the heart*. Editors: Spooner, P.M., Joyner, R.W., Jalife, J.

Jongsma, H.J. (1999) Modulation of gap junction properties in failing hearts. *Journal of Cardiovascular Electrophysiology* **10**:1421-1424.

Jongsma, H.J. and Wilders, R. (2000) MiniReview: Gap junctions in cardiovascular disease. *Circulation Research* **86**:1193-1197.

Johnson C.M., Green K.G., Kanter E.M., Bou-Abboud E., Saffitz J.E., and Yamada K.A. (1999) Voltage-gated Na⁺ channel activity and connexin expression in Cx43-deficient cardiac myocytes. *Journal of Cardiovascular Electrophysiology* **10**:1390-1401.

Joyner, R.W. (1986) Modulation of repolarisation by electrotonic interactions. *Japanese Heart Journal* **27 (Suppl 1)**:167-183.

Keevil V.L., Huang C.L-H., Chau P-L., Sayeed R.A., and Vandenberg J.I. (2000) The effect of heptanol on the electrical and contractile function of the isolated, perfused rabbit heart. *Pflugers Archive - European Journal of Physiology* **440**:275-282.

Kimber, S., Downar, E., Masse, S., Sevaptisidis, E., Chen, T., Mickleborough, L., and Parsons, I. (1996) A Comparison of unipolar and bipolar electrodes during cardiac mapping studies. *PACE* **19**:1196-1204.

Kleber, A.G., Janse, M.J., and Fast, V.G. (2001) Normal and abnormal conduction in the heart. In: *Handbook of Physiology. Section 2 the cardiovascular system. Volume 1: The heart.* Oxford University Press.

Korsgren, M., Leskinen, E., Sjostrand, U., and Varnauskas, E. (1966) Intracardiac recording of monophasic action potentials in the human heart. *Scandinavian Journal of Clinical & Laboratory Investigation.* **18(5)**:561-4, 1966.

Kuo, C.S., Munakata, K., Reddy, C.P., and Surawicz, M.D. (1983) Characteristic and possible mechanism of ventricular arrhythmia dependent on the dispersion of action potential duration. *Circulation* **67(6)**:1356-1367.

Kuo, C.S, Amlie, J.P., Munakata, K., Reddy, C.P. and Surawicz, P. (1983) Dispersion of monophasic action potential duration and activation times during atrial pacing, ventricular pacing, and ventricular premature stimulation in canine ventricles. *Cardiovascular Research* **17**:152-161.

Kurz, R., Xiao-Lin, R., and Franz, M.R. (1993) Increased dispersion of ventricular repolarisation and ventricular tachyarrhythmias in the globally ischaemic rabbit heart. *European Heart Journal* **14**:1561-1571.

Lab, M.J. (1982) Contraction-excitation feedback in myocardium. Physiological basis and clinical relevance. *Circulation Research* **50(6)**:757-766.

Lars Bastiaanse E.M., Jongsma H.J., van der Laarse A., and Takens-Kwak B.R. (1993) Heptanol-induced Decrease in Cardiac Gap Junctional Conductance Is Mediated by a Decrease in the Fluidity of Membranous Cholesterol-rich Domains. *Journal of Membrane Biology* **136**:135-145.

Laurita K.R., Girouard D.S., and Rosenbaum D.S. (1996) Modulation of ventricular repolarisation by premature stimulus. Role of epicardial dispersion of repolarisation kinetics demonstrated by optical mapping of the intact guinea pig heart. *Circulation Research* **79**:493-503.

Leerssen, H.M., Vos, M.A., den Dulk, K., van der Zande, J., and Wellens, HJ. (1994) Is the ventricular effective refractory period different when determined by incremental versus decremental scanning?: The effect of pacing cycle length, d-sotalol, and levocromakalim. *Pacing & Clinical Electrophysiology* **7(11 Pt 2)**:2084-9.

Leirner and Cestari (1999) Monophasic action potentials. *Arq Bras Cardiology*: **72(2)** (Internet source).

Lesh M.D., Pring M., and Spear J.F. (1989) Cellular uncoupling can unmask dispersion of APD in ventricular myocardium. A computer modelling study. *Circulation Research* **65**:1426-1440.

Leslie, J., Nolan, M.F., Logan, S.D., and Spanswick, D. (1998) Actions of carbenoxolone on rat sympathetic preganglionic neurones *in vitro*. *Journal of Physiology* **506.P**, 146P.

Levine, J.H., Moore, E.N., and Kadish, A. (1986) The monophasic action potential upstroke: A means of characterizing local conduction. *Circulation* **74**:1147-1155.

Li, G-R., Feng, J., Yue, L., and Carrier, M. (1999) Transmural heterogeneity of action potentials and I_{to1} in myocytes isolated from the human right ventricle. *American Journal of Physiology* **275**:H369-H377.

- Litovsky, S.H. and Antzelevitch, C. (1989) Rate dependence of action potential duration and refractoriness in canine ventricular endocardium differed from that of the epicardium: role of the transient outward current. *Journal of American College of Cardiology* **14**:1053-1066.
- Luo, C. and Rudy, Y. (1991) A model of the ventricular cardiac action potential: depolarisation, repolarisation and their interaction. *Circulation Research* **68**:1501-1526.
- McIntosh, M.A., Cobbe, S.M., and Smith, G.L. (1998) Non uniform changes in action potential duration and intracellular Ca^{2+} in the left ventricular myocyte subtypes isolated from rabbits with heart failure. *Personal correspondence*.
- McIntosh, M.A., Cobbe, S.M., and Smith, G.L. (2000) Heterogeneous changes in action potential and intracellular Ca^{2+} in left ventricular myocyte sub-types from rabbits with heart failure. *Cardiovascular Research*. **45**(2):397-409.
- Mines, G.R. (1914): On circulating excitations in heart muscle and their possible relation to tachycardia and fibrillation. *Transactions Of The Royal Society Of Canada* **8**:43-52.
- Morady, F., Kadish, A.H., Toivonen, L.K., Kushner, J.A., and Schmaltz, S. (1988) The maximum effect of an increase in rate on human ventricular refractoriness. *Pacing Clinical Electrophysiology* **11**(12):2223-34.
- Morgan, J.M., Cunningham, D., and Rowland, E. (1992) Electrical restitution in the endocardium of the intact human right ventricle. *British Heart Journal* **67**:42-46.
- Ng, G.A. (1998) Mechanical performance, intracellular Ca^{2+} handling and ventricular repolarisation in isolated hearts from rabbits with heart failure. *Ph.D. Thesis*.

- Peters, N.S. (1996) New insights in to myocardial arrhythmogenesis: distribution of gap-junctional coupling in normal, ischaemic and hypertrophied human hearts. *Clinical Science* **90**:447-452.
- Pye, M.P. and Cobbe, S.M. (1992) Mechanisms of ventricular arrhythmias in cardiac failure and hypertrophy. *Cardiovascular Research* **26**:740-750. (Abstract)
- Qin, D., Zhang, Z-H., Caref, E.B. Boutjdir, M., Jain, P., and El-Sherif, N. (1996) Cellular and ionic basis of arrhythmias in postinfarction remodeled ventricular myocardium. *Circulation Research* **79**:461-473.
- Ramdat Misier, A.R.R., Opthof, T., Van Hemel, N.M., Vermeulen, J.T., de Bakker, J.M.T., Defauw, J.J.A.M., van Capelle, F.J.L., and Janse, M.J. (1995) Dispersion of 'refractoriness' in noninfarcted myocardium of patients with ventricular tachycardia or ventricular fibrillation after myocardial infarction. *Circulation* **91**:2566-2572.
- Ramza, B.M., Tan, R.C., Osaka, T., and Joyner, R.W. (1990) Cellular mechanism of the functional refractory period in ventricular muscle. *Circulation Research* **66**(1):147-62.
- Reiter, M.J., Synhorst, D.P., and Mann, D.E. (1988) Electrophysiological effects of acute ventricular dilatation in the isolated rabbit heart. *Circulation Research* **62**:554-562.
- Reuter, H. (1973) Time- and voltage-dependent contractile responses in mammalian cardiac muscle. *European Journal of Cardiology* **1**:177-181.
- Riccio, M.L., Koller, M.L., and Gilmour Jr., R.F. (1999) Electrical restitution and spatiotemporal organisation during ventricular fibrillation. *Circulation Research* **84**:955-963.
- Rudisuli A. and Weingart R. (1999) Electrical Properties of Gap Junction Channels in Guinea-pig Ventricular Cell Pairs Revealed by Exposure to Heptanol. *Pflugers Arch* **415**:12-21.

- Rudy, Y. and Shaw, R.M. (1997) Membrane factors and gap junction factors as determinants of ventricular conduction and re-entry. From: Spooner, P.M., Joyner, R.W. and Jalife, J. *Discontinuous conduction in the heart*.
- Runnalls, M.E., Sutton, P.M., and Taggart, P. (1987) Modifications of electrode design for recording monophasic action potentials in animals and humans. *American Journal of Physiology* **253**:H1315-H1320.
- Sabatine, M.S., Antman, E.M., Ganz, L.I., Strichartz, G.R., and Lilly, L.S. Mechanisms of Cardiac Arrhythmias. In: Lilly, L.S. Ed. *Pathophysiology of Heart Disease 2nd Edition*. Philadelphia, Pa: Williams & Wilkins; 1997: 233-248.
- Schmitt, F.O., and Erlanger, J. (1928) Directional differences in the conduction of the impulse through heart muscle and their possible relation to extrasystolic and fibrillatory contractions. *American Journal of Physiology* **87**:326-347.
- Segawa, D., Sjoquist, P-O., Norlander, M., Wang, Q-D., Gonon, A., and Ryden, L. (1999) Cardiac inotropic vs. chronotropic selectivity of isradipine, nifedipine and celvidipine, a new ultrashort-acting dihydropyridine. *European Journal of Pharmacology* **380**:123-128.
- Severs, N.J. (1994) Pathophysiology of gap junctions in heart and disease. *Journal of Cardiovascular Electrophysiology* **5**:462-475.
- Shaw R.M. and Rudy Y. (1997) Ionic mechanisms of propagation in cardiac tissue: Roles of the sodium and L-type calcium currents during reduced excitability and decreased gap junction coupling, *Circulation Research* **81(5)**:727-741, 1997.
- Sicouri, S. and Antzelevitch, C.A. (1991) A subpopulation of cells with unique electrophysiological properties in the deep subepicardium of the canine ventricle. The M cells. *Circulation Research* **68**:1729-1741.
- Spach, M.S., Miller, W.T., and Dolber, P.C. (1982) The functional role of structural complexities in the propagation of depolarisation in the atrium of the

dog. Cardiac conduction disturbances due to discontinuities of effective axial resistivity. *Circulation Research* **50**:175-191.

Spear J.S., Balke C.W., Lesh M.D., Kadish A.H., Levine J.L., and Moore E.N. (1990) Effect of cellular uncoupling by heptanol on conduction in infarcted myocardium. *Circulation* **66**:202-207. (Abstract)

Surawicz, M.D. (1997) Ventricular fibrillation and dispersion of repolarisation. *Journal of Cardiovascular Electrophysiology* **8**:1009-1012.

Surawicz, B. (1990) Dispersion of refractoriness in ventricular arrhythmias. *In Cardiac Electrophysiology: From cell to bedside*. Editors: Zipes, D.P., and Jalife, J.

Swartz, J.F., Jones, J.L. and Fletcher, R.D. (1993) Characteristics of ventricular fibrillation based on monophasic action potential morphology in human heart. *Circulation* **87**:1907-1914.

Takens-Kwak B.R., Jongasma H.J., Rook M.B., and Van Ginneken A.C.G. (1992) Mechanisms of heptanol-induced uncoupling of cardiac gap junctions: a perforated patch-clamp study. *American Journal of Physiology* **262**(2 Pt 1):c1531-1538.

Taggart, P., Sutton, P.M., Opthof, T., Coronel, R., Trimlett, R., Pugsley, W., and Kallis, P. (2001) Transmural repolarisation in the left ventricle in humans during normoxia and ischaemia. *Cardiovascular Research*. **50**(3):454-62.

Tomaselli, G.F., Beuckelmann, D.J., Calkins, H., Berger, R.D., Kessler, P.D., Lawrence, J.H., Kass, D., Feldman, A.M., and Marban, E. (1994) Sudden cardiac death in heart failure: The role of abnormal repolarisation. *Circulation* **90**(5):2534-2539.

Vasello, J.A., Cassidy, D.M., and Kindwall, K.E., Marchlinski, F.E., and Josephson, M.E. (1988) Nonuniform recovery of excitability in the left ventricle. *Circulation* **78**:1365-1372.

Van Ginneken, A.C.G. and Veldkamp, M.W. (1999) Editorial: Implications of inhomogeneous distribution of I_{Ks} and I_{Kr} channels in ventricle with respect to effects of class III agents and beta-agonists. *Cardiovascular Research* **43**:20-22.

VanTyn, R.A. and MacLean, L.D. (1961) Factors of importance in determining ventricular fibrillation threshold. *American Journal of Physiology* **201**(3):457-461.

Viswanathan, P.C., Shaw, R.M., and Rudy, Y. (1999) Effects of I_{Kr} and I_{Ks} on action potential duration and its rate dependence: A simulation study. *Circulation* **99**(18):2466-2474.

Watanabe, M., Otani, N.F., and Gilmour, R.F. (1995) Biphasic restitution of action potential duration and complex dynamics in ventricular myocardium. *Circulation Research* **76**(5):915-921.

Weidman, S. and Draper, M.H. (1951) Cardiac resting and action potentials recorded with an intracellular electrode. *Journal of Physiology* **115**:74-94.

Weissenburger J., Nesterenko V.V., and Antzelevitch C. (2000) Transmural heterogeneity of ventricular repolarisation under baseline and long QT conditions in the canine heart in vivo: Torsades de pointes develops with halothane but not pentobarbitol anaesthesia. *Journal of Cardiovascular Electrophysiology* **11**:290-304.

Wit, A.L. and Dillon, S.M. Mechanisms of arrhythmia development. In: Zipes, D.P. and Jalife, J. Eds. *Cardiac Electrophysiology: From Cell to Bedside*. Philadelphia, Pa: W.B. Saunders Company.

Wolk, R., Cobbe, S.M., Hicks, M.N., and Kane, K.A. (1999) Functional, structural and dynamic bases of electrical heterogeneity in healthy and diseased cardiac muscle: implications for arrhythmogenesis and antiarrhythmic drug therapy. *Pharmacology & Therapeutics*. **84**(2):207-31.

Wu, J., Biermann, M., Rubart, M., and Zipes, DP. (1998) Cytochalasin D as excitation-contraction uncoupler for optically mapping action potentials in wedges of ventricular myocardium. *Journal of Cardiovascular Electrophysiology* 9(12):1336-47.

Yuan, S., Blomstrom-Lundqvist, C., and Bertil Olsson, S. (1994) Monophasic action potentials: Concepts to practical applications. *Journal of Cardiovascular Electrophysiology* 5(3):287-308.

Zhang, Y.M., Miura, M., and ter Keurs, H.E.D.J. (1996) Triggered propagated contractions in rat cardiac trabeculae. Inhibition by octanol and heptanol. *Circulation Research* 79:1077-1085.

